

**WestminsterResearch**

<http://www.westminster.ac.uk/westminsterresearch>

**Deiminated Proteins and Extracellular Vesicles - Novel Serum**

**Biomarkers in Whales and Orca**

**Magnadóttir, B., Uysal Organer, P., Kraev, I., Svansson, V.,**

**Hayes, P.M. and Lange, S.**

NOTICE: this is the authors' version of a work that was accepted for publication in Comparative Biochemistry and Physiology - Part D: Genomics and Proteomics.

Changes resulting from the publishing process, such as peer review, editing, corrections, structural formatting, and other quality control mechanisms may not be reflected in this document. Changes may have been made to this work since it was submitted for publication. A definitive version was subsequently published in Comparative Biochemistry and Physiology - Part D: Genomics and Proteomics, DOI: 10.1016/j.cbd.2020.100676, 2020.

The final definitive version in Comparative Biochemistry and Physiology - Part D: Genomics and Proteomics is available online at:

<https://dx.doi.org/10.1016/j.cbd.2020.100676>

© 2020. This manuscript version is made available under the CC-BY-NC-ND 4.0 license

<https://creativecommons.org/licenses/by-nc-nd/4.0/>

---

The WestminsterResearch online digital archive at the University of Westminster aims to make the research output of the University available to a wider audience. Copyright and Moral Rights remain with the authors and/or copyright owners.

---

Whilst further distribution of specific materials from within this archive is forbidden, you may freely distribute the URL of WestminsterResearch: (<http://westminsterresearch.wmin.ac.uk/>).

In case of abuse or copyright appearing without permission e-mail [repository@westminster.ac.uk](mailto:repository@westminster.ac.uk)

1      **Deiminated Proteins and Extracellular Vesicles - Novel Serum Biomarkers in Whales and Orca**

2  
3  
4      Bergljot Magnadottir<sup>a</sup>, Pinar Uysal-Onganer<sup>b</sup>, Igor Kraev<sup>c</sup>, Vilhjalmur Svansson<sup>a</sup>, Polly Hayes<sup>d</sup>, Sigrun  
5      Lange<sup>d\*</sup>

6  
7      <sup>a</sup>*Institute for Experimental Pathology, University of Iceland, Keldur v. Vesturlandsveg, 112 Reykjavik,  
8      Iceland; bergmagn@hi.is; vsvanss@hi.is*

9      <sup>b</sup>*Cancer Research Group, School of Life Sciences, University of Westminster, London W1W 6UW, UK;  
10     email: P.onganer@westminster.ac.uk*

11     <sup>c</sup>*Electron Microscopy Suite, Faculty of Science, Technology, Engineering and Mathematics, Open  
12     University, Milton Keynes, MK7 6AA, UK; igor.kraev@open.ac.uk.*

13     <sup>d</sup>*Tissue Architecture and Regeneration Research Group, School of Life Sciences, University of  
14     Westminster, London W1W 6UW, UK; p.hayes@westminster.ac.uk; S.Lange@westminster.ac.uk*

15  
16     \*Corresponding author: [S.Lange@westminster.ac.uk](mailto:S.Lange@westminster.ac.uk)

20    **Abstract**

21    Peptidylarginine deiminases (PADs) are a family of phylogenetically conserved calcium-dependent  
22    enzymes which cause post-translational protein deimination. This can result in neo-epitope  
23    generation, affect gene regulation and allow for protein moonlighting via functional and structural  
24    changes in target proteins. Extracellular vesicles (EVs) carry cargo proteins and genetic material and  
25    are released from cells as part of cellular communication. EVs are found in most body fluids where  
26    they can be useful biomarkers for assessment of health status. Here, serum-derived EVs were profiled,  
27    and post-translationally deiminated proteins and EV-related microRNAs are described in 5 cetaceans:  
28    minke whale, fin whale, humpback whale, Cuvier's beaked whale and orca. EV-serum profiles were  
29    assessed by transmission electron microscopy and nanoparticle tracking analysis. EV profiles varied  
30    between the 5 species and were identified to contain deiminated proteins and selected key  
31    inflammatory and metabolic microRNAs. A range of proteins, critical for immune responses and  
32    metabolism were identified to be deiminated in cetacean sera, with some shared KEGG pathways of  
33    deiminated proteins relating to immunity and physiology, while some KEGG pathways were species-  
34    specific. This is the first study to characterise and profile EVs and to report deiminated proteins and  
35    putative effects of protein-protein interaction networks via such post-translational deimination in  
36    cetaceans, revealing key immune and metabolic factors to undergo this post-translational  
37    modification. Deiminated proteins and EVs profiles may possibly be developed as new biomarkers for  
38    assessing health status of sea mammals.

39

40    **Key words:** Peptidylarginine deiminases (PADs); protein deimination; extracellular vesicles (EVs);  
41    microRNAs; cetaceans (*Balaenoptera acutorostrata*; *Balaenoptera physalus*; *Megaptera*  
42    *novaengliae*; *Ziphius cavirostris*; *Orcinus orca*); immunity; metabolism.

43

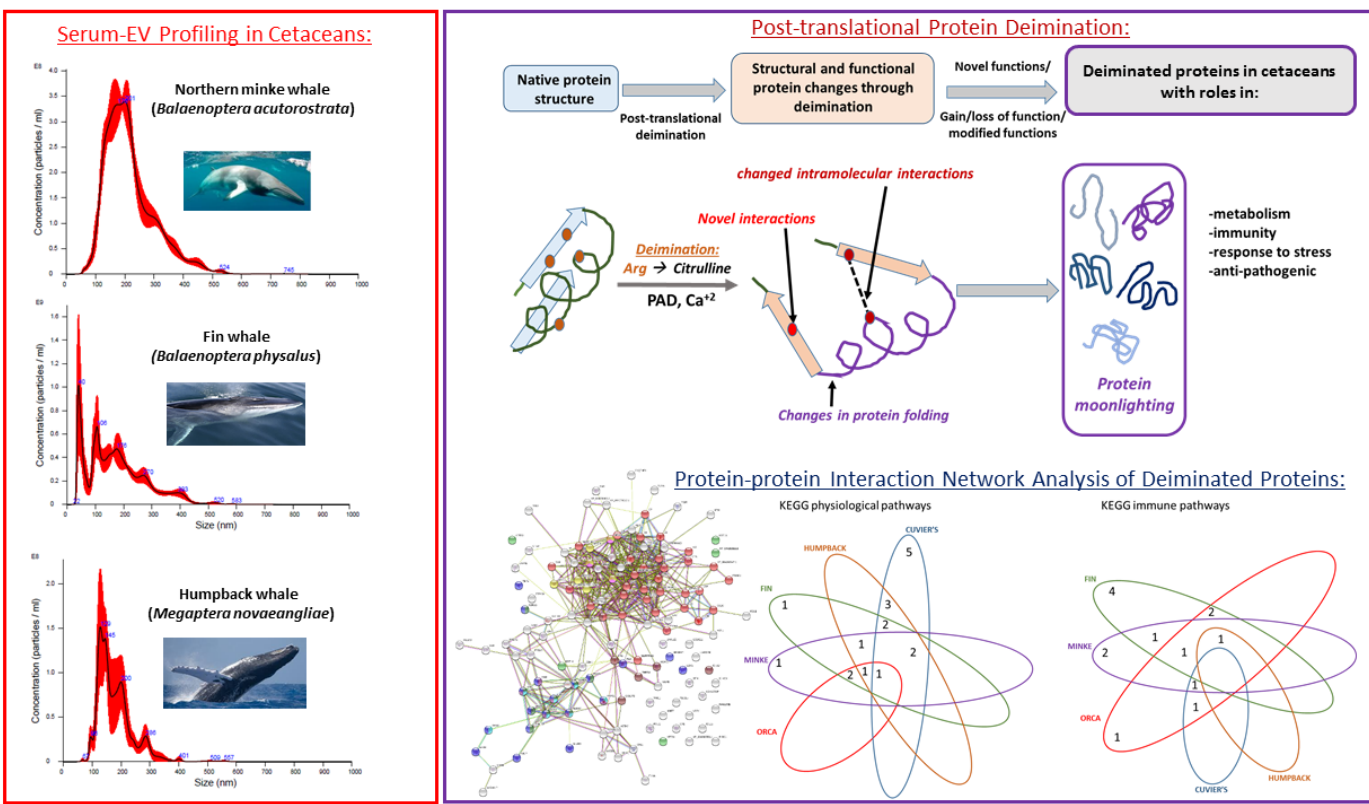
44    **Highlights**

- 45       • Deiminated proteins were identified in whales and orca  
46       • Key proteins of innate and adaptive immunity are deiminated in cetacean sera  
47       • EV profiles were characterised in sera of 5 cetacean species  
48       • Whale and orca serum-EVs are enriched in microRNAs compared to whole sera  
49       • EV-cargo of immune related miR21, miR155 and metabolic miR210 expression varies  
50          between cetacean species  
51       • Deiminated proteins and EV profiles are novel biomarkers in cetaceans

52

53

54 GRAPHIC ABSTRACT



55

56

57 **1. Introduction**

58 Peptidylarginine deiminases (PADs) are phylogenetically conserved calcium-dependent enzymes  
59 which post-translationally convert arginine into citrulline in target proteins in an irreversible manner,  
60 causing functional and structural protein changes (Vossenaar, 2003; György et al., 2006; Wang and  
61 Wang, 2013; Bicker and Thompson, 2013). Protein deimination can affect gene regulation, cause  
62 generation of neoepitopes (Witalison et al., 2015; Lange et al., 2017) and may also allow for protein  
63 moonlighting, an evolutionary acquired phenomenon facilitating proteins to exhibit several  
64 physiologically relevant functions within one polypeptide chain (Henderson and Martin, 2014; Jeffrey,  
65 2018). Regulation of proteins through such post-translational changes and protein moonlighting of  
66 post-translationally modified proteins in health and disease are of great interest, also with regard to  
67 effects on function of protein networks in evolutionary conserved and adapted pathways. PADs have  
68 been widely studied in a range of human pathologies, including cancer, autoimmune and  
69 neurodegenerative diseases (Wang and Wang, 2013; Witalison et al., 2015; Lange et al., 2017). Crucial  
70 roles for PADs have also been described in CNS regeneration and hypoxia (Lange et al., 2011; Lange et  
71 al., 2014; Fan et al., 2018; Yu et al., 2018). PADs are phylogenetically conserved and have been  
72 identified in diverse taxa from bacteria to mammals, with 5 tissue specific PAD isozymes in mammals,  
73 3 in birds, 1 in bony fish and arginine deiminase homologues in parasites and bacteria (Vossenaar et  
74 al., 2003; Rebl et al., 2010; Lange et al., 2011; Magnadottir 2018a, Magnadottir et al., 2019a; Gavinho  
75 et al., 2019; Kosgodage et al., 2019). In whales some PADs have been reported as gene sequences, for  
76 example PADI2 (Gene ID: 102988183) and PADI3 (Gene ID: 102986659) in sperm whale (*Physeter*  
77 *catodon*) (see Supplementary Fig. 1 for phylogenetic analysis of known PADs in cetaceans). Hitherto,  
78 PAD-related studies or investigations into their deiminated protein products are though almost non-  
79 existent, besides recent studies on cetacean extracellular trap formation (ETosis), which is a  
80 phylogenetically conserved innate defence mechanism that can be mediated via PADs (Li et al., 2010;  
81 Villagra-Blanco et al., 2019; Imlau et al., 2020). Research on PADs in normal vertebrate physiology has  
82 furthermore been limited compared to studies on pathophysiology. Putative control of physiological  
83 and immunological processes via post-translational deimination of proteins remains therefore a  
84 relatively unexplored field and has been a focus of recent ongoing comparative studies in our  
85 laboratory in a range of taxa throughout phylogeny (Criscitiello et al., 2019 and 2020; Kosgodage et  
86 al., 2019; Pamenter et al., 2019; Magnadottir et al., 2018a,b and 2019a,b; Kosgodage et al., 2019;  
87 Magnadottir et al., 2020a,b; Lange et al., 2020; Phillips et al., 2020). This also includes the identification  
88 of regulatory effects of PADs on extracellular vesicle (EV) release as a phylogenetically conserved  
89 mechanism (Kholia et al., 2015; Gavinho et al., 2019; Kosgodage et al., 2019).

EVs participate in cellular communication via transfer of cargo proteins and genetic material, including microRNAs (Inal et al., 2013; Colombo et al., 2014; Lange et al., 2017; Kosgodage et al., 2018; Turchinovich et al., 2019; Vagner et al., 2019). EVs can be isolated from most body fluids and be used as biomarkers for assessment of health status (Hessvik and Llorente, 2018; Ramirez et al., 2018). While work on EVs has hitherto largely focussed on human pathologies, roles for EVs in normal physiology and immunity also play important roles. Furthermore, key roles for PADs have been established in cellular release of EVs and EV biogenesis (Kholia et al., 2015; Kosgodage et al., 2017; Kosgodage et al., 2018; Kosgodage et al., 2019). Comparative studies assessing EVs and EV cargo have highlighted important roles for EVs in response to infection (Iliev et al., 2018; Yang et al., 2019), in mucosal immunity (Magnadottir et al., 2019b) and in host-pathogen interactions (Gavinho et al., 2019). Importantly, EVs were also recently identified by our group as novel biomarkers in teleost fish in response to environmental sea temperature changes (Magnadottir et al., 2020a). In elasmobranchs, EVs have been characterised in shark, where deiminated proteins were also identified as part of EV cargo (Criscitiello et al., 2019), and a recent studies have been carried out on EV profiling and protein deimination in penguins (Phillips et al., 2020) and pinnipeds (Magnadottir et al., 2020b).

Whales belong to cetaceans, which also include dolphins and porpoises, and have undergone extensive underwater adaptions, both anatomically and immunologically, to physiological stress linked to their marine environments (Beineke et al., 2010; Yim et al., 2013; Tsagkogeorga et al., 2015). Whales are thought to have diverged from terrestrial mammals about 50 million years ago, with toothed whales and baleen whales separated about 30 million years ago (McGowen et al., 2009; Meredith et al., 2011; Gatesy et al., 2013). Marine mammals are of considerable interest for comparative and evolutionary immunology due to their shared lineage with terrestrial mammals (Beineke et al., 2010; Meredith et al., 2011; Villagra-Blanco et al., 2019). Research into their immune systems may also further current understanding for resistance to cancer, insulin resistance and adaptions to hypoxia, highly relevant to a number of human pathologies (Tsagkogeorga et al., 2015; Tian et al., 2016; Seluanov et al., 2018). While cetaceans have been studied for a range of immunological factors (Beineke et al., 2010; Zhou et al., 2018; Gelain and Bonsembiante, 2019) and assessed for conserved immunological and physiological mechanisms, including at the genetic level (Yim et al., 2014; McGowen et al., 2014; Braun et al., 2015; Lopes-Marques et al., 2018; Zhou et al., 2018), less emphasis has been on proteomic studies. No studies have hitherto assessed aspects of putative regulation via post-translational modifications, such as deimination, which may affect protein-protein interaction networks and therefore be critical for physiological and immunological functions. Furthermore, comparative studies on EVs are scarce, including basic EV characterisation and identification, and have hitherto not been carried out in a cetacean species. While EVs are critical

124 factors in cellular communication and acknowledged biomarkers in a range of human  
125 pathophysiologies, their potential for assessments of physiological status or the level of  
126 environmental or immunological challenges in other taxa remains a vastly underexplored area. In  
127 ongoing studies on deiminated protein pathways and EV profiling throughout phylogeny in our  
128 laboratory, including in species with unusual metabolic and immunological adaptions, as well as in  
129 human disease, we felt that a study on these parameters in cetaceans was warranted.

130 In order to identify putative PAD-mediated roles for regulation of physiological and immune pathways,  
131 the current study assessed deiminated proteins and serum-derived EV profiles, including microRNA  
132 (miR) markers, in five cetaceans. The species under study were northern minke whale (*Balaenoptera*  
133 *acutorostrata*), fin whale (*Balaenoptera physalus*), humpback whale (*Megaptera novaeangliae*),  
134 Cuvier's beaked whale (*Ziphius cavirostris*) and orca (*Orcinus orca*). The minke whale, fin whale and  
135 humpback whale are mysticetes, while the orca is an odontocete and belongs to the family  
136 Delphinidae. The Cuvier's beaked whale is most common beaked whale, an odontocete of the family  
137 Ziphiidae, and the only member of the genus *Ziphius*, believed to represent the remant of an ancient  
138 evolutionary lineage.

139 Whales are long-lived sea mammals and are, like other sea life, exposed to ongoing changes in sea  
140 temperatures due to global warming as well as a range of environmental contaminants. This can  
141 change sea animals' exposure to pathogens, some of which are adapted to certain temperatures, and  
142 therefore result in opportunistic infections, including due to shift in habitat. Effects of virus-induced  
143 immunosuppression, as well as increased bacterial and parasitic infections due to xenobiotic pollution,  
144 affect a range of marine mammals globally (Kennedy 1998; Martinau et al., 1999; Jepson et al., 1999,  
145 Wünschmann et al., 2001; Müller et al., 2004; Siebert et al., 2006; Siebert et al., 2009; Beineke et al.,  
146 2010). Such increased disease susceptibility due to environmental factors, alongside effects of chronic  
147 diseases and starvation, has received considerable attention although many aspects of aquatic  
148 mammal's immune functions still remain to be fully understood (Beineke et al., 2010). A range of  
149 critical knowledge gaps in cetacean host-pathogen interactions have furthermore recently been  
150 highlighted, urging research in the field of cetacean immunology (Di Guardo et al., 2018). As  
151 accumulative effects of pollution may impact long-living sea mammals, changes in inflammatory- and  
152 other parameters in their biofluids, such as EVs and deiminated proteins, may be novel biomarkers  
153 which could be used for assessment of environmental effects on their health status. Furthermore,  
154 studying long-lived mammals that display cancer resistance, such as cetaceans, may be of translational  
155 value for furthering current understanding of putative underlying pathophysiological mechanisms and  
156 for longevity (Ma and Gladyshev, 2017; Seluanov et al., 2018).

157 Here we report for the first time deimination of key immune and metabolic proteins in whale and orca  
158 sera, characterise serum-derived EVs and assess EV-mediated export of key miRs involved in immune  
159 responses and metabolism. Our findings indicate both shared KEGG pathways for immunological and  
160 physiological functions in these cetaceans, as well as some differences in these parameters between  
161 the species under study. Furthermore, our findings verify that EVs are a better source for assessment  
162 of miR expression, compared to whole sera. This report is a first base-line study, indicating the  
163 potential for the development of a health-index biomarker test, based on deiminated proteins and EV  
164 profiling, as a novel tool to assess sea mammal health.

165

## 166 **2. Materials and Methods**

167

### 168 **2.1 Sampling of whale and orca sera**

169 Blood utilised in this study was collected from one individual animal of each of the following cetacean  
170 species: Northern minke whale (*Balaenoptera acutorostrata*), fin whale (*Balaenoptera physalus*),  
171 humpback whale (*Megaptera novaeangliae*), Cuvier's beaked whale (*Ziphius cavirostris*) and orca  
172 (*Orcinus orca*). Protocols for blood collection were ethically approved and conducted under licences  
173 of the Chief Veterinary Officer, the Icelandic Government's Ministry of Industries and Innovation  
174 (98020047; 13-23-04; 13-08-02). *Balenoptera acutorostrata* and *Balaenoptera physalus* were free  
175 ranging (South-Western Iceland) and samples collected post-mortem following euthanasia;  
176 *Megaptera novaeangliae* and *Ziphius cavirostris* were free ranging (South-Eastern Iceland) and blood  
177 samples were collected following stranding. *Orcinus orca* was captive (The Whale Sanctuary Project,  
178 Klettsvik Bay, Iceland) and blood was collected during routine health checks. Blood was collected live  
179 from the dorsal fin *vena caudalis* of the orca, but post-mortem from an intrathoracic vessel of the  
180 minke whale, fin whale, humpback whale and beaked whale, using vacutainers. After collection, the  
181 blood was processed by storing at room temperature for 2 h and thereafter overnight at 4 °C. Serum  
182 was collected after centrifugation at 2000 g for 20 min, aliquoted and frozen at -20 °C until further  
183 use. The animals were considered healthy upon sampling (further information available on these  
184 individuals on age, sex and reproductive status/maturity is provided in Supplementary Table 1).

185

### 186 **2.2 Extracellular vesicle isolation and NTA analysis**

187 For isolation of EVs, step-wise centrifugation and ultracentrifugation was used, based on previously  
188 established protocols (Kosgodage et al., 2018; Magnadottir et al., 2019b) and according to the  
189 recommendations of MISEV2018 (the minimal information for studies of extracellular vesicles 2018;  
190 Théry et al., 2018). Whale sera were diluted 1:4 in Dulbecco's PBS (DPBS which was ultrafiltered using

191 a 0.22 µm filter) by adding 250 µl serum to 750 µl DPBS per EV isolation. The diluted sera were  
192 centrifuged at 4,000 g for 30 min at 4 °C for removal of cells and cell debris and thereafter the  
193 supernatant was collected and centrifuged at 100,000 g for 1 h at 4 °C for EV enrichment. The resulting  
194 EV pellet was then resuspended and washed in 1 ml DPBS and ultracentrifuged again at 100,000 g for  
195 1 h at 4 °C. The final EV-enriched pellet was then resuspended in 100 µl DPBS for nanoparticle tracking  
196 analysis (NTA), based on Brownian motion of particles in suspension (Soo et al., 2012). The EV samples  
197 were diluted 1/100 in DPBS and applied to the NanoSight NS300 system (Malvern, U.K.) using a syringe  
198 pump to ensure continuous flow of the sample. Videos were recorded for 5 x 90 sec, with  
199 approximately 30-60 particles per frame. The replicate histograms generated from the recordings  
200 were averaged for assessment of EV size distribution profiles.

201

### 202 **2.3 Transmission Electron Microscopy**

203 For electron microscopic imaging of EVs, these were isolated from whale and orca sera as described  
204 above. EV pellets were then fixed with 2.5 % glutaraldehyde in 100 mM sodium cacodylate buffer (pH  
205 7.0) at 4 °C for 1 h and resuspended in 100 mM sodium cacodylate buffer (pH 7.0). The EVs were  
206 placed on to a grid containing a glow discharged carbon support film and stained with 2 % aqueous  
207 uranyl acetate (Sigma-Aldrich). Imaging was performed using a JEOL JEM 1400 transmission electron  
208 microscope (JEOL, Japan) operated at 80 kV at a magnification of 80,000 to 100,000. Digital images  
209 were recorded using an AMT XR60 CCD camera (Deben, UK).

210

### 211 **2.4 Western blotting**

212 Sera and serum-derived EV isolates (with each EV pellet isolated from 250 µl serum and reconstituted  
213 in 100 µl PBS after isolation and purification) were diluted 1:1 in 2x Laemmli sample buffer (containing  
214 5 % beta-mercaptoethanol) and boiled for 5 min at 100 °C before separation on 4-20 % gradient TGX  
215 gels (BioRad U.K.). Following SDS-PAGE, transfer to nitrocellulose membranes was performed using  
216 semi-dry Western blotting at 15 V for 1 h. The membranes were blocked in 5 % bovine serum albumin  
217 (BSA, Sigma-Aldrich, U.K.) diluted in TBS-T (tris-buffered saline containing 0.1 % Tween-20) at room  
218 temperature (RT) for 1 h, followed by overnight incubation at 4 °C with the primary antibodies, which  
219 were diluted in TBS-T as follows: F95 (MABN328, Merck, U.K.) 1/1000; anti-PAD2 (ab50257, Abcam)  
220 1/1000; anti-PAD3 (ab50246) 1/1000; anti-citH3-r2-r8-r17 (ab5103) 1/1000; CD63 (ab216130) 1/1000;  
221 Flotillin-1 (ab41927) 1/2000. After incubation with the primary antibodies, the membranes were  
222 washed in TBS-T for 3 x 10 min at room temperature (RT) and thereafter incubated in the  
223 corresponding secondary antibody (anti-rabbit IgG BioRad or anti-mouse IgM BioRad respectively,  
224 diluted 1/4000 in TBS-T) for 1 h, at RT. Membranes were then washed for 5 x 10 min in TBS-T, followed

225 by one wash for 10 min in TBS. Visualisation was performed using electrochemiluminescence (ECL,  
226 Amersham, U.K.) and the UVP BioDoc-ITM System (Thermo Fisher Scientific, U.K.).

227

## 228 **2.5 Immunoprecipitation and protein identification**

229 For isolation of deiminated proteins from whale and orca sera, the F95 pan-deimination antibody  
230 (MABN328, Merck), which is developed against a deca-citrullinated peptide and specifically detects  
231 proteins modified by citrullination (Nicholas and Whitaker, 2002), was used in conjunction with the  
232 Catch and Release immunoprecipitation kit (Merck, U.K.). According to the manufacturer's  
233 instructions (Merck), 50 µl of serum was used per sample for F95 enrichment and  
234 immunoprecipitation was carried out overnight on a rotating platform at 4 °C. The F95 bound proteins  
235 were eluted using denaturing elution buffer (according to the manufacturer's instructions, Merck) and  
236 the F95 enriched eluates were thereafter analysed both by Western blotting and by liquid  
237 chromatography mass spectrometry (LC-MS/MS) for identification of deiminated protein targets  
238 (Cambridge Proteomics, U.K.). For LC-MS/MS, peak files were submitted to in-house Mascot (Matrix  
239 Science, Cambridge Proteomics) using the following databases for identification of species-specific  
240 protein matches: *Balaenoptera\_acutorostrata\_20190523* (32,118 sequences; 20,395,764 residues);  
241 *Balaenoptera\_physalus\_20190523* (333 sequences; 92,646 residues);  
242 *Megaptera\_novaeangliae\_20190523* (259 sequences; 50,653 residues);  
243 *Ziphius\_cavirostris\_20190523* (176 sequences; 49,360 residues) and *Orcinus\_orca\_20190523* (333  
244 sequences; 105,106 residues). Furthermore, the LC-MS/MS peak files from all five species under study  
245 were also submitted to a larger cetacean UniProt database (CCP\_Cetacea Cetacea\_20191213; 252,001  
246 sequences; 150,129,595 residues; Cambridge Proteomics).

247

## 248 **2.6 Protein interaction network analysis**

249 STRING analysis (Search Tool for the Retrieval of Interacting Genes/Proteins; <https://string-db.org/>)  
250 was used for the identification of putative protein-protein interaction networks for the deiminated  
251 proteins identified in northern minke whale, fin whale, humpback whale, Cuvier's beaked whale and  
252 orca, respectively. Species selection in the STRING database was set to "cetacean" and protein-  
253 interaction network analysis was based on hits with "minke whale" for minke whale, but on hits with  
254 "orca" for fine whale, humpback whale, Cuvier's beaked whale and orca (note that protein-interaction  
255 network analysis for minke whale using corresponding orca hits revealed a similar analysis as when  
256 using the minke whale STRING database, therefore the minke whale database was used for minke  
257 whale). Protein networks were built by using the function of "search multiple proteins" in STRING and  
258 applying basic settings and medium confidence, with colour lines between nodes indicating evidence-

259 based interactions for network edges as follows: known interactions (based on curated databases,  
260 experimentally determined), predicted interactions (based on gene neighbourhood, gene fusion, gene  
261 co-occurrence) or via text mining, co-expression or protein homology. Annotations for KEGG (Kyoto  
262 Encyclopedia of Genes and Genomes) pathways identified were highlighted for physiological and  
263 immunological pathways identified by STRING (Fig. 4-8).

264

## 265 **2.7. PAD sequence alignment and phylogenetic reconstruction**

266 Pre-existing predicted PAD protein sequences for a number of cetaceans (Indo-Pacific humpback  
267 dolphin, *Sousa chinensis*; narwhal, *Monodon Monoceros*; sperm whale, *Physeter catodon*; common  
268 bottlenose dolphin, *Tursiops truncatus*; long-finned pilot whale, *Globicephala melas*; Pacific white-  
269 sided dolphin, *Lagenorhynchus obliquidens*; beluga *Delphinapterus leucas*; **narrow-ridged finless**  
270 **porpoise**, *Neophoncaena asiaeorientalis*; baiji, *Lipotes vexillifer*; minke whale, *Balaenoptera*  
271 *acutorostrata*; fin whale, *Balaenoptera physalus*; killer whale, *Orcinus orca*) were retrieved from NCBI  
272 searches (<https://blast.ncbi.nlm.nih.gov/Blast.cgi?PAGE=Proteins>) or by searching specific genome  
273 resources (*Balaena mysticetus*; <http://www.bowhead-whale.org/>). For the remaining cetacea species  
274 (Indo-Pacific bottlenose dolphin, *Tursiops aduncus*; North Pacific right whale, *Eubalaena japonica*;  
275 Sowerby's beaked whale, *Mesoplodon bidens*; Amazon River dolphin, *Inia geoffrensis*; Antarctic minke  
276 whale, *Balaenoptera bonaerensis*; Indus river dolphin, *Platanista minor*; harbour porpoise, *Phocoena*  
277 *phocoena*; vaquita, *Phocena sinus*; La Plata dolphin, *Potoporia blainvilliei*; humpback whale,  
278 *Megaptera novaeangliae*), and the common hippopotamus, *Hippopotamus amphibius* (included as  
279 the closest living terrestrial relative of the cetacea), which had no pre-existing predicted PAD  
280 sequences, tBLASTn searches (<https://blast.ncbi.nlm.nih.gov/Blast.cgi?PROGRAM=tblastn>) searches  
281 using reference PAD protein sequences (*Orcinus orca*) were performed against available none  
282 annotated genome assemblies found NCBI. Where possible resultant scaffold matches were then used  
283 to predict PAD sequences using the FGENESH gene finder tool in Softberry  
284 (<http://www.softberry.com>). Resultant predicted PAD protein sequences were checked using BLASTp  
285 searches to ensure accuracy for the FGENESH protein prediction. Multiple sequence alignment was  
286 performed using ClustalW in Bioedit version 7 (Hall, 1999). Evolutionary analyses were conducted in  
287 MEGAX (Kumar et al., 2018). Phylogenetic relationships of the cetacean PAD proteins were inferred  
288 using the Neighbour-Joining method under the conditions of the Poisson correction distance model,  
289 with 1000 bootstrap replicates used to assess nodal support.

290

## 291 **2.8 MicroRNA analysis in whale serum and EVs**

292 Total whale and orca sera as well as the corresponding EV isolates, were assessed for relative changes  
293 in the expression of three key miRs related to inflammation (miR21), stress-response (miR155),  
294 hypoxia and metabolic activity (miR210), respectively. RNA was extracted from whole sera (50 µl of  
295 serum per isolation) and from EV preparations of the sera from each species (each EV pellet prepared  
296 from 250 µl serum per sample as before), using Trizol (Sigma, U.K.). The purity and concentration of  
297 the isolated RNA were measured using the NanoDrop Spectrophotometer at 260 nm and 280 nm  
298 absorbance. For cDNA production, the qScript microRNA cDNA Synthesis Kit (Quantabio, U.K.) was  
299 used according to the manufacturer's instructions. The cDNA was used to assess the expression of  
300 miR21, miR155 and miR210. U6-snRNA and has-let-7a-5p were used as reference RNAs for  
301 normalization of miR expression levels. The PerfeCTa SYBR Green SuperMix (Quantabio, U.K.) was  
302 used together with MystiCq microRNA qPCR primers for the miR21 (hsa-miR-21-5p), mir155 (hsa-miR-  
303 155-5p) and miR210 (hsa-miR-210-5p). All miR primers were obtained from Sigma (U.K.).  
304 Thermocycling conditions were used as follows: denaturation at 95 °C for 2 min, followed by 40 cycles  
305 of 95 °C for 2 sec, 60 °C for 15 sec, and extension at 72 °C for 15 sec. The  $2\Delta\Delta CT$  method (Livak and  
306 Schmittingen, 2001) was used for calculating relative miR expression levels and for normalisation. Each  
307 experiment was repeated three times.

308

### 309 **2.8 Statistical Analysis**

310 GraphPad Prism version 7 (GraphPad Software, San Diego, U.S.A.) was used to prepare graphs and  
311 NTA curves were generated using the NanoSight 3.0 software (Malvern Panalytical, UK). Significant  
312 differences were considered as  $p \leq 0.05$ , following one-way ANOVA.

313

## 314 **3. Results**

315

### 316 **3.1 EV profile analysis of whale and orca sera**

317 EVs from whale and orca sera were characterised by NTA for size profiling, by morphological analysis  
318 using transmission electron microscopy (TEM) and by Western blotting using EV-specific markers (Fig  
319 1). NTA profiles of EVs revealed poly-dispersed EV populations which overall fell within a range of  
320 approximately 50 – 500 nm, albeit with some variation between the 5 cetaceans. For minke whale,  
321 main EV peaks were seen at 176 and 201 nm and a smaller peak at 524 nm (Fig. 1A); in fin whale main  
322 EV peaks were observed at 40, 108, 176, 270 and 393 nm; in humpback whale an EV profile between  
323 67-401 nm, with main peaks at 129, 145, 200 and 286 nm was observed (Fig. 1C); Cuvier's beaked  
324 whale had a more monodispersed profile with one main EV peak at 146 nm within a 50-400 nm overall  
325 EV distribution (Fig. D); orca showed main EV peaks at 51 and 123 nm, with a smaller peak at 470 nm

326 (Fig. 1E). Western blotting confirmed that the EVs were positive for the EV-specific markers CD63 and  
327 Flot-1 (Fig. 1 A-E, see Western blot inserts for each species), which have been shown to be  
328 phylogenetically conserved from fish to mammals (Iliev et al., 2018; Criscitiello et al., 2019;  
329 Magnadottir et al., 2020a,b; Criscitiello et al., 2020). EVs were further characterised by morphology  
330 using TEM, confirming typical EV morphology and a poly-dispersed population (Fig. 1A-E, see inserted  
331 TEM images for each whale species). Overall yield of serum-derived EVs varied between the 5 species  
332 (Fig 2A), with  $2.27 \times 10^9$  (+/-  $4.21 \times 10^8$ ) EVs/ml for minke whale;  $4.6 \times 10^9$  (+/-  $2.14 \times 10^8$ ) EVs/ml for  
333 fin whale;  $5.48 \times 10^8$  (+/-  $4.85 \times 10^7$ ) EVs/ml for humpback whale;  $7.52 \times 10^9$  (+/-  $9.65 \times 10^7$ ) EVs/ml for  
334 Cuvier's beaked whale; and  $8.84 \times 10^9$  (+/-  $1.29 \times 10^8$ ) EVs/ml for orca (Fig. 2A). Some variation in modal  
335 size of EVs was also observed between the species (Fig. 2B).

336

### 337 **3.2 PAD and deiminated proteins in whale and orca sera and serum-derived EVs**

338 The presence of a PAD homologue was assessed in whale and orca sera by Western blotting via cross  
339 reaction with human PAD2 and PAD3 antibodies, showing expected 70-75 kDa size bands observed  
340 for PAD2 and PAD3, although more specifically for PAD2 (Fig. 3A), which is the phylogenetically most  
341 conserved PAD form. Deiminated histone H3 was detected in cetacean sera at the expected  
342 approximate 20 kDa size (Fig. 3B). Total deiminated proteins were detected in the whale and orca sera  
343 and in serum-derived EVs using the F95 pan-deimination antibody, with deimination positive bands  
344 detected in the range of 15-150 kDa (Fig. 3C-D), both in serum-derived EVs (Fig. 3C) and in whole sera  
345 (Fig. 3D).

346

### 347 **3.3 LC-MS/MS analysis of deiminated proteins in whale and orca sera**

348 Deiminated protein candidates were further identified in the sera of the wales and orca using F95  
349 enrichment and LC-MS/MS analysis. Results for deiminated protein hits against species-specific  
350 databases for each species are listed below in Tables 1-5. It must be noted that differences in the  
351 number of peptide hits in this species-specific analysis is partly down to differences in the amount of  
352 annotated proteins available in the species-specific databases used for protein identification for the 5  
353 species under study (see section 2.5). In Northern minke whale (*Balaenoptera acutorostrata*) over 90  
354 deiminated protein candidates specific to minke whale were identified (Table 1); in fin whale  
355 (*Balaenoptera physalus*) 3 species specific proteins were identified to be deiminated (Table 2), but  
356 further hits were identified with other species (not shown); in humpback whale (*Megaptera*  
357 *novaengliae*) 2 species-specific deiminated proteins (Table 3) and further hits (not shown) with other  
358 species were identified to be deiminated; in Cuvier's beaked whale (*Ziphius cavirostris*) 2 species  
359 specific (Table 4) and also further hits with other species (not shown) were identified as deiminated

360 protein candidates; in orca (*Orcinus orca*) 2 species specific hits (Table 5) and further hits with other  
 361 species (not shown) were identified as deiminated protein candidates. Species-specific hits only, are  
 362 listed in Tables 1-5. The protein hits identified by LC-MS/MS in all five cetacean species were  
 363 furthermore assessed against a larger cetacean database (CCP\_Cetacea\_Cetacea\_20191213; 252,001  
 364 sequences; 150,129,595 residues), showing 137 cetacean hits for minke whale; 244 cetacean hits for  
 365 fin whale, 155 cetacean hits for humpback whale, 88 cetacean hits for Cuvier's beaked whale and 106  
 366 cetacean hits for orca; these are represented in Supplementary Tables 2-6.

367

368 **Table 1. Deiminated proteins identified by F95 enrichment in serum of Northern minke whale (*Balaenoptera***

369 *acutorostrata*). Deiminated proteins were isolated by immunoprecipitation using the pan-deimination F95  
 370 antibody. The F95 enriched eluate was analysed by LC-MS/MS and peak list files were submitted to mascot. Only  
 371 peptide sequence hits scoring with *B. acutorostrata* are included. Peptide sequences and m/z values are listed.  
 372 For protein hits identified against the full cetacean database see Supplementary Table 2.

Protein name	m/z	Peptide sequence	Score (p<0.05) <sup>†</sup>	Total score
AOA452CHV5_BALAS <i>Apolipoprotein B-100</i>	393.2478	R.LLLNGVR.T	34	3805
	394.2573	K.FIIPGLK.L	34	
	401.2408	K.LVEEALK.K	35	
	401.2451	K.LNVGGTIK.G	48	
	408.7322	K.VGVELSGR.A	53	
	419.7792	R.VQIPLLR.M	46	
	420.7687	K.ITQLLPR.E	53	
	423.2292	K.FLDSHVK.F	23	
	427.2443	K.ALDFFIK.S	33	
	430.2469	K.TLQELQK.L	31	
	448.7325	K.HINIDER.M	44	
	463.7402	R.AFYELQR.D	36	
	465.2867	K.LVEEALKK.S	41	
	472.2370	K.HVSEAICK.E	43	
	474.2468	R.TMFEQLTPK.L	27	
	475.2409	K.SKDFPEAR.A	34	
	477.2687	R.ASTALVYTK.N	79	
	480.7716	K.ALSDLQSVK.T	49	
	482.2586	K.LEGTSSLTR.K	61	
	486.2612	R.SISTALDHK.I	41	
	508.7799	R.TWLQEALR.N	48	
	509.3010	K.LATALLSNK.L	53	
	523.3055	K.IPSVQINFK.K	47	
	524.2568	K.LDVTNNDR.K	50	
	526.7632	R.VPQTGMTFR.H	28	
	527.7561	K.LDNIYSSDK.F	69	
	528.3140	K.LQDLQLLGR.L	79	
	530.7622	K.VQGTEFSHR.L	29	
	539.7800	R.EVTIDAQFR.D	29	
	569.7801	K.QGFFPD SVNKA	39	
	570.2720	K.EVYGFNPEGK.A	43	
	576.2888	K.LDFSSQADLR.S	91	
	386.2034	K.SNTVAGLHTEK.N	23	
	583.8014	K.NSLFFSAQPR.A	51	
	586.8195	K.VDGWNLEVKE	38	
	394.5385	K.LHVSEQNAQR.A	37	

	592.7663	K.NSEEFAAAMSK.Y	56	
	594.7802	K.ATGASYDYVNK.Y	59	
	604.3036	R.DLSGMDTILAR.I	54	
	607.7716	K.FSALDMTNNGK.L	76	
	609.8400	K.TLVEQGFTVPK.I	36	
	611.3148	R.VNQNIVYESR.F	73	
	633.3312	R.IYAIWEQNTK.N	35	
	633.8564	K.TEVIPPLVENR.Q	61	
	643.3612	K.AGQLEFIVPSPK.R	67	
	644.3610	K.NTLELSNGVLVK.V	21	
	649.8460	R.VPELDDEIQIK.A	66	
	437.2271	K.SKPTVSSSMELK.Y	46	
	439.5771	R.KGNVATEISIER.N	62	
	659.2654	R.DFSAEYEEDGR.Y	46	
	664.3650	K.SISLPSLDPVSGR.I	37	
	671.8826	R.ALSNEAVTSLLPK.L	35	
	673.8498	K.VNNQLTLDNSNTK.Y	66	
	680.8447	R.ALTASTNNEGNLR.V	77	
	465.5612	K.YHQEYTGLDLR.D	30	
	701.8931	K.IAELSTSAQEIIK.S	49	
	709.8564	K.ALYWVDGQVPDR.V	64	
	474.5720	K.FQETLEDIRDR.V	35	
	482.9245	R.LGGFLFTSGEHTSK.A	50	
	736.8526	R.DPATGQLNGESNLR.F	26	
	491.6045	K.QVLLYPEKEEPK.H	22	
	748.8682	K.AASSFPVDSLSDYPK.S	31	
	779.4096	R.ITENDLQIALDNAK.I	36	
	793.8498	R.VYQMMDMQQEVR.Y	97	
	530.2961	R.AYLHILGEELGFVK.L	52	
	535.6262	R.LFGSNTLHLVSTTK.T	46	
	810.4105	R.GLQNSAEQVYQGAVR.Q	66	
	873.9498	R.DAVDQPQEFTLVASVK.Y	26	
	591.6442	K.ADAVV DLLSYHVQGSAK.T	72	
	607.6126	R.NDCTGNEDHTYLILR.V	83	
	630.3152	K.TEHESEVLFVGNTIEGK.S	68	
	476.7531	K.FLHSIFQEIEEDLKR.L	49	
	645.3337	R.EVLLQTFLDDTSPGDKR.L	97	
	666.0055	R.FELELKPTGEVEQYSAR.A	78	
	674.3291	K.SLYQELLAQEDHSGFQR.L	66	
	685.6516	R.SGVQMNTNFFHETGLEAR.V	71	
	894.4321	K.SQVQVHSGSLQNNIQLSNDQEEAR.L	47	
A0A384B912_BALAS <i>Alpha-2-macroglobulin isoform X2</i>	383.2107	R.GEAFTLK.A	27	2013
	403.7056	K.GPTQEFK.K	28	
	408.7685	K.RTTVLVK.N	35	
	442.2842	R.DLKPAIVK.V	41	
	443.7246	K.YGAATFTR.T	57	
	445.7268	K.SLDEEAVK.E	40	
	447.2201	R.VTINMCR.K	33	
	452.2178	K.DMYSFLK.D	32	
	460.7271	K.DLSGFPER.L	33	
	467.7532	K.GPTQEFKK.R	39	
	484.2370	K.RQEFEEMK.I	37	
	507.7535	R.YLNTGYQR.Q	47	
	509.8003	K.ATVLNYLPK.C	43	
	510.7849	R.GIPFFGQVR.L	29	
	516.2911	K.TQQLTAEIK.S	43	
	530.7842	R.IMQWQNLK.V	39	

	552.7985	<i>R.SSGSLLNNAIK.G + Deamidated (NQ)</i>	74	
	558.8060	<i>R.QTVSWAVTPK.S</i>	80	
	387.2121	<i>K.AHTSFQISLR.V</i>	43	
	581.2902	<i>K.ICPQPQQYK.I</i>	21	
	587.7799	<i>K.MLETSDHVS.R.T</i>	72	
	398.8926	<i>K.SFVHLEPLPR.E</i>	44	
	605.8249	<i>K.LPPNVVEESAR.A</i>	63	
	620.7793	<i>K.YEVENCLANK.V + Deamidated (NQ)</i>	67	
	629.8445	<i>R.LLSSPVVAEMGR.G</i>	96	
	429.2349	<i>K.VFTNSNIHKPK.I + Deamidated (NQ)</i>	46	
	651.8457	<i>K.VTASPQSLCALR.A</i>	73	
	669.8295	<i>R.NALFCLESAWK.S</i>	51	
	472.9477	<i>K.MVSGFIPLKPTVK.M</i>	50	
	716.8622	<i>K.IQEEGTEVELTGK.G</i>	90	
	726.7958	<i>K.EQETQCICGNR.Q + Deamidated (NQ)</i>	72	
	497.6242	<i>M.VLVPSLLHTGTPEK.G</i>	58	
	507.9207	<i>R.SGTHVLPVHQGDMK.G + Oxidation (M)</i>	31	
	763.3966	<i>K.AAQVTIQSSGTFSTK.F</i>	88	
	548.9582	<i>R.TEVSNHHVLIYLDK.V</i>	60	
	555.6386	<i>R.VHLEASPAFLAVPGEK.E</i>	56	
	861.4429	<i>R.APSNEEVMFQTIQVK.G + Oxidation (M)</i>	53	
	594.0087	<i>K.DTVIKPLLVEPEGLEK.E</i>	53	
	914.9600	<i>K.QLTFPLSSEPFQGSYK.V</i>	48	
	943.4475	<i>K.FSQQLNSQGCFSQQVK.T</i>	54	
	631.0072	<i>K.GHFPLSVPVESDIAPVAR.L</i>	64	
	477.7818	<i>R.KDTVIKPLLVEPEGLEK.E</i>	36	
	969.9594	<i>K.EATFNSLLCPGAEVSEK.L</i>	58	
	494.2693	<i>K.VGLNFSPAQSLPASHAHLK.V</i>	51	
	681.6161	<i>K.YSNPSNCFGGESHAVCEK.F</i>	71	
	683.0209	<i>K.AGALCLSSDTGLGLSPTASLR.A</i>	96	
	713.7236	<i>R.AQTVQAHYVLNGQVLQELK.E</i>	63	
	724.6433	<i>R.KYSNPSNCFGGESHAVCEK.F + Deamidated (NQ)</i>	75	
	549.7866	<i>R.GHELMHIIHISEPPTETVR.K</i>	72	
	801.7352	<i>R.QQNSQGGFSSTQDTVVALHALSK.Y</i>	67	
	812.0687	<i>K.KEEFPALEVQTLQTCDFGPK.A</i>	60	
	622.3431	<i>K.NEESLVIVQTDKPIYKPGQTVK.F</i>	63	
	845.3623	<i>K.VYDYYETDEFAVAЕYNAPCSK.D</i>	49	
	649.3291	<i>K.SLDEEAVKEDNSVHWTRPQPK.A + Deamidated (NQ)</i>	31	
	775.3732	<i>R.VHLEASPAFLAVPGEKEQETQCICGNR.Q + Deamidated (NQ)</i>	89	
	793.8655	<i>R.HYDGSYSTFGEQHGNNNEGNTWLAFVLK.S</i>	85	
	824.3633	<i>K.EDNEDCISHHNIYLNGIMYSPVSNTNEK.D + Deamidated (NQ)</i>	46	
	863.6284	<i>K.DHSPCYGYQWLSEEEAYHTANLVFSR.S</i>	28	
A0A383Z2B4_BALAS <i>Complement C3</i>	385.7113	<i>K.ENIPAAR.Q</i>	38	<b>2339</b>
	388.7367	<i>K.GVFVLNK.K</i>	39	
	400.7474	<i>R.VGLVAVDK.G</i>	52	
	402.2076	<i>K.VVPEGMR.V + Oxidation (M)</i>	34	
	417.2477	<i>R.LPYSVVR.N</i>	27	
	430.7455	<i>K.LLSTGVDR.Y</i>	41	
	437.7315	<i>R.DGTLELAR.S</i>	40	
	444.2327	<i>R.NEQVEIR.A</i>	47	
	451.7527	<i>K.IWDIVEK.A</i>	36	
	472.2767	<i>R.QEALELIK.K</i>	51	
	473.2628	<i>R.QPMTITVR.T</i>	54	
	476.2483	<i>K.FLNTATER.N</i>	37	
	479.7636	<i>K.LENDLLNK.F</i>	48	

	499.2950	<i>R.ISLAHSLTR.V</i>	63	
	539.2842	<i>R.DSCVGTLLVK.N</i>	42	
	546.8188	<i>K.NTLIYLDK.V</i>	56	
	550.2806	<i>K.GYTQQPLAYR.Q</i>	44	
	550.3271	<i>K.RQEALELIK.K</i>	39	
	551.2747	<i>R.VPITDGNGEAK.L + Deamidated (NQ)</i>	56	
	569.2968	<i>R.TLDPEHLGQK.G</i>	27	
	572.8036	<i>K.DFDTVPPVVR.W</i>	42	
	583.2883	<i>K.GSMILDICTR.Y</i>	62	
	587.3353	<i>R.IVWESASLLR.S</i>	67	
	587.8500	<i>R.HQQTLIIPPK.S</i>	32	
	597.7969	<i>R.YTYLVMNK.G</i>	37	
	605.3170	<i>R.QPNSAYAAFLK.R</i>	36	
	409.8866	<i>K.KGYTQQPLAYR.Q</i>	21	
	650.7977	<i>R.ACEPGVDYVYK.I</i>	30	
	673.3193	<i>K.FYYIDDPDGLK.V</i>	61	
	675.3480	<i>R.AQFILQGDACVK.A</i>	32	
	676.8200	<i>K.ENEDFTLTAQGK.G</i>	54	
	681.3184	<i>K.SGSDEVQVQQER.R</i>	88	
	685.8696	<i>K.TIYTPGSTVLYR.I</i>	57	
	687.3571	<i>R.EVVADSVWVDVDR.D</i>	69	
	699.4239	<i>K.SSVPVPYVIVPLK.V</i>	33	
	473.9027	<i>K.VSHTLEDCLAFK.V</i>	42	
	526.5914	<i>K.AGDFLEDHYLELR.R</i>	58	
	829.8872	<i>K.AFLDCCEYIAQLR.L</i>	69	
	833.4464	<i>K.FVTVQADFGNVLVEK.V</i>	35	
	833.4814	<i>R.VLNGVQPSQAAALVGK.S + Deamidated (NQ)</i>	22	
	852.9000	<i>K.AANLSDQVPDTESETK.I</i>	39	
	590.6614	<i>K.VHQYFNVGLIQPGAVK.V</i>	26	
	898.9664	<i>R.VELLYNPAFCSLATAK.K</i>	60	
	601.3332	<i>R.TGIPIVTSPYQIHFTK.T</i>	53	
	467.2613	<i>R.VELKPGETLNVNFHLR.T</i>	68	
	642.9693	<i>R.SEETKENEDFTLTAQGK.G</i>	36	
	704.3283	<i>K.AHYEDSPQQVFSAEFEVK.E</i>	51	
	715.0278	<i>K.ILLQGTPVAQMTEAINGDR.L + Deamidated (NQ)</i>	89	
	1222.0769	<i>K.ADIGCTPGSGSDYAGVFTDAGLALK.T</i>	26	
	892.7664	<i>R.TMQALPYNTQDNSNNYLHLSVPR.V</i>	81	
A0A383ZXR0_BALAS <i>Serum albumin</i>	395.2394	<i>K.IVTDLTK.V</i>	46	2314
	423.7320	<i>K.VTEEQLK.T</i>	22	
	433.7164	<i>K.ADFAEVSK.I</i>	49	
	445.2480	<i>K.LCAVASLR.E</i>	26	
	449.7443	<i>R.LCVLHEK.T</i>	28	
	457.2168	<i>K.DDNPDLPK.L</i>	34	
	457.2427	<i>K.YLYEIGR.R</i>	34	
	481.2510	<i>R.EQVLASSAR.Q + Deamidated (NQ)</i>	50	
	506.8237	<i>K.QIALVELVK.H</i>	50	
	509.2718	<i>K.SLHTLFGDK.L</i>	43	
	534.2449	<i>K.QNCELFEK.L</i>	61	
	536.2664	<i>K.SHCIAEVQK.D</i>	38	
	558.3192	<i>K.LVNEVTELAK.A</i>	57	
	569.7526	<i>K.CCTESLVNR.R</i>	58	
	570.8713	<i>K.KQJALVELVK.H</i>	72	
	576.2747	<i>K.ETCFALEGPK.L</i>	69	
	393.5316	<i>K.HKDDNPDLPK.L</i>	36	
	606.7807	<i>R.FNDLGEENFK.G</i>	77	
	646.3051	<i>K.ECCDKPLLEK.S</i>	25	
	657.3641	<i>R.HPEYSVSLLR.I</i>	69	

	658.3209	<i>K.TVMGNFAAFVDK.C + Oxidation (M)</i>	79	
	678.2900	<i>K.GVFAECCQAADK.G</i>	56	
	699.3409	<i>K.YICENQATISAK.L</i>	66	
	705.7853	<i>K.ACVADESAANCDK.S</i>	84	
	717.7708	<i>R.ETYGEMADCCAK.Q</i>	74	
	490.6128	<i>R.RHPEYSVSLLR.I</i>	63	
	753.9302	<i>K.LQPLVDEPQNLIK.Q</i>	38	
	756.4252	<i>K.VPQVSTPTLVEVSR.N</i>	83	
	756.8379	<i>K.DDPPACYATVFEK.L</i>	54	
	511.5983	<i>K.LKECCDKPLLEK.S</i>	62	
	768.4313	<i>K.LGEYLFQNALIVR.Y</i>	24	
	517.2570	<i>K.LKPDPTLCSEFK.E</i>	55	
	547.3178	<i>K.KVPQVSTPTLVEVSR.N</i>	78	
	583.8923	<i>K.ECCHGDLLECADDR.A</i>	27	
	638.3090	<i>R.RPCFSALTVDETYEPK.A</i>	50	
	641.6367	<i>K.TFTFHADLCTLPENEK.Q</i>	43	
	980.4632	<i>K.DELPENLSPVAADFAEDK.E</i>	59	
	678.0515	<i>R.YTKKVPQVSTPTLVEVSR.N</i>	73	
	545.2658	<i>K.LKPDPTLCSEFKENEQK.F</i>	42	
	735.0268	<i>R.HPYFYAPELYYYAHQYK.G</i>	35	
	562.7404	<i>K.ECCHGDLLECADDRADLAK.Y</i>	36	
	826.0563	<i>K.DELPENLSPVAADFAEDKEVCK.N</i>	55	
	753.8626	<i>K.SHCIAEVQKDEL PENLSPVAADFAEDKEVCK.E</i>	61	
	706.5385	<i>K.SHCIAEVQKDEL PENLSPVAADFAEDKEVCK.N</i>	76	
A0A384ALG4_BALAS <i>Ceruloplasmin isoform X2</i>	394.7163	<i>K.GSLLANGR.L + Deamidated (NQ)</i>	51	1968
	401.7099	<i>K.DPVCLAK.M</i>	20	
	458.7643	<i>R.KGSLLANGR.L + Deamidated (NQ)</i>	73	
	507.2159	<i>K.TYCSEPEK.V</i>	22	
	549.7883	<i>R.SYSIHAHGVK.T</i>	46	
	583.7699	<i>K.ANDEFIESNK.M</i>	76	
	587.7759	<i>K.MYYSAVDPTK.D</i>	45	
	595.2596	<i>R.EYTDGSFTNR.K</i>	49	
	403.5436	<i>R.IYHSHIDAPR.D</i>	43	
	629.8504	<i>K.HYLQVFNPBK.K</i>	48	
	637.3489	<i>R.SAPPPSASHVVPK.G</i>	28	
	664.8300	<i>K.GTFTYEWTVPK.E</i>	37	
	681.8541	<i>R.DTANLFPQTSLR.L</i>	59	
	456.2263	<i>K.AETGDTVYVHFK.N</i>	52	
	701.3909	<i>K.GTYPLSIEPIGVR.V</i>	75	
	746.3721	<i>K.ALYLQYTDETFK.T</i>	61	
	503.2819	<i>R.DIATGLIGPLIHCK.K</i>	60	
	756.3602	<i>R.QFTDSTFQVPGER.K</i>	57	
	506.9391	<i>R.RDTANLFPQTSLR.L</i>	43	
	785.8897	<i>K.TENPTVTPTAPGETR.T</i>	79	
	526.2732	<i>K.EVGPTYKDPVCLAK.M</i>	63	
	532.5693	<i>K.VDKDNEDFQESNR.M</i>	38	
	724.0344	<i>K.LISVDTEHSNIYLQNGPNR.I</i>	93	
	556.7984	<i>R.KPEEEHLGILGPQLHAGVGDK.V</i>	77	
	575.3015	<i>K.KLISVDTEHSNIYLQNGPNR.I</i>	37	
	777.3522	<i>R.SGAGIDDSPCIPWAYYSTVDR.V</i>	59	
	596.0428	<i>K.VRPGEQCMYILHANPEQGPGK.E</i>	69	
	796.7537	<i>R.GPEEEHLGILGPVISAEVGDTIR.V</i>	70	
	800.0380	<i>K.HYYIGIIETTWWDYASDHGEK.K</i>	52	
	825.0328	<i>R.MFTTAPDQVDKENEDFQESNK.M</i>	50	
	648.2806	<i>K.TYCSEPEKVDKDNE DFQESNR.M</i>	94	
	866.0801	<i>K.AGLQAFFWVQDCQKPSSENDIR.G</i>	53	
	669.1016	<i>K.ERGPEEEHLGILGPVISAEVGDTIR.V</i>	69	

	744.3796 998.7731 669.3148	K.ELHHLQELNLSNAFLDKEEFYIGSK.Y R.LFMQPDTETGTFDVECLTTDHYTGGMK.Q + Deamidated (NQ) K.VRPGEQCMYILHANPEQGPGKEDSNCVTR.I	50 37 36	
AOA383Z5R5_BALAS <i>Serotransferrin</i>	397.7057 426.7085 455.7112 461.7534 468.2747 475.2332 500.2445 503.7895 531.7373 542.2485 564.2920 575.8166 597.7642 426.9117 431.1960 656.2932 678.3365 696.8361 701.8334 705.8417 723.3185 765.8958 550.2707 878.3733 602.2895 956.9316 662.6082 665.6106 1028.0111 758.3589 589.5130 601.0450 665.8179	K.GTDFNLK.D K.DSANGFLK.I + Deamidated (NQ) R.GSVDEFEK.C K.KGTDFNLK.D R.VPSHAVVAR.S K.LCQLCAGK.G K.TSYIDCIK.A K.YVTAVANLR.Q K.INHCEFDK.F R.YYGYSGAFR.C K.KTSYIDCIK.A K.THYYAVAVVK.K R.ECLPNNYER.Y K.THYYAVAVVKK.G R.WCTVSSHEASK.C K.FFSEGCAPGSPPR.N K.VFDTGPVFVSCVK.K R.EILDAQQDEFGK.H K.SSDPDLNWNNLK.D K.CLMDGVGDVAFVK.H K.ENTGGNNPEEWAK.T K.FTPESGYYAVAVVK.K K.GISEDFQLFSSPHGK.D K.IECESAESTEECIAK.I K.GEADAMSLDDGGHIYIAGK.C K.TLQEDDFELLCTDGTR.K K.HGSDCCSSFCFHSETK.D K.CACSNHEPYFGYSGAFK.C K.CLAPLQNATYESYLGNK.Y K.SVEEASDCFLAQGPNAVSR.E K.INHCEFDFKFFSEGCAPGSPPR.N R.KSVEEASDCFLAQGPNAVSR.E K.HTTVLENLPDEADKDEYELLCR.D	23 27 36 49 59 45 26 62 24 48 38 50 47 48 39 81 69 58 41 79 94 42 44 48 40 82 76 47 30 81 51 47 77	1707
AOA384B6G0_BALAS <i>Kininogen-1</i>	390.7158 423.2580 436.7635 478.7635 489.2745 493.2605 500.8110 530.7878 542.2828 542.8111 567.7400 603.3133 668.2909 692.3344 698.3058 723.8487 918.4359 967.5248 688.0506 869.3638	R.IASFSQLK.C K.AVDTALKK.Y K.ATVQVVAGK.K K.YSIVFTAR.E K.AYVDIQLR.I K.HSLILNCK.A + Deamidated (NQ) K.KATVQVVAGK.K K.RPPGFSPFR.S K.SGNQFVLYR.V K.KYSIVFTAR.E K.EGDCPVQSDK.T K.ADVYVVPWEK.K R.TDDPDTFSFK.Y K.ENFLFLTPDCK.S K.SLSNGNIGECTDK.A + Deamidated (NQ) K.LNVENNGTFYFK.I + Deamidated (NQ) K.CDLYPVEDFVQPPTR.I K.IYPTVNCQSLGQISLLK.R K.KIYPTVNCQSLGQISLLK.R K.TWQDCDYGDSAQAATGECTATVAK.R	30 40 58 55 43 59 86 35 78 44 50 35 47 72 82 30 36 64 59 64	1145

	725.8627 1190.0765	R.ICAGCPRPIPVDSPELEELDHSIAK.L K.FSVATQTCQITPAEGPVVTAQYDCLGCLHPISTESPDL R.H	38 39	
AOA383ZCJ5_BALAS <i>Hemopexin</i>	416.7208 472.7288 495.7317 498.7498 503.7473 524.2593 551.3079 579.7387 669.3749 674.3301 727.3198 759.3982 547.2525 558.6348 932.4734 999.4752 814.8939 890.0217	R.GPVDAAFR.H R.FWDFTTK.T K.LDPDVMER.C K.VNSLLGCPH.- K.VDAALCTEK.S K.VWEYPPEK.E R.QLWWLDLK.L R.DYFMPCPGR.G + Oxidation (M) K.LNVTEALPQPQK.V K.GDKVWEYPPEK.E R.SWQAVGNCSSAMR.W R.CSPDLVLSALLSDK.H K.HGATYAFSGSHYWR.L K.RCSPDLVLSALLSDK.H K.LGAQATWTELPWPHEK.V R.FNPVTGDMYPNYPLDVR.D K.EFGSPHGINLDTVDAACTCPGSSLLHVMAGR.Q K.LLQEEFPGIPSPVDAAVECHHEECLHEGVLFQGNHMR.F + Deamidated (NQ); Oxidation (M)	58 46 55 73 52 40 28 43 66 31 97 82 68 58 79 95 74 52	1094
AOA383ZWG8_BALAS <i>Keratin, type II cytoskeletal 5</i>	405.7086 414.2185 442.7271 453.7370 469.7508 473.2596 508.2349 513.7318 533.7618 541.8033 547.2675 567.2844 571.2634 576.7801 597.7913 619.7900 621.7853 640.3489 649.8187 436.8897 453.5542 476.2464 565.9468	R.QSSVSFR.S R.FASFIDK.V R.TSFTSVSR.S R.FLEQQNK.V R.SLYNLGGSK.R R.GRLDSEL.R.N K.HEISEMNR.M K.DVDAAYMNK.V K.YEDEINKR.T R.FASFIDKVR.F K.AQYEEIANR.S R.KLLEGEECR.L K.DYQELMNTK.L K.NKYEDEINK.R K.YEELQQTAGR.H R.NMQDLVEDFK.N R.TEAESWYQTK.Y K.LSLDVEIATYR.K R.TTAENEFVMLK.K + Oxidation (M) K.NKYEDEINKR.T R.NTKHEISEMNR.M R.TTAENEFVMLKK.D + Oxidation (M) K.DVDAAYMNKVELEAK.V	21 39 57 25 52 36 39 41 41 64 50 64 58 41 67 55 41 53 42 55 52 54 48	1092
AOA384ALK4_BALAS <i>Fibronectin</i>	386.2217 397.2442 555.7750 569.2718 585.2289 611.2642 646.3669 441.9092 694.3301 477.9213 716.3938	K.SEPLIGR.K R.ITGYVIK.Y R.STTPDITGYR.I R.FTNVGPDTMR.V R.YQCYCYGR.G R.TFYSCCTTEGR.Q R.GATYNIIIVEAIK.D K.LGVRPSQGGEAPR.E R.TFYQIGESWEK.F R.WSRPQAPITGYR.I R.VPGTSASATLGLTR.G	32 23 49 40 22 71 49 78 54 22 96	1016

	772.3859 515.2748 797.4046 542.5823 622.6376 691.9559 727.7036 604.5263 830.7435 863.1167	R.SYTITGLQPGBTDYK.I K.EATIPGHLNSYTIK.G K.QYNVGPSATQYPLR.N K.LSCQCLGFGSGHFR.C R.HTTLQTTSAGSGSFTDVR.T R.GFNCESKPEPEETCFDK.Y K.NLHLETNPDTGVLTWSWER.S R.RPAGAEPGHEGSTGHSYNQYSQR.Y R.TEIDKPSQMQLVTDVQDNSISVR.W R.TKTETITGFQVDAIPANGQTPIQR.T + Deamidated (NQ)	32 31 60 71 78 39 55 47 47 23	
A0A383YWT8_BALAS <i>Complement factor H-like isoform X1</i>	433.2243 434.2106 457.7689 486.2400 508.2472 511.2604 547.7775 554.2986 603.2486 624.2720 663.2846 722.9049 741.8846 499.9125 556.2786 610.3134 955.9242 688.0054 758.3656 976.7631	K.SGEQVAFK.C K.FSCIQGR.I K.VENAIIQKE K.HTICINGR.W + Deamidated (NQ) R.DVSCVNPPK.V R.EAFTMIGPR.S K.EYLQGETVR.V R.TLGSIVMVCK.D K.CTSGFEYGER.G K.LSYTCEDGFR.I K.SCDMPVFENAR.A K.QPTILNGYPLSLK.E + Deamidated (NQ) K.SCAPPQLLSGEVK.E R.CSFKPCDFPVIK.H K.LSCSQPPQVDHGTIK.S K.WTQPPQCIATEELKK.C R.GDAVCTEFGWTPVPSCK.E K.EEAQIQSCPPPPQIPNTR.D R.LGQQQFTYHCDQYFVTPLR.T K.DSYQHGEEVIYNCDEFGFIDGPASIR.C	65 40 38 66 30 41 58 21 83 64 49 25 48 27 53 33 21 33 64 74	929
A0A383Z8T4_BALAS <i>C4b-binding protein alpha chain isoform X7</i>	418.2499 489.3052 556.2587 561.7481 585.7771 587.2454 603.2824 426.8777 434.2032 668.2800 474.9221 736.8660 743.8723 779.8806 866.9597 938.9174 744.6987 580.0076	R.LALEVYK.L K.LISSFLGLK.S K.QSIVFDCK.G R.CTADGTWSPK.T K.CEPPPAISNGK.H + Deamidated (NQ) K.SGIDNSCTYR.Y + Deamidated (NQ) K.ADGPPTVTCQR.N R.YYCLSGYKPK.A R.KSGIDNSCTYR.Y R.YGDEVSYTCNK.K K.ALCLKPEIEHGR.L K.LMQCLPTPEEVRL K.TISVWNPSPPPTCK.K R.CGNPGELLNGQVTAK.T + Deamidated (NQ) K.LYVEIQQLELQNDK.A K.SGDAIYECDEGYTLVGK.N K.YGYQKPTEEEVYDIGTALR.Y K.TPECYPDCSDSPPVIAHGHHK.L	35 61 64 27 38 71 65 23 41 42 61 57 33 57 65 40 46 39	864
PODMA6 APOA1_BALAS <i>Apolipoprotein A-I</i>	413.2325 430.2295 450.2508 492.2794 506.7929 530.2787 540.7534 558.3066	R.AHVETLR.Q K.VQELQDK.L R.EQLGPVTR.E K.VAPLGEELR.E K.AKPALEDLR.Q K.LTPLAEEEMR.D R.EFWDNLEK.E R.QKVQELQDK.L	26 35 56 63 59 66 40 47	856

	385.5595 608.8429 612.3716 416.2120 632.8199 633.8221 464.9137 714.8544 490.2732 599.2880	K.VREQLGPVTR.E K.VSILAAIDEASK.K R.QGLLPVLENLK.V K.EGGGSLVQYHAK.A + Deamidated (NQ) K.WQEELQIYR.Q K.VQPYLDEFQK.K K.KWQEELQIYR.Q R.DYVTQFEASALGK.Q R.VKDFATVYVDAIK.D R.EFWDNLEKETESLR.Q	39 74 54 25 48 26 40 79 48 31	
A0A384BF87_BALAS <i>Haptoglobin</i>	393.2293 419.2086 429.7501 437.2558 460.7349 490.7511 492.7956 573.7747 587.8271 425.5507 667.3484 674.3165 843.9261 604.3366 648.6652 718.7053	K.DIAPTLR.L K.DYVEVGR.V K.QLVEIEK.V R.IIGGSLDAK.G K.GSFPWQAK.M R.VGYVSGWGR.N K.AKDIAPTLR.L K.HYEGSTVPEK.K K.VSSILDWVQK.T K.HYEGSTVPEKK.T R.NANFIFTEHLK.Y K.SCATAEYGVVK.V K.VPTDETVMPICLPSK.D K.VLLHPDYSEVDIGLIK.L R.EKVPTDETVMPICLPSK.D K.SPGVGQPILNNEHTFCAGLSK.Y	36 27 39 68 27 68 42 33 57 40 42 53 29 58 34 69	722
A0A383ZI56_BALAS <i>Inter-alpha-trypsin inhibitor heavy chain H4 isoform X2</i>	420.7505 430.2478 474.2815 500.2831 571.3327 633.3223 668.3364 452.5808 695.8338 563.9771 973.4864	K.ILGDLGPR.D K.GSELVVAGK.L K.NVIFVIDK.S K.LALDNGGLAR.R K.AGLLLLSSPDR.V R.ITGGSSADPVFSK.R K.AAAQEQYSAAVAR.G K.LRDQNPDVLSAK.V R.VAEQEEAFQSPR.Y R.KTEQFQVSVSVAAPAAK.V K.SPEQQQDTVLGNFIVR.Y	46 34 26 46 63 88 26 48 87 72 48	584
A0A383ZCZ3_BALAS <i>Hemoglobin subunit beta</i>	463.7501 473.7715 518.7888 563.7844 575.3408 637.8652 640.4269 664.8438 712.8574 739.8492 882.9093	M.VHLTAEEK.S K.SAVTALWAK.V K.VLASFSDGLK.H K.LHVDPENFR.L K.VVAGVANALAHK.Y R.LLVVYPWTQRF R.LLGNVLVIVLAR.H K.VNVEEVGGEALGR.L K.EFTPELQAAYQK.V K.GTFATLSELHCDK.L R.FFEAFGDLSTADAVMK.N	31 58 32 20 73 55 76 88 67 87 118	705
A0A383ZRJ1_BALAS <i>Keratin, type I cytoskeletal 14</i>	404.2033 405.2238 515.3005 532.8088 553.7667 572.7508 575.2972 629.7778	R.LAADDFR.T R.LASYLDK.V R.VLDELTALAR.A R.LASYLDKVR.A K.VTMQNLNDR.L + Oxidation (M) K.DAEDWFFSK.T R.DVTSSSRQIR.T + Deamidated (R) K.NHEEEMNALR.G + Oxidation (M)	55 46 54 53 92 37 28 42	512

	701.3325 538.7844	<i>R.GQVGGDVNVEMDAAPGVDSL.R.I + Oxidation (M)</i> <i>K.VTMQNLNDRASYLDKVR.A + Oxidation (M)</i>	81 26	
AOA383ZST7_BALAS <i>Complement C5 isoform X1</i>	432.7446 447.7866 456.2365 474.2325 549.3197 555.7875 591.2880 668.8057 674.3805 676.3415 513.5767 814.4074	<i>R.VFQTLEK.N</i> <i>R.LPLDLVPK.T</i> <i>R.IVACASYK.L</i> <i>K.WLSEEQR.Y</i> <i>K.LQGTLPIEAR.E</i> <i>R.VTFDSETAIK.E</i> <i>R.ESYAGTTLDPK.G</i> <i>K.TTCVNADLEEGK.Q</i> <i>K.IIAITEENAFVK.Y</i> <i>R.VDQQLTDYEIK.D</i> <i>K.TSTSEEICSFHLK.I</i> <i>R.GEQIQLSGTVNYR.T</i>	40 34 38 41 65 38 31 62 55 47 22 23	<b>493</b>
AOA384BAA9_BALAS <i>Apolipoprotein A-IV</i>	429.7251 493.2884 544.2851 558.2883 638.8320 437.9069 692.8688 613.9874 653.9971	<i>K.GNAAELQ.R.S</i> <i>K.LAPLTESVR.G</i> <i>K.IDQNVEELK.A</i> <i>K.IDQNVEELR.R</i> <i>R.SLAPYAQDVQGK.L</i> <i>K.LVPFATELHER.L</i> <i>R.TQVNAQAQQQLQR.Q</i> <i>K.LGPLAGDVEDHLSFLEK.D</i> <i>R.SLAKLSSHLDQQVETFR.H + Deamidated (NQ)</i>	33 40 42 82 40 55 74 58 68	<b>491</b>
AOA383Z9Z9_BALAS <i>Alpha-mannosidase</i>	542.8118 558.8038 568.2965 597.8640 623.8615 482.2321 910.9919 620.6356	<i>R.WGPETLLL.R</i> <i>R.ETTLAANQLR.A</i> <i>K.LATAQGQQYR.T</i> <i>K.EVLAPQVVLAR.G</i> <i>R.VLVIQNEYIR.A</i> <i>R.LEHQFAVGEDSGR.N</i> <i>R.IYITDGNVQLTVLTD.R.S</i> <i>R.SQGGSSLSDGSLELMVHR.R</i>	46 33 79 53 68 29 81 67	<b>456</b>
AOA383ZV20_BALAS <i>Alpha-1-antitrypsin</i>	440.7245 444.7557 504.7717 548.7980 440.5420 533.2636 553.9299 461.9787 938.9814	<i>K.INDYVEK.G</i> <i>K.AVLTIDEK.G</i> <i>K.KINDYVEK.G</i> <i>K.LSISGTYDLK.T</i> <i>R.DFHVDEETTVK.V</i> <i>K.NLYHSEAFSINFR.D</i> <i>K.WEKPFEAEHTTER.D</i> <i>K.VFSNGADLSGITEEVPLK.L</i> <i>K.VFSNGADLSGITEEVPLK.L + Deamidated (NQ)</i>	33 45 48 69 51 63 42 58 23	<b>431</b>
AOA383ZW6_BALAS <i>Keratin, type II cytoskeletal 6A-like isoform X2</i>	414.2185 453.7370 541.8033 567.2844 570.2737 590.3036 602.3222 640.3489	<i>R.FASFIDK.V</i> <i>R.FLEQQNK.V</i> <i>R.FASFIDKVR.F</i> <i>R.KLEGEECR.L</i> <i>K.DYQELMNVK.L</i> <i>K.YEELQLTAGR.H</i> <i>K.WTLLQEQQGT.K.T</i> <i>K.LSLDVEIATYR.K</i>	39 25 64 64 41 56 47 53	<b>388</b>
AOA383ZRG8_BALAS <i>Keratin, type I cytoskeletal 15</i>	404.2033 561.7931 601.8044 651.3330 453.5722 460.5807	<i>R.LAADDFR.L</i> <i>R.LEQEIATYR.S</i> <i>R.QSVEADINGLR.R + Deamidated (NQ)</i> <i>R.ALEEANADLEV.K.I</i> <i>R.QSVEADINGLRR.V + Deamidated (NQ)</i> <i>K.TRLEQEIATYR.S</i>	55 68 81 78 47 43	<b>369</b>

A0A384A3E4_BALAS <i>Hemoglobin subunit alpha isoform X1</i>	380.2158 395.7083 559.7540 626.8616 539.5939 466.2274 593.7971	M.VLSPTDK.S R.VDPANFK.L R.MFMNFPSTK.T + Oxidation (M) K.FLASVSTVLTSK.Y K.IGNHSAEYGAEALER.M K.TYFPHFDLGHDSAQVK.G K.AVGHMDNLLDALSDLHAKH.L	47 23 43 86 59 31 57	365
A0A384AZC9_BALAS <i>Clusterin</i>	454.2658 455.2451 485.7313 523.7895 616.8101 719.8353 666.6522	K.YINKEIK.N R.GSLFFNPK.S K.FMETVAEK.A K.SLLGSLEEAK.K K.TLIEQTNEER.K R.ASNIMDELFQDR.F R.KFQDTQYYSPFSSFPR.G	21 46 42 46 71 80 32	338
A0A452CBF7_BALAS <i>Desmoplakin isoform X1</i>	416.7299 431.7552 454.2658 459.7684 471.7719 565.3095 587.8157 610.7909	K.VTQLTDR.W R.GLVGIEFK.E R.YIELLTR.S R.LPVDIAYK.R R.QVQNLVNK.S K.IEVLEELR.L R.LLQLQEQQMR.A + Oxidation (M) R.ETQSQLETER.S	47 33 45 36 38 57 42 40	334
A0A384B1Q0_BALAS <i>Vitamin D-binding protein</i>	407.2576 469.7449 489.7603 588.7716 433.5865 678.8436 614.9946 903.0740	K.ILEPTLK.S R.DLSSFIEK.G K.ELPEYTVK.I R.ICSQYSAYGK.E R.KTHIPEVFSLK.I K.VLDQYTDFLSR.K R.GKLPDATETEELVAK.R K.HQPQEFPYVEPTNDEICEAFR.K	41 35 24 70 24 64 36 35	328
A0A384A7N6_BALAS <i>Dipeptidyl peptidase 4</i>	428.7480 552.2830 604.7866 755.8278 607.6143 858.4322	K.AGAVNPTVK.F R.VLEDNSALDK.M K.MLQDVQMPSK.K + 2 Oxidation (M) K.WEYYDSVYTER.Y R.YMGLPTPEDNLDHYR.N R.AENFKQVEYLLIHGTAADDNVHFQQSAQISK.A	52 79 41 59 34 59	323
A0A383ZRE5_BALAS <i>Keratin, type I cytoskeletal 17 isoform X1</i>	405.2238 515.3005 531.7534 561.7931 629.7778 460.5807	R.LASYLDK.V R.VLDELTLAR.A K.ATMQNLNDR.L R.LEQEIATYR.R K.NHEEMNALR.G + Oxidation (M) K.TRLEQEIATYR.R	46 54 54 68 43 42	306
A0A383ZRY6_BALAS <i>Junction plakoglobin</i>	406.7840 412.8674 618.8478 684.8066 714.4056	R.LVQLLVK.A R.ISEDKNPDYR.K R.VSVELTNSLFK.H R.TMQNTSDLTAR.C + Oxidation (M) R.ALMGSPQLVAAVVR.T + Oxidation (M)	26 55 36 96 36	275
A0A452CBL8_BALAS <i>Tubulin beta-2A chain isoform X2</i>	527.3082 546.2818 653.6653 776.3582	R.YLTVAIFR.G R.LHFFMPGFAPLTSR.G + Oxidation (M) K.GHYTEGAELVDSVLDVVR.K K.FWEVISDEHGIDPTGSYHGDSLQLER.I	66 76 94 35	272
A0A384AFQ0_BALAS <i>Plasminogen</i>	406.7473 425.2395 510.7323 549.2380 561.7552	R.LPVIENK.V R.DVVLFEK.R R.TPENFPCR.N R.NLEENYCR.N R.WEFCDIPR.C	28 21 26 31 30	262

	432.5549 491.5804 784.0802	K.HNIFTPEANPR.A R.GTVAVTVSGHTCQR.W K.VVLAGHQAETAVEDSVQEIQVAK.L	29 46 51	
A0A383ZM34_BALAS <i>Dimethylglycine dehydrogenase, mitochondrial isoform X1</i>	566.3240 614.7959 575.2853 779.4244	R.VGVIDLSPFGK.F K.WTTTQYTEAK.A R.ISYTGEGLWELYHR.R K.KADIINIVNGPITYSPDILPMVGPHQGVR.N	106 67 57 27	257
A0A383ZRY3_BALAS <i>Keratin, type I cytoskeletal 19</i>	404.2033 521.3062 553.7667 561.7931	R.LAADDFR.T R.IVLQIDNAR.L K.VTMQNLNDR.L + Oxidation (M) R.LEQEIATYR.N	55 37 92 68	252
A0A383YQI3_BALAS <i>Xaa-Pro dipeptidase</i>	467.7716 484.2400 557.3424 489.2755 493.9339	K.AIYEAVL.R.S R.EASFEGISK.F K.VPLALFALNR.R R.LADRIHHEELTR.I R.VFKTDMELEVLR.Y	34 59 27 31 41	192
A0A384B2P9_BALAS <i>Complement factor B</i>	401.2265 481.7398 497.2843 501.2668 696.8091	R.DLLDIGR.N R.LPQSTTCR.Q K.ALFVSELSK.D K.DVSEVVTPR.F R.LEDSVTYYCSR.G	41 52 39 29 31	191
A0A384B2W1_BALAS <i>Complement C4</i>	448.2590 454.7454 585.3170 769.3969 778.4198	R.GQIVSVH.R.E R.SGFLSIER.L K.LQDAPSGQVVR.G K.VENSISSANTFLGAK.V K.ISLAQEQVGGSPEK.L	21 42 41 28 50	181
A0A383Z8T4_BALAS <i>C4b-binding protein alpha chain isoform X7</i>	868.8886 938.9143	K.LSCTSSGWSAPAAPQCK.A K.SGDAIYECDEGYTLVGK.N	87 88	176
A0A384B7A3_BALAS <i>selenoprotein P</i>	463.7584 528.7536 549.7421 623.0826	K.QPPAWSIK.D K.DDFLIYDR.C K.TLEDEGFCK.N R.LVYHLGLPYSFLTSSHVEDAIK.T	23 39 49 50	160
A0A383ZWH5_BALAS <i>Keratin, type I cytoskeletal 18</i>	404.2033 521.3062 533.2643 553.8142	R.LAADDFR.V R.IVLQIDNAR.L R.AQYDELAQK.N R.LASYLERVR.S	55 37 25 38	155
A0A452C4G6_BALAS <i>lysozyme C</i>	490.2336 492.2796 700.8442	R.ATNYNPGR.S R.VVQDPQGIK.A R.STDYGIFQINSR.Y	47 21 86	154
A0A383ZW41_BALAS <i>Tubulin alpha chain</i>	543.3140 470.9295 573.6323 777.3443	K.EIDLVLDR.I R.QLFHPEQLITGK.E R.NLDIERPTYTNLNR.L R.AVFHWYVGEGMEEGEFSEAR.E	57 23 36 37	153
A0A452C7H9_BALAS <i>Ferritin heavy chain-like</i>	438.7630 449.2144 515.9064	R.IFLQDIK.K K.YFLHQSHERR.E R.QNYHQDSEAAINR.Q	41 31 72	144
A0A384AF15_BALAS <i>Actin, cytoplasmic 2</i>	488.7278 566.7672 652.0265	K.AGFAGDDAPR.A R.GYSFTTTAER.E R.VAPEEHPVLLTEAPLNPK.A	64 55 22	141
A0A383YRP6_BALAS <i>Antithrombin-III</i>	420.2108 456.2691 764.3883	K.FDTISEK.T R.LPGIVAEGR.N K.AFLEVNEEGSEAAASTVIGIAGR.S	45 59 32	136
A0A383ZRJ1_BALAS <i>Keratin, type I cytoskeletal 14</i>	404.2033 405.2238 1043.4943	R.LAADDFR.T R.LASYLDK.V R.GQVGGDVNVEMDAAPGVDSL.R.I	36 23 78	135

A0A384AFN8_BALAS <i>Superoxide dismutase</i>	845.1037 698.3638	K.LTAVSVGVQGSGWGW/LGFNKEQGR.L K.EKLTAVSVGVQGSGWGW/LGFNKEQGR.L	80 50	130
A0A452CDN2_BALAS <i>Keratin, type I cytoskeletal 12</i>	405.2238 532.8088 561.7629	R.LASYLDK.V R.LASYLDKVR.A K.MTMKNLNDR.L	46 53 21	120
A0A383Z527_BALAS <i>Triosephosphate isomerase</i>	489.5794 801.9481 434.7322	K.TATPQQAQEVHEK.L K.VVLAYEPVWAIGTGK.T K.TATPQQAQEVHEKLR.G	42 30 46	118
A0A452C549_BALAS <i>Immunoglobulin lambda-1 light chain</i>	830.9147	K.YAASSYLALTASEWK.S	117	117
A0A384AEC5_BALAS <i>Beta-2-glycoprotein 1</i>	505.2635 477.5748 872.9594	R.ATVIYEGEK.V R.TCPKPDELPFAR.V K.LPVCAPTTCPPPPPIP.K.F	40 37 34	111
A0A384AU56_BALAS <i>Arginase</i>	474.7794 557.2958	K.DIVYIGLR.D R.GGVEEGPTVLR.K	33 76	109
A0A384B6M8_BALAS <i>Fetuin-B</i>	500.3157 595.2817	K.LVVLPPFSK.E K.SVSVTCDFFK.S	73 35	108
A0A383ZV15_BALAS <i>Heat shock protein HSP 90-alpha</i>	408.2605 757.3957	R.ALLFVPR.R R.GVVDSEDLPLNISR.E	41 67	108
A0A384B2D0_BALAS <i>Heat shock protein HSP 90-beta</i>	415.2681 757.3957	R.ALLFIPR.R R.GVVDSEDLPLNISR.E	36 67	102
A0A384AGF6_BALAS <i>Fructose-bisphosphate aldolase</i>	401.2451 566.7927 745.8580	R.ALQASALK.A R.ALANSLACQGK.Y R.LQSIGTENTENNR.R	33 35 32	101
A0A383ZNS6_BALAS <i>Fibrinogen beta chain</i>	490.7239 891.4093	R.QDGSVDFGR.K K.DNENVINEYSSQLEK.H	30 69	99
A0A383YX88_BALAS <i>Inter-alpha-trypsin inhibitor heavy chain H2</i>	465.7194 494.9440 791.9318	K.HADPDFTK.K K.AHVTFKPTVAQQR.K K.IQPSGGTNINEALLR.A	25 26 42	93
A0A384A960_BALAS <i>Alpha-2-antiplasmin</i>	574.7888 648.8311 761.7364	R.NPNPGAQPEPK.E K.LGNQEPPGQTAPK.K R.GISDQLSVSSVQHQSTLELR.E	27 34 30	90
A0A384BAB1_BALAS <i>Apolipoprotein C-III</i>	865.9330	K.DALTSVQESQVAQQAR.G	87	87
A0A452C549_BALAS <i>Immunoglobulin lambda-1 light chain</i>	830.9166	K.YAASSYLALTASEWK.S	89	89
A0A383ZWG2_BALAS <i>Keratin, type II cuticular Hb6</i>	453.7370 611.8196 632.3506	R.FLEQQNK.L R.ATAENEFVTLK.K K.LGLDIEIATYR.R	25 32 25	82
A0A384BC72_BALAS <i>Unconventional myosin-Vb isoform X4</i>	396.2076 429.7501 444.2327	R.IIGANMR.T + Deamidated (NQ); Oxidation (M) K.LVQLEK.K + Deamidated (NQ) K.NELNELR.K	31 22 30	82
A0A384A9E5_BALAS <i>Vitronectin</i>	645.2896 675.3448	R.GLYCYELDEK.A K.GIPDNVDAALALPAHSYSGR.E	31 50	80
A0A383ZQR0_BALAS <i>Histone H3.1-like</i>	416.2502 495.2926	K.STELLIR.K K.VFLENVIR.D	28 50	77
A0A384BAE9_BALAS <i>Phosphotriesterase-related protein</i>	565.8066	R.VLQEAGADISK.T	76	76
A0A452CPB6_BALAS <i>Complement component C9</i>	516.2723 699.3558	K.VVEESELAR.T R.AIADYINEFSVR.K	50 25	76

A0A452CB89_BALAS <i>Unconventional myosin-XV</i>	422.2686 523.3142	<i>K.IILLQSR.A + Deamidated (NQ)</i> <i>K.TEATKLILR.Y + Deamidated (R)</i>	46 30	75
A0A383ZIC9_BALAS <i>L-lactate dehydrogenase</i>	624.8040	<i>R.VIGSGCNLDSAR.F</i>	74	74
A0A384A978_BALAS <i>14-3-3 protein epsilon isoform X1</i>	628.7988	<i>R.YLAEFATGNDR.K</i>	68	68
A0A384A061_BALAS <i>Cathepsin G-like</i>	451.9123 849.7634	<i>R.RTDTLHDVQIR.V</i> <i>R.AIPHPGYNPQNNENDIMLLQLRS</i>	28 39	66
A0A383ZVX9_BALAS <i>Protein kinase C-binding protein NELL2</i>	572.2315	<i>R.LDQCYCYER.T</i>	64	64
A0A384AG73_BALAS <i>Histone H2A</i>	425.7666 458.2725	<i>R.HLQLAIR.N</i> <i>K.KMRIIIPR.H + 2 Deamidated (R)</i>	31 31	62
A0A384BA01_BALAS <i>Heparin cofactor 2 isoform X1</i>	449.2447 544.7905	<i>K.FALDLYR.A</i> <i>K.QVPVLDDFR.A</i>	40 22	62
A0A384B0X4_BALAS <i>Glutathione synthetase</i>	436.7455	<i>K.ILSNNPNSK.G</i>	60	60
A0A452CCD2_BALAS <i>Alpha-1B-glycoprotein</i>	567.3012	<i>R.FPLGAVTGDR.G</i>	60	60
A0A383YT12_BALAS <i>Annexin</i>	622.8151	<i>R.TNQELQEINR.V</i>		
A0A383ZP87_BALAS <i>Charged multivesicular body protein 5</i>	466.7456 572.8304	<i>K.KMREGPAK.N + Oxidation (M)</i> <i>K.ISRLDAELVK.Y + Deamidated (R)</i>	21 36	57
A0A383Z9P7_BALAS <i>Polymeric immunoglobulin receptor</i>	486.2736 758.7378	<i>K.IVEGEPSLK.V</i> <i>K.SNALQVLKPETELIYGDLR.G</i>	32 24	56
A0A383Z8Q9_BALAS <i>Heterogeneous nuclear ribonucleoproteins A2/B1 isoform X1</i>	594.8271	<i>K.IDTIEIITDR.Q</i>	56	56
A0A452CGT3_BALAS <i>Periplakin</i>	473.2628 487.2586	<i>R.QSLQLLEAR.R + Deamidated (NQ)</i> <i>R.GELQQQLQR.R + 2 Deamidated (NQ)</i>	21 37	
A0A383ZLI1_BALAS <i>Microtubule-associated protein 1B</i>	528.3140 626.8099	<i>R.AIGNIELGIR.S</i> <i>K.ETKNAANTSTSK.S + Deamidated (NQ)</i>	25 30	54
A0A383ZSV7_BALAS <i>Tenascin isoform X1</i>	568.2903	<i>K.APTTQVESFR.V</i>	51	51
A0A383YY16_BALAS <i>Serine/threonine-protein phosphatase</i>	466.2614 473.2596	<i>K.QTIETAIR.G</i> <i>R.AAARAESLR.A + Deamidated (R)</i>	21 29	50
A0A384B0M0_BALAS <i>E3 ubiquitin-protein ligase SH3RF1</i>	452.2299	<i>K.EDELELR.K</i>	47	47
A0A384A314_BALAS <i>Hydroxyacylglutathione hydrolase, mitochondrial isoform X1</i>	435.7740	<i>K.ALLEVLR.L</i>	46	46
A0A383ZYA9_BALAS <i>F-box only protein 50</i>	410.2362	<i>R.TVIAQHHVAPR.T</i>	46	46
A0A383YRQ8_BALAS <i>Histone H2B</i>	408.7324	<i>R.EIQTAVR.L</i>	45	45
A0A383ZNS6_BALAS	474.7266	<i>R.ECEEIIR.N</i>	45	45

<b>Fibrinogen beta chain</b>				
A0A384ATV8_BALAS <b>Glycerol-3-phosphate dehydrogenase [NAD(+)]</b>	436.2840	K.GALGISLIK.G	44	44
A0A383Z1U4_BALAS <b>Complement C3-like isoform X1</b>	652.8309	R.VFVSNPDGSPASK.V	43	43
A0A383ZQ81_BALAS <b>Trypsin-like</b>	588.3214	R.TLNNDIMLIK.L + Deamidated (NQ)	43	43
A0A383YW83_BALAS <b>Desmoglein-1</b>	513.7371	R.TMNNFLDR.E + Oxidation (M)	43	43
A0A383ZI24_BALAS <b>Rootletin</b>	453.7302 487.2586	R.TLSEEATR.L K.GQLQQELR.R + 2 Deamidated (NQ)	21 22	43
A0A383ZUP7_BALAS <b>Protein S100</b>	494.7593	K.LLQTECPK.F	42	42
A0A383ZJG1_BALAS <b>Basement membrane-specific heparan sulfate proteoglycan core protein</b>	549.7988	R.IGAPTNLEQR.A	42	42
A0A384AJC0_BALAS <b>protrudin isoform X1</b>	610.8038	R.IGAPTNLEQR.A	42	42
A0A452C841_BALAS <b>Ankyrin repeat domain-containing protein 24</b>	539.5939	R.ARQAQSRAQEALER.A + Deamidated (NQ); 2 Deamidated (R)	42	42
A0A452C9S2_BALAS <b>DnaJ homolog subfamily C member 14-like</b>	492.2611 398.8752	R.RKEYIMK.R + Oxidation (M) R.SPGRHQLGGKR.S + Deamidated (NQ); Deamidated (R)	22 22	40
A0A383ZSX3_BALAS <b>Protein AMBP</b>	483.7103	K.ECLQTCR.T	39	39
A0A383YSS2_BALAS <b>Thioredoxin reductase 1</b>	624.3392	R.QFVPIKVEQIEAGTPGR.L + 2 Deamidated (NQ)	39	39
A0A452CBX0_BALAS <b>Myosin-1-like</b>	468.2629	K.CASLKKTK.Q	38	38
A0A383YQ74_BALAS <b>60S ribosomal protein L30</b>	879.4589	R.VCTLAIIDPGDSDII.R.S	36	36
A0A383ZYI4_BALAS <b>Carbonic anhydrase 2</b>	527.9437	K.YAAELHLVHWNTK.Y		
A0A383ZZQ3_BALAS <b>N6-adenosine-methyltransferase catalytic subunit</b>	508.7721	K.QLDSLRRER.L	36	36
A0A384ANP8 A0A384ANP8_BALAS <b>HERV-H LTR-associating protein 1</b>	460.5570	K.QKCLENICKSV.- + Deamidated (NQ)	35	35
A0A384A168 A0A384A168_BALAS <b>Catalase</b>	487.7490	K.NLSVEDAAR.L	35	35
A0A384AEC5_BALAS <b>Beta-2-glycoprotein 1</b>	759.6873	K.TSYAPGEEIVYTCQPGYVSR.G	34	34
A0A384A9V8 A0A384A9V8_BALAS <b>SWI/SNF-related matrix-associated actin-dependent regulator of chromatin subfamily A</b>	424.7348	K.KNVFNPK.R + 2 Deamidated (NQ)	34	34

<i>containing DEAD/H box 1 isoform X2</i>				
A0A384BAV9_BALAS <i>Collagen alpha-1(IV) chain isoform X1</i>	642.3357	<i>K.ILYHGYSLLYVQGNER.A</i>	34	34
A0A452CIN7_BALAS <i>Pleckstrin homology domain-containing family G member 3</i>	483.2744	<i>K.SKVYQLAR.Q + Deamidated (NQ)</i>	34	34
A0A383YWG2_BALAS <i>Kinesin-like protein KIF21A</i>	483.2744	<i>R.ASQQINALR.S + 2 Deamidated (NQ)</i>	33	33
A0A384ACX2_BALAS <i>Charged multivesicular body protein 4c</i>	514.8088	<i>K.RAACQALKR.K + Deamidated (NQ); Deamidated (R)</i>	33	33

373     <sup>†</sup>Ions score is -10\*Log(P), where P is the probability that the observed match is a random event. Individual ions  
 374     scores > 32 indicated identity or extensive homology ( $p < 0.05$ ). Protein scores were derived from ions scores as  
 375     a non-probabilistic basis for ranking protein hits. Cut-off was set at Ions score 20.

376

377     **Table 2. Deiminated proteins identified by F95 enrichment in serum of fin whale (*Balaenoptera physalus*).**  
 378     Deiminated proteins were isolated by immunoprecipitation using the pan-deimination F95 antibody. The F95  
 379     enriched eluate was analysed by LC-MS/MS and peak list files were submitted to mascot. Only peptide sequence  
 380     hits scoring with *B. physalus* are included. Peptide sequences and m/z values are listed. For protein hits against  
 381     the full cetacean database see Supplementary Table 3.

Protein name	m/z	Peptide sequence	Score (p<0.05) <sup>†</sup>	Total score
Q0QES7_BALPH <i>Glyceraldehyde-3-phosphate dehydrogenase</i>	406.2101 435.2576 685.3741 778.9081 539.2985 910.4540	<i>K.LTGMAFR.V</i> <i>K.VIPELNGK.L</i> <i>R.GAAQNIIPASTGAAK.A</i> <i>R.VPTPNVSVDLTCR.L</i> <i>K.AITIFQERDPANIK.W</i> <i>K.IVSNASCTTNCLAPLAK.V</i>	40 42 77 97 33 92	381
O02673_BALPH <i>Gamma fibrinogen</i>	486.5787	<i>R.SDGPAKPNGIDSATK.I</i>	46	46
Q0QE03_BALPH <i>Isocitrate dehydrogenase 1</i>	690.3438	<i>K.VEISYTPSDGSPK.T</i>	22	22

382     <sup>†</sup>Ions score is -10\*Log(P), where P is the probability that the observed match is a random event. Individual ions  
 383     scores > 15 indicated identity or extensive homology ( $p < 0.05$ ). Protein scores were derived from ions scores as  
 384     a non-probabilistic basis for ranking protein hits. Cut-off was set at Ions score 20.

385

386     **Table 3. Deiminated proteins identified by F95 enrichment in serum of humpback whale (*Megaptera novaeangliae*).** Deiminated proteins were isolated by immunoprecipitation using the pan-deimination F95  
 387     antibody. The F95 enriched eluate was analysed by LC-MS/MS and peak list files were submitted to mascot. Only  
 388     peptide sequence hits scoring with *M. novaeangliae* are included. Peptide sequences and m/z values are listed.  
 389     For protein hits against the full cetacean database see Supplementary Table 4.

Protein name	m/z	Peptide sequence	Score (p<0.05) <sup>†</sup>	Total score
A1E0X3_MEGNO <i>Beta-actin</i>	488.7276 652.0251	<i>K.AGFAGDDAPR.A</i> <i>R.VAPEEHPVLLTEAPLNPK.A</i>	51 27	78
R9S009_MEGNO <i>Myoglobin</i>	479.0133	<i>K.YLEFISDAIHVVLHSR.H</i>	47	47

391     <sup>†</sup>Ions score is -10\*Log(P), where P is the probability that the observed match is a random event. Individual ions  
 392     scores > 13 indicated identity or extensive homology ( $p < 0.05$ ). Protein scores were derived from ions scores as  
 393     a non-probabilistic basis for ranking protein hits. Cut-off was set at Ions score 20.

394

395 **Table 4. Deiminated proteins identified by F95 enrichment in serum of Cuvier's beaked whale (*Ziphius*  
 396 *cavirostris*).** Deiminated proteins were isolated by immunoprecipitation using the pan-deimination F95  
 397 antibody. The F95 enriched eluate was analysed by LC-MS/MS and peak list files were submitted to mascot. Only  
 398 peptide sequence hits scoring with *Z. cavirostris* are included. Peptide sequences and m/z values are listed. For  
 399 protein hits against the full cetacean database see Supplementary Table 5.

Protein name	m/z	Peptide sequence	Score (p<0.05) <sup>†</sup>	Total score
<b>MYG_ZIPCA</b> <i>Myoglobin</i>	395.7186	<i>K.ASEDLKK.H</i>	31	696
	455.7348	<i>K.GHPETLEK.F</i>	31	
	475.7403	<i>K.YKELGFHG.-</i>	46	
	434.2224	<i>K.GHPETLEKFDFK.F</i>	37	
	708.9197	<i>K.HGHTVLTALGGILK.K</i>	89	
	773.8487	<i>R.HPSDFGADAAQAAAMTK.A</i>	126	
	818.9368	<i>K.VEADLSGHGQEILR.L</i>	102	
	464.2471	<i>K.GHHEAELKPLAQSHATK.H</i>	51	
	933.5031	<i>M.GLSEAEWQLVLHVWAK.V</i>	85	
	638.3455	<i>K.YLEFISDAIIHVLHSR.H</i>	57	
	397.2168	<i>K.KGHHEAELKPLAQSHATK.H</i>	42	
<b>A8IY74_ZIPCA</b> <i>Recombination activating protein 1</i>	612.8331	<i>R.KGHQPSTQLTK.K</i>	23	23

400 <sup>†</sup>Ions score is -10\*Log(P), where P is the probability that the observed match is a random event. Individual ions  
 401 scores > 14 indicated identity or extensive homology (p < 0.05). Protein scores were derived from ions scores as  
 402 a non-probabilistic basis for ranking protein hits. Cut-off was set at Ions score 20.  
 403

404 **Table 5. Deiminated proteins identified by F95 enrichment in serum of orca (*Orcinus orca*).** Deiminated  
 405 proteins were isolated by immunoprecipitation using the pan-deimination F95 antibody. The F95 enriched  
 406 eluate was analysed by LC-MS/MS and peak list files were submitted to mascot. Only peptide sequence hits  
 407 scoring with *O. orca* are included. Peptide sequences and m/z values are listed. For protein hits against the full  
 408 cetacean database see Supplementary Table 6.

Protein name	m/z	Peptide sequence	Score (p<0.05) <sup>†</sup>	Total score
G8Z0F2_ORCOR <i>Adiponectin</i>	533.7796	<i>R.SAFSVGLETR.V</i>	42	42
G8Z0E8_ORCOR <i>Cytoplasmic beta-actin</i>	398.2398	<i>K.IIAPPER.K</i>	33	101
	895.9500	<i>K.SYELPDGQVITIGNER.F</i>	68	

409 <sup>†</sup>Ions score is -10\*Log(P), where P is the probability that the observed match is a random event. Individual ions  
 410 scores > 15 indicated identity or extensive homology (p < 0.05). Protein scores were derived from ions scores as  
 411 a non-probabilistic basis for ranking protein hits. Cut-off was set at Ions score 20.  
 412

### 413 **3.4 Protein interaction network analysis**

414 STRING analysis (Search Tool for the Retrieval of Interacting Genes/Proteins; <https://string-db.org/>)  
 415 was used for the identification of putative protein-protein interaction networks for the deiminated  
 416 proteins identified in northern minke whale, fin whale, humpback whale, Cuvier's beaked whale and  
 417 orca, respectively – based on identification of protein hits using the larger cetacean database following  
 418 LC-MS/MS analysis. These networks were based on the STRING cetacean database for minke whale  
 419 (constructed using minke whale hits), while hits with orca were used for constructing protein-  
 420 interaction networks for fin whale, humpback whale, Cuvier's beaked whale and orca. As protein-  
 421 interaction network analysis for minke whale, using the corresponding orca STRING database,  
 422 revealed a similar analysis as when using the minke whale STRING database, the minke whale STRING

423 database was used for the analysis of protein-interaction networks in minke whale (Figure 4). The PPI  
424 enrichment *p*-value for all protein networks identified in the 5 cetaceans under study was *p* < 1.0 x  
425 10<sup>-16</sup>, indicating that the deiminated protein hits have more interactions among themselves than what  
426 would be expected for a random set of proteins of similar size. Annotations for KEGG (Kyoto  
427 Encyclopedia of Genes and Genomes) pathways identified for the deiminated protein hits, which  
428 relate to physiological and immunological pathways, are represented in Fig. 4-8, with some shared  
429 pathways common between all or some of the species, while other pathways identified were species-  
430 specific (see Venn Diagram in Fig. 9). Physiological KEGG pathways identified for deiminated proteins  
431 included the complement and coagulation cascades, renin-angiotensin system, oestrogen signalling  
432 pathway, cholesterol metabolism, vitamin digestion and absorption, glycolysis/gluconeogenesis,  
433 biosynthesis of amino acids, fat digestion and absorption, metabolic pathways, carbon metabolism,  
434 ECM-receptor interaction, nitrogen metabolism, pentose phosphate pathway, HIF-1 signalling, thyroid  
435 hormone synthesis and proximal tubule bicarbonate reclamation (Fig. 4A, 5A, 6A, 7A, 8A). KEGG  
436 pathways for immune defences/host-pathogen interactions included *Staphylococcus aureus* infection,  
437 systemic lupus erythematosus (SLE), amoebiasis, ferroptosis, phagosome, necroptosis, prion diseases,  
438 pertussis, metabolism of xenobiotics, cancer, prion diseases and tryptamomiasis (Fig. 4B, 5B, 6B, 7B,  
439 8B). Figures 4-8 highlight the different KEGG pathways for deiminated proteins identified in the  
440 cetaceans under study, while the Venn diagrams in Fig. 9 show the number of common and species-  
441 specific physiological (Fig. 9A) and immune related (Fig. 9B) pathways identified for the deiminated  
442 protein hits identified. Relevance of these KEGG pathways for physiology and immunity of the  
443 cetacean species under study are further discussed in the discussion.

444

### 445 **3.5 Phylogenetic reconstruction of PAD sequences.**

446 Five well supported and distinct clades representing each PAD were formed within the Neighbour-  
447 joining phylogeny (Supp. Fig. 1). The PAD1 clade appeared to resolve the best supported phylogenetic  
448 topology with the cetacean sequences falling into two subclades, one for the Odontoceti and one for  
449 the Mysticeti, with La Planta dolphin (*Pontoporia blainvilliei*) as a paraphyletic group. The first PAD1  
450 “Odontoceti” subclade was further split into two clades, one representing members of the Lipotidae  
451 and Iniidae, and the other further split into a Delphinidae clade and another clade comprising  
452 Montodontidae and Phocoenidae lineages. The second PAD1 “Mysticeti” subclade also formed two  
453 further clades, one representing members of the Ziphidae and the other representing members of  
454 the Physeteridae, Balaenidae and Balaenopteridae.

455 The PAD2, PAD3, PAD4 and PAD6 clades do not show the same differentiation into such distinct groups  
456 as for PAD1 (Supp. Fig. 1). Interestingly, the PAD sequences for the common hippopotamus,  
457 *Hippopotamus amphibius*, were intermingled with the cetacean sequences within each of the

458 respective PAD clades, with the exception of the *H. amphibius* PAD3 which formed the expected  
459 paraphyletic clade (Supp. Fig. 1).

460

### 461 **3.6 Analysis of inflammatory and metabolic microRNAs in whale sera and serum derived EVs**

462 The inflammatory and stress related miR21, miR155 and the metabolic and hypoxia related miR210  
463 were assessed both in whole sera and in EVs isolated from sera of the 5 cetaceans. Species-specific  
464 differences were observed in the relative expression all three miRs as shown in Fig. 10. Furthermore,  
465 EVs were found to be a better source of miRs, compared to whole sera (Fig. 10). The highest relative  
466 levels of miR21 were found in humpback whale EVs, followed by minke whale (Fig. 10A), while relative  
467 miR155 expression was highest in minke whale EVs (Fig. 10B) and miR210 relative levels were highest  
468 in orca, followed by humpback whale (Fig. 10C).

469

## 470 **4. Discussion**

471 This is the first study to characterise deiminated protein networks, extracellular vesicles (EVs) and  
472 microRNA (miR) EV-cargo in cetacean sera. Deiminated proteins were identified and compared in the  
473 5 different cetacean species under study: Northern minke whale (*Balaenoptera acutorostrata*), fin  
474 whale (*Balaenoptera physalus*), humpback whale (*Megaptera novaeangliae*), Cuvier's beaked whale  
475 (*Ziphius cavirostris*) and orca (*Orcinus orca*). The findings presented here unravel novel aspects of post-  
476 translational deimination in key proteins of metabolism, innate and adaptive immunity in these sea  
477 mammals.

478 PAD homologues were identified in whale sera by Western blotting via cross reaction with human  
479 PAD2 and PAD3. PAD2 is the phylogenetically most conserved PAD form (Vossenaar et al., 2003;  
480 Magnadottir et al., 2018a), and in cetacean sera PAD-positive bands were seen at an expected 70 - 75  
481 kDa size, similar to as seen for other mammalian PADs.

482 Deiminated histone H3, a marker of neutrophil extracellular trap formation (NETosis), was detected  
483 in the whale and orca sera. NETosis is partly driven by PADs (Li et al., 2010), is conserved throughout  
484 phylogeny (Magnadottir et al., 2018a; Magnadottir et al., 2019a; Criscitiello et al., 2019), and is  
485 important in innate immune defences against a range of pathogens including bacteria, viruses and  
486 helminths (Brinkmann et al., 2004; Palić et al., 2007; Branzk et al., 2014; Schönrich and Raftery, 2016).  
487 Indeed, NET/ETosis has recently been related to parasitic defence mechanisms in cetaceans (Villagra-  
488 Blanco et al., 2019). NETosis has furthermore been associated with clearance of apoptotic cells and  
489 tissue remodelling (Magnadottir et al., 2018a; Magnadottir et al., 2019a) as well as being associated  
490 with chronic pathologies (Lee et al., 2017; O'Neil and Kaplan, 2019), neurodegenerative diseases  
491 (Pietronigro et al., 2017) and cancer (Gonzalez-Aparicio and Alfaro, 2019). Histones undergo various

492 post-translational modifications that affect gene regulation and can also act in concert (Bird, 2007;  
493 Latham et al., 2007). In addition to acetylation, phosphorylation and ubiquitination, histones are  
494 indeed known to undergo deimination, including H2B (Sohn et al., 2015) and H3 as identified here in  
495 minke whale. Other histones known to undergo deimination are H2A (Hagiwara et al., 2005) and H4  
496 (Chen et al., 2014; Kosgodage et al., 2018), both of which were also identified here as deimination  
497 targets based on the larger cetacean database search (Supplementary Tables 2-5).

498 Further deiminated proteins identified here in whale and orca sera by F95 enrichment and LC-MS/MS  
499 analysis included key immune, nuclear and metabolic proteins. Most species-specific protein hits were  
500 found for minke whale which, has to be noted, also had the largest searchable species-specific  
501 database and therefore the most annotations for identification of species-specific proteins.  
502 Furthermore, all protein hits from the LC-MS/MS analysis for deiminated proteins isolated from the  
503 individual cetaceans were also assessed against a larger common cetacean database (Supplementary  
504 Tables 2-6). The protein list for species-specific deiminated proteins identified in minke whale was  
505 submitted to STRING (Search Tool for the Retrieval of Interacting Genes/Proteins) analysis  
506 (<https://string-db.org/>) to predict putative protein-protein interaction networks. For deiminated  
507 proteins identified in minke whale serum, PPI enrichment value for 85 of the identified deiminated  
508 proteins was found to be  $p < 1 \times 10^{-16}$ , which indicates that these proteins have more interactions among  
509 themselves than what would be expected for a random set of proteins of similar size, drawn from the  
510 genome. Such enrichment indicates that the proteins are at least partially biologically connected, as a  
511 group. KEGG pathways involved in immunity and metabolism are highlighted for the minke whale  
512 species-specific derived STRING protein network analysis in Supplementary Fig 2.

513 In addition to the species-specific analysis of protein interaction networks, based on the species-  
514 specific UniProt databases for each of the cetaceans under study, a wider analysis of deiminated  
515 protein hits based on a larger cetacean UniProt database was used to create protein-protein  
516 interaction networks in STRING (Figures 4-8). These revealed both common/shared deiminated  
517 protein pathways related to physiology and immunity as well as highlighting some differences in  
518 deiminated KEGG pathways between the species under study (Fig. 9). KEGG pathways for the  
519 complement and coagulation cascades were identified in all 5 cetacean species, and form part of the  
520 acute phase response and first line of immune defences against invading pathogens as well as in the  
521 clearance of necrotic or apoptotic cells (Dodds and Law, 1998; Fishelson et al., 2001; Gelain and  
522 Bonsembiante, 2019). Pathways for glycolysis/gluconeogenesis were identified in minke, fin,  
523 humpback and Cuvier's beaked whale. Recent studies in dolphins have identified low activity of the  
524 glycolysis metabolic pathway (Suzuki et al., 2018) and changes in glycolysis pathways has been  
525 assessed in diving vertebrates (Hochachka et al., 1975). Post-translationally deiminated proteins in

526 glycolysis pathways have been recently identified in the naked mole-rat (*Heterocephalus glaber*)  
527 (Pamenter et al., 2019), where changes in glycolysis has for example been related to anoxia resistance  
528 (Park et al., 2017). How deimination of glycolysis pathway related proteins play roles in hypoxia  
529 tolerance and cancer-resistance remains to be further investigated. Oestrogen signalling pathways  
530 were identified as deiminated in minke whale, fin whale and humpback whale. Oestrogen has been  
531 studied in a range of cetaceans, including during pregnancy (Robeck et al., 2016) and as a marker for  
532 environmental pollution in orca at the mRNA expression level (Buckman et al., 2011), while post-  
533 translational modification and putative effects of deimination on oestrogen signalling remains to be  
534 investigated. KEGG pathways relating to cholesterol metabolism were identified in minke whale, fin  
535 whale, humpback whale and orca, while KEGG pathways for fat digestion and absorption were  
536 identified to be deiminated in minke whale, fin whale and orca. Cholesterol has been studied in whales  
537 in relation to lifespan (Borchman et al., 2017) and lipidomics are being developed as a diagnostic tool  
538 for metabolic and physiological state in whales, including cholesterol (Tang et al., 2018). Roles for post-  
539 translational modifications, including deimination, in cholesterol metabolism remain to be fully  
540 understood. KEGG pathways relating to vitamin digestion and absorption were identified to be  
541 deiminated in minke whale, fin whale and orca. Disruption of vitamin profiles has been identified in  
542 cetaceans in response to exposure to environmental pollutants (Desforges et al., 2013; Pedro et al.,  
543 2019), but to what extend deimination plays a role in vitamin processing is not known. KEGG pathways  
544 for biosynthesis of amino acids were identified to be deiminated in minke whale, fin whale, humpback  
545 whale and Cuvier's beaked whale. Such deimination may be of considerable interest as amino acid  
546 assessment for mammalian metabolism is being developed for health management of cetaceans  
547 (Suzuki et al, 2018) and for research into ageing and disease, including in cetacean samples (Fry and  
548 Carter, 2019). Pathways for carbon metabolism were identified in fin whale, humpback whale and  
549 Cuvier's beaked whale, while nitrogen metabolism pathways were identified in humpback whale and  
550 Cuvier's beaked whale. Both pathways have been utilised to assess environmental contamination in  
551 whales (Borrell et al., 2018; Pinzone et al., 2019). Pathways relating to HIF-1 signalling were identified  
552 in Cuvier's beaked whale and humpback whale, which correlates with these two cetaceans being the  
553 most deep diving of the species under study; for example gas and fat embolic syndrome is a pathologic  
554 condition of *Ziphiidae* and mirrors decompression sickness identified in human divers (Fernández et  
555 al., 2005; Di Guardo et al., 2019). Deiminated protein pathways related to HIF-1 signalling have also  
556 recently been identified in the naked mole-rat, which is known for unusual resistance to hypoxia  
557 (Pamenter et al., 2019), while studies on hypoxia in the CNS have revealed roles for PAD-mediated  
558 pathways (Lange et al., 2014; Fan et al., 2018; Yu et al., 2018).

559 Other deiminated KEGG physiological pathways identified to be species-specific were renin-  
560 angiotensin system (minke whale), proximal tubule bicarbonate reclamation (Cuvier's beaked  
561 whale), ECM-receptor interaction (fin whale), and in Cuvier's beaked whale KEGG pathways for thyroid  
562 hormone synthesis, fructose, mannose and pyruvate metabolism, as well as mineral absorption were  
563 identified to be deiminated. The renin-angiotensin system plays pivotal roles in maintaining blood  
564 pressure and extracellular volume homeostasis (Yang and Xu, 2017). It is critical for osmoregulation in  
565 cetaceans and has been studied in relation to adaptions due to their evolutionary transition from  
566 terrestrial to hyperosmotic environments (Ortiz, 2001; Zu et al., 2013). Cetacean kidneys have several  
567 evolutionary adaptions, including larger size and relatively large ratio of medulla to renal cortex, which  
568 allows for production of highly concentrated urine (Zu et al., 2013). Furthermore, hormonal regulation  
569 of salt and water balance is of great importance, while overall molecular mechanisms underlying these  
570 specialised pathways still remain to be fully explored. Proximal tubule bicarbonate reclamation  
571 pathways were here identified to be deiminated in Cuvier's beaked whale, and these are critical for  
572 kidney function in whales (Maluf and Gassman, 1998) and are primary target of kidney injury in human  
573 and animal models (Chevalier, 2016). Therefore post-translational regulation of proteins  
574 involved in these pathways, including deimination identified here, may be of some interest for  
575 osmoregulation and specialised kidney function in cetaceans as well as for advancing therapeutic  
576 strategies in kidney disease (Chevalier, 2016). ECM-receptor interactions play direct and indirect roles  
577 in control of a range of cellular activities including adhesion, migration, differentiation, proliferation  
578 and apoptosis and are widely studied in cancer, including at the transcriptome level (Bao et al., 2019).  
579 KEGG pathways for both ECM-receptor interaction and focal adhesion have been identified to be  
580 enriched in EVs of mesenchymal stem cells (Mardpour et al., 2019), and both pathways were here  
581 found enriched in deiminated proteins in fin whale only. Roles for regulation of these pathways via  
582 post-translational deimination have not been investigated. Thyroid hormones have been studied in a  
583 range of whales and dolphins, including for evaluation of energetics and stress (Suzuki et al., 2018;  
584 Hunt et al., 2019), as well as environmental pollution (Buckmann et al., 2011; Villanger et al., 2011;  
585 Hunt et al., 2017; Simond et al., 2019). PADs have been related to thyroid cancer (Guo et al., 2017)  
586 and deimination of histone H3 has been linked to autoimmune thyroid disease (Morshed et al., 2019),  
587 while physiological effects of deimination on thyroid hormone synthesis remain to be investigated.  
588 Fructose, mannose and pyruvate metabolism are associated with glycolytic pathways, which have  
589 been found to be of low activity in cetaceans (Suzuki et al., 2018) and therefore regulatory  
590 mechanisms via deimination may be of relevance for understanding of cancer and insulin resistance  
591 pathways (Brown et al., 2016; Guzmán-Flores et al., 2018). In cetaceans, ATP-mediated control of  
592 pyruvate is associated with aerobic-anaerobic transition during diving (Storey and Hochachka, 1974),

593 but to what extent post-translational modifications are involved in regulating proteins involved in  
594 these processes remains to be investigated.

595 Notably, KEGG pathways for host-pathogen interactions were enriched in all five cetacean species  
596 under study, with pathways relating to bacterial infection in all five species, amoebiasis in minke whale  
597 and fin whale and trypanosomiasis in Cuvier's beaked whale and orca. KEGG immune pathways for  
598 viral infection were identified in fin whale only, as well as cancer related pathways and metabolism of  
599 xenobiotics by cytochrome P450, a detoxification system in a range of marine mammals (Goksøyr et  
600 al., 1995) and a biomarker for environmental stress (Waugh et al., 2011; Bachman et al., 2015; Righetti  
601 et al., 2019). KEGG pathways relating to autoimmunity were identified in minke whale, fin whale and  
602 orca. Pathways relating to ferroptosis, a form of regulated cell death and implicated in multiple  
603 physiological and pathological processes (Xie et al., 2016; Shi et al., 2019), were furthermore identified  
604 in minke whale, Cuvier's beaked whale and orca, while pathways relating to phagosome and  
605 necroptosis, critical for necrotic and infectious diseases (Xia et al., 2020), were identified in minke  
606 whale. These findings highlight novel roles for protein deimination in infection, chronic diseases and  
607 host-pathogen interactions in cetaceans. While exact mechanistic pathways will need to be followed  
608 up and validated, the current findings of post-translational deimination in these KEGG pathways add  
609 to the acknowledged lack of information for host-pathogen interactions in cetaceans (Di Guardo et  
610 al., 2018). Transmission of marine morbilliviruses for example requires further research into host-  
611 specific factors (Jo et al., 2018; Di Guardo and Mazzariol, 2019; Ohishi et al., 2019) and research into  
612 immune mechanisms in relation to bacterial infections, including multidrug-resistant bacteria and  
613 opportunistic infection, are of pivotal importance (Reif et al., 2017; Mazzariol et al., 2018). In addition,  
614 specific roles for deiminated protein cargo exported in EVs will also need to be assessed as deiminated  
615 protein enrichment has been shown to differ in EVs compared to whole plasma and serum (Criscitiello  
616 et al., 2019 and 2020; Pamener et al., 2019; Magnadottir et al., 2020a). Further to previously  
617 identified roles for PAD-mediated NETosis/ETosis in cetaceans in response to zoonotic diseases  
618 (Villagara-Blance et al., 2019; Imlau et al., 2020), also verified in the present study, newly recognized  
619 targets of deimination in cetaceans are identified here and highlight putative roles for regulation of  
620 immunological pathways via such post-translational deimination. Selected deiminated protein  
621 candidates, based on identification from the species-specific search for the individual cetaceans under  
622 study, which are involved in immune, nuclear and metabolic functions are discussed below in relation  
623 to roles in physiology and pathology:

624

625 **Adiponectin** was identified to be deiminated in orca only and is in human the most abundant secreted  
626 adipokine with pleiotropic roles in physiological and pathophysiological processes (Fiaschi, 2019). It

627 has received considerable interest in the field of metabolic and obesity research (Frankenberg et al.,  
628 2017; Spracklen et al., 2019), as well as in diabetes (Yamauchi et al., 2003), due to its key function in  
629 regulating glucose (Yamauchi et al., 2002; Kadokawa & Yamauchi, 2005; Almabouada et al., 2013).  
630 Adiponectin is furthermore linked to longevity (Chen et al., 2019), regenerative functions (Fiaschi et  
631 al., 2014), myopathies (Gamberi et al., 2019) and cancer (Parida et al., 2019). Adiponectin also plays  
632 roles in reproduction, embryo pre-implantation and embryonic development (Barbe et al., 2019). Due  
633 to the range of functions in relation to key pathophysiologies, there is a great interest in drug  
634 development to modulate adiponectin signalling (Fiaschi, 2019). Recent studies in rheumatoid arthritis  
635 made a correlation between inflammation, autoantibodies and adiponectin levels (Hughes-Austin et  
636 al., 2018; Liu et al., 2019). Post-translational deimination may be a hitherto unrecognized mechanism  
637 for adiponectin and of relevance for metabolic adaptions, as adiponectin was recently identified as a  
638 deimination candidate in naked mole-rat and llama (*Lama glama*), both which display unusual  
639 metabolism and adaption to extreme environments (Pamenter et al., 2019; Criscitiello et al., 2020).  
640 Deimination may allow for protein moonlighting functions via changes in protein folding and therefore  
641 interaction with other proteins. Adiponectin is a small 244 aa protein (NP\_001171271.1) in humans  
642 and contains 2 unfolded regions and 7 arginine sites, while orca adiponectin (XP\_004278522.1) has  
643 also 2 unfolded regions and 7 arginine sites, that could be subjected to PAD-mediated deimination  
644 and therefore modulate adiponectin folding and function, depending on which arginine is deiminated.  
645 STRING analysis for orca adiponectin and relevant KEGG pathways are shown in Supplementary Fig. 3  
646 (Supplementary Fig. 3A and 3B). Given that orca will have some unique physiological characteristics,  
647 the identification of post-translational deimination of this key metabolic protein may be of great  
648 interest for comparative metabolic studies.

649

650 **Albumin** is a major acidic plasma protein in vertebrates and serves as a transport molecule for fatty  
651 acids, bilirubin, steroids, amino acids and copper, as well as having roles in maintaining the colloid  
652 osmotic pressure of blood (Peters, 1996; Metcalf et al., 2007). In aquatic animals, albumin has been  
653 identified as a putative health marker in response to environmental conditions in porpoises (Nabi et  
654 al., 2017) and for assessment of serum chemistry in wild beluga whales (*Delphinapterus leucas*)  
655 (Norman et al., 2012). In teleost fish, albumin levels were shown to be raised upon heavy metal  
656 exposure in water (Firat and Kargin, 2010). While albumin is known to be a glycoprotein in some  
657 species (Metcalf et al., 1998; Tao et al., 2019), roles for post-translational deimination remain to be  
658 further understood. Indeed, albumin was recently found to be deiminated in teleost fish (Magnadottir  
659 et al., 2019a).

660

661 **Alpha-2-macroglobulin** was found deiminated in minke whale serum. It forms part of the innate  
662 immune system and clears active proteases from tissue fluids (Armstrong and Quigley, 1999). Alpha-  
663 2-M is phylogenetically conserved from arthropods to mammals, is found at high levels in mammalian  
664 plasma and is closely related to other thioester containing proteins, complement proteins C3, C4 and  
665 C5 (Sottrup-Jensen et al., 1987; Davies and Sim, 1981). Alpha-2-M was recently found to be deiminated  
666 in shark (Criscitiello et al., 2019), camelid (Criscitiello et al., 2020), naked mole-rat and Antarctic  
667 seabirds (Phillips et al., 2020) and this may contribute to phylogenetically conserved and adapted  
668 functions in immune responses.

669

670 **Alpha-1-microglobulin/bikunin precursor (AMBP protein)** was here found deiminated in minke whale  
671 serum. It has been linked to oxidative stress and altered protein composition of subcutaneous adipose  
672 tissue in chronic disease (Gertow et al., 2017) but has not been identified as deiminated in any species  
673 before to our knowledge.

674

675 **Antithrombin-III** was here found to be deiminated in minke whale serum. It is a phylogenetically  
676 conserved hepatic glycoprotein and found in blood plasma (Jordan, 1983). Antithrombin forms part  
677 of the coagulation system and in whales, intestinal heparin has been found to bind with high affinity  
678 for antithrombin III (Uchiyama et al., 1990) and studied in coagulation (Oshima, 1990). Roles in disease  
679 are linked to thrombosis, pulmonary embolism (Amiral and Seghatchian, 2018) and angiogenesis in  
680 cancer (O'Reilly et al., 1999). Antithrombin-III furthermore has anti-inflammatory action and is linked  
681 to kidney diseases (Lu et al., 2017). Glycosylation has been found to affect the activity of antithrombin  
682 (McCoy al., 2003). Post-translational deimination has also been shown to affect its function by  
683 converting antithrombin to a form with a four-fold higher affinity for heparin pentasaccharide (Pike et  
684 al., 1997) and its deimination was recently identified also in seabirds (Phillips et al., 2020). Therefore  
685 post-translational modifications, including deimination, seem to play important roles in the functional  
686 diversity of antithrombin-III.

687

688 **Apolipoproteins A-I, A-IV, B-100 and C-III** were here identified as deiminated in minke whale serum.  
689 Apolipoprotein A-I is primarily involved in lipid metabolism where conformational plasticity and  
690 flexibility are of importance (Arciello et al., 2016). Apo A-I is also associated with regulation of  
691 mitochondrial function and bioenergetics (White et al., 2017). Furthermore, Apo A-I has been shown  
692 to have a regulatory role in the complement system by affecting membrane attach complex (MAC)  
693 assembly (Hamilton et al., 1993; Jenne et al., 1991; French et al., 1994). ApoB-100 is conserved  
694 between cetacean and other mammals (Amrine-Madsen et al., 2003), synthesised by the liver and

695 plays parts of innate immune responses (Peterson et al., 2008). ApoB-100 is furthermore associated  
696 with ER stress and insulin resistance (Su et al., 2009) as well as lipid metabolism disorders (Andersen  
697 et al., 2016). ApoA-IV is a lipid binding protein, primarily synthesized in the small intestine and involved  
698 in a range of physiological proteins including lipid absorption and metabolism, glucose homeostasis,  
699 platelet aggregation and thrombosis (Qu et al., 2019). Apo-CIII is a glycoprotein secreted by liver and  
700 small intestine and has roles in secretion of triglyceride-rich VLDL particles from hepatic cells under  
701 lipid rich conditions (Sundaram et al., 2010). Apo-CIII is also produced within pancreatic islets and  
702 linked to diabetes (Juntti-Berggren and Berggren, 2017). The roles for post-translational deimination  
703 in protein moonlighting of these apolipoproteins in whale physiology may be of considerable interest.  
704 Deimination of some apolipoproteins has previously been also identified for in other vertebrates,  
705 including camelids (Criscitiello et al., 2020), naked mole-rat (Pamerter et al., 2019) and teleost fish  
706 (Magnadottir et al., 2019a).

707

708 **Beta-2-glycoprotein 1 (apolipoprotein H)** was here identified as deiminated in minke whale. It is a 38  
709 kDa multifunctional plasma protein which binds cardiolipin. It has roles in agglutination and has anti-  
710 coagulation activity in serum (Rikarni et al., 2015). Furthermore it is implicated in anti-phospholipid  
711 syndrome (Radic and Pattanaik, 2018; Yin et al, 2018). Its post-translational deimination has recently  
712 been identified also in naked mole-rat (Pamerter et al., 2019) and may be of some interest in relation  
713 to moonlighting functions in physiology, in addition to roles in autoimmunity.

714

715 **Ceruloplasmin** is a serum ferroxidase with antioxidative function and roles in iron homeostasis and  
716 carries over 90 % of the copper in plasma (Liu et al., 2011). In aquatic animals, ceruloplasmin has been  
717 shown to contribute to acute immune responses in teleost fish (Lü et al., 2013). It is also upregulated  
718 as an acute phase protein in response to growth hormone (Yada, 2007) and upon heavy metal  
719 exposure (Firat and Kargin, 2010), as well as being upregulated in response to bacterial challenge (Liu  
720 et al., 2011). Ceruloplasmin is furthermore related to bacterial resistance (Sahoo et al., 2013) and  
721 parasitic infection (Kovacevic et al., 2015; Henry et al., 2015). As fish have been shown to use iron  
722 deprivation as a nutritional immunity mechanism, by withholding iron from iron-requiring pathogens  
723 (Lange et al., 2001; Martínez et al., 2017), such uses in other aquatic animals, including whales, may  
724 be possible. Ceruloplasmin has been identified to be deiminated in teleost fish (Magnadottir et al.,  
725 2019a) as well as in the naked mole-rat (Pamerter et al., 2019) and it may be postulated that post-  
726 translational deimination may facilitate the diverse functions of ceruloplasmin.

727

728 **Clusterin** (apolipoprotein J) was identified here as deiminated in minke whale serum. It is a  
729 glycoprotein and a stress-activated ATP-independent molecular chaperone for protein folding and  
730 involved in clearance of cellular debris and apoptosis (Jones and Jomary, 2002; Wilson and Zoubeidi,  
731 2017). Furthermore, clusterin is involved in a range of diseases related to oxidative stress, including  
732 inflammatory diseases, neurodegeneration, cancer and ageing (Yao et al., 2018; Foster et al., 2019).  
733 In seal brains, clusterin has been found to be four-fold higher expressed than in any other mammalian  
734 brain transcriptome. It has been postulated that elevation of this stress related gene may contribute  
735 to the hypoxia tolerance of diving mammals (Fabrizius et al., 2016). Roles for post-translational  
736 deimination in the function of clusterin in whale physiology may therefore be of interest.

737

738 A range of **complement components** was here identified as deiminated in minke whale serum. This  
739 included complement component C3, C5, C9, C1q, complement component C4-binding protein,  
740 complement factor B and factor H. The complement system forms part of the first line of immune  
741 defences against invading pathogens and also participates in the clearance of necrotic or apoptotic  
742 cells (Dodds and Law, 1998; Sunyer and Lambris, 1998; Fishelson et al., 2001; Carroll and Sim, 2011).  
743 The complements system is furthermore implicated in regeneration (Del-Rio-Tsonis et al., 1998;  
744 Haynes et al., 2013) and tissue remodelling (Lange et al., 2004a; 2004b; Lange et al., 2005; Lange et  
745 al., 2006; Lange et al., 2019). **Complement component C3** plays a central role in all pathways of  
746 complement activation and can also be directly activated by self- and non-self surfaces via the  
747 alternative pathway without a recognition molecule (Dodds and Law, 1998; Dodds, 2002). This is to  
748 our knowledge the first report of deiminated complement C3 in a mammalian species, while C3 was  
749 recently identified by our group in deiminated form in teleost fish (Magnadottir et al., 2019a and  
750 2019b) as well as in elasmobranch shark (Criscitiello et al., 2019). Post-translational deimination of C3  
751 may possibly influence its function including in the generation of the convertase, its cleavage ability,  
752 binding and deposition. **Complement component C5** plays important roles in inflammation and  
753 apoptosis. It is cleaved into C5a, which has pleiotropic biologic functions including as anaphylatoxin  
754 (Klos et al., 2009) while C5b forms the basis of the membrane attach complex (MAC) (Morgan et al.,  
755 2016). In cellular *in vitro* models, C5 has previously been reported to undergo deimination by  
756 *Porphyromonas gingivalis*, which evades complement-mediated killing by disabling anaphylatoxin C5a  
757 protein function via deimination of a critical C-terminal arginine (Bielecka et al., 2014). **Complement**  
758 **component C9** participates in the formation of the membrane attack complex, leading to lysis of the  
759 pathogen. C9 has previously been found to be deiminated in teleost fish (Magnadottir et al., 2019a).  
760 **Complement C1q** can activate the classical complement system by binding to the Fc region of  
761 immunoglobulins that are bound to antigen (Reid et al., 2002; Reid, 2018). Interestingly, an essential

762 role for arginine in C1q has been suggested for C1q-IgG interaction (Kojouharova et al., 2004). C1q  
763 also serves as a potent pattern recognition molecule which recognises self, non-self and altered self-  
764 signals (Nayak et al., 2012; Reid, 2018). **Complement component C4-binding protein** (C4BP) is a large  
765 glycoprotein, synthesised in the liver. It acts as an inhibitor of the classical and lectin pathways of the  
766 complement system and has multifaceted roles in immunity and homeostasis. C4BP is a cofactor for  
767 serine protease factor I, and besides C4-binding functions, it can also bind to C3b and accelerate decay  
768 of the C3 convertase. C4BP binds necrotic and apoptotic cells, as well as DNA, and therefore is involved  
769 in tissue clearance post injury (Ermert and Bloom, 2016). **Complement factor B** is a phylogenetically  
770 conserved activation protease of the complement system (Nonaka, 2014). **Complement factor H** is a  
771 major regulator of the alternative complement pathway and factor H family proteins are involved in  
772 modulating a range of cellular functions (Józsi et al., 2019). The deimination of the various  
773 complement components identified here may have diverse effects on complement activity and add to  
774 moonlighting functions of the complement system in homeostasis and immune defences. Recent  
775 comparative studies have indeed highlighted deimination of a range of complement proteins, and this  
776 is of considerable importance for understanding the diversity of complement function throughout  
777 phylogeny (Magnadottir et al., 2018a; Magnadottir et al., 2019a; Lange et al., 2019; Pameneter et al.,  
778 2019; Criscitiello et al., 2019 and 2020).

779

780 **Charged multivesicular body protein 4c** was identified as deiminated in minke whale serum. It is a  
781 core component of the endosomal sorting required for transport complex III (ESCRT-III) which is  
782 involved in multivesicular bodies (MVBs) formation and sorting of endosomal cargo proteins into  
783 MVBs and is furthermore involved in cell division (Carlton et al., 2012). It is also associated to cancer  
784 (Sadler et al., 2018) and to the regulation of viral replication (Li et al., 2013).

785

786 **Desmoplakin** was here identified to be deiminated in minke whale serum. Desmoplakin is a unique  
787 and critical component of desmosomal cell-cell junctions and involved in integrity of the cytoskeletal  
788 intermediate filament network (Bendrick et al., 2019). It has been shown to be required for epidermal  
789 integrity and embryo morphogenesis (Bharathan and Dickinson, 2019), as well as in the coordination  
790 of cell migration (Bendrick et al., 2019). Mutations in desmoplakin have been linked to multiple  
791 allergies, severe dermatitis and metabolic wasting (SAM) syndrome (Liang et al., 2019). It is also linked  
792 to Carvajal syndrome, involving altered skin and hair abnormalities, and heart diseases (Reichl et al.,  
793 2018; Yermakovich et al., 2018; Chen et al., 2019). Desmosomal proteins have been shown to have  
794 both tumour-promoting and tumour-suppressive functions, depending of cancer types and can  
795 regulate cell proliferation, differentiation, migration, apoptosis, and impact treatment sensitivity in

796 different types of cancers (Zhou et al., 2017). Desmoplakin was recently identified to be also  
797 deiminated in camelid serum EVs, but not whole plasma (Criscitiello et al., 2020). As the roles of  
798 desmosomal proteins in cancer and metastasis are not fully understood, the identification of  
799 deiminated desmoplakin in minke whale serum may be of some interest and add to understanding of  
800 pleiotropic functions throughout phylogeny via such post-translational modification.

801

802 ***Dimethylglycine dehydrogenase (DMGDH), mitochondrial isoform X1*** was here identified as  
803 deiminated in minke whale serum. It is a mitochondrial matrix enzyme with roles in choline  
804 degradation, one-carbon metabolism and electron transfer to the respiratory chain (Augustin et al.,  
805 2016). DMGDH is a key metabolic enzyme, linked to diabetes, kidney disease (Zhu et al., 2018;  
806 Magnusson et al., 2015), carcinoma and metastasis (Liu et al., 2016).

807

808 ***Dipeptidylpeptidase 4*** (DPP4, also known as CD26) was here identified to be deiminated in minke  
809 whale serum. DPP4 controls glucose homeostasis and has complex roles in inflammation and  
810 homeostasis, including in liver cytokine expression, while its activity in plasma has been shown to  
811 correlate with body weight and fat mass (Varin et al., 2019). Furthermore, roles for DDP4 in cancer  
812 have been found to relate to its post-translational processing of chemokines, thereby limiting  
813 lymphocyte migration to sites of inflammation and tumours (Barreira da Silva et al., 2015). DPP4  
814 inhibitors have therefore been suggested as a strategy to enhance tumour immunotherapy (Barreira  
815 da Silva et al., 2015). Furthermore, serum DDP4 activity levels in primary HIV infection were found to  
816 be significantly decreased and to correlate with inflammation and HIV-induced intestinal damage  
817 (Ploquin et al., 2018). The identification of DPP4 as a deimination candidate has previously been  
818 verified in camelids (Criscitiello et al., 2020) and may be of some relevance as such post-translational  
819 modification can affect DPP4 structure and function, allowing for moonlighting functions in  
820 pathological and pathophysiological milieus throughout phylogeny.

821

822 ***Fetuin-B*** was identified as deiminated in minke whale. It is a member of the fetuin family and part of  
823 the cystatin superfamily of cysteine protease inhibitors (Lee et al., 2009). Fetuin-B is a hepatokine,  
824 secreted by hepatocytes and linked to the regulation of the insulin and hepatocyte growth factor  
825 receptors, to metabolism as well as metabolic dysfunction, including insulin resistance and chronic  
826 kidney disease (Meex and Watt, 2017; Lin et al., 2019). Fetusins have further functions in osteogenesis  
827 and bone resorption, response to systemic inflammation and infection (Qu et al., 2018; Li et al., 2017)  
828 as well as in fertilisation (Stöcker et al., 2014; Fang et al., 2019). The structure of mammalian plasma  
829 fetuin-B has been extensively studied and fetuin-B is described throughout phylogeny from

830 cartilaginous fishes to mammals (Cuppari et al., 2019). Post-translational deimination of fetuin-B has  
831 not been reported before.

832

833 **Fibrinogen** is a glycoprotein, synthesised in liver (Tennent et al., 2007) and forms part of the acute  
834 phase response as part of the coagulation cascade (Tiscia and Margaglione, 2018). Fibrinogen is well  
835 described in cetaceans (Gatesy, 1997; Terasawa et al., 2008). In humans, impaired mechanism of  
836 fibrinogen formation and fibrin polymerization are implicated in various pathologies including  
837 coagulopathies and ischemic stroke (Weisel and Litvinov, 2013). Acquired fibrinogen disorders are also  
838 associated with cancer, liver disease or post-translational modifications (Besser and MacDonald,  
839 2016). Fibrinogen is indeed a known deimination candidate and this post-translational modification  
840 contributes for example to its antigenicity in autoimmune diseases (Hida et al., 2004; Okumura et al.,  
841 2009; Muller and Radic, 2015; Blachère et al., 2017), and deimination has also been identified in other  
842 taxa, including camelids (Criscitiello et al., 2020) and naked mole-rat (Pamenter et al., 2019). In aquatic  
843 animals, fibrinogen has been associated with teleost host defence against pathogens (Blanco-Abad et  
844 al., 2018), in acute phase and stress responses during temperature acclimation (Dietrich et al., 2018)  
845 and upon exposure to tetrodotoxin (Kiriake et al., 2016). Fibrinogen and gamma-fibrinogen were here  
846 found to be deiminated in minke whale and fin whale respectively.

847

848 **Glyceraldehyde-3-phosphate dehydrogenase** (GAPDH) was identified as deiminated in fin whale  
849 (*Balaenoptera physalus*). GAPDH has key metabolic functions in glycolysis but also has pleiotropic non-  
850 metabolic functions including in apoptosis, transcription activation and axonal transport (Tarze et al.,  
851 2007; Zala et al., 2013; Sirover 2018; Butera et al., 2019). GAPDH has been identified to have a range  
852 of moonlighting functions, including in iron metabolism (Boradia et al., 2014) and is associated to  
853 various pathologies (Sirover 2018). GAPDH has been shown to be regulated via post-translational  
854 modifications (Tristan et al., 2011; White and Garcin, 2017; Butera et al., 2019) and was recently  
855 identified as a deimination candidate in brain-cancer (Kosgodage et al., 2018), as well as in plasma-  
856 EVs of naked mole-rat and in harbour seal (Magnadottir et al., 2020b). Deimination of GAPDH  
857 identified here in fin whale may contribute to its multifaceted physiological functions.

858

859 **Haptoglobin** is an acute phase plasma protein and is in mammals involved in protection of oxidative  
860 damage by binding to haemoglobin (Andersen et al., 2017; Redmond et al., 2018). Haptoglobin has  
861 been described in a range of whales and dolphins, with some specific features identified (Travis et al.,  
862 1971; Yim et al., 2014). In aquatic animals it has been found to have roles in anti-viral immunity  
863 (Cordero et al., 2017). Haptoglobin was here found to be deiminated in minke whale serum and has

864 previously been identified as deiminated in nurse shark (Criscitiello et al., 2019), possibly adding to  
865 some of its functional diversity throughout phylogeny.

866

867 **Heat shock protein 90** (Hsp90) was here found to be deiminated in minke whale. Hsp90 is a  
868 phylogenetically highly conserved chaperone protein involved in protein folding, the stabilisation of  
869 proteins against heat stress and aids in protein degradation (Buchner 1999; Picard, 2002). Hsp90 also  
870 stabilizes a number of proteins required for tumour growth and is therefore important in anti-cancer  
871 drug investigations (Goetz et al., 2003). Hsp90 is responsible for most of the ATPase activity of the  
872 proteasome (Imai et al., 2003) and has an ATP binding region, which also is the main binding site of  
873 drugs, including anti-tumour drugs, that can be used to target Hsp90 (Chiosis et al., 2006). Hsp90 has  
874 previously been described to be post-translationally deiminated in rheumatoid arthritis, allowing  
875 deimination-induced shifts in protein structure to generate cryptic epitopes capable of bypassing B  
876 cell tolerance (Travers et al., 2016). HSP90 has also been verified as a deimination candidate in  
877 camelids (Criscitiello et al., 2020). Finding post-translational deimination of this protein throughout  
878 phylogeny supports translational investigations between species to further current understanding of  
879 HSP90 function, both in physiology and pathologies.

880

881 **Hemopexin** is a plasma glycoprotein and scavenger protein of haemoglobin and a predominant heme  
882 binding protein, which contributes to heme homeostasis (Smith and McCulloch, 2015; Immenschuh et  
883 al., 2017). Hemopexin also associates with high density lipoproteins (HDL), influencing their  
884 inflammatory properties (Mehta and Reddy, 2015). In relation to aquatic animals, hemopexin has  
885 been associated with physiological stresses, including increased water temperature, immune  
886 response and heavy metal exposure in fish (Kwon and Ghil, 2017; Diaz-Rosales et al., 2014). Here,  
887 hemopexin was found deiminated in minke whale serum. Previously, deimination of hemopexin has  
888 been found in teleost fish (Magnadottir et al., 2019a), in elasmobranch shark (Criscitiello et al., 2019),  
889 in naked mole-rat (Pamenter et al., 2019) and in camelid (Criscitiello et al., 2020). While hemopexin is  
890 a known glycoprotein, little is known regarding post-translational deimination for its function.

891

892 **Immunoglobulin (Ig) proteins** were identified here as being deiminated in minke whale serum. Ig's  
893 are key molecules in adaptive immunity and have been studied in whales (Andrésdóttir et al., 1987;  
894 Nollens et al., 2008). Furthermore, serum immunoglobulin levels have been associated with more  
895 active immune defences in free ranging bottlenose dolphins (*Tursiops truncatus*) compared to  
896 managed dolpins (Ruiz et al., 2009). Ig quantification assays have also been developed to assess  
897 immune function in orca (Taylor et al., 2002). Post-translational deimination of Ig's and roles in Ig

function have hitherto received little attention. In patients with bronchiectasis and RA, post-translational deimination of the IgG Fc region has been identified (Hutchinson et al., 2017). Deimination of Ig's in a range of taxa has recently been described by our group including teleost fish (Magnadottir et al., 2019a), elasmobranchs (Criscitiello et al., 2019), camelid (Criscitiello et al., 2020) and penguin seabirds (Phillips et al., 2020). Given the increased interest in furthering understanding of Ig diversity throughout phylogeny (Dooley and Flajnik, 2006; Smith et al., 2012; Zhang et al., 2013; de los Rios et al., 2015; Zhang et al., 2016; Zhang et al., 2017; Stanfield et al., 2018) our current finding of deimination of whale Ig's highlights a novel concept of diversification of their function via post-translational deimination.

907

908 ***Isocitrate dehydrogenase 1*** (IDH1) was here identified to be deiminated in fin whale only. It is found  
909 in the cytosol and in peroxisomes and involved in a major pathway for cellular NADPH generation  
910 (Golub et al., 2019). Mutations in IDH have been associated with cancer, leading to development of  
911 targeted cancer therapeutics (Golub et al., 2019), while post-translational deimination has, to our  
912 knowledge, not been described in any species before.

913

914 ***Keratins*** were here identified as deiminated in minke whale serum. Keratin cytoskeleton evolution  
915 has been extensively studied, including in marine mammals and whales (Sun et al., 2017; Ehrlich et al.,  
916 2019), with cetaceans displaying impaired terminal keratinocyte differentiation (Lopes-Marques et al.,  
917 2018). Baleen keratin is furthermore of some interest as a bioengineering material (Wang et al.,  
918 2019). In aquatic animals, roles for keratin in anti-bacterial defences have been shown in skin mucus,  
919 as keratin has pore-forming abilities. Keratin also serves as a first barrier to injury as a cytoskeletal  
920 protein (Molle et al., 2011). Downregulation of keratin II has for example been observed in *vibrio*  
921 infected fish (Rajan et al., 2013), while deiminated keratin was recently identified in teleost fish mucus  
922 (Magnadottir et al., 2018a), in birds (Phillips et al., 2020), naked mole-rat (Pamenter et al., 2019) and  
923 camelids (Criscitiello et al., 2020). In mammals, deimination of keratin is important including in skin  
924 physiology associated to cutaneous diseases (Chavanas et al., 2006; Ying et al., 2009); deimination  
925 indeed seems a phylogenetically conserved mechanism for facilitation of moonlighting functions of  
926 keratin.

927

928 ***Kininogen*** forms part of the acute phase response, has been described in whales (Semba et al., 2000)  
929 and was here identified to be deiminated in minke whale serum. Kininogen has been previously found  
930 to be deiminated in teleost fish (Magadottir et al., 2019a), Antarctic birds (Phillips et al., 2020), camelid  
931 (Criscitiello et al., 2020) and naked mole-rat (Pamenter et al., 2019). In mammals, elevated levels of

932 kininogen are linked to sepsis (Hofman et al., 2018) and inflammatory and oxidative stress pathways  
933 in type I diabetes (Al Hariri et al., 2017). To what extent kininogen function is dependent on post-  
934 translational deimination remains to be further investigated.

935

936 **Myoglobin** was identified as deiminated in humpback whale (*Megaptera novaeangliae*) and Cuvier's  
937 beaked whale (*Ziphius cavirostris*), while **hemoglobin** was identified as deiminated in minke whale.  
938 Both haemoglobin and myoglobin are key molecules in molecular oxygen transport in the bloodstream  
939 and for its storage in skeletal muscle. In diving cetaceans they contribute to hypoxia tolerance (Tian  
940 et al., 2016; Fago et al., 2017). Hemoglobin has furthermore been found to be a major binding protein  
941 for methylmercury in the liver of dolphins (Zayas et al., 2014). Myoglobin is found at higher  
942 concentrations in myocytes of deep diving animals compared to terrestrial animals and has been  
943 described in a range of whales (Isogai et al., 2018; Iwanami et al., 2006; Jones et al., 1979), including  
944 in humpback whale (Lehman et al., 1978), finback whale (DiMarchi et al., 1978) and minke whale  
945 (Lehman et al., 1977). The diving capacity of mammals is related to the myoglobin concentration in  
946 their myocytes. A more positive net surface charges of myoglobin are seen in diving animals compared  
947 to terrestrial animals, possibly to cause electrostatic repulsion among myoglobin molecules and to  
948 prevent their aggregation and maintain high protein concentration (Mirceta et al., 2013; Isogai et al.,  
949 2018). Therefore, post-translational deimination of myoglobin identified here in whales may be of  
950 considerable interest in relation to their physiological adaption to deep-diving. This correlates also  
951 with our recent findings of deiminated myoglobin and hemoglobin in pinnipeds, possibly playing roles  
952 in their adaption to hypoxic conditions (Magnadottir et al., 2020b).

953

954 **Plakoglobin** ( $\gamma$ -catenin) was here found to be deiminated in minke whale serum. It forms part of the  
955 Wnt signalling pathway, is a component of adherens junctions and desmosomes and plays therefore  
956 a vital role in the regulation of cell-cell adhesion (Aktary et al., 2017). Plakoglobin is also involved in  
957 the regulation of tumourigenesis and metastasis (Aktary et al., 2017). Plakoglobin is important in heart  
958 development and regeneration (Piven and Winata, 2017). Mutations in plakoglobin are for example  
959 linked to cardiomyopathies and Naxos disease (Li et al., 2018). Phosphorylation of plakoglobin has  
960 been described, through which it associates with cadherins (Shibata et al., 1994), and deimination of  
961 plakoglobin (junction plakoglobin) was recently identified in the naked mole-rat (Pamenter et al.,  
962 2019). Therefore its deimination identified here in whales, also long-lived and cancer-resistant  
963 animals, may be of some interest and further understanding of such post-translational changes  
964 contributing to plakoglobin functional diversity.

965

966 **Protein S100** was here identified as deiminated in minke whale. The S100 family of proteins in  
967 vertebrates participate in a variety of intracellular and extracellular functions. This includes regulation  
968 of protein phosphorylation and transcription factors, regulation of enzyme activities, cell growth and  
969 differentiation and inflammatory responses, including as damage associated molecular patterns  
970 (DAMPs) (Donato, 2003; Marenholz et al., 2004). In whales, S100B, a calcium-binding stress protein  
971 with pleiotropic function, has been found to be significantly enriched in the brain transcriptome  
972 compared to terrestrial mammals, possibly contributing to hypoxia tolerance (Fabrizius et al., 2016).  
973 Deimination of S100 proteins, as identified here, may indeed contribute to their pleiotropic functions  
974 throughout phylogeny.

975

976 **14-3-3 protein epsilon isoform X1** was here identified as deiminated in minke whale serum. 14-3-3  
977 protein are a conserved family of regulatory molecules, involved in signalling via binding to a range of  
978 kinases, transmembrane receptors and phosphatases (Bridges and Moorhead., 2005). 14-3-3 proteins  
979 are involved in a range of pathologies and linked to cancer, age-related neurodegenerative diseases  
980 and ageing (Fan et al., 2019). Furthermore, 14-3-3 proteins play roles in immunoglobulin class switch  
981 recombination and are therefore important for the immune response (Xu et al., 2012; Lam et al., 2013;  
982 Li et al., 2017). 14-3-3 proteins act also via conformational change (Bridges and Moorhead, 2005) and  
983 therefore the identification of post-translational deimination here may be of considerable interest.

984

985 **Recombination activating protein 1** (RAG1) was here identified as deiminated in Cuvier's beaked  
986 whale (*Ziphius cavirostris*) only. It is involved in immunoglobulin V-D-J recombination, which facilitates  
987 the generation of diverse repertoires of antigen receptors (Rodgers, 2017). RAG proteins are therefore  
988 critical for adaptive immune responses and are believed to have evolved from a mobile DNA element  
989 into a tightly controlled DNA recombinase in lymphocytes (Fugmann, 2010). In humans, mutation in  
990 RAG genes are related to a range of pathologies related to immune dysregulation (Notarangelo et al.,  
991 2016). In cetaceans, RAG1 has been identified in a range of species (McGowen et al., 2009). Post-  
992 translational deimination of RAG1 has not been identified in any species before to our knowledge and  
993 may possibly contribute to the diversification of adaptive immunity throughout phylogeny.

994

995 **Rootletin**, also known as ciliary rootlet coiled-coil protein (CROCC), was here identified as deiminated  
996 in minke whale. It is a protein that is required for centrosome cohesion and therefore plays important  
997 roles in mitosis (Bahe et al., 2005; Graser et al., 2007). Rootletin has been shown to be phosphorylated  
998 and to have the ability to form centriole-associated fibers, suggesting a dynamic model for centrosome  
999 cohesion based on entangling filaments (Bahe et al., 2005). Deletion of rootletin in mouse models

1000 causes photoreceptor degeneration and impaired mucociliary clearance, supporting its key function  
1001 in rootlet structures (Yang et al., 2005). Rootlets have been studied in the development of the nervous  
1002 terminalis in toothed whales (Oelschläger et al., 1987) and baleen whales (Oelschläger, 1989).  
1003 Rootletin was recently identified to be deiminated in camelid serum (Criscitiello et al., 2020) and its  
1004 deimination also identified here in minke whale may provide novel insights into its dynamic functions  
1005 via such post-translational modification.

1006

1007 **Selenoprotein P** (Sepp1) is a plasma glycoprotein, mainly secreted from liver but also other tissues  
1008 and contains most of the selenium in plasma (Mosert, 2000; Persson-Mochos, 2000; Burk and Hill,  
1009 2009). It has antioxidant properties (Mosert, 2000) and serves in homeostasis and distribution of  
1010 selenium (Burk and Hill, 2009). Phylogenetically Sepp1 is believed to have appeared in early metazoan  
1011 species and terrestrial animals have fewer selenoproteins than marine animals, which may be  
1012 reflected in different functions (Lobanov et al., 2008). While Sepp1 is known to be glycosylated, other  
1013 post-translational changes have not been studied. Besides its identification here as a protein  
1014 candidate for post-translational deimination, deimination was recently reported in Sepp1 in Antarctic  
1015 seabirds (Phillips et al., 2020).

1016

1017 **Serotransferrin** was here identified as deiminated in minke whale serum. It acts as an antimicrobial  
1018 agent and is at the frontier in innate immune mechanisms in some aquatic animals (Stafford and  
1019 Belosevic, 2003; Mohd-Padil et al., 2013). In bottlenose dolphins (*Tursiops truncatus*), differences in  
1020 transferrin levels of managed versus wild dolphins has been observed (Mazzaro et al., 2012), while in  
1021 fish increased serotransferrin is found in response to toxins (Kiriake et al., 2016). Serotransferrin was  
1022 recently identified to be deiminated in teleost fish (Magnadottir et al., 2018a), as well as in the naked  
1023 mole-rat (Pamenter et al., 2019).

1024

1025 **STE20-like serine/threonine-protein kinase isoform X2** was here found deiminated in minke whale  
1026 serum. STE20-like kinases form part of the Hippo signalling pathway which regulates the balance  
1027 between cell proliferation and apoptosis and is therefore involved in controlling organ size and tissue  
1028 homeostasis (Bae and Luo, 2018). It is for example involved in liver size control and regeneration, as  
1029 well as in tumourigenesis (Hong et al., 2015). Its deimination is here described for the first time to our  
1030 knowledge.

1031

1032 **Triose phosphate isomerase** (TPI) was here identified as deiminated in minke whale serum. TPI plays  
1033 an important role in glycolysis and is essential for efficient energy production. Besides roles in

1034 glycolysis, TPI is linked to lipid metabolism and is involved in ageing, metabolism and a range of human  
1035 diseases (Olivares-Illana et al., 2017). Other moonlighting functions identified for TPI are in sperm-egg  
1036 interactions (Petit et al., 2014). Deimination of TPI has not been described before to our knowledge.

1037

1038 **Vitamin D-binding protein (VDBP)** is a multifaceted protein mainly produced in the liver, where its  
1039 regulation is influenced by estrogen, glucocorticoids and inflammatory cytokines (Bikle and Schwartz,  
1040 2019). It is secreted into the blood circulation and is able to bind the various forms of vitamin D  
1041 (Verboven et al., 2002; Norman, 2008). It transports vitamin D metabolites between skin, liver and  
1042 kidney, as well as various target tissues (Norman, 2008). In minke whale, VDBP has been identified in  
1043 the liver transcriptome, is negatively correlated with polychlorinated biphenyl levels and therefore  
1044 may be a putative toxicology marker (Niimi et al., 2014). In humans, VDBP has been tested as an anti-  
1045 cancer agent via activation of macrophages against cancer cells (Yamamoto et al., 2008). Some  
1046 association has also been made between polymorphisms of VDBP and the risk of coronary artery  
1047 disease (Tarighi et al., 2017). Post-translational modifications of VDBP have been associated with  
1048 multiple sclerosis (MS) (Perga et al., 2015), although it remains to be exactly identified which these  
1049 post-translational modifications are. On the other hand, protein deimination is well known to be  
1050 associated with MS (Moscarello et al., 2013), while a link to VDBP has not been made in MS. VDBP has  
1051 previously been identified to be glycosylated (Kilpatrick and Phinney, 2017) and was found to be  
1052 deiminated in camelids (Criscitiello et al., 2020). Here it was identified as a deimination candidate in  
1053 minke whale. Post-translational deimination may contribute to various functions of VDBP in  
1054 physiological as well as pathophysiological processes.

1055

1056 **Vitronectin** (VTN) is a glycoprotein of the hemopexin family which is abundantly found in serum, the  
1057 extracellular matrix and in bone. VTN is identified as a key controller of mammalian tissue repair and  
1058 remodelling activity (Leavesley et al., 2013). It promotes cell adhesion and spreading. It also inhibits  
1059 the membrane-damaging effect of the terminal cytolytic complement pathway and binds to several  
1060 serine protease inhibitors (Felding-Habermann and Cheresh, 1993). VTN is also involved in  
1061 haemostasis and tumour malignancy (Preissner and Seiffert, 1998; Hurt et al., 2009). Deimination of  
1062 VTN has recently been described in wandering albatross (*Diomedea exulans*) plasma (Phillips et al.,  
1063 2020) and was here identified in minke whale, possibly contributing to some of its pleiotropic  
1064 functions throughout phylogeny.

1065

1066 **Xaa-Pro dipeptidase**, also known as prolidase, was here identified as deiminated in minke whale  
1067 serum. Post-translational modifications of prolidase have been shown to regulate its enzymatic

1068 abilities and in humans, deficiency in prolidase can cause a range of chronic, debilitating health  
1069 conditions (Viglio et al., 2006; Kitchener et al., 2012). Increased serum prolidase activity has also  
1070 been associated with oxidative stress in humans in relation to obesity (Aslan et al., 2017). Increased  
1071 levels of prolidase activity are associated to some cancers, leading to the development of proline  
1072 prodrugs (Mittal et al., 2005). Serum prolidase enzyme activity is also currently being explored as a  
1073 biomarker for diseases including chronic hepatitis B and liver fibrosis (Duygu et al., 2013; Şen et al.,  
1074 2014; Stanfliet et al., 2015). Phosphorylation of prolidase has been shown to increase its activity while  
1075 dephosphorylation leads to a decrease in enzyme activity. Post-translational demination of prolidase  
1076 has recently been described in the llama (Criscitiello et al., 2020), a species adapted to high altitude  
1077 and therefore tolerant of low oxygen levels. Studies into post-translational demination of Xaa-Pro  
1078 dipeptidase may add to current understanding of how this enzyme is regulated.

1079

1080 **MicroRNAs** (miRs) are highly conserved small non-coding RNAs that control gene expression and  
1081 regulate biological processes by targeting messenger RNAs (mRNAs). MiRs can inhibit post-  
1082 transcriptional translation of mRNA or enhance mRNA degradation (Bavelloni et al., 2017). Hitherto  
1083 no studies have been carried out on miRs in whales, while some expression profiling has been carried  
1084 out in dolphins with the aim to identify health related biomarkers in relation to organ injury (Segawa  
1085 et al., 2016). Diving animals, such as whales and orca, undergo physiological and morphological  
1086 changes needed for life in an aquatic environment, which are marked by resistance to physiological  
1087 stresses caused by a lack of oxygen, increased amounts of reactive oxygen species and high salt levels  
1088 (Yim et al., 2014). MiR210 has previously been identified as a major miR induced under hypoxia and  
1089 has important roles in mitochondrial metabolism, DNA damage response, cell proliferation and  
1090 apoptosis (Bavelloni et al., 2017). MiR210 has a role in regulating mitochondrial metabolism (Chen  
1091 et al., 2010) and cell glycolytic activity and is also linked to inflammation (Voloboueva et al., 2017).  
1092 MiR210 is also involved in angiogenesis and vascular remodelling (Fasanaro et al., 2008); for example,  
1093 mesenchymal stem cell derived EVs have been identified to be enriched in miR210 and to promote  
1094 angiogenesis in ischemic myocardium (Wang et al., 2017). MiR210 has been identified as a regulator  
1095 of the hypoxia pathway and to have pro-apoptotic functions under normal oxygen conditions, but  
1096 anti-apoptotic effects under hypoxic conditions (Favarro et al., 2010; Huang et al., 2010). In the current  
1097 study, miR210 was found to be highest expressed in orca, followed by humpback whale, Cuvier's  
1098 beaked whale, fin whale and minke whale and this may possibly reflect physiological differences  
1099 between these species in relation to mitochondrial metabolism and oxygen transport.  
1100 MiR21 is strongly conserved throughout evolution, is a main immunoregulatory and onco-related miR  
1101 and is also associated to chronic diseases (Musso et al., 2016, Južwik et al., 2019; Li et al., 2019). While

1102 many experimentally verified targets of miR21 are tumour suppressors, miR21 is also linked to cardiac  
1103 disease and oxidative stress (Xu et al., 2019). In the current study miR21 was found to be highly  
1104 expressed in humpback EVs, followed by minke whale EVs, but at lower levels in the other three  
1105 species, with lowest levels detected in Cuvier's beaked whale. Whether this difference is innate to the  
1106 whale's and orca's normal physiology, or due to differences in immune and health status of the  
1107 individual animals, remains to be further investigated as this could not be assessed in the current study  
1108 due to only one individual used per species. Roles for miR21 in immune responses of aquatic animals  
1109 have previously been identified in teleost fish, where miR21 was found to be up-regulated after  
1110 immune stimulation and to inhibit the expression of cytokines via regulation of Toll-like receptor  
1111 signalling (Bi et al., 2017).

1112 In mammals, miR155 is known to be a major inflammatory related miR, linked to inflammatory and  
1113 stress responses (Xiaoyan et al., 2017). In the current study miR155 was by far most highly expressed  
1114 in minke whale EVs, while fin whale, humpback whale and orca showed similar levels of miR155 and  
1115 lowest levels were seen in Cuvier's beaked whale. As no previous studies have been carried out on  
1116 these two miRs in cetaceans it remains to be fully understood which specific functions these have in  
1117 whale physiology. Furthermore, both miR21 and miR155 have been associated to viral infections in  
1118 fish (Andreassen and Høyheim, 2017), been found to be upregulated in fish exposed to chronic  
1119 [C<sub>8</sub>mim]Br induced inflammation (Ma et al., 2019) and related to changes in sea temperature in teleost  
1120 fish (Magnadottir et al., 2020a). Interspecies differences in miR expression observed here may indicate  
1121 that levels of these miRs vary between species, depending on their habitat and metabolic activity. This  
1122 may though also reflect different health status of the 5 animals used. As only one animal per species  
1123 was assessed in this pilot study, such species-specific differences need to be further evaluated in larger  
1124 sample cohorts.

1125  
1126 This is the first study to assess EV profiles and PAD-mediated protein deimination in cetaceans, while  
1127 recent studies on other pelagic animals such as teleost and elasmobranch fish as well as pinnipeds and  
1128 seabirds have recently been carried out (Iliev et al., 2018; Magnadottir et al., 2019b; 2020a; 2020b;  
1129 Criscitiello et al., 2019; Phillips et al., 2020), as well as on other mammals with unusual metabolism  
1130 (Pamenter et al., 2019; Criscitiello et al., 2020). Roles for PADs and EVs in have also been described in  
1131 parasite host-pathogen interactions (Gavinho et al., 2019), but remain to be further investigated for  
1132 parasite infections and other zoonotic diseases in aquatic mammals. Furthermore, we identified here  
1133 post-translational deimination of key immune factors of innate and adaptive immunity, as well as in  
1134 metabolism of the cetaceans assessed in the current study. These findings highlight novel aspects of  
1135 protein moonlighting functions of these immune proteins in sea mammals via post-translational

1136 deimination. Due to the limited annotation of the whale and orca genomes, the hits identified in this  
1137 study may though underestimate the amount of deiminated protein targets present in their sera,  
1138 although this was compensated for to some extent using a wider search by assessing protein targets  
1139 against a larger cetacean database, revealing a number of common KEGG pathways. Roles for miRs in  
1140 gene regulation, including in stress responses due to environmental changes, toxicology and infection,  
1141 are increasingly acknowledged and as miRs are known to be exported via EVs, changes in such EV  
1142 cargo may be of considerable interest. An important finding of the current study is that EVs were a  
1143 better source for miR analysis compared to whole sera, with EVs posing as better diagnostic markers  
1144 than whole serum.

1145 Findings of the current study touch upon a hugely understudied and emerging field of EV research in  
1146 diverse taxa, in relation to sea mammal health and for the development of EV-related biomarkers to  
1147 assess health status of wild sea animals in response to pollution, opportunistic infections as well as in  
1148 response to changing sea temperatures and shift in habitat due to global warming. Orcas are for  
1149 example among the world's most PCB-contaminated marine mammals, raising concerns about  
1150 implications for their health (Buckman et al., 2011). Furthermore, findings in long-lived mammals that  
1151 display cancer resistance, including cetaceans, may be of considerable translational value for  
1152 furthering understanding of mechanisms underlying cancer resistance for improved development of  
1153 human cancer therapies (Seluanov et al., 2018) and novel insights into potentially unique non-age-  
1154 related mechanisms of carcinogenesis across species (Pesavento et al., 2018). Such comparative  
1155 studies furthermore provide translational value for mechanisms involved insulin resistance  
1156 (Tsagkogeorga et al., 2015), as well as revealing molecular signatures of longevity (Ma and Gladyshev,  
1157 2017).

1158 In continuation of the current pilot study, further assessment of changes in deiminated proteins, EV  
1159 profile and miR expression will be of great interest to assess health status of wild sea mammals in  
1160 response to infection, environmental temperature and toxicology. In addition, wider sampling within  
1161 and between populations would enable comparisons with normal physiological protein deimination  
1162 status and EV-profiles. This would be particularly valuable for assessing natural and anthropogenic  
1163 stresses in cetaceans in general, many of which face increasing threats related to changing climate.  
1164 While the current study lays a base-line for these novel biomarkers, future studies will need to further  
1165 refine and develop these markers as an applicable tool in the evaluation of cetacean health status.

1166

1167 **Acknowledgements**

1168 The authors would like to thank Michael Deery and Yagnesh Umrania at the Cambridge Centre for  
1169 Proteomics for the LC-MS/MS analysis. This study was funded in part by a University of Westminster  
1170 start-up grant to SL. Thanks are also due to The Guy Foundation for funding the purchase of equipment  
1171 utilised in this work.

1172

1173 **Credit Author Statement**

1174 **BM:** Resources; Validation; Writing - review & editing

1175 **PU-O:** Formal analysis; Resources; Validation; Visualisation, Writing - review & editing.

1176 **IK:** Formal analysis; Resources; Validation; Visualization.

1177 **VS:** Resources; Validation; Writing - review & editing.

1178 **PH:** Formal analysis; Validation; Visualisation, Writing - review & editing.

1179 **SL:** Conceptualization; Data curation; Formal analysis; Funding acquisition; Investigation;  
1180 Methodology; Project administration; Resources; Validation; Visualization; Writing - original draft;  
1181 Writing - review & editing.

1182

1183 **References**

1184 Aktary, Z., Alaee, M., Pasdar, M., 2017. Beyond cell-cell adhesion: Plakoglobin and the regulation of  
1185 tumorigenesis and metastasis. *Oncotarget* 8(19), 32270-32291.

1186

1187 Al Hariri, M., Elmedawar, M., Zhu, R., Jaffa, M.A., Zhao, J., Mirzaei, P., Ahmed, A., Kobeissy, F., Ziyadeh,  
1188 F.N., Mechref,Y., Jaffa, A.A., 2017. Proteome profiling in the aorta and kidney of type 1 diabetic rats.  
1189 *PLoS One* 12(11), e0187752.

1190

1191 Almabouada, F., Diaz-Ruiz, A., Rabanal-Ruiz, Y., Peinado, J.R., Vazquez-Martinez, R., Malagon, M.M.,  
1192 2013. Adiponectin receptors form homomers and heteromers exhibiting distinct ligand binding and  
1193 intracellular signaling properties. *J. Biol. Chem.* 288(5), 3112-25.

1194

1195 Amiral, J., Seghatchian, J., 2018. Revisiting antithrombin in health and disease, congenital deficiencies  
1196 and genetic variants, and laboratory studies on  $\alpha$  and  $\beta$  forms. *Transfus. Apher. Sci.* 57(2), 291-297.

1197

1198 Amrine-Madsen, H., Koepfli, K.P., Wayne, R.K., Springer, M.S., 2003. A new phylogenetic marker,  
1199 apolipoprotein B, provides compelling evidence for eutherian relationships. *Mol. Phylogenetic. Evol.*  
1200 28(2), 225-40.

1201

1202 Andersen, L.H., Miserez, A.R., Ahmad, Z., Andersen, R.L., 2016. Familial defective apolipoprotein B-  
1203 100: A review. *J. Clin. Lipidol.* 10(6), 1297-1302.

1204

1205 Andersen, C.B.F., Stødkilde, K., Sæderup, K.L., Kuhlee, A., Raunser, S., Graversen, J.H., Moestrup, S.K.  
1206 Haptoglobin., 2017. *Antioxid Redox Signal.* 26(14), 814-831.

1207

1208 Andreassen, R., Høyheim, B., 2017. miRNAs associated with immune response in teleost fish. *Dev.*  
1209 *Comp. Immunol.* 75, 77-85.

1210

- 1211 Andrésdóttir, V., Magnadóttir, B., Andrésson, O.S., Pétursson, G., 1987. Subclasses of IgG from whales.  
1212 Dev. Comp. Immunol. 11(4), 801-6.
- 1213
- 1214 Arciello, A., Piccoli, R., Monti, D.M., 2016. Apolipoprotein A-I: the dual face of a protein. FEBS Lett.  
1215 590(23), 4171-4179.
- 1216
- 1217 Armstrong, P. B., Quigley, J.P., 1999. Alpha2-macroglobulin: an evolutionarily conserved arm of the  
1218 innate immune system. Dev. Comp. Immunol. 23, 375.
- 1219
- 1220 Aslan, M., Duzenli, U., Esen, R., Soyoral, Y.U., 2017. Serum prolidase enzyme activity in obese subjects  
1221 and its relationship with oxidative stress markers. Clin. Chim. Acta. 473, 186-190.
- 1222
- 1223 Augustin, P., Hromic, A., Pavkov-Keller, T., Gruber, K., Macheroux, P., 2016. Structure and biochemical  
1224 properties of recombinant human dimethylglycine dehydrogenase and comparison to the disease-  
1225 related H109R variant. FEBS J. 283(19), 3587-3603.
- 1226
- 1227 Bachman, M.J., Foltz, K.M., Lynch, J.M., West, K.L., Jensen, B.A., 2015. Using cytochrome P4501A1  
1228 expression in liver and blubber to understand effects of persistent organic pollutant exposure in  
1229 stranded Pacific Island cetaceans. Environ. Toxicol. Chem. 34(9), 1989-95.
- 1230
- 1231 Bae, S.J., Luo, X., 2018. Activation mechanisms of the Hippo kinase signaling cascade. Biosci.Rep. 38(4),  
1232 pii, BSR20171469.
- 1233
- 1234 Bahe, S., Stierhof, Y.D., Wilkinson, C.J., Leiss, F., Nigg, E.A., 2005. Rootletin forms centriole-associated  
1235 filaments and functions in centrosome cohesion. J. Cell. Biol. 171(1), 27-33.
- 1236
- 1237 Bao, Y., Wang, L., Shi, L. et al., 2019. Transcriptome profiling revealed multiple genes and ECM-  
1238 receptor interaction pathways that may be associated with breast cancer. Cell Mol. Biol. Lett. 24, 38.
- 1239
- 1240 Barbe, A., Bongrani, A., Mellouk, N., Estienne, A., Kurowska, P., Grandhaye, J., Elfassy, Y., Levy, R., Rak,  
1241 A., Froment, P., et al., 2019. Mechanisms of adiponectin action in fertility: An overview from  
1242 gametogenesis to gestation in humans and animal models in normal and pathological conditions. Int.  
1243 J. Mol. Sci. 20, 1526.
- 1244
- 1245 Barreira da Silva, R., Laird, M.E., Yatim, N., Fiette, L., Ingersoll, M.A., Albert, M.L., 2015. Dipeptidylpeptidase 4 inhibition enhances lymphocyte trafficking, improving both naturally occurring  
1246 tumor immunity and immunotherapy. Nat. Immunol. 16(8), 850-8.
- 1247
- 1248 Bavelloni, A., Ramazzotti, G., Poli, A., Piazzesi, M., Focaccia, E., Blalock, W., Faenza, I., 2017. Anticancer  
1249 Res. 37(12), 6511-6521.
- 1250
- 1251 Beineke, A., Siebert, U., Wohlsein, P., Baumgärtner, W, 2010. Immunology of whales and dolphins.  
1252 Vet. Immunol. Immunopathol. 133(2-4), 81-94.
- 1253
- 1254 Bendrick, J.L., Eldredge, L.A., Williams, E.I., Haight, N.B., Dubash, A.D., 2019. Desmoplakin Harnesses  
1255 Rho GTPase and p38 Mitogen-Activated Protein Kinase Signaling to Coordinate Cellular Migration. J.  
1256 Invest. Dermatol. 139(6), 1227-1236.
- 1257
- 1258 Besser, M.W., MacDonald, S.G., 2016. Acquired hypofibrinogenemia: Current perspectives. J. Blood  
1259 Med. 7, 217–225.
- 1260
- 1261

- 1262 Bharathan, N.K., Dickinson, A.J.G., 2019. Desmoplakin is required for epidermal integrity and  
1263 morphogenesis in the *Xenopus laevis* embryo. Dev. Biol. 450(2), 115-131.
- 1264
- 1265 Bi, D., Cui, J., Chu, Q., Xu, T., 2017. MicroRNA-21 contributes to suppress cytokines production by  
1266 targeting TLR28 in teleost fish. Mol. Immunol. 83, 107-114.
- 1267
- 1268 Bicker, K.L., Thompson, P.R., 2013. The protein arginine deiminases: Structure, function, inhibition,  
1269 and disease. Biopolymers 99(2), 155-63.
- 1270
- 1271 Bielecka, E., Scavenius, C., Kantyka, T., Jusko, M., Mizgalska, D., Szmigielski, B., Potempa, B., Enghild,  
1272 J.J., Prossnitz, E.R., Blom, A.M., Potempa, J., 2014. Peptidyl arginine deiminase from *Porphyromonas*  
1273 *gingivalis* abolishes anaphylatoxin C5a activity. J. Biol. Chem. 289(47), 32481-7.
- 1274
- 1275 Bikle, D.D., Schwartz, J., 2019. Vitamin D Binding Protein, Total and Free Vitamin D Levels in Different  
1276 Physiological and Pathophysiological Conditions. Front. Endocrinol. (Lausanne). 10,317.
- 1277
- 1278 Bird, A., 2007. Perceptions of epigenetics. Nature 447, 396–398.
- 1279
- 1280 Blachère, N.E., Parveen, S., Frank, M.O., Dill, B.D., Molina, H., Orange, D.E., 2017. High-Titer  
1281 Rheumatoid Arthritis Antibodies Preferentially Bind Fibrinogen Citrullinated by Peptidylarginine  
1282 Deiminase 4. Arthritis Rheumatol. 69(5), 986-995.
- 1283
- 1284 Blanco-Abad, V., Noia, M., Valle, A., Fontenla, F., Folgueira, I., De Felipe, A.P., Pereiro, P., Leiro, J.,  
1285 Lamas, J., 2018. The coagulation system helps control infection caused by the ciliate parasite  
1286 *Philasterides dicentrarchi* in the turbot *Scophthalmus maximus* (L.). Dev. Comp. Immunol. 87, 147-  
1287 156.
- 1288
- 1289 Boradia, V.M., Raje, M., Raje, C.I., 2014. Protein moonlighting in iron metabolism: glyceraldehyde-3-  
1290 phosphate dehydrogenase (GAPDH). Biochem. Soc. Trans. 42(6), 1796-801.
- 1291
- 1292 Borchman, D., Stimmelmayr, R., George, J.C., 2017. Whales, lifespan, phospholipids, and cataracts. J  
1293 Lipid Res. 58(12), 2289-2298.
- 1294
- 1295 Borrell, A., Saiz, L., Víkingsson, G.A., Gaufier, P., López Fernández, A., Aguilar, A., 2018. Fin whales as  
1296 bioindicators of multi-decadal change in carbon and oxygen stable isotope shifts in the North Atlantic.  
1297 Mar. Environ. Res. 138, 129-134.
- 1298
- 1299 Braun, B.A., Marcovitz, A., Camp, J.G., Jia, R., Bejerano, G., 2015. Mx1 and Mx2 key antiviral proteins  
1300 are surprisingly lost in toothed whales. Proc. Natl. Acad. Sci. USA 112, 8036–8040.
- 1301
- 1302 Branzk, N., Lubojemska, A., Hardison, S.E., Wang, Q., Gutierrez, M.G., Brown, G.D., Papayannopoulos,  
1303 V., 2014. Neutrophils sense microbe size and selectively release neutrophil extracellular traps in  
1304 response to large pathogens. Nat. Immunol. 15(11), 1017-25.
- 1305
- 1306 Bridges, D., Moorhead, G.B., 2005. 14-3-3 proteins: a number of functions for a numbered protein.  
1307 Sci. STKE. 2005 (296), re10.
- 1308
- 1309 Brinkmann, V., Reichard, U., Goosmann, C., Fauler, B., Uhlemann, Y., Weiss, D.S., Weinrauch, Y.,  
1310 Zychlinsky, A., 2004. Neutrophil extracellular traps kill bacteria. Science 303, 1532–1535.
- 1311

- 1312 Brown, D.G., Rao, S., Weir, T.L., O'Malia, J., Bazan, M., Brown, R.J., Ryan, E.P., 2016. Metabolomics and  
1313 metabolic pathway networks from human colorectal cancers, adjacent mucosa, and stool. *Cancer*  
1314 *Metab.* 4, 11.
- 1315
- 1316 Buchner, J., 1999. Hsp90 & Co. - a holding for folding. *Trends Biochem. Sci.* 24 (4), 136–41.
- 1317
- 1318 Buckman, A.H., Veldhoen, N., Ellis, G., Ford, J.K., Helbing, C.C., Ross, P.S., 2011. PCB-associated  
1319 changes in mRNA expression in killer whales (*Orcinus orca*) from the NE Pacific Ocean. *Environ. Sci.*  
1320 *Technol.* 45(23), 10194-202.
- 1321
- 1322 Burk, R.F., Hill, K.E., 2009. Selenoprotein P-expression, functions, and roles in mammals. *Biochim.*  
1323 *Biophys. Acta* 1790(11), 1441-7.
- 1324
- 1325 Butera, G., Mullappilly, N., Masetto, F., Palmieri, M., Scupoli, M.T., Pacchiana, R., Donadelli, M., 2019.  
1326 Regulation of Autophagy by Nuclear GAPDH and Its Aggregates in Cancer and Neurodegenerative  
1327 Disorders. *Int. J. Mol. Sci.* 20(9), pii E2062.
- 1328
- 1329 Carlton, J.G., Caballe, A., Agromayor, M., Kloc, M., Martin-Serrano, J., 2012. ESCRT-III governs the  
1330 Aurora B-mediated abscission checkpoint through CHMP4C. *Science* 336(6078), 220-5.
- 1331
- 1332 Carroll, M.V., Sim, R.B., 2011. Complement in health and disease. *Adv. Drug Deliv. Rev.* 63(12), 965-  
1333 75.
- 1334
- 1335 Chavanas, S., Méchin, M.C., Nachat, R., Adoue, V., Coudane, F., Serre, G., Simon, M., 2006.  
1336 Peptidylarginine deiminases and deimination in biology and pathology: relevance to skin homeostasis.  
1337 *J. Dermatol. Sci.* 44(2), 63-72.
- 1338
- 1339 Chen, Z., Li, Y., Zhang, H., Huang, P., Luthra, R., 2010. Hypoxia-regulated microRNA-210 modulates  
1340 mitochondrial function and decreases ISCU and COX10 expression. *Oncogene* 29, 4362-4368.
- 1341
- 1342 Chen R., Kang R., Fan X.-G., Tang D., 2014. Release and activity of histone in diseases. *Cell Death Dis.*  
1343 5, e1370.
- 1344
- 1345 Chen, L., Song, J., Chen, X., Chen, K., Ren, J., Zhang, N., Rao, M., Hu, Z., Zhang, Y., Gu, M., Zhao, H.,  
1346 Tang, H., Yang, Z., Hu, S., 2019. A novel genotype-based clinicopathology classification of  
1347 arrhythmogenic cardiomyopathy provides novel insights into disease progression. *Eur. Heart J.* 40(21),  
1348 1690-1703.
- 1349
- 1350 Chen, Y.L., Tao, J., Zhao, P.J., Tang, W., Xu, J.P., Zhang, K.Q., Zou, C.G., 2019. Adiponectin receptor  
1351 PAQR-2 signaling senses low temperature to promote *C. elegans* longevity by regulating autophagy.  
1352 *Nat. Commun.* 10(1), 2602.
- 1353
- 1354 Chevalier, R.L., 2016. The proximal tubule is the primary target of injury and progression of kidney  
1355 disease: role of the glomerulotubular junction. *Am. J. Physiol. Renal Physiol.* 311(1), F145-61.
- 1356
- 1357 Chiosis, G., Caldas Lopes, E., Solit, D., 2006. Heat shock protein-90 inhibitors: a chronicle from  
1358 geldanamycin to today's agents. *Curr. Opin. Investigig. Drugs* 7 (6), 534–41.
- 1359
- 1360 Colombo, M., Raposo, G., Théry, C., 2014. Biogenesis, secretion, and intercellular interactions of  
1361 exosomes and other extracellular vesicles. *Annu. Rev. Cell Dev. Biol.* 30, 255–289.
- 1362

- 1363 Cordero, H., Li, C.H., Chaves-Pozo, E., Esteban, M.Á., Cuesta, A., 2017. Molecular identification and  
1364 characterization of haptoglobin in teleosts revealed an important role on fish viral infections. Dev.  
1365 Comp. Immunol. 76, 189-199.
- 1366
- 1367 Criscitiello, M.F., Kraev, I., Lange, S. 2019. Deiminated Proteins in Extracellular Vesicles and Plasma of  
1368 Nurse Shark (*Ginglymostoma cirratum*)- Novel Insights into Shark Immunity. Fish Shellfish Immunol.  
1369 92, 249-255.
- 1370
- 1371 Cuppari, A., Körschgen, H., Fahrenkamp, D., Schmitz, C., Guevara, T., Karmilin, K., Kuske, M., Olf, M.,  
1372 Dietzel, E., Yiallouros, I., de Sanctis, D., Goulas, T., Weiskirchen, R., Jahnens-Decent, W., Floehr, J.,  
1373 Stoecker, W., Jovine, L., Gomis-Rüth, F.X., 2019. Structure of mammalian plasma fetuin-B and its  
1374 mechanism of selective metallopeptidase inhibition. IUCrJ. 6(Pt 2), 317-330.
- 1375
- 1376 Davies, S.G., Sim, R.B., 1981. Intramolecular general acid catalysis in the binding reactions of alpha 2-  
1377 macroglobulin and complement components C3 and C4. Biosci. Rep. 1(6), 461-8.
- 1378
- 1379 de los Rios, M., Criscitiello, M.F., Smider, V.V., 2015. Structural and genetic diversity in antibody  
1380 repertoires from diverse species. Curr. Opin. Struct. Biol. 33, 27-41.
- 1381
- 1382 Desforges, J.P., Ross, P.S., Dangerfield, N., Palace, V.P., Whiticar, M., Loseto, L.L., 2013. Vitamin A and  
1383 E profiles as biomarkers of PCB exposure in beluga whales (*Delphinapterus leucas*) from the western  
1384 Canadian Arctic. Aquat. Toxicol. 142-143, 317-28.
- 1385
- 1386 Del Rio-Tsonis, K., Tsonis, P.A., Zarkadis, I.K., Tsagas, A.G., Lambris, J.D., 1998. Expression of the third  
1387 component of complement, C3, in regenerating limb blastema cells of urodeles. J. Immunol. 161(12),  
1388 6819-24.
- 1389
- 1390 Di Guardo, G., Centellegher, C., Mazzariol, S., 2018. Cetacean Host-Pathogen Interaction(s): Critical  
1391 Knowledge Gaps. Front. Immunol. 9, 2815.
- 1392
- 1393 Di Guardo, G., Mazzariol, S., 2019. Cetacean morbillivirus: A Land-to-Sea Journey and Back? Virol. Sin.  
1394 34(3), 240-242.
- 1395
- 1396 Diaz-Rosales, P., Pereiro, P., Figueras, A., Novoa, B., Dios, S., 2014. The warm temperature acclimation  
1397 protein (Wap65) has an important role in the inflammatory response of turbot (*Scophthalmus*  
1398 *maximus*). Fish Shellfish Immunol. 41(1), 80-92.
- 1399
- 1400 Dietrich, M.A., Hliwa, P., Adamek, M., Steinhagen, D., Karol, H., Ciereszko A., 2018. Acclimation to cold  
1401 and warm temperatures is associated with differential expression of male carp blood proteins involved  
1402 in acute phase and stress responses, and lipid metabolism. Fish Shellfish Immunol. 76, 305-315.
- 1403
- 1404 Di Guardo, G., Criscitiello, M.F., Sierra, E., Mazzariol, S., 2019. Editorial: Comparative Immunology of  
1405 Marine Mammals. Front. Immunol. 10, 2300.
- 1406
- 1407 DiMarchi, R.D., Wang, C.C., Hemenway, J.B., Gurd, F.R., 1978. Complete amino acid sequence of the  
1408 major component myoglobin of finback whale (*Balaenoptera physalus*). Biochemistry 17(10), 1968-  
1409 70.
- 1410
- 1411 Dodds, A.W., 2002. Which came first, the lectin/classical pathway or the alternative pathway of  
1412 complement? Immunobiology 205(4-5), 340-54.
- 1413

- 1414 Dodds, A.W., Law, S.K., 1998. The phylogeny and evolution of the thioester bond-containing proteins  
1415 C3, C4 and alpha 2-macroglobulin. *Immunol. Rev.* 166, 15-26.
- 1416
- 1417 Donato, R., 2003. Intracellular and extracellular roles of S100 proteins. *Microsc. Res. Tech.* 60(6), 540-  
1418 51.
- 1419
- 1420 Dooley, H., Flajnik, M.F., 2006. Antibody repertoire development in cartilaginous fish. *Dev. Comp.  
1421 Immunol.* 30(1-2), 43-56.
- 1422
- 1423 Duygu, F., Aksoy, N., Cicek, A.C., Butun, I., Unlu, S., 2013. Does prolidase indicate worsening of  
1424 hepatitis B infection? *J. Clin. Lab. Anal.* 27 (5), 398-401.
- 1425
- 1426 Ehrlich, F., Fischer, H., Langbein, L., Praetzel-Wunder, S., Ebner, B., Figlak, K., Weissenbacher, A., Sipos,  
1427 W., Tschachler, E., Eckhart, L., 2019. Differential Evolution of the Epidermal Keratin Cytoskeleton in  
1428 Terrestrial and Aquatic Mammals. *Mol. Biol. Evol.* 36(2), 328-340.
- 1429
- 1430 Ermert, D., Blom, A.M., 2016. C4b-binding protein: The good, the bad and the deadly. Novel functions  
1431 of an old friend. *Immunol. Lett.* 169, 82-92.
- 1432
- 1433 Fabrizius, A., Hoff, M.L., Engler, G., Folkow, L.P., Burmester, T., 2016. When the brain goes diving:  
1434 transcriptome analysis reveals a reduced aerobic energy metabolism and increased stress proteins in  
1435 the seal brain. *BMC Genomics* 17, 583.
- 1436
- 1437 Fago, A., Parraga, D.G., Petersen, E.E., Kristensen, N., Giouri, L., Jensen, F.B., 2017. A comparison of  
1438 blood nitric oxide metabolites and hemoglobin functional properties among diving mammals. *Comp.  
1439 Biochem. Physiol. A Mol. Integr. Physiol.* 205, 35-40.
- 1440
- 1441 Fan, X., Cui, L., Zeng, Y., Song, W., Gaur, U., Yang, M., 2019. 14-3-3 Proteins Are on the Crossroads of  
1442 Cancer, Aging, and Age-Related Neurodegenerative Disease. *Int. J. Mol. Sci.* 20(14), pii, E3518.
- 1443
- 1444 Fang, L., Hu, X., Cui, L., Lv, P., Ma, X., Ye, Y., 2019. Serum and follicular fluid fetuin-B levels are  
1445 correlated with fertilization rates in conventional IVF cycles. *J. Assist. Reprod. Genet.* 36(6), 1101-1107.
- 1446
- 1447 Fasanaro, P., D'Alessandra, Y., Di Stefano, V., Melchionna, R., Romani, S., Pompilio, G., Capogrossi,  
1448 M.C., Martelli, F., 2008. MicroRNA-210 modulates endothelial cell response to hypoxia and inhibits  
1449 the receptor tyrosine kinase ligand ephrin-A3. *J. Biol. Chem.* 283, 15878-15883.
- 1450
- 1451 Favaro, E., Ramachandran, A., McCormick, R., Gee, H., Blancher, C., Crosby, M., Devlin, C., Blick, C.,  
1452 Buffa, F., Li, J-L., Vojnovic, B., Pires das Neves, R., Glazer, P., Iborra, F., Ivan, M., Ragoussis, J., Harris,  
1453 A.L., 2010. MicroRNA-210 regulates mitochondrial free radical response to hypoxia and krebs cycle in  
1454 cancer cells by targeting iron sulfur cluster protein ISCU. *PLoS One* 5, e10345.
- 1455
- 1456 Felding-Habermann, B., Cheresh, D.A., 1993. Vitronectin and its receptors. *Curr. Opin. Cell Biol.* 5 (5),  
1457 864-8.
- 1458
- 1459 Fernández, A., Edwards, J.F., Rodríguez, F., Espinosa de los Monteros, A., Herráez, P., Castro, P., Jaber,  
1460 J.R., Martín, V., Arbelo, M. 2005. "Gas and fat embolic syndrome" involving a mass stranding of beaked  
1461 whales (family *Ziphiidae*) exposed to anthropogenic sonar signals. *Vet. Pathol.* 42, 446-57.
- 1462
- 1463 Fiaschi, T., 2019. Mechanisms of Adiponectin Action. *Int J Mol Sci.* 20(12), pii, E2894.
- 1464

- 1465 Fiaschi, T., Magherini, F., Gamberi, T., Modesti, P.A., Modesti, A., 2014. Adiponectin as a tissue  
1466 regenerating hormone: More than a metabolic function. *Cell. Mol. Life Sci.* 71, 1917–1925.  
1467
- 1468 Fan, T., Zhang, C., Zong, M., Fan, L., 2018. Hypoxia-induced autophagy is inhibited by PADI4  
1469 knockdown, which promotes apoptosis of fibroblast-like synoviocytes in rheumatoid arthritis. *Mol.*  
1470 *Med. Rep.* 17(4), 5116-5124.  
1471
- 1472 Firat, O., Kargin, F., 2010. Individual and combined effects of heavy metals on serum biochemistry of  
1473 Nile tilapia *Oreochromis niloticus*. *Arch. Environ. Contam. Toxicol.* 58(1), 151-7.  
1474
- 1475 Fishelson, Z., Attali, G., Mevorach, D., 2001. Complement and apoptosis. *Mol. Immunol.* 38(2-3) 207-  
1476 19.  
1477 Foster, E.M., Dangla-Valls, A., Lovestone, S., Ribe, E.M., Buckley, N.J., 2019. Clusterin in Alzheimer's  
1478 Disease: Mechanisms, Genetics, and Lessons From Other Pathologies. *Front. Neurosci.* 13, 164.  
1479
- 1480 Frankenberg, A.D.V., Reis, A.F., Gerchman, F., 2017. Relationships between adiponectin levels, the  
1481 metabolic syndrome, and type 2 diabetes: a literature review. *Arch. Endocrinol. Metab.* 61(6), 614-  
1482 622.  
1483
- 1484 French, L.E., Wohlwend, A., Sappino, A.P., Tschoopp, J., Schifferli, J.A., 1994. Human clusterin gene  
1485 expression is confined to surviving cells during in vitro programmed cell death. *J. Clin. Invest.* 93(2),  
1486 877-84.  
1487
- 1488 Fry, B., Carter, J.F., 2019. Stable carbon isotope diagnostics of mammalian metabolism, a high-  
1489 resolution isotomics approach using amino acid carboxyl groups. *PLoS One* 14(10), e0224297.  
1490
- 1491 Fugmann, S.D., 2010. The origins of the Rag genes--from transposition to V(D)J recombination. *Semin.*  
1492 *Immunol.* 22(1), 10-6.  
1493
- 1494 Gamberi, T., Magherini, F., Fiaschi, T., 2019. Adiponectin in myopathies. *Int. J. Mol. Sci.* 20, 1544.  
1495
- 1496 Gatesy, J., 1997. More DNA support for a Cetacea/Hippopotamidae clade: the blood-clotting protein  
1497 gene gamma-fibrinogen. *Mol. Biol. Evol.* 14(5), 537-43.  
1498
- 1499 Gatesy, J., Geisler, J.H., Chang, J., Buell, C., Berta, A., Meredith, R.W., Springer, M.S., McGowen, M.R.,  
1500 2013. A phylogenetic blueprint for a modern whale. *Mol. Phylogenet. Evol.* 66(2), 479-506.  
1501
- 1502 Gavinho, B., Rossi, I. V., Evans-Osses, I., Lange, S., Ramirez, M. I., 2019. Peptidylarginine deiminase  
1503 inhibition abolishes the production of large extracellular vesicles from *Giardia intestinalis*, affecting  
1504 host-pathogen interactions by hindering adhesion to host cells. *bioRxiv* 586438. 10.1101/586438.  
1505
- 1506 Gelain, ME, Bonsembiante, F., 2019. Acute Phase Proteins in Marine Mammals: State of Art,  
1507 Perspectives and Challenges. *Front. Immunol.* 10, 1220.  
1508
- 1509 Gertow, J., Ng, C.Z., Mamede Branca, R.M., Werngren, O., Du, L., Kjellqvist, S., Hemmingsson, P.,  
1510 Bruchfeld, A., MacLaughlin, H., Eriksson, P., Axelsson, J., Fisher, R.M., 2017. Altered Protein  
1511 Composition of Subcutaneous Adipose Tissue in Chronic Kidney Disease. *Kidney Int. Rep.* 2(6), 1208-  
1512 1218.  
1513

- 1514 Goetz, M.P., Toft, D.O., Ames, M.M., Erlichman, C., 2003. The Hsp90 chaperone complex as a novel  
1515 target for cancer therapy. *Ann. Oncol.* 14 (8), 1169–76.
- 1516
- 1517 Golub, D., Iyengar, N., Dogra, S., Wong, T., Bready, D., Tang, K., Modrek, A.S., Placantonakis, D.G.,  
1518 2019. Mutant Isocitrate Dehydrogenase Inhibitors as Targeted Cancer Therapeutics. *Front. Oncol.* 9,  
1519 417.
- 1520
- 1521 Gonzalez-Aparicio, M., Alfaro, C., 2019. Influence of Interleukin-8 and Neutrophil Extracellular Trap  
1522 (NET) Formation in the Tumor Microenvironment: Is There a Pathogenic Role? *J. Immunol. Res.* 2019,  
1523 6252138.
- 1524
- 1525 Goksøyr, A., 1995. Cytochrome P450 in marine mammals: isozyme forms, catalytic functions, and  
1526 physiological regulations. *Dev. in Marine Biol.* 4, 629–639.
- 1527
- 1528 Graser, S., Stierhof, Y.D., Nigg, E.A., 2007. Cep68 and Cep215 (Cdk5rap2) are required for centrosome  
1529 cohesion. *J. Cell Sci.* 120 (24), 4321–31.
- 1530
- 1531 Guo, W., Zheng, Y., Xu, B., Ma, F., Li, C., Zhang, X., Wang, Y., Chang, X., 2017. *Onco Targets Ther.* 10,  
1532 1475–1485.
- 1533
- 1534 Guzmán-Flores, J.M., Flores-Pérez, E.C., Hernández-Ortiz, M., Vargas-Ortiz, K., Ramírez-Emiliano, J.,  
1535 Encarnación-Guevara, S., Pérez-Vázquez, V., 2018. Protein Expression Profile of Twenty-Week-Old  
1536 Diabetic db/db and Non-Diabetic Mice Livers: A Proteomic and Bioinformatic Analysis. *Biomolecules*  
1537 8(2), pii E35.
- 1538
- 1539 György, B., Toth, E., Tarcsa, E., Falus, A., Buzas, E.I., 2006. Citrullination: a posttranslational  
1540 modification in health and disease. *Int. J. Biochem. Cell Biol.* 38, 1662–77.
- 1541
- 1542 Hagiwara T., Hidaka Y., Yamada M., 2005. Deimination of histone H2A and H4 at arginine 3 in HL-60  
1543 granulocytes. *Biochemistry* 44, 5827–5834.
- 1544
- 1545 Hall, T.A., 1999. BioEdit: a user-friendly biological sequence alignment editor and analysis program  
1546 for Windows 95/98/NT. *Nucl. Acids. Symp. Ser.* 41, 95–98.
- 1547
- 1548 Hamilton, K.K., Zhao, J., Sims, P.J., 1993. Interaction between apolipoproteins A-I and A-II and the  
1549 membrane attack complex of complement. Affinity of the apoproteins for polymeric C9. *J. Biol. Chem.*  
1550 268(5), 3632–8.
- 1551
- 1552 Haynes, T., Luz-Madrigal, A., Reis, E.S., Echeverri Ruiz, N.P., Grajales-Esquivel, E., Tzekou, A., Tsionis,  
1553 P.A., Lambris, J.D., Del Rio-Tsonis, 2013. Complement anaphylatoxin C3a is a potent inducer of  
1554 embryonic chick retina regeneration. *Nat. Commun.* 4, 2312.
- 1555
- 1556 Henderson, B., Martin, A.C., 2014. Protein moonlighting: a new factor in biology and medicine.  
1557 *Biochem. Soc. Trans.* 42(6), 1671–8.
- 1558
- 1559 Henry, M.A., Nikoloudaki, C., Tsigenopoulos, C., Rigos, G., 2015. Strong effect of long-term Sparicotyle  
1560 chrysophrii infection on the cellular and innate immune responses of gilthead sea bream, *Sparus*  
1561 *aurata*. *Dev. Comp. Immunol.* 51(1), 185–93.
- 1562
- 1563 Hessvik, N.P., Llorente, A., 2018. Current knowledge on exosome biogenesis and release. *Cell Mol. Life  
1564 Sci.* 75, 193–208.

- 1565  
1566 Hida, S., Miura, N.N., Adachi, Y., Ohno, N., 2004. Influence of arginine deimination on antigenicity of  
1567 fibrinogen. *J. Autoimmun.* 23(2), 141-50.  
1568  
1569 Hochachka, P.W., Owen, T.G., Allen, J.F., Whittow, G.C., 1975. Multiple end products of anaerobiosis  
1570 in diving vertebrates. *Comp. Biochem. Physiol. B.* 50(1), 17-22.  
1571  
1572 Hofman, Z.L.M., De Maat, S., Maas, C., 2018. High-molecular-weight kininogen: breaking bad in  
1573 lethal endotoxemia. *J. Thromb. Haemost.* 16(2), 193-195.  
1574  
1575 Hong, L., Cai, Y., Jiang, M., Zhou, D., Chen, L., 2015. The Hippo signaling pathway in liver regeneration  
1576 and tumorigenesis. *Acta Biochim. Biophys. Sin (Shanghai)*. 47(1), 46-52.  
1577  
1578 Huang, X., Le, Q-T., Giaccia, A.J., 2010. MiR-210 – micromanager of the hypoxia pathway. *Trends Mol.*  
1579 *Med.* 16, 230-237.  
1580  
1581 Hughes-Austin, J.M., Deane, K.D., Giles, J.T., Derber, L.A., Zerbe, G.O., Dabelea, D.M., Sokolove, J.,  
1582 Robinson, W.H., Holers, V.M., Norris, J.M., 2018. Plasma adiponectin levels are associated with  
1583 circulating inflammatory cytokines in autoantibody positive first-degree relatives of rheumatoid  
1584 arthritis patients. *PLoS One* 13(6), e0199578.  
1585  
1586 Hunt, K.E., Lysiak, N.S., Robbins, J., Moore, M.J., Seton, R.E., Torres, L., Buck, C.L., 2017. Multiple  
1587 steroid and thyroid hormones detected in baleen from eight whale species. *Conserv. Physiol.* 5(1),  
1588 cox061.  
1589  
1590 Hunt, K.E., Robbins, J., Buck, C.L., Bérubé, M., Rolland, R.M., 2019. Evaluation of fecal hormones for  
1591 noninvasive research on reproduction and stress in humpback whales (*Megaptera novaeangliae*).  
1592 *Gen. Comp. Endocrinol.* 280, 24-34.  
1593  
1594 Hutchinson, D., Clarke, A., Heesom, K., Murphy, D., Eggleton, P., 2017. Carbamylation/citrullination of  
1595 IgG Fc in bronchiectasis, established RA with bronchiectasis and RA smokers: a potential risk factor for  
1596 disease. *ERJ. Open Res.* 3(3), pii, 00018-2017.  
1597  
1598 Hurt, Elaine, M. Chan, King Serrat, Maria Ana Duhagon, Thomas, Suneetha B., Veenstra, Timothy D.,  
1599 Farrar, William L., 2009. Identification of Vitronectin as an Extrinsic Inducer of Cancer Stem Cell  
1600 Differentiation and Tumor Formation. *Stem Cells* 28: N/A–N/A. doi:10.1002/stem.271  
1601  
1602 Iliev, D., Strandskog, G., Nepal, A., Aspar, A., Olsen, R., Jørgensen, J., Wolfson, D., Ahluwalia, B.S.,  
1603 Handzhiyski, J., Mironova, R., 2018. Stimulation of exosome release by extracellular DNA is conserved  
1604 across multiple cell types. *FEBS J.* doi: 10.1111/febs.14601.  
1605  
1606 Imai, J., Maruya, M., Yashiroda, H., Yahara, I., Tanaka, K., 2003. The molecular chaperone Hsp90 plays  
1607 a role in the assembly and maintenance of the 26S proteasome. *EMBO J.* 22 (14), 3557–67.  
1608  
1609 Imlau, M., Conejeros, I., Muñoz-Caro, T., Zhou, E., Gärtner, U., Ternes, K., Taubert, A., Hermosilla, C.,  
1610 2020. Dolphin-derived NETosis results in rapid *Toxoplasma gondii* tachyzoite ensnarement and  
1611 different phenotypes of NETs. *Dev. Comp. Immunol.* 103:103527.  
1612  
1613 Immenschuh, S., Vijayan, V., Janciauskiene, S., Gueler, F., 2017. Heme as a Target for Therapeutic  
1614 Interventions. *Front. Pharmacol.* 8, 146  
1615

- 1616 Inal, J.M., Ansa-Addo, E.A., Lange, S., 2013. Interplay of host-pathogen microvesicles and their role in  
1617 infectious disease. *Biochem. Soc. Trans.* 1;41(1), 258-62.
- 1618
- 1619 Isogai, Y., Imamura, H., Nakae, S., Sumi, T., Takahashi, K.I., Nakagawa, T., Tsuneshige, A., Shirai, T.,  
1620 2018. Tracing whale myoglobin evolution by resurrecting ancient proteins. *Sci. Rep.* 8(1), 16883.
- 1621
- 1622 Iwanami, K., Mita, H., Yamamoto, Y., Fujise, Y., Yamada, T., Suzuki, T., 2006. cDNA-derived amino acid  
1623 sequences of myoglobins from nine species of whales and dolphins. *Comp. Biochem. Physiol. B*  
1624 *Biochem. Mol. Biol.* 145(2), 249-56.
- 1625
- 1626 Jeffrey, C.J., 2018. Protein moonlighting: what is it, and why is it important? *Philos. Trans. R. Soc. Lond.*  
1627 *B. Biol. Sci.* 373(1738), pii 20160523.
- 1628
- 1629 Jenne, D.E., Lowin, B., Peitsch, M.C., Böttcher, A., Schmitz, G., Tschopp, J., 1991. Clusterin  
1630 (complement lysis inhibitor) forms a high density lipoprotein complex with apolipoprotein A-I in  
1631 human plasma. *J. Biol. Chem.* 266(17), 11030-6.
- 1632
- 1633 Jepson, P.D. , Bennett, P.M., Allchin, C.R. , Law, R.J. , Kuiken, T., Baker, J.R. , Rogan, E. , Kirkwood, J.K.,  
1634 1999. Investigating potential associations between chronic exposure to polychlorinated biphenyls and  
1635 infectious disease mortality in harbour porpoises from England and Wales. *Sci. Total Environ.* 243/244,  
1636 339-348.
- 1637
- 1638 Jo, W.K., Kruppa, J., Habierski, A., van de Bildt, M., Mazzariol, S., Di Guardo, G., Siebert, U., Kuiken, T.,  
1639 Jung, K., Osterhaus, A., Ludlow, M., 2018. Evolutionary evidence for multi-host transmission of  
1640 cetacean morbillivirus. *Emerg. Microbes Infect.* 7(1), 201.
- 1641
- 1642 Jones, B.N., Rothgeb, T.M., England, R.D., Gurd, F.R., 1979. Complete amino acid sequence of the  
1643 myoglobin from the Pacific sei whale, *Balaenoptera borealis*. *Biochim. Biophys. Acta* 577(2), 464-74.
- 1644
- 1645 Jones, S.E., Jomary, C., 2002. Clusterin. *Int. J. Biochem. Cell Biol.* 34(5), 427-31.
- 1646
- 1647 Jordan, R.E., 1983. Antithrombin in vertebrate species: Conservation of the heparin-dependent  
1648 anticoagulant mechanism. *Arch. Biochem. Biophys.* 227 (2), 587–595.
- 1649
- 1650 Józsi, M., Schneider, A.E., Kárpáti, É., Sándor, N., 2019. Complement factor H family proteins in their  
1651 non-canonical role as modulators of cellular functions. *Semin. Cell. Dev. Biol.* 85, 122-131.
- 1652
- 1653 Juntti-Berggren, L., Berggren, P.O., 2017. Apolipoprotein CIII is a new player in diabetes. *Curr. Opin.*  
1654 *Lipidol.* 28(1), 27-31.
- 1655
- 1656 Juźwik, C.A., Drake, S.S., Zhang, Y., Paradis-Isler, N., Sylvester, A., Amar-Zifkin, A., Douglas, C.,  
1657 Morquette, B., Moore, C.S., Fournier, A., 2019. *Prog. Neurobiol.* 26, 101664.
- 1658
- 1659 Kadowaki, T., Yamauchi, T., 2005. Adiponectin and adiponectin receptors. *Endocr. Rev.* 26, 439–451.
- 1660
- 1661 Kennedy, S., 1998. Morbillivirus infections in aquatic mammals *J. Comp. Pathol.* 119, 201-225.
- 1662
- 1663 Kholia, S., Jorfi, S., Thompson, P.R., Causey, C.P., Nicholas, A.P., Inal, J.M., Lange, S., 2015. A novel role  
1664 for peptidylarginine deiminases in microvesicle release reveals therapeutic potential of PAD inhibition  
1665 in sensitizing prostate cancer cells to chemotherapy. *J. Extracell. Vesicles.* 4, 26192.
- 1666

- 1667 Kilpatrick, L.E., Phinney, K.W., 2017. Quantification of Total Vitamin-D-Binding Protein and the  
1668 Glycosylated Isoforms by Liquid Chromatography-Isotope Dilution Mass Spectrometry. *J. Proteome*  
1669 *Res.* 16(11), 4185-4195.
- 1670
- 1671 Kiriake, A., Ohta, A., Suga, E., Matsumoto, T., Ishizaki, S., Nagashima, Y., 2016. Comparison of  
1672 tetrodotoxin uptake and gene expression in the liver between juvenile and adult tiger pufferfish,  
1673 *Takifugu rubripes*. *Toxicon.* 111, 6-12.
- 1674
- 1675 Kitchener, R.L., Grunden, A.M., 2012. Prolidase function in proline metabolism and its medical and  
1676 biotechnological applications. *J. Applied Microbiol.* 113 (2), 233–47.
- 1677
- 1678 Klos, A., Tenner, A.J., Johswich, K.O., Ager, R.R., Reis, E.S., Köhl, J., 2009. The role of the anaphylatoxins  
1679 in health and disease. *Mol. Immunol.* 46(14), 2753-66.
- 1680
- 1681 Kojouharova, M.S., Gadjeva, M.G., Tsacheva, I.G., Zlatarova, A., Roumenina, L.T., Tchorbadjieva, M.I.,  
1682 Atanasov, B.P., Waters, P., Urban, B.C., Sim, R.B., Reid, K.B., Kishore, U., 2004. Mutational analyses of  
1683 the recombinant globular regions of human C1q A, B, and C chains suggest an essential role for  
1684 arginine and histidine residues in the C1q-IgG interaction. *J. Immunol.* 172(7), 4351-8.
- 1685
- 1686 Kosgodage, U.S., Trindade, R.P., Thompson, P.R., Inal, J.M., Lange, S., 2017. Chloramidine/Bisindolylmaleimide-I-Mediated Inhibition of Exosome and Microvesicle Release and  
1687 Enhanced Efficacy of Cancer Chemotherapy. *Int. J. Mol. Sci.* 18, 1007.
- 1688
- 1689 Kosgodage, U.S., Onganer, P.U., Maclatchy, A., Nicholas, A.P., Inal, J.M., Lange, S., 2018. Peptidylarginine Deiminases Post-translationally Deiminate Prohibitin and Modulate Extracellular  
1690 Vesicle Release and miRNAs 21 and 126 in Glioblastoma Multiforme. *Int. J. Mol. Sci.* 20(1), pii, E103.
- 1691
- 1692 Kosgodage, U.S., Matewele, P., Mastroianni, G., Kraev, I., Brotherton, D., Awamaria, B., Nicholas, A.P.,  
1693 Lange, S., Inal, J.M., 2019. Peptidylarginine Deiminase Inhibitors Reduce Bacterial Membrane Vesicle  
1694 Release and Sensitize Bacteria to Antibiotic Treatment. *Front. Cell Infect. Microbiol.* 9, 227.
- 1695
- 1696 Kovacevic, N., Hagen, M.O., Xie J., Belosevic, M., 2015. The analysis of the acute phase response during  
1697 the course of Trypanosoma carassii infection in the goldfish (*Carassius auratus* L.). *Dev. Comp.  
1700 Immunol.* 53(1), 112-22.
- 1701
- 1702 Kumar, S., Stecher, G., Li, M., Knyaz, C., Tamura, K., 2018. MEGAX: Molecular Evolutionary Analysis  
1703 across computing platforms. *Mol. Biol. Evol.* 35, 1547-1549.
- 1704
- 1705 Kwon, G., Ghil, S., 2017. Identification of warm temperature acclimation-associated 65-kDa protein-2  
1706 in Kumgang fat minnow *Rhynchocypris kumgangensis*. *J. Exp. Zool. A. Ecol. Integr. Physiol.* 327(10),  
1707 611-619.
- 1708
- 1709 Lam, T., Thomas, L.M., White, C.A., Li, G., Pone, E.J., Xu, Z., Casali, P., 2013. Scaffold functions of 14-3-  
1710 3 adaptors in B cell immunoglobulin class switch DNA recombination. *PLoS One* 8(11), e80414.
- 1711
- 1712 Lange, S., Gudmundsdottir, B.K., Magnadottir, B., 2001. Humoral immune parameters of cultured  
1713 Atlantic halibut (*Hippoglossus hippoglossus* L.). *Fish Shellfish Immunol.* 11(6), 523-35.
- 1714
- 1715 Lange, S., Bambir, S., Dodds, A.W., Magnadottir, B., 2004a. The ontogeny of complement component  
1716 C3 in Atlantic Cod (*Gadus morhua* L.)—an immunohistochemical study. *Fish Shellfish Immunol.* 16,  
1717 359-367.

- 1718  
1719 Lange, S., Bambir, S., Dodds, A.W., Magnadottir, B., 2004b. An immunohistochemical study on  
1720 complement component C3 in juvenile Atlantic halibut (*Hippoglossus hippoglossus* L.). Dev. Comp.  
1721 Immunol. 28(6), 593-601.
- 1722  
1723 Lange, S., Dodds, A.W., Gudmundsdóttir, S., Bambir, S.H., Magnadottir, B., 2005. The ontogenetic  
1724 transcription of complement component C3 and Apolipoprotein A-I tRNA in Atlantic cod (*Gadus*  
1725 *morhua* L.) - a role in development and homeostasis? Dev. Comp. Immunol. 29(12), 1065-77.
- 1726  
1727 Lange, S., Bambir, S.H., Dodds, A.W., Bowden, T., Bricknell, I., Espelid, S., Magnadottir, B., 2006.  
1728 Complement component C3 transcription in Atlantic halibut (*Hippoglossus hippoglossus* L.) larvae. Fish  
1729 Shellfish Immunol. 20(3), 285-94.
- 1730  
1731 Lange, S., Gögel, S., Leung, K.Y., Vernay, B., Nicholas, A.P., Causey, C.P., Thompson, P.R., Greene, N.D.,  
1732 Ferretti, P., 2011. Protein deiminases: new players in the developmentally regulated loss of neural  
1733 regenerative ability. Dev. Biol. 355(2), 205-14.
- 1734  
1735 Lange, S., Rocha-Ferreira, E., Thei, L., Mawjee, P., Bennett, K., Thompson, P.R., Subramanian, V.,  
1736 Nicholas, A.P., Peebles, D., Hristova, M., Raivich, G., 2014. Peptidylarginine deiminases: novel drug  
1737 targets for prevention of neuronal damage following hypoxic ischemic insult (HI) in neonates. J.  
1738 Neurochem. 130(4), 555-62.
- 1739  
1740 Lange, S., Gallagher, M., Kholia, S., Kosgodage, U.S., Hristova, M., Hardy, J., Inal, J.M., 2017.  
1741 Peptidylarginine Deiminases-Roles in Cancer and Neurodegeneration and Possible Avenues for  
1742 Therapeutic Intervention via Modulation of Exosome and Microvesicle (EMV) Release? Int. J. Mol. Sci.  
1743 18(6), pii E1196.
- 1744  
1745 Lange, S., Kraev, I., Magnadóttir, B., Dodds, A.W., 2019. Complement component C4-like protein in  
1746 Atlantic cod (*Gadus morhua* L.) - Detection in ontogeny and identification of post-translational  
1747 deimination in serum and extracellular vesicles. Dev. Comp. Immunol. 101, 103437.
- 1748  
1749 Latham J.A., Dent S.Y., 2007. Cross-regulation of histone modifications. Nat. Struct. Mol. Biol. 14,  
1750 1017–1024.
- 1751  
1752 Leavesley, D.I., Kashyap, A.S., Croll, T., Sivaramakrishnan, M., Shokoohmand, A., Hollier, B.G., Upton,  
1753 Z., 2013. Vitronectin--master controller or micromanager? IUBMB Life. 65(10), 807-18.
- 1754  
1755 Lee, C., Bongcam-Rudloff, E., Sollner, C., Jahnens-Dechent, W., Claesson-Welsh, L., 2009. Type 3  
1756 cystatins; fetuins, kininogen and histidine-rich glycoprotein. Front. Biosci. (Landmark Ed). 14, 2911-22.
- 1757  
1758 Lee, K.H., Kronbichler, A., Park, D.D., Park, Y., Moon, H., Kim, H., Choi, J.H., Choi, Y., Shim, S., Lyu, I.S.,  
1759 et al., 2017. Neutrophil extracellular traps (NETs) in autoimmune diseases: A comprehensive review.  
1760 Autoimmun. Rev. 16(11), 1160-1173.
- 1761  
1762 Lehman, L.D., Dwulet, F.E., Bogardt, R.A. Jr, Jones, B.N., Gurd, F.R., 1977. The complete amino acid  
1763 sequence of the major component myoglobin from the arctic minke whale, *Balaenoptera*  
1764 *acutorostrata*. Biochemistry 16(4), 706-9.
- 1765  
1766 Lehman, L.D., Dwulet, F.E., Jones, B.N., Bogardt, R.A. Jr., Krueckeberg, S.T., Visscher, R.B., Gurd,F.R.,  
1767 1978. Complete amino acid sequence of the major component myoglobin from the humpback whale,  
1768 *Megaptera novaeangliae*. Biochemistry 17(18), 3736-9.

- 1769  
1770 Li, P., Li, M., Lindberg, M.R., Kennett, M.J., Xiong, N., Wang, Y., 2010. PAD4 is essential for antibacterial  
1771 innate immunity mediated by neutrophil extracellular traps. *J. Exp. Med.* 207(9), 1853-62.  
1772  
1773 Li, X., Li, X., Cao, H., Wang, Y., Zheng, S.J., 2013. Engagement of new castle disease virus (NDV) matrix  
1774 (M) protein with charged multivesicular body protein (CHMP) 4 facilitates viral replication. *Virus Res.*  
1775 171(1), 80-8.  
1776  
1777 Li, C., Gao, C., Fu, Q., Su, B., Chen, J., 2017. Identification and expression analysis of fetuin B (FETUB) in  
1778 turbot (*Scophthalmus maximus* L.) mucosal barriers following bacterial challenge. *Fish Shellfish*  
1779 *Immunol.* 68, 386-394.  
1780  
1781 Li, F., Huang, Y., Huang, Y.Y., Kuang, Y.S., Wei, Y.J., Xiang, L., Zhang, X.J., Jia, Z.C., Jiang, S., Li, J.Y., Wan,  
1782 Y., 2017. MicroRNA-146a promotes IgE class switch in B cells via upregulating 14-3-3 $\sigma$  expression. *Mol.*  
1783 *Immunol.* 92, 180-189.  
1784  
1785 Li, G.L., Saguner, A.M., Fontaine, G.H., 2018. Naxos disease: from the origin to today. *Orphanet J. Rare*  
1786 *Dis.* 13(1), 74.  
1787  
1788 Li, J., Li, K., Chen, X., 2019. Inflammation-regulatory microRNAs: Valuable targets for intracranial  
1789 atherosclerosis. *J. Neurosci. Res.* 97(10), 1242-1252.  
1790  
1791 Liang, J., Li C., Zhang, Z., Ni, C., Yu, H., Li, M., Yao, Z., 2019. Severe dermatitis, multiple allergies and  
1792 metabolic wasting (SAM) syndrome caused by de novo mutation in the DSP gene misdiagnosed as  
1793 generalized pustular psoriasis and treatment of acitretin with gabapentin. *J. Dermatol.* 46(7), 622-625.  
1794  
1795 Lin, M., Liu, C., Liu, Y., Wang, D., Zheng, C., Shi, X., Chen, Z., Liu, J., Li, X., Yang, S., Li, Z., 2019. Fetuin-B  
1796 Links Nonalcoholic Fatty Liver Disease to Chronic Kidney Disease in Obese Chinese Adults: A Cross-  
1797 Sectional Study. *Ann. Nutr. Metab.* 74(4), 287-295.  
1798  
1799 Liu, H., Peatman, E., Wang, W., Abernathy, J., Liu, S., Kucuktas, H., Terhune, J., Xu, D.H., Klesius, P., Liu,  
1800 Z., 2011. Molecular responses of ceruloplasmin to *Edwardsiella ictaluri* infection and iron overload in  
1801 channel catfish (*Ictalurus punctatus*). *Fish Shellfish Immunol.* 30(3), 992-7.  
1802  
1803 Liu, G., Hou, G., Li, L., Li, Y., Zhou, W., Liu, L., 2016. Potential diagnostic and prognostic marker  
1804 dimethylglycine dehydrogenase (DMGDH) suppresses hepatocellular carcinoma metastasis in vitro  
1805 and in vivo. *Oncotarget* 7(22), 32607-16.  
1806  
1807 Liu, R., Zhao, P., Zhang, Q., Che, N., Xu, L., Qian, J., Tan, W., Zhang, M., 2019. Adiponectin promotes  
1808 fibroblast-like synoviocytes producing IL-6 to enhance T follicular helper cells response in rheumatoid  
1809 arthritis. *Clin Exp Rheumatol.* 2019 Apr 11. [Epub ahead of print]  
1810  
1811 Livak, K.J., Schmittgen, T.D., 2001. Analysis of relative gene expression data using real-time  
1812 quantitative PCR and the 2(-Delta Delta C(T)) method. *Methods* 25, 402-408.  
1813  
1814 Lobanov, A.V., Hatfield, D.L., Gladyshev, V.N., 2008. Reduced reliance on the trace element selenium  
1815 during evolution of mammals. *Genome Biol.* 9, R62.  
1816  
1817 Lopes-Marques, M., Machado, A.M., Barbosa, S., Fonseca, M.M., Ruivo, R., Castro, L.F.C., 2018.  
1818 Cetacea are natural knockouts for IL20. *Immunogenetics* 70(10), 681-687.  
1819

- 1820 Lu, Z., Wang, F., Liang, M., 2017. SerpinC1/Antithrombin III in kidney-related diseases. *Clin. Sci (Lond)*.  
1821 131(9), 823-831.
- 1822
- 1823 Lü, A., Hu, X., Wang, Y., Shen, X., Zhu, A., Shen, L., Ming, Q., Feng, Z., 2013. Comparative analysis of  
1824 the acute response of zebrafish *Danio rerio* skin to two different bacterial infections. *J. Aquat. Anim.*  
1825 *Health* 25(4), 243-51.
- 1826
- 1827 Ma, S., Gladyshev, V.N., 2017. Molecular signatures of longevity: Insights from cross-species  
1828 comparative studies. *Semin. Cell Dev. Biol.* 70, 190-203.
- 1829
- 1830 Ma, J., Chen, X., Xin, G., Li, X., 2019. Chronic exposure to the ionic liquid [C8mim]Br induces  
1831 inflammation in silver carp spleen: Involvement of oxidative stress-mediated p38MAPK/NF-κB  
1832 signalling and microRNAs. *Fish Shellfish Immunol.* 84, 627-638.
- 1833
- 1834 Magnadottir, B., Hayes, P., Hristova, M., Bragason, B.P., Nicholas, A.P., Dodds, A.W., Guðmundsdóttir,  
1835 S., Lange, S., 2018a. Post-translational Protein Deimination in Cod (*Gadus morhua* L.) Ontogeny –  
1836 Novel Roles in Tissue Remodelling and Mucosal Immune Defences? *Dev. Comp. Immunol.* 87, 157-  
1837 170.
- 1838
- 1839 Magnadottir, B., Hayes, P., Gísladóttir, B., Bragason, B.P., Hristova, M., Nicholas, A.P.,  
1840 Guðmundsdóttir, S., Lange, S., 2018b. Pentraxins CRP-I and CRP-II are post-translationally deiminated  
1841 and differ in tissue specificity in cod (*Gadus morhua* L.) ontogeny. *Dev. Comp. Immunol.* 87, 1-11.
- 1842
- 1843 Magnadottir, B., Bragason, B.T., Bricknell, I.R., Bowden T., Nicholas, A.P., Hristova, M.,  
1844 Guðmundsdóttir, S., Dodds, A.W., Lange, S., 2019a. Peptidylarginine Deiminase and Deiminated  
1845 Proteins are detected throughout Early Halibut Ontogeny - Complement Components C3 and C4 are  
1846 post-translationally Deiminated in Halibut (*Hippoglossus hippoglossus* L.). *Dev. Comp. Immunol.* 92, 1-  
1847 19.
- 1848
- 1849 Magnadottir, B., Kraev, I., Guðmundsdóttir, S., Dodds, A.W., Lange S., 2019b. Extracellular Vesicles  
1850 from Cod (*Gadus morhua* L.) Mucus contain Innate Immune Factors and Deiminated Protein Cargo.  
1851 *Dev. Comp. Immunol.* 99, 103397.
- 1852
- 1853 Magnadottir, B., Uysal-Organer, P., Kraev, I., Dodds, A.W., Guðmundsdóttir, S., Lange, S., 2020a.  
1854 Extracellular vesicles, deiminated protein cargo and microRNAs are novel serum biomarkers for  
1855 environmental rearing temperature in Atlantic cod (*Gadus morhua* L.). *Aquaculture Research* 16,  
1856 100245.
- 1857
- 1858 Magnadottir, B., Uysal-Organer, P., Kraev, I., Svansson, V., Skirnisson, K., Lange, S., 2020b. Deiminated  
1859 Proteins and Extracellular Vesicles as Novel Biomarkers in Pinnipeds: Grey seal (*Halichoerus grypus*)  
1860 and Harbour seal (*Phoca vitulina*). *Biochimie, under review*.
- 1861
- 1862 Magnusson, M., Wang, T.J., Clish, C., Engström, G., Nilsson, P., Gerszten, R.E., Melander, O., 2015.  
1863 Dimethylglycine Deficiency and the Development of Diabetes. *Diabetes* 64(8), 3010-6.
- 1864
- 1865 Maluf, N.S.R., Gassman, J.J., 1998. Kidneys of the killer whale and significance of reniculism. *Anat. Rec.*  
1866 250, 34-44.
- 1867
- 1868 Mardpour, S., Hamidieh, A.A., Taleahmad, S., Sharifzad, F., Taghikhani, A., Baharvand, H., 2019.  
1869 Interaction between mesenchymal stromal cell-derived extracellular vesicles and immune cells by  
1870 distinct protein content. *J. Cell Physiol.* 234(6), 8249-8258.

- 1871  
1872 Marenholz, I., Heizmann, C.W., Fritz, G., 2004. S100 proteins in mouse and man: from evolution to  
1873 function and pathology (including an update of the nomenclature). *Biochem. Biophys. Res. Commun.*  
1874 322(4), 1111-22.  
1875  
1876 Martínez, D., Oyarzún, R., Pontigo, J.P., Romero, A., Yáñez, A.J., Vargas-Chacoff, L., 2017. Nutritional  
1877 Immunity Triggers the Modulation of Iron Metabolism Genes in the Sub-Antarctic Notothenioid  
1878 *Eleginops maclovinus* in Response to *Piscirickettsia salmonis*. *Front. Immunol.* 8, 1153.  
1879  
1880 Martineau, D., Lair, S., De Guise, S., Lipscomb, T.P., Beland, P., 1999. Cancer in beluga whales from the  
1881 St Lawrence estuary, Quebec, Canada: a potential biomarker of environmental contamination  
1882 *J. Cetacean Res. Manage.* 83, 249-265  
1883  
1884 Mazzariol, S., Corrò, M., Tonon, E., Biancani, B., Centellegher, C., Gili, C., 2018. Death Associated to  
1885 Methicillin Resistant *Staphylococcus aureus* ST8 Infection in Two Dolphins Maintained Under Human  
1886 Care, Italy. *Front. Immunol.* 9, 2726.  
1887  
1888 Mazzaro, L.M., Johnson, S.P., Fair, P.A., Bossart, G., Carlin, K.P., Jensen, E.D., Smith, C.R., Andrews,  
1889 G.A., Chavey, P.S., Venn-Watson, S., 2012. Iron indices in bottlenose dolphins (*Tursiops truncatus*).  
1890 *Comp. Med.* 62(6), 508-15.  
1891  
1892 McCoy, A.J., Pei, X.Y., Skinner, R., Abrahams, J.P., Carrell, R.W., 2003. Structure of beta-antithrombin  
1893 and the effect of glycosylation on antithrombin's heparin affinity and activity. *J. Mol. Biol.* 326 (3),  
1894 823–833.  
1895  
1896 McGowen, M.R., Spaulding, M., Gatesy, J., 2009. Divergence date estimation and a comprehensive  
1897 molecular tree of extant cetaceans. *Mol. Phylogenet. Evol.* 53(3), 891-906.  
1898  
1899 McGowen, M.R., Gatesy, J., Wildman, D.E., 2014. Molecular evolution tracks macroevolutionary  
1900 transitions in Cetacea. *Trends Ecol. Evol.* 29, 336–346.  
1901  
1902 Mehta, N.U., Reddy, S.T., 2015. Role of hemoglobin/heme scavenger protein hemopexin in  
1903 atherosclerosis and inflammatory diseases. *Curr. Opin. Lipidol.* 26(5), 384-7.  
1904  
1905 Meex, R.C.R., Watt, M.J., 2017. Hepatokines: linking nonalcoholic fatty liver disease and insulin  
1906 resistance. *Nat. Rev. Endocrinol.* 13(9), 509-520.  
1907  
1908 Meredith, R.W., Janečka, J.E., Gatesy, J., Ryder, O.A., Fisher, C.A., Teeling, E.C., Goodbla, A., Eizirik, E.,  
1909 Simão, T.L., Stadler, T., Rabosky, D.L., Honeycutt, R.L., Flynn, J.J., Ingram, C.M., Steiner, C., Williams,  
1910 T.L., Robinson, T.J., Burk-Herrick, A., Westerman, M., Ayoub, N.A., Springer, M.S., Murphy, W.J., 2011.  
1911 Impacts of the Cretaceous Terrestrial Revolution and KPg extinction on mammal diversification.  
1912 *Science* 334(6055), 521-4.  
1913  
1914 Metcalf, V.J., Brennan, S.O., Chambers, G.K., George, P.M., 1998. The albumin of the brown trout  
1915 (*Salmo trutta*) is a glycoprotein. *Biochim. Biophys. Acta.* 1386(1), 90-6.  
1916  
1917 Metcalf, V.J., George, P.M., Brennan, S.O., 2007. Lungfish albumin is more similar to tetrapod than to  
1918 teleost albumins: purification and characterisation of albumin from the Australian lungfish,  
1919 *Neoceratodus forsteri*. *Comp. Biochem. Physiol. B Biochem. Mol. Biol.* 147(3), 428-37.  
1920

- 1921 Mirceta, S., Signore, A.V., Burns, J.M., Cossins, A.R., Campbell, K.L., Berenbrink, M., 2013. Evolution of  
1922 mammalian diving capacity traced by myoglobin net surface charge. *Science* 340(6138), 1234192.
- 1923
- 1924 Mittal, S., Song, X., Vig, B.S., Landowski, C.P., Kim, I., Hilfinger, JM., Amidon, G.L., 2005. Prolidase, a  
1925 potential enzyme target for melanoma: design of proline-containing dipeptide-like prodrugs. *Mol.*  
1926 *Pharm.* 2 (1), 37–46.
- 1927
- 1928 Mohd-Padil, H., Mohd-Adnan, A., Gabaldón, T., 2013. Phylogenetic analyses uncover a novel clade of  
1929 transferrin in nonmammalian vertebrates. *Mol. Biol. Evol.* 30(4), 894-905.
- 1930
- 1931 Molle, V., Campagna, S., Bessin, Y., Ebran, N., Saint, N., Molle, G., 2008. First evidence of the pore-  
1932 forming properties of a keratin from skin mucus of rainbow trout (*Oncorhynchus mykiss*, formerly  
1933 *Salmo gairdneri*). *Biochem. J.* 411, 33-40.
- 1934
- 1935 Morgan, B.P., Walters, D., Serna, M., Bubeck, D., 2016. Terminal complexes of the complement  
1936 system: new structural insights and their relevance to function. *Immunol. Rev.* 274(1),141-151.
- 1937
- 1938 Morshed, S.A., Ma, R., Latif, R., Davies, T.F., 2019. Cleavage Region Thyrotropin Receptor Antibodies  
1939 Influence Thyroid Cell Survival In Vivo. *Thyroid* 29(7), 993-1002.
- 1940
- 1941 Moscarello, M.A., Lei, H., Mastronardi, F.G., Winer, S., Tsui, H., Li, Z., Ackerley, C., Zhang, L., Raijmakers,  
1942 R., Wood, D.D., 2013. Inhibition of peptidyl-arginine deiminases reverses protein-hypercitrullination  
1943 and disease in mouse models of multiple sclerosis. *Dis. Model Mech.* 6(2), 467-78.
- 1944
- 1945 Mostert, V., 2000. Selenoprotein P: properties, functions, and regulation. *Arch. Biochem. Biophys.*  
1946 376(2), 433-8.
- 1947
- 1948 Muller, S., Radic, M., 2015. Citrullinated Autoantigens: From Diagnostic Markers to Pathogenetic  
1949 Mechanisms. *Clin. Rev. Allergy Immunol.* 49(2), 232-9.
- 1950
- 1951 Musso, G., Cassader, M., Cohney, S., De Michieli, F., Pinach, S., Saba, F., Gambino, R., 2016. Fatty Liver  
1952 and Chronic Kidney Disease: Novel Mechanistic Insights and Therapeutic Opportunities. *Diabetes Care.*  
1953 39(10), 1830-45.
- 1954
- 1955 Müller, G., Wohlsein, P., Beineke, A., Haas, L., Greiser-Wilke, I., Siebert, U., Fonfara, S., Harder, T.,  
1956 Stede, M., Gruber, A.D., Baumgartner, W., 2004. Phocine distemper in German seals, 2002. *Emerg.*  
1957 *Infect. Dis.* 10, 723-725
- 1958
- 1959 Nabi, G., Hao, Y., Zeng, X., Jinsong, Z., McLaughlin, R.W., Wang, D., 2017. Hematologic and biochemical  
1960 differences between two free ranging Yangtze finless porpoise populations: The implications of  
1961 habitat. *PLoS One.* 12(11), e0188570.
- 1962
- 1963 Nayak, A., Pednekar, L., Reid, K.B., Kishore, U., 2012. Complement and non-complement activating  
1964 functions of C1q: a prototypical innate immune molecule. *Innate Immun.* 18(2), 350-63.
- 1965
- 1966 Nicholas, A.P., Whitaker, J.N., 2002. Preparation of a monoclonal antibody to citrullinated epitopes:  
1967 its characterization and some applications to immunohistochemistry in human brain. *Glia* 37(4), 328-  
1968 36.
- 1969
- 1970 Niimi, S., Imoto, M., Kunisue, T., Watanabe, M.X., Kim, E.Y., Nakayama, K., Yasunaga, G., Fujise, Y.,  
1971 Tanabe, S., Iwata, H., 2014. Effects of persistent organochlorine exposure on the liver transcriptome

- 1972 of the common minke whale (*Balaenoptera acutorostrata*) from the North Pacific. Ecotoxicol. Environ.  
1973 Saf. 108, 95-105.
- 1974
- 1975 Nollens, H.H., Ruiz, C., Walsh, M.T., Gulland, F.M., Bossart, G., Jensen, E.D., McBain, J.F., Wellehan,  
1976 J.F., 2008. Cross-reactivity between immunoglobulin G antibodies of whales and dolphins correlates  
1977 with evolutionary distance. Clin. Vaccine Immunol. 15(10), 1547-54.
- 1978
- 1979 Nonaka, M., 2014. Evolution of the complement system. Subcell. Biochem. 80, 31-43.
- 1980
- 1981 Norman, A.W., 2008. A vitamin D nutritional cornucopia: new insights concerning the serum 25-  
1982 hydroxyvitamin D status of the US population. Am. J. Clin. Nutr. 88(6), 1455-6.
- 1983
- 1984 Norman, S.A., Goertz, C.E., Burek, K.A., Quakenbush, L.T., Cornick, L.A., Romano, T.A., Spoon, T., Miller,  
1985 W., Beckett, L.A., Hobbs, R.C., 2012. Seasonal hematology and serum chemistry of wild beluga whales  
1986 (*Delphinapterus leucas*) in Bristol Bay, Alaska, USA. J. Wildl. Dis. 48(1), 21-32.
- 1987
- 1988 Notarangelo, L.D., Kim, M.S., Walter, J.E., Lee, Y.N., 2016. Human RAG mutations: biochemistry and  
1989 clinical implications. Nat. Rev. Immunol. 16(4), 234-46.
- 1990
- 1991 Oelschläger, H.A., Buhl, E.H., Dann, J.F., 1987. Development of the nervus terminalis in mammals  
1992 including toothed whales and humans. Ann. NY Acad. Sci. 519, 447-64.
- 1993
- 1994 Oelschläger, H.A., 1989. Early development of the olfactory and terminalis systems in baleen whales.  
1995 Brain Behav. Evol. 34(3), 171-83.
- 1996
- 1997 Okumura, N., Haneishi, A., Terasawa, F., 2009. Citrullinated fibrinogen shows defects in FPA and FPB  
1998 release and fibrin polymerization catalyzed by thrombin. Clin. Chim. Acta 401(1-2), 119-23.
- 1999
- 2000 Olivares-Illana, V., Riveros-Rosas, H., Cabrera, N., Tuena de Gómez-Puyou, M., Pérez-Montfort, R.,  
2001 Costas, M., Gómez-Puyou, A., 2017. A guide to the effects of a large portion of the residues of  
2002 triosephosphate isomerase on catalysis, stability, druggability, and human disease. Proteins 85(7),  
2003 1190-1211.
- 2004
- 2005 O'Neil, L.J., Kaplan, M.J., 2019. Neutrophils in Rheumatoid Arthritis: Breaking Immune Tolerance and  
2006 Fueling Disease. Trends Mol. Med. 25(3), 215-227.
- 2007
- 2008 O'Reilly, M.S., Pirie-Shepherd, S., Lane, W.S., Folkman, J., 1999. Antiangiogenic activity of the cleaved  
2009 conformation of the serpin antithrombin. Science 285 (5435), 1926-1928.
- 2010
- 2011 Ohishi K, Maruyama T, Seki F, Takeda M., 2019. Marine Morbilliviruses: Diversity and Interaction with  
2012 Signaling Lymphocyte Activation Molecules. Viruses 11(7), pii: E606.
- 2013
- 2014 Ortiz, R.M., 2001. Osmoregulation in marine mammals. J. Exp. Biol. 204(Pt 11), 1831-44.
- 2015
- 2016 Oshima G., 1990. Effects of different heparins on the enhancement of the thrombin-antithrombin  
2017 reaction. Biol. Chem. Hoppe Seyler. 371(1), 37-42.
- 2018
- 2019 Palić, D., Ostojic, J., Andreasenc, C., Roth, J.A., 2007. Fish cast NETs: neutrophil extracellular traps are  
2020 released from fish neutrophils. Dev. Comp. Immunol. 31, 805e16.
- 2021

- 2022 Pamenter, M.E., Uysal-Onganer, P., Huynh, K.W., Kraev, I., Lange, S. 2019. Post-translational  
2023 Deimination of Immunological and Metabolic Protein Markers in Plasma and Extracellular Vesicles of  
2024 Naked Mole-Rat (*Heterocephalus glaber*). *Int. J. Mol. Sci.* 20(21), pii, E5378.
- 2025
- 2026 Parida, S., Siddharth, S., Sharma, D., 2019. Adiponectin, obesity, and cancer: Clash of the bigwigs in  
2027 health and disease. *Int. J. Mol. Sci.* 20, 2519.
- 2028
- 2029 Park, T.J., Reznick, J., Peterson, B.L., Blass, G., Omerbasic, D., Bennett, N.C., Kuich, P.H.J.L., Zasada, C.,  
2030 Browe, B.M., Hamann, W., et al., 2017. Fructose-driven glycolysis supports anoxia resistance in the  
2031 naked mole-rat. *Science* 356, 305–308.
- 2032
- 2033 Pedro, S., Dietz, R., Sonne, C., Rosing-Asvid, A., Hansen, M., McKinney, M.A., 2019. Are vitamins A and  
2034 E associated with persistent organic pollutants and fatty acids in the blubber of highly contaminated  
2035 killer whales (*Orcinus orca*) from Greenland? *Environ. Res.* 177, 108602.
- 2036
- 2037 Perga, S., Giuliano Albo, A., Lis, K., Minari, N., Falvo, S., Marnetto, F., Caldano, M., Reviglione, R., et al.,  
2038 2015. Vitamin D Binding Protein Isoforms and Apolipoprotein E in Cerebrospinal Fluid as Prognostic  
2039 Biomarkers of Multiple Sclerosis. *PLoS One.* 10(6), e0129291.
- 2040
- 2041 Persson-Moschos, M.E., Stavenow, L., Akesson, B., Lindgärde, F., 2000. Selenoprotein P in plasma in  
2042 relation to cancer morbidity in middle-aged Swedish men. *Nutr. Cancer.* 36(1), 19-26.
- 2043
- 2044 Pesavento, P.A., Agnew, D., Keel, M.K., Woolard, K.D., 2018. Cancer in wildlife: patterns of emergence.  
2045 *Nat. Rev. Cancer.* 18(10), 646-661.
- 2046
- 2047 Peters, T., Jr., 1996. All about albumin. *Biochemistry, Genetics, and Medical Applications*. Academic  
2048 Press, Inc, San Diego (1996).
- 2049
- 2050 Peterson, M.M., Mack, J.L., Hall, P.R., Alsup, A.A., Alexander, S.M., Sully, E.K., Sawires, Y.S., Cheung,  
2051 A.L., Otto, M., Gresham, H.D., 2008. Apolipoprotein B Is an innate barrier against invasive  
2052 *Staphylococcus aureus* infection. *Cell Host Microbe* 4(6),555-66.
- 2053
- 2054 Petit, F.M., Serres, C., Auer, J., 2014. Moonlighting proteins in sperm-egg interactions. *Biochem. Soc.*  
2055 *Trans.* 42(6),1740-3.
- 2056
- 2057 Phillips, R.A., Kraev, I., Lange, S., 2020. Protein Deimination and Extracellular Vesicle Profiles in  
2058 Antarctic Seabirds. *Biology* 9(1), 15.
- 2059
- 2060 Picard, D., 2002. Heat-shock protein 90, a chaperone for folding and regulation. *Cell. Mol. Life Sci.* 59  
2061 (10), 1640–8.
- 2062
- 2063 Pietronigro, E.C., Della Bianca, V., Zenaro, E., Constantin, G., 2017. NETosis in Alzheimer's Disease.  
2064 *Front. Immunol.* 8, 211.
- 2065
- 2066 Pike, R.N., Potempa, J., Skinner, R., Fitton, H.L., McGraw, W.T., Travis, J., Owen, M., Jin, L., Carrell,  
2067 R.W., 1997. Heparin-dependent modification of the reactive center arginine of antithrombin and  
2068 consequent increase in heparin binding affinity. *J. Biol. Chem.* 272(32), 19652-5.
- 2069
- 2070 Pinzone, M., Damseaux, F., Michel, L.N., Das, K., 2019. Stable isotope ratios of carbon, nitrogen and  
2071 sulphur and mercury concentrations as descriptors of trophic ecology and contamination sources of  
2072 Mediterranean whales. *Chemosphere* 237, 124448.

- 2073  
2074 Piven, O.O., Winata, C.L., 2017. The canonical way to make a heart:  $\beta$ -catenin and plakoglobin in heart  
2075 development and remodeling. *Exp. Biol. Med (Maywood)*. 242(18), 1735-1745.  
2076  
2077 Ploquin, M.J., Casrouge, A., Madec, Y., Noël, N., Jacquelin, B., Huot, N., Duffy, D., Jochems, S.P., Micci,  
2078 L., et al., 2018. Systemic DPP4 activity is reduced during primary HIV-1 infection and is associated with  
2079 intestinal RORC+ CD4+ cell levels: a surrogate marker candidate of HIV-induced intestinal damage. *J.*  
2080 *Int. AIDS Soc.* 21(7), e25144.  
2081  
2082 Preissner, K.T., Seiffert, D., 1998. Role of vitronectin and its receptors in haemostasis and vascular  
2083 remodeling. *Thrombosis Research*. 89 (1), 1–21.  
2084  
2085 Qu, H., Qiu, Y., Wang, Y., Liao, Y., Zheng, Y., Zheng, H., 2018. Plasma fetuin-B concentrations are  
2086 associated with insulin resistance and first-phase glucose-stimulated insulin secretion in individuals  
2087 with different degrees of glucose tolerance. *Diabetes Metab.* 44(6), 488-492.  
2088  
2089 Qu, J., Ko, C.W., Tso, P., Bhargava, A., 2019. Apolipoprotein A-IV: A Multifunctional Protein Involved in  
2090 Protection against Atherosclerosis and Diabetes. *Cells* 8(4), pii, E319.  
2091  
2092 Radic, M., Pattanaik, D., 2018. Cellular and Molecular Mechanisms of Anti-Phospholipid Syndrome.  
2093 *Front. Immunol.* 9, 969.  
2094  
2095 Rajan, B., Lokesh, J., Kiron, V., Brinchmann, M.F., 2013. Differentially expressed proteins in the skin  
2096 mucus of Atlantic cod (*Gadus morhua*) upon natural infection with *Vibrio anguillarum*. *BMC Vet. Res.*  
2097 9, 103.  
2098  
2099 Ramirez, S.H., Andrews, A.M., Paul, D., Pachter, J.S., 2018. Extracellular vesicles: mediators and  
2100 biomarkers of pathology along CNS barriers. *Fluids Barriers CNS*. 15(1), 19.  
2101  
2102 Rebl, A., Köllner, B., Anders, E., Wimmers, K., Goldammer, T., 2010. Peptidylarginine deiminase gene  
2103 is differentially expressed in freshwater and brackish water rainbow trout. *Mol. Biol. Rep.* 37(5), 2333-  
2104 9.  
2105  
2106 Redmond, A.K., Ohta, Y., Criscitiello, M.F., Macqueen, D.J., Flajnik, M.F., Dooley, H., 2018. Haptoglobin  
2107 Is a Divergent MASP Family Member That Neofunctionalized To Recycle Hemoglobin via CD163 in  
2108 Mammals. *J. Immunol.* 201(8), 2483-2491.  
2109  
2110 Reichl, K., Kreykes, S.E., Martin, C.M., Shenoy, C., 2018. Desmoplakin Variant-Associated  
2111 Arrhythmogenic Cardiomyopathy Presenting as Acute Myocarditis. *Circ. Genom. Precis. Med.* 11(12),  
2112 e002373.  
2113  
2114 Reid, K.B., Colomb, M., Petry, F., Loos, M., 2002. Complement component C1 and the collectins--first-  
2115 line defense molecules in innate and acquired immunity. *Trends Immunol.* 23(3), 115-7.  
2116  
2117 Reid, K.B.M., 2018. Complement Component C1q: Historical Perspective of a Functionally Versatile,  
2118 and Structurally Unusual, Serum Protein. *Front. Immunol.* 9, 764.  
2119  
2120 Reif, J.S., Schaefer, A.M., Bossart, G.D., Fair, P.A., 2017. Health and Environmental Risk Assessment  
2121 Project for bottlenose dolphins *Tursiops truncatus* from the southeastern USA. II. Environmental  
2122 aspects. *Dis. Aquat. Organ.* 125(2), 155-166.  
2123

- 2124 Rikarni, Dharma, R., Tambunan, K.L., Isbagyo, H., Dewi, B.E., Acang, N., Setiabudy, R., Aman, A.K., 2015.  
2125 Prothrombotic Effect of Anti-beta-2 Glycoprotein-1 Antibodies on the Expression of Tissue Factor,  
2126 Thrombomodulin, and Plasminogen Activator Inhibitor-1 in Endothelial Cells. *Acta Med Indones.* 47(1),  
2127 31-7.
- 2128
- 2129 Righetti, B.P.H., Mattos, J.J., Siebert, M.N., Daura-Jorge, F.G., Bezamat, C., Fruet, P.F., Genoves, R.C.,  
2130 Taniguchi, S., da Silva, J., Montone, R.C., Simões-Lopes, P.C.A., Bainy, A.C.D., Lüchmann, K.H., 2019.  
2131 Biochemical and molecular biomarkers in integument biopsies of free-ranging coastal bottlenose  
2132 dolphins from southern Brazil. *Chemosphere* 225, 139-149.
- 2133
- 2134 Robeck, T.R., Steinman, K.J., O'Brien, J.K., 2016. Characterization and longitudinal monitoring of serum  
2135 progestagens and estrogens during normal pregnancy in the killer whale (*Orcinus orca*). *Gen. Comp.*  
2136 *Endocrinol.* 236, 83-97.
- 2137
- 2138 Rodgers, K.K., 2017. Riches in RAGs: Revealing the V(D)J Recombinase through High-Resolution  
2139 Structures. *Trends Biochem. Sci.* 42(1), 72-84.
- 2140
- 2141 Ruiz, C.L., Nollens, H.H., Venn-Watson, S., Green, L.G., Wells, R.S., Walsh, M.T., Nolan, E.C., McBain,  
2142 J.F., Jacobson, E.R., 2009. *Dev. Comp. Immunol.* 33(4), 449-55.
- 2143
- 2144 Sadler, J.B.A., Wenzel, D.M., Williams, L.K., Guindo-Martínez, M., Alam, S.L., Mercader, J.M., Torrents,  
2145 D., Ullman, K.S., Sundquist, W.I., Martin-Serrano, J., 2018. A cancer-associated polymorphism in  
2146 ESCRT-III disrupts the abscission checkpoint and promotes genome instability. *Proc Natl. Acad. Sci.*  
2147 USA 115(38), E8900-E8908.
- 2148
- 2149 Sahoo, P.K., Das, S., Mahapatra, K.D., Saha, J.N., Baranski, M., Ødegård, J., Robinson, N., 2013.  
2150 Characterization of the ceruloplasmin gene and its potential role as an indirect marker for selection to  
2151 *Aeromonas hydrophila* resistance in rohu, *Labeo rohita*. *Fish Shellfish Immunol.* 34(5), 1325-34.
- 2152
- 2153 Schönrich, G., Raftery, M.J., 2016. Neutrophil Extracellular Traps Go Viral. *Front. Immunol.* 7, 366.
- 2154
- 2155 Segawa, T., Kobayashi, Y., Inamoto, S., Suzuki, M., Endoh, T., Itou, T., 2016. Identification and  
2156 Expression Profiles of microRNA in Dolphin. *Zoolog. Sci.* 33(1), 92-7.
- 2157
- 2158 Seluanov, A., Gladyshev, V.N., Vijg, J., Gorbunova, V., 2018. Mechanisms of cancer resistance in long-  
2159 lived mammals. *Nat. Rev. Cancer.* 18(7), 433-441.
- 2160
- 2161 Semba, U., Shibuya, Y., Okabe, H., Hayashi, I., Yamamoto, T., 2000. Whale high-molecular-weight and  
2162 low-molecular-weight kininogens. *Thromb. Res.* 97(6), 481-90.
- 2163
- 2164 Şen, V., Uluca, Ü., Ece, A., Kaplan, İ., Bozkurt, F., Aktar, F., Bağlı, S., Tekin ,R., 2014. Serum prolidase  
2165 activity and oxidant-antioxidant status in children with chronic hepatitis B virus infection. *Ital. J.*  
2166 *Pediatr.* 40 (1), 95.
- 2167
- 2168 Shi, Z.Z., Fan, Z.W., Chen, Y.X., Xie, X.F., Jiang, W., Wang, W.J., Qiu, Y.T., Bai, J., 2019. Ferroptosis in  
2169 Carcinoma: Regulatory Mechanisms and New Method for Cancer Therapy. *Onco Targets Ther.* 12,  
2170 11291-11304.
- 2171
- 2172 Shibata, T., Gotoh, M., Ochiai, A., Hirohashi, S., 1994. Association of plakoglobin with APC, a tumor  
2173 suppressor gene product, and its regulation by tyrosine phosphorylation. *Biochem. Biophys. Res.*  
2174 *Commun.* 203(1), 519-22.

- 2175  
2176 Siebert, U., Tolley, K., Víkingsson, G.A., Olafsdottir, D., Lehnert, K., Weiss, R., Baumgärtner, W., 2006.  
2177 Pathological findings in harbour porpoises (*Phocoena phocoena*) from Norwegian and Icelandic  
2178 waters. *J. Comp. Pathol.* 134, 134-142.
- 2179  
2180 Siebert, U., Prenger-Beringhoff, E., Weiss, R., 2009. Regional differences in bacterial flora in harbour  
2181 porpoises from the North Atlantic: environmental effects? *J. Appl. Microbiol.* 106, 329-337.
- 2182  
2183 Simond, A.E., Houde, M., Lesage, V., Michaud, R., Zbinden, D., Verreault, J., 2019. Associations  
2184 between organohalogen exposure and thyroid- and steroid-related gene responses in St. Lawrence  
2185 Estuary belugas and minke whales. *Mar. Pollut. Bull.* 145, 174-184.
- 2186  
2187 Sirover, M.A., 2018. Pleiotropic effects of moonlighting glyceraldehyde-3-phosphate dehydrogenase  
2188 (GAPDH) in cancer progression, invasiveness, and metastases. *Cancer Metastasis Rev.* 37(4), 665-676.
- 2189  
2190 Smith, L.E., Crouch, K., Cao, W., Müller, M.R., Wu, L., Steven, J., Lee, M., Liang, M., Flajnik, M.F., Shih,  
2191 H.H., Barelle, C.J., Paulsen, J., Gill, D.S., Dooley, H., 2012. Characterization of the immunoglobulin  
2192 repertoire of the spiny dogfish (*Squalus acanthias*). *Dev. Comp. Immunol.* 36(4), 665-79.
- 2193  
2194 Smith, A., McCulloh, R.J., 2015. Hemopexin and haptoglobin: allies against heme toxicity from  
2195 hemoglobin not contenders. *Front. Physiol.* 6, 187.
- 2196  
2197 Sohn, D.H., Rhodes, C., Onuma, K., Zhao, X., Sharpe, O., Gazitt, T., Shiao, R., Fert-Bober, J., Cheng, D.,  
2198 Lahey, L.J., et al., 2015. Local Joint inflammation and histone citrullination in a murine model of the  
2199 transition from preclinical autoimmunity to inflammatory arthritis. *Arthritis Rheumatol.* 67, 2877–  
2200 2887.
- 2201  
2202 Soo, C. Y., Song, Y., Zheng, Y., Campbell, E. C., Riches, A. C., Gunn-Moore, F., et al., 2012. Nanoparticle  
2203 tracking analysis monitors microvesicle and exosome secretion from immune cells. *Immunology* 136,  
2204 192–197.
- 2205  
2206 Sottrup-Jensen, L., Stepanik, T.M., Kristensen, T., Lønblad, P.B., Jones, C.M., Wierzbicki, D.M.,  
2207 Magnusson, S., Domdey, H., Wetsel, R.A., Lundwall, A., et al., 1985. Common evolutionary origin of  
2208 alpha 2-macroglobulin and complement components C3 and C4. *Proc. Natl. Acad. Sci. USA* 82(1), 9-13.
- 2209  
2210 Spracklen, C.N., Karaderi, T., Yaghootkar, H., Schurmann, C., Fine, R.S., et al., 2019. Exome-Derived  
2211 Adiponectin-Associated Variants Implicate Obesity and Lipid Biology. *Am. J. Hum. Genet.* pii, S0002-  
2212 9297(19)30188-0.
- 2213  
2214 Stafford, J.L., Belosevic, M., 2003. Transferrin and the innate immune response of fish: identification  
2215 of a novel mechanism of macrophage activation. *Dev. Comp. Immunol.* 27(6-7), 539-54.
- 2216  
2217 Stanfield, R.L., Haakenson, J., Deiss, T.C., Criscitiello, M.F., Wilson, I.A., Smider, V.V., 2018. The Unusual  
2218 Genetics and Biochemistry of Bovine Immunoglobulins. *Adv. Immunol.* 137, 135-164.
- 2219  
2220 Stanfliet, J.C., Locketz, M., Berman, P., Pillay, T.S., 2015. Evaluation of the utility of serum prolidase as  
2221 a marker for liver fibrosis. *J. Clin. Lab. Anal.* 29(3), 208-13.
- 2222  
2223 Storey, K.B., Hochachka, P.W., 1974. Glycolytic enzymes in muscle of the pacific dolphin: role of  
2224 pyruvate kinase in aerobic-anaerobic transition during diving. *Comp. Biochem. Physiol. B.* 49(1B), 119-  
2225 28.

- 2226  
2227 Stöcker, W., Karmilin, K., Hildebrand, A., Westphal, H., Yiallouros, I., Weiskirchen, R., Dietzel, E., Floehr,  
2228 J., Jahnens-Dechent, W., 2014. Mammalian gamete fusion depends on the inhibition of ovastacin by  
2229 fetuin-B. *Biol. Chem.* 395(10), 1195-9.  
2230  
2231 Su, Q., Tsai, J., Xu, E., Qiu, W., Bereczki, E., Santha, M., Adeli, K., 2009. Apolipoprotein B100 acts as a  
2232 molecular link between lipid-induced endoplasmic reticulum stress and hepatic insulin resistance.  
2233 *Hepatology* 50(1), 77-84.  
2234  
2235 Sun, X., Zhang, Z., Sun, Y., Li, J., Xu, S., Yang, G., 2017. Comparative genomics analyses of alpha-keratins  
2236 reveal insights into evolutionary adaptation of marine mammals. *Front. Zool.* 14, 41.  
2237  
2238 Sundaram, M., Zhong, S., Bou Khalil, M., Links, P.H., Zhao, Y., Iqbal, J., Hussain, M.M., Parks, R.J., Wang,  
2239 Y., Yao, Z., 2010. Expression of apolipoprotein C-III in McA-RH7777 cells enhances VLDL assembly and  
2240 secretion under lipid-rich conditions. *Lipid Res.* 51(1), 150-61.  
2241  
2242 Sunyer, J.O., Lambris, J.D., 1998. Evolution and diversity of the complement system of poikilothermic  
2243 vertebrates. *Immunol. Rev.* 166, 39-57.  
2244  
2245 Suzuki M, Yoshioka M, Ohno Y, Akune Y., 2018. Plasma metabolomic analysis in mature female  
2246 common bottlenose dolphins: profiling the characteristics of metabolites after overnight fasting by  
2247 comparison with data in beagle dogs. *Sci. Rep.* 8(1), 12030.  
2248  
2249 Suzuki, M., Banno, K., Usui, T., Funasaka, N., Segawa, T., Kirihata, T., Kamisako, H., Ueda, K., Munakata,  
2250 A., 2018. *Gen. Comp. Endocrinol.* 262, 20-26.  
2251  
2252 Tao, P., Li, Z., Woolfork, A.G., Hage, D.S., 2019. Characterization of tolazamide binding with glycated  
2253 and normal human serum albumin by using high-performance affinity chromatography. *J. Pharm.*  
2254 *Biomed. Anal.* 166, 273-280.  
2255  
2256 Tarighi, S., Najafi, M., Hosseini-Nezhad, A., Ghaedi, H., Meshkani, R., Moradi, N., Fadaei, R., Kazerouni,  
2257 F., Shanaki, M., 2017. Association Between Two Common Polymorphisms of Vitamin D Binding Protein  
2258 and the Risk of Coronary Artery Disease: A Case-control Study. *J. Med. Biochem.* 36(4), 349-357.  
2259  
2260 Tarze, A., Deniaud, A., Le Bras, M., Maillier, E., Molle, D., Laroquette, N., Zamzami, N., Jan, G., Kroemer,  
2261 G., Brenner, C., 2007. GAPDH, a novel regulator of the pro-apoptotic mitochondrial membrane  
2262 permeabilization. *Oncogene* 26 (18), 2606–20.  
2263  
2264 Taylor, B.C., Brotheridge, R.M., Jessup, D.A., Stott, J.L., 2002. Measurement of serum immunoglobulin  
2265 concentration in killer whales and sea otters by radial immunodiffusion. *Vet. Immunol. Immunopathol.*  
2266 89(3-4), 187-95.  
2267  
2268 Tennent, G.A., Brennan, S.O., Stangou, A.J., O'Grady, J., Hawkins, P.N., Pepys, M.B., 2007. Human  
2269 plasma fibrinogen is synthesized in the liver. *Blood* 109, 1971–1974.  
2270  
2271 Terasawa, F., Arai, T., Tokura, T., Ohshita, I., 2008. Fibrinogen concentrations in captive bottlenose  
2272 dolphins during pregnancy. *J. Vet. Med. Sci.* 70(11), 1277-9.  
2273  
2274 Théry, C., Witwer, K.W., Aikawa, E., Alcaraz, M.J., Anderson, J.D., Andriantsitohaina, R., Antoniou, A.,  
2275 Arab, T., Archer, F., Atkin-Smith, G.K., et al., 2018. Minimal information for studies of extracellular

- 2276 vesicles 2018 (MISEV2018): A position statement of the International Society for Extracellular Vesicles  
2277 and update of the MISEV2014 guidelines. *J. Extracell. Vesicles* 7, 1535750.
- 2278
- 2279 Tian, R., Wang, Z., Niu, X., Zhou, K., Xu, S., Yang, G., 2016. Evolutionary Genetics of Hypoxia Tolerance  
2280 in Cetaceans during Diving. *Genome Biol Evol.* 8(3), 827-39.
- 2281
- 2282 Tiscia, G.L., Margaglione, M., 2018. Human Fibrinogen: Molecular and Genetic Aspects of Congenital  
2283 Disorders. *Int. J. Mol. Sci.* 19(6), pii, E1597.
- 2284
- 2285 Travers, T.S., Harlow, L., Rosas, I.O., Gochuico, B.R., Mikuls, T.R., Bhattacharya, S.K., Camacho, C.J.,  
2286 Ascherman, D.P., 2016. Extensive Citrullination Promotes Immunogenicity of HSP90 through Protein  
2287 Unfolding and Exposure of Cryptic Epitopes. *J. Immunol.* 197(5), 1926-36.
- 2288
- 2289 Travis, J.C., Sanders, B.G., Cushing, J.E., 1971. Electrophoretic properties of haptoglobin and  
2290 hemoglobin in four species of whales. *Comp. Biochem. Physiol. B.* 39(2), 299-303.
- 2291
- 2292 Tristan, C., Shahani, N., Sedlak, T.W., Sawa, A., 2011. The diverse functions of GAPDH: views from  
2293 different subcellular compartments. *Cell. Signal.* 23(2), 317–23.
- 2294
- 2295 Tsagkogeorga, G., McGowen, M.R., Davies, .K. T. J., Jarman, S., Polanowsk, A., Bertelsen, M.F., Rossiter,  
2296 S.J., 2015. A phylogenomic analysis of the role and timing of molecular adaptation in the aquatic  
2297 transition of cetartiodactyl mammals. *R. Soc. Open Sci.* 2(9), 150156.
- 2298
- 2299 Turchinovich, A., Drapkina, O., Tonevitsky, A., 2019. Transcriptome of Extracellular Vesicles: State-of-  
2300 the-Art. *Front. Immunol.* 10, 202.
- 2301
- 2302 Uchiyama, H., Metori, A., Ogamo, A., Nagasawa, K., 1990. Contribution of chemical 6-O-sulfation of  
2303 the aminodeoxyhexose residues in whale heparin with high affinity for antithrombin III to its  
2304 anticoagulant properties. *J. Biochem.* 107(3), 377-80.
- 2305
- 2306 Vagner, T., Chin, A., Mariscal, J., Bannykh, S., Engman, D.M., Di Vizio, D., 2019. Protein Composition  
2307 Reflects Extracellular Vesicle Heterogeneity. *Proteomics*, e1800167.
- 2308
- 2309 Varin, E.M., Mulvihill, E.E., Beaudry, J.L., Pujadas, G., Fuchs, S., Tanti, J.F., Fazio, S., Kaur, K., Cao, X.,  
2310 Baggio, L.L., Matthews, D., Campbell, J.E., Drucker, D.J., 2019. Circulating Levels of Soluble Dipeptidyl  
2311 Peptidase-4 Are Dissociated from Inflammation and Induced by Enzymatic DPP4 Inhibition. *Cell  
Metab.* 29(2), 320-334.
- 2312
- 2313 Verboven, C., Rabijns, A., De Maeyer, M., Van Baelen, H., Bouillon, R., De Ranter, C., 2002. A structural  
2314 basis for the unique binding features of the human vitamin D-binding protein. *Nat. Struct. Biol.* 9(2),  
2315 131-6.
- 2316
- 2317 Viglio, S., Annovazzi, L., Conti, B., Genta, I., Perugini, P., Zanone, C., Casado, B., Cetta, G., Iadarola, P.,  
2318 2006. The role of emerging techniques in the investigation of prolidase deficiency: from diagnosis to  
2319 the development of a possible therapeutical approach. *J. Chromatogr. B Analyt. Technol. Biomed. Life  
Sci.* 832 (1), 1–8.
- 2320
- 2321 Villagra-Blanco, R., Silva, L.M.R., Conejeros, I., Taubert, A., Hermosilla, C., 2019. Pinniped- and  
2322 Cetacean-Derived ETosis Contributes to Combating Emerging Apicomplexan Parasites (*Toxoplasma  
gondii*, *Neospora caninum*) Circulating in Marine Environments. *Biology (Basel)*. 8(1).
- 2323
- 2324
- 2325
- 2326

- 2327 Villanger, G.D., Lydersen, C., Kovacs, K.M., Lie, E., Skaare, J.U., Jenssen, B.M., 2011. Disruptive effects  
2328 of persistent organohalogen contaminants on thyroid function in white whales (*Delphinapterus*  
2329 *leucas*) from Svalbard. *Sci. Total Environ.* 409(13), 2511-24.
- 2330
- 2331 Vossenaar, E.R., Zendman, A.J., van Venrooij, W.J., Pruijn, G.J., 2003. PAD, a growing family of  
2332 citrullinating enzymes: genes, features and involvement in disease. *Bioessays* 25(11), 1106-18.
- 2333
- 2334 Voloboueva, L.A., Sun, X., Xu, L., Ouyang, Y.-B., Giffard, R.G., 2017. Distinct effects of miR-210 reduction  
2335 on neurogenesis: increased neuronal survival of inflammation but reduced proliferation associated  
2336 with mitochondrial enhancement. *J. Neurosci.* 37, 3072-3084.
- 2337
- 2338 Wang, S., Wang, Y., 2013. Peptidylarginine deiminases in citrullination, gene regulation, health and  
2339 pathogenesis. *Biochim. Biophys. Acta* 1829(10), 1126-35.
- 2340
- 2341 Wang, N., Chen, C., Yang, D., Liao, Q., Luo, H., Wang, X., Zhou, F., Yang, X., Yang, J., Zeng, C., Wang,  
2342 W.E., 2017. Mesenchymal stem cells-derived extracellular vesicles, via miR-210, improve infarcted  
2343 cardiac function by promotion of angiogenesis. *Biochim. Biophys. Acta* 1863, 2085-2092.
- 2344
- 2345 Wang, B., Sullivan, T.N., Pisarenko, A., Zaheri, A., Espinosa, H.D., Meyers, M.A., 2019. Lessons from  
2346 the Ocean: Whale Baleen Fracture Resistance. *Adv. Mater.* 31(3), e1804574.
- 2347
- 2348 Waugh, C.A., Huston, W.M., Noad, M.J., Bengtson Nash, S., 2011. Cytochrome P450 isozyme protein  
2349 verified in the skin of southern hemisphere humpback whales (*Megaptera novaeangliae*): implications  
2350 for biochemical biomarker assessment. *Mar. Pollut. Bull.* 62(4), 758-61.
- 2351
- 2352 Weisel, J.W., Litvinov, R.I., 2013. Mechanisms of fibrin polymerization and clinical implications. *Blood*  
2353 121, 1712-1719.
- 2354
- 2355 White, C.R., Datta, G., Giordano, S., 2017. High-Density Lipoprotein Regulation of Mitochondrial  
2356 Function. *Adv. Exp. Med. Biol.* 982, 407-429.
- 2357
- 2358 White, M.R., Garcin, E.D., 2017. D-Glyceraldehyde-3-Phosphate Dehydrogenase Structure and  
2359 Function. *Subcell. Biochem.* 83, 413-453.
- 2360
- 2361 Wilson, M.R., Zoubeidi, A., 2017. Clusterin as a therapeutic target. *Expert Opin. Ther. Targets* 21(2),  
2362 201-213.
- 2363
- 2364 Witalison, E.E., Thompson, P.R., Hofseth, L.J., 2015. Protein Arginine Deiminases and Associated  
2365 Citrullination: Physiological Functions and Diseases Associated with Dysregulation. *Curr. Drug Targets*  
2366 16(7), 700-10.
- 2367
- 2368 Wünschmann, A., Siebert, U., Frese, K., Weiss, R., Lockyer, C., Heide-Jørgensen, M.P., Müller, G.,  
2369 Baumgärtner, W., 2001. Evidence of infectious diseases in harbour porpoises (*Phocoena phocoena*)  
2370 hunted in the waters of Greenland and by-caught in the German North Sea and Baltic Sea. *Vet. Rec.*  
2371 148, 715-720
- 2372
- 2373 Xia, X., Lei L., Wang, S., Hu, J., Zhang, G., 2020. Necroptosis and its role in infectious diseases. *Apoptosis*.  
2374 2020 Jan 7. doi: 10.1007/s10495-019-01589-x. [Epub ahead of print]
- 2375
- 2376 Xiaoyan, W., Pais, E.M., Lan, L., Jingrui, C., Lin, M., Fordjour, P.A., Guanwei, F., 2017. MicroRNA-155: a  
2377 Novel Armamentarium Against Inflammatory Diseases. *Inflammation* 40(2), 708-716.

- 2378  
2379 Xie, Y., Hou, W., Song, X., Yu, Y., Huang, J., Sun, X., Kang, R., Tang, D., 2016. Ferroptosis: process and  
2380 function. *Cell. Death Differ.* 23(3), 369-79.  
2381  
2382 Xu, Z., Zan, H., Pone, E.J., Mai, T., Casali, P., 2012. Immunoglobulin class-switch DNA recombination:  
2383 induction, targeting and beyond. *Nat. Rev. Immunol.* 12(7), 517-31.  
2384  
2385 Xu, S., Yang, Y., Zhou, X., Xu, J., Zhou, K., Yang, G., 2013. Adaptive evolution of the osmoregulation-  
2386 related genes in cetaceans during secondary aquatic adaptation. *BMC Evol. Biol.* 13, 189.  
2387  
2388 Xu, H.X., Pan, W., Qian, J.F., Liu, F., Dong, H.Q., Liu, Q.J., 2019. MicroRNA-21 contributes to the  
2389 puerarin-induced cardioprotection via suppression of apoptosis and oxidative stress in a cell model of  
2390 ischemia/reperfusion injury. *Mol. Med. Rep.* 20(1), 719-727.  
2391  
2392 Yada T., 2007. Growth hormone and fish immune system. *Gen. Comp. Endocrinol.* 152(2-3), 353-8.  
2393  
2394 Yamamoto, N., Suyama, H., Yamamoto, N., 2008. Immunotherapy for Prostate Cancer with Gc Protein-  
2395 Derived Macrophage-Activating Factor, GcMAF. *Transl. Oncol.* 1(2), 65-72.  
2396  
2397 Yamauchi, T., Kamon, J., Minokoshi, Y., Ito, Y.; Waki, H., Uchida, S., Yamashita, S., Noda, M., Kita, S.,  
2398 Ueki, K., et al., 2002. Adiponectin stimulates glucose utilization and fatty-acid oxidation by activating  
2399 AMP-activated protein kinase. *Nat. Med.* 8, 1288–1295.  
2400  
2401 Yamauchi, T., Kamon, J., Ito, Y., Tsuchida, A., Yokomizo, T., Kita, S., Sugiyama, T., Miyagishi, M., Hara,  
2402 K., Tsunoda, M., et al., 2003. Cloning of adiponectin receptors that mediate antidiabetic metabolic  
2403 effects. *Nature* 423, 762–769.  
2404  
2405 Yao, M., Fang, M., Zheng, W., Dong, Z., Yao, D., 2018. Role of secretory clusterin in  
2406 hepatocarcinogenesis. *Transl. Gastroenterol. Hepatol.* 3, 48.  
2407  
2408 Yang, J., Gao, J., Adamian, M., Wen, X.H., Pawlyk, B., Zhang, L., Sanderson, M.J., Zuo, J., Makino, C.L.,  
2409 Li, T., 2005. The ciliary rootlet maintains long-term stability of sensory cilia. *Mol. Cell. Biol.* 25, 4129–  
2410 4137.  
2411  
2412 Yang, T., Xu, C., 2017. Physiology and Pathophysiology of the Intrarenal Renin-Angiotensin System: An  
2413 Update. *J. Am. Soc. Nephrol.* 28(4), 1040-1049.  
2414  
2415 Yang, H., Li, X., Ji, J., Yuan, C., Gao, X., Zhang, Y., Lu, C., Li, F., Zhang, X., 2019. Changes of microRNAs  
2416 expression profiles from red swamp crayfish (*Procambarus clarkia*) hemolymph exosomes in response  
2417 to WSSV infection. *Fish Shellfish Immunol.* 84, 169-177.  
2418  
2419 Yermakovich, D., Sivitskaya, L., Vaikhanskaya, T., Danilenko, N., Motuk, I., 2018. Novel desmoplakin  
2420 mutations in familial Carvajal syndrome. *Acta Myol.* 37(4), 263-266.  
2421  
2422 Yim HS, Cho YS, Guang X, Kang SG, Jeong JY, Cha SS, Oh HM, Lee JH, Yang EC, Kwon KK, Kim YJ, Kim  
2423 TW, Kim W, Jeon JH, Kim SJ, Choi DH, Jho S, Kim HM, Ko J, Kim H, Shin YA, Jung HJ, Zheng Y, Wang Z,  
2424 Chen Y, Chen M, Jiang A, Li E, Zhang S, Hou H, Kim TH, Yu L, Liu S, Ahn K, Cooper J, Park SG, Hong CP,  
2425 Jin W, Kim HS, Park C, Lee K, Chun S, Morin PA, O'Brien SJ, Lee H, Kimura J, Moon DY, Manica A,  
2426 Edwards J, Kim BC, Kim S, Wang J, Bhak J, Lee HS, Lee JH., 2014. Minke whale genome and aquatic  
2427 adaptation in cetaceans. *Nat. Genet.* 46(1), 88-92.  
2428

- 2429 Yin, D., de Laat, B., Devreese, K.M.J., Kelchtermans, H., 2018. The clinical value of assays detecting  
2430 antibodies against domain I of  $\beta$ 2-glycoprotein I in the antiphospholipid syndrome. Autoimmun. Rev.  
2431 17(12), 1210-1218.
- 2432
- 2433 Ying, S., Dong, S., Kawada, A., Kojima, T., Chavanas, S., Méchin, M.C., Adoue, V., Serre, G., Simon, M.,  
2434 Takahara, H., 2009. Transcriptional regulation of peptidylarginine deiminase expression in human  
2435 keratinocytes. J. Dermatol. Sci. 53(1), 2-9.
- 2436
- 2437 Yu, R., Li, C., Sun, L., Jian, L., Ma, Z., Zhao, J., Liu, X., 2018. Hypoxia induces production of citrullinated  
2438 proteins in human fibroblast-like synoviocytes through regulating HIF1 $\alpha$ . Scand. J. Immunol. 87(4),  
2439 e12654.
- 2440
- 2441 Zala, D., Hinckelmann, M.V., Yu, H., Lyra da Cunha, M.M., Liot, G., Cordelières, F.P., Marco, S., Saudou,  
2442 F., (2013). Vesicular glycolysis provides on-board energy for fast axonal transport. Cell 152 (3), 479–  
2443 91.
- 2444
- 2445 Zayas, Z.P., Ouerdane, L., Mounicou, S., Lobinski, R., Monperrus, M., Amouroux, D., 2014. Hemoglobin  
2446 as a major binding protein for methylmercury in white-sided dolphin liver. Anal. Bioanal. Chem. 406(4),  
2447 1121-9.
- 2448
- 2449 Zhang, C., Du Pasquier, L., Hsu, E., 2013. Shark IgW C region diversification through RNA processing  
2450 and isotype switching. J. Immunol. 191(6), 3410-8.
- 2451
- 2452 Zhang, N., Zhang, X.J., Song, Y.L., Lu, X.B., Chen, D.D., Xia, X.Q., Sunyer, J.O., Zhang, Y.A., 2016.  
2453 Preferential combination between the light and heavy chain isotypes of fish immunoglobulins. Dev.  
2454 Comp. Immunol. 61, 169-79.
- 2455
- 2456 Zhang, N., Zhang, X.J., Chen, D.D., Sunyer, O.J., Zhang, Y.A., 2017. Molecular characterization and  
2457 expression analysis of three subclasses of IgT in rainbow trout (*Oncorhynchus mykiss*). Dev. Comp.  
2458 Immunol. 70, 94-105.
- 2459
- 2460 Zhou, X., Sun, D., Guang, X., Ma, S., Fang, X., Mariotti, M., Nielsen, R., Gladyshev, V.N., Yang, G., 2018.  
2461 Molecular Footprints of Aquatic Adaptation Including Bone Mass Changes in Cetaceans. Genome Biol.  
2462 Evol. 10(3), 967-975.
- 2463
- 2464 Zhou, G., Yang, L., Gray, A., Srivastava, A.K., Li, C., Zhang, G., Cui, T., 2017. The role of desmosomes in  
2465 carcinogenesis. Onco Targets Ther. 10, 4059-4063.
- 2466
- 2467 Zhu, K., Zheng, T., Chen, X., Wang, H., 2018. Bioinformatic Analyses of Renal Ischaemia-Reperfusion  
2468 Injury Models: Identification of Key Genes Involved in the Development of Kidney Disease. Kidney  
2469 Blood Press. Res. 43(6), 1898-1907.
- 2470
- 2471
- 2472 **Figure legends**
- 2473
- 2474 **Fig. 1. Extracellular vesicles (EVs) isolated from sera of whales and orca.** Nanoparticle tracking  
2475 analysis (NTA), Western blotting (WB) and transmission electron microscopy (TEM) for  
2476 characterisation of EVs from: **A.** Minke whale (*Balaenoptera acutorostrata*); **B.** Fin whale

2477 (*Balaenoptera physalus*); **C.** Humpback whale (*Megaptera novaeangliae*); **D.** Cuvier's beaked whale  
2478 (*Ziphius cavirostris*); **E.** Orca (*Orcinus orca*). For all profiles, a poly-dispersed population of EVs in the  
2479 size range of mainly 50-400 nm is seen, with main peaks of EV sizes differing between species, as seen  
2480 in the individual NTA profiles. Analysis of EVs from whale serum by TEM confirms size and typical  
2481 morphology of EVs; scale bar (100 nm) is indicated in all figures.

2482

2483 **Fig. 2. EV yield and modal size of EVs from whale and orca sera.** **A.** Total yield of EVs from whale sera  
2484 varied between the sera from the 5 species under study. Highest levels of EV were seen in orca (*O.  
2485 orca*) and Cuvier's beaked whale (*Z. cavi*), while the lowest EV serum yield was found in humpback  
2486 whale (*M. Nova*). Similar EV yield was observed in minke (*B. acut*) and fin whale (*B. phys*). **B.** Modal  
2487 size of EVs isolated from sera of the five cetacean species varied somewhat within an overall range of  
2488 100-170 nm. Minke whale showed larger EV modal size compared to the other whale species.

2489

2490 **Fig. 3. Western blotting of deiminated proteins and PAD in whale and orca sera.** **A.** PAD homologues  
2491 were identified in whale sera at the expected size of approximately 70-75 kDa, using human PAD2 and  
2492 PAD3 specific antibodies. The presence of deiminated histone H3 (cithH3), representative of  
2493 (neutrophil) extracellular traps (NET/ETs) was also identified, at approximately 20 kDa. **B.** Total  
2494 deiminated proteins were identified in EVs from whale sera, using the F95 pan-deimination specific  
2495 antibody. **C.** Western blotting confirmed the presence of deiminated proteins in total sera from whales  
2496 and orca, as assessed by immunoprecipitation of deiminated proteins from whole sera using the F95  
2497 pan-deimination antibody.

2498

2499 **Fig. 4 Protein-protein interaction networks of deiminated protein hits identified in serum of minke  
2500 whale (*Balaenoptera acutorostrata*).** Reconstruction of protein-protein interactions based on known  
2501 and predicted interactions using STRING analysis and the minke whale protein database in STRING. **A.**  
2502 **KEGG pathways relating physiological pathways** are highlighted as follows: red=complement and  
2503 coagulation cascade; blue=renin-angiotensin system; light green=oestrogen signalling;  
2504 yellow=cholesterol metabolism; pink=vitamin digestion and absorption; dark  
2505 green=glycolysis/gluconeogenesis; light blue=biosynthesis of amino acids; orange=fat digestion and  
2506 absorption. **B. KEGG pathways relating to immunity:** red=*Staphylococcus aureus* infection; blue=SLE;  
2507 light green=amoebiasis; yellow=ferroptosis; pink=phagosome; dark green=necroptosis. Coloured lines  
2508 indicate whether protein interactions are identified via known interactions (curated databases,  
2509 experimentally determined), predicted interactions (gene neighbourhood, gene fusion, gene co-

2510 occurrence) or via text mining, co-expression or protein homology (see the colour key for connective  
2511 lines included in the figure). PPI enrichment p-value:  $p < 1.0 \times 10^{-16}$

2512

2513 **Fig. 5 Protein-protein interaction networks of deiminated protein hits identified in serum of fin**  
2514 **whale (*Balaenoptera physalus*)**. Reconstruction of protein-protein interactions based on known and  
2515 predicted interactions using STRING analysis and the orca protein database in STRING. **A. KEGG**  
2516 **pathways relating physiological pathways** are highlighted as follows: red=complement and  
2517 coagulation cascade; blue=metabolic pathways; light green=oestrogen signalling; yellow=cholesterol  
2518 metabolism; pink=vitamin digestion and absorption; dark green=glycolysis/gluconeogenesis; light  
2519 blue=biosynthesis of amino acids; orange=fat digestion and absorption; purple=carbon metabolism;  
2520 brown=ECM-receptor interaction. **B. KEGG pathways relating to immunity**: red=*Staphylococcus*  
2521 *aureus* infection; blue=SLE; light green=amoebiasis; yellow=prion diseases; pink=pertussis; dark  
2522 green=proteoglycans in cancer; orange=metabolism of xenobiotics by cytochrome P450; light  
2523 blue=human papillomavirus infection; purple=focal adhesion. Coloured lines indicate whether protein  
2524 interactions are identified via known interactions (curated databases, experimentally determined),  
2525 predicted interactions (gene neighbourhood, gene fusion, gene co-occurrence) or via text mining, co-  
2526 expression or protein homology (see the colour key for connective lines included in the figure). PPI  
2527 enrichment p-value:  $p < 1.0 \times 10^{-16}$

2528

2529 **Fig. 6 Protein-protein interaction networks of deiminated protein hits identified in serum of**  
2530 **humpback whale (*Megaptera novaeangliae*)**. Reconstruction of protein-protein interactions based  
2531 on known and predicted interactions using STRING analysis and the orca protein database in STRING.  
2532 **A. KEGG pathways relating physiological pathways** are highlighted as follows: red=complement and  
2533 coagulation cascade; blue=metabolic pathways; light green=oestrogen signalling; yellow=cholesterol  
2534 metabolism; pink=HIF-1 signalling pathway; dark green=glycolysis/gluconeogenesis; light  
2535 blue=biosynthesis of amino acids; orange=carbon metabolism; purple=nitrogen metabolism;  
2536 brown=pentose phosphate pathway. **B. KEGG pathways relating to immunity**: red=complement and  
2537 coagulation cascade; blue=*Staphylococcus aureus* infection. Coloured lines indicate whether protein  
2538 interactions are identified via known interactions (curated databases, experimentally determined),  
2539 predicted interactions (gene neighbourhood, gene fusion, gene co-occurrence) or via text mining, co-  
2540 expression or protein homology (see the colour key for connective lines included in the figure). PPI  
2541 enrichment p-value:  $p < 1.0 \times 10^{-16}$ .

2542

2543 **Fig. 7 Protein-protein interaction networks of deiminated protein hits identified in serum of Cuvier's**  
2544 **beaked whale (*Ziphius cavirostris*)**. Reconstruction of protein-protein interactions based on known  
2545 and predicted interactions using STRING analysis and the orca protein database in STRING. **A. KEGG**  
2546 **pathways relating physiological pathways** are highlighted as follows: red=complement and  
2547 coagulation cascade; blue=metabolic pathways; light green=mineral absorption; yellow=thyroid  
2548 hormone synthesis; pink=HIF-1 signalling pathway; dark green=glycolysis/gluconeogenesis; light  
2549 blue=biosynthesis of amino acids; orange=carbon metabolism; purple=nitrogen metabolism;  
2550 brown=proximal tubule bicarbonate reclamation. **B. KEGG pathways relating to immunity (and**  
2551 **metabolism)**: red=African trypanosomiasis; pink=ferroptosis; blue=pentose phosphate pathway; light  
2552 green=fructose and mannose metabolism; yellow=pyruvate metabolism. Coloured lines indicate  
2553 whether protein interactions are identified via known interactions (curated databases, experimentally  
2554 determined), predicted interactions (gene neighbourhood, gene fusion, gene co-occurrence) or via  
2555 text mining, co-expression or protein homology (see the colour key for connective lines included in  
2556 the figure). PPI enrichment p-value:  $p < 1.0 \times 10^{-16}$

2557  
2558 **Fig. 8 Protein-protein interaction networks of deiminated protein hits identified in serum of orca**  
2559 **(*Orcinus orca*)**. Reconstruction of protein-protein interactions based on known and predicted  
2560 interactions using STRING analysis and the orca protein database in STRING. **A. KEGG pathways**  
2561 **relating physiological pathways** are highlighted as follows: red=complement and coagulation  
2562 cascade; blue=fat digestion and absorption; light green=cholesterol metabolism; yellow=vitamin  
2563 digestion and absorption. **B. KEGG pathways relating to immunity**: red=*Staphylococcus aureus*  
2564 infection; blue=SLE; light green=pertussis; yellow=prion diseases; pink=Chagas disease (American  
2565 trypanosomiasis); dark green=African trypanosomiasis; light blue=ferroptosis. Coloured lines indicate  
2566 whether protein interactions are identified via known interactions (curated databases, experimentally  
2567 determined), predicted interactions (gene neighbourhood, gene fusion, gene co-occurrence) or via  
2568 text mining, co-expression or protein homology (see the colour key for connective lines included in  
2569 the figure). PPI enrichment p-value:  $p < 1.0 \times 10^{-16}$

2570  
2571 **Fig. 9. Venn diagram for physiological and immunological KEGG pathways in cetaceans. A.**  
2572 Deiminated KEGG protein pathways identified in STRING for the 5 cetaceans under study reveal a  
2573 number of common/shared and species-specific pathways relating to physiological functions. **B.**  
2574 Deiminated KEGG protein pathways immune functions, identified in STRING for the 5 cetaceans under  
2575 study, reveal a number of common/shared and species-specific pathways.

2576

2577 **Fig. 10. MicroRNA expression in whale and orca sera and serum-derived EVs.** A-B. MiR21, miR155  
2578 and miR210 relative expression was assessed for key inflammatory and metabolic miRs respectively,  
2579 in whale and orca sera and serum derived EVs. **A.** MiR21 expression was compared in EVs and sera of  
2580 the 5 species under study, with highest levels found in EVs of humpback whale and minke whale; **B.**  
2581 MiR155 expression was compared in EVs and sera of the 4 whales and orca, with the highest levels  
2582 observed in minke whale; **C.** MiR210 expression was compared in EVs and sera of whales and orca,  
2583 showing highest relative levels in orca EVs.

2584

2585 **Supplementary Fig. 1. Phylogenetic tree for PAD isozymes in cetacea.** Neighbour-joining phylogeny  
2586 derived using the conditions of the Poisson distance correction model in MEGAX (Kumar et al., 2018),  
2587 showing the relationships of cetacea and *Hippopotamus amphibius* PADs. Bootstrap values > 50 based  
2588 on 1000 replicates are shown as nodal support. PADs for the 4 whales and orca focused on in this  
2589 study, northern minke whale (*Balaenoptera acutorostrata*), fin whale (*Balaenoptera physalus*),  
2590 humpback whale (*Megaptera novaeangliae*), Cuvier's beaked whale (*Ziphius cavirostris*) and orca  
2591 (*Orcinus orca*), are highlighted by silhouettes.

2592

2593 **Supplementary Fig. 2. Protein-protein interaction networks of deiminated protein hits identified in**  
2594 **serum of minke whale (*Balaenoptera acutorostrata*).** Reconstruction of protein-protein interactions  
2595 based on known and predicted interactions using STRING analysis. As not all target proteins are  
2596 present in STRING for minke whale, 85 minke whale proteins could be used for this analysis. KEGG  
2597 pathways relating to the identified proteins and reported in STRING are highlighted as follows:  
2598 red=complement and coagulation cascade; light blue=*Staphylococcus aureus* infection;  
2599 orange=systemic lupus erythematosus (SLE); dark blue=cholesterol metabolism; pink=ECM receptor  
2600 interaction; dark green=amoebiasis; yellow=estrogen signalling pathway; light green=glycolysis.  
2601 Coloured lines indicate whether protein interactions are identified via known interactions (curated  
2602 databases, experimentally determined), predicted interactions (gene neighbourhood, gene fusion,  
2603 gene co-occurrence) or via text mining, co-expression or protein homology (see the colour key for  
2604 connective lines included in the figure).

2605

2606 **Supplementary Fig. 3. Protein-protein interaction networks of adiponectin in orca (*Orcinus orca*).**  
2607 Reconstruction of protein-protein interactions of orca adiponectin, based on known and predicted  
2608 interactions using STRING analysis. **A.** Coloured nodes represent query proteins and first shell of  
2609 interactors (ADIPOQ=adiponectin and highlighted in red). **B.** KEGG pathways related to adiponectin  
2610 (ADIPOQ) and interacting proteins, reported in STRING and highlighted as follows: Yellow=non-

2611 alcoholic fatty liver disease (NAFLD); pink=AMPK signalling pathway; dark green=longevity regulating  
2612 pathway; red=adipocytokine signalling pathway; light blue=PPAR signalling pathway; orange=type II  
2613 diabetes mellitus; purple=regulation of lipolysis in adipocytes; light green=HIF-1 signalling pathway;  
2614 dark blue=insulin resistance; brown=FoxO signalling pathway. Coloured nodes represent query  
2615 protein (adiponectin=ADIPOQ) and first shell of interactors, white nodes are second shell of  
2616 interactors. Coloured lines indicate whether protein interactions are identified via known interactions  
2617 (curated databases, experimentally determined), predicted interactions (gene neighbourhood, gene  
2618 fusion, gene co-occurrence) or via text mining, co-expression or protein homology (see colour key for  
2619 connective lines shown in the figure).

2620

2621 **Supplementary Table 1.** A summary on data available for the individual cetaceans from which serum  
2622 samples were utilised in this study.

2623

2624 **Supplementary Table 2. Deiminated proteins identified by F95 enrichment in serum of Northern**  
2625 **minke whale (*Balaenoptera acutorostrata*).** Deiminated proteins were isolated by  
2626 immunoprecipitation using the pan-deimination F95 antibody. The F95 enriched eluate was analysed  
2627 by LC-MS/MS and peak list files were submitted to mascot. Peptide hits scoring with the cetacean  
2628 database (CCP\_Cetacea Cetacea\_20191213; 252,001 sequences; 150,129,595 residues) are shown.  
2629 Species hit names and total scores are shown.

2630

2631 **Supplementary Table 3. Deiminated proteins identified by F95 enrichment in serum of fin whale**  
2632 **(*Balaenoptera physalus*).** Deiminated proteins were isolated by immunoprecipitation using the pan-  
2633 deimination F95 antibody. The F95 enriched eluate was analysed by LC-MS/MS and peak list files were  
2634 submitted to mascot. Peptide hits scoring with the cetacean database (CCP\_Cetacea  
2635 Cetacea\_20191213; 252,001 sequences; 150,129,595 residues) are shown. Species hit names and  
2636 total scores are shown.

2637

2638 **Supplementary Table 4. Deiminated proteins identified by F95 enrichment in serum of humpback**  
2639 **whale (*Megaptera novaeangliae*).** Deiminated proteins were isolated by immunoprecipitation using  
2640 the pan-deimination F95 antibody. The F95 enriched eluate was analysed by LC-MS/MS and peak list  
2641 files were submitted to mascot. Peptide hits scoring with the cetacean database (CCP\_Cetacea  
2642 Cetacea\_20191213; 252,001 sequences; 150,129,595 residues) are shown. Species hit names and  
2643 total scores are shown.

2644

2645 **Supplementary Table 5. Deiminated proteins identified by F95 enrichment in serum of Cuvier's**  
 2646 **beaked whale (*Ziphius cavirostris*)**. Deiminated proteins were isolated by immunoprecipitation using  
 2647 the pan-deimination F95 antibody. The F95 enriched eluate was analysed by LC-MS/MS and peak list  
 2648 files were submitted to mascot. Peptide hits scoring with the cetacean database (CCP\_Cetacea  
 2649 Cetacea\_20191213; 252,001 sequences; 150,129,595 residues) are shown. Species hit names and  
 2650 total scores are shown.

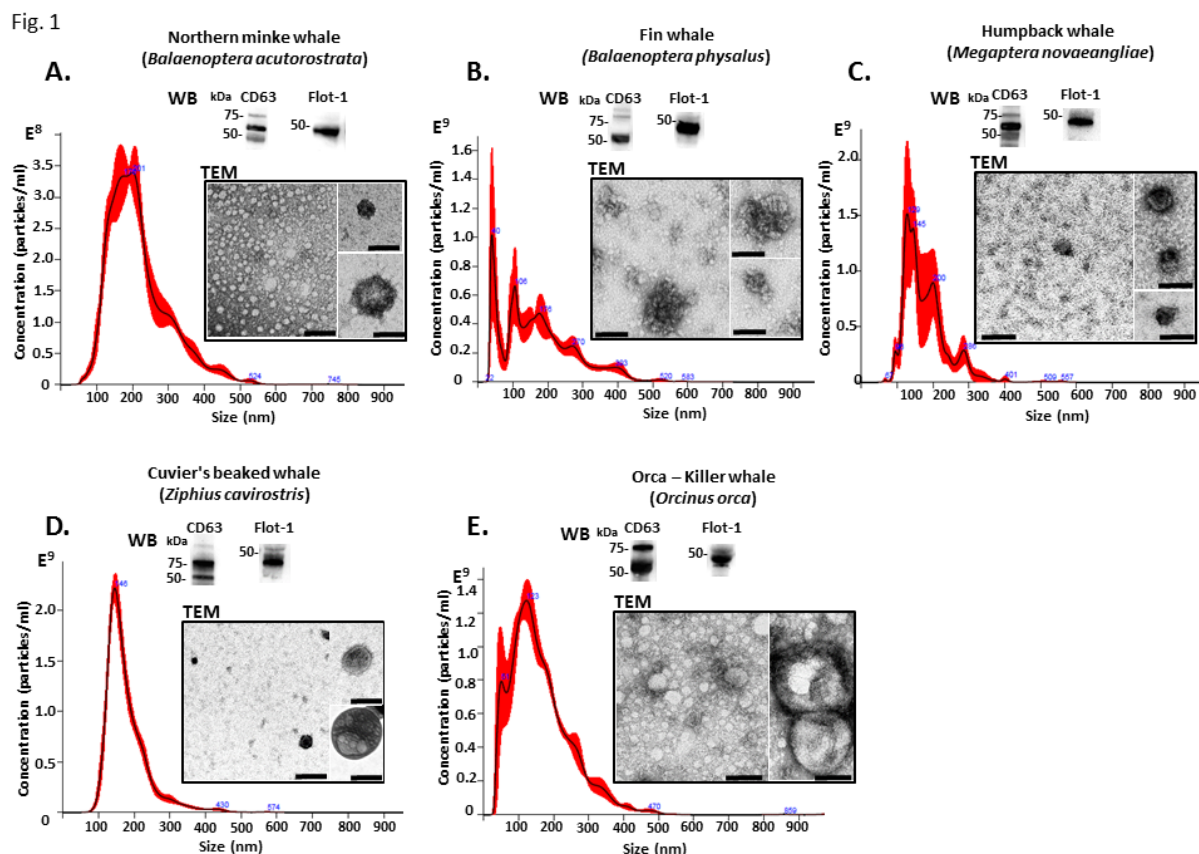
2651

2652 **Supplementary Table 6. Deiminated proteins identified by F95 enrichment in serum of orca (*Orcinus***  
 2653 ***orca*)**. Deiminated proteins were isolated by immunoprecipitation using the pan-deimination F95  
 2654 antibody. The F95 enriched eluate was analysed by LC-MS/MS and peak list files were submitted to  
 2655 mascot. Peptide hits scoring with the cetacean database (CCP\_Cetacea Cetacea\_20191213; 252,001  
 2656 sequences; 150,129,595 residues) are shown. Species hit names and total scores are shown.

2657

2658

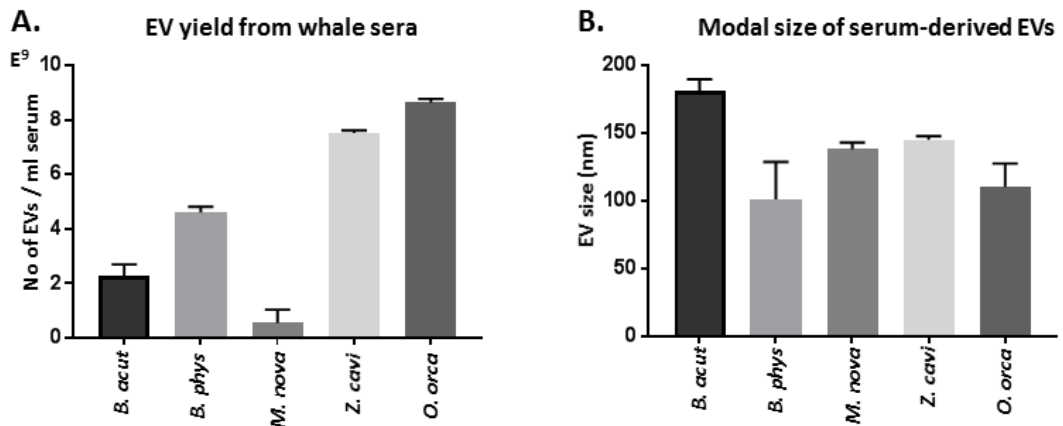
Fig. 1



2659

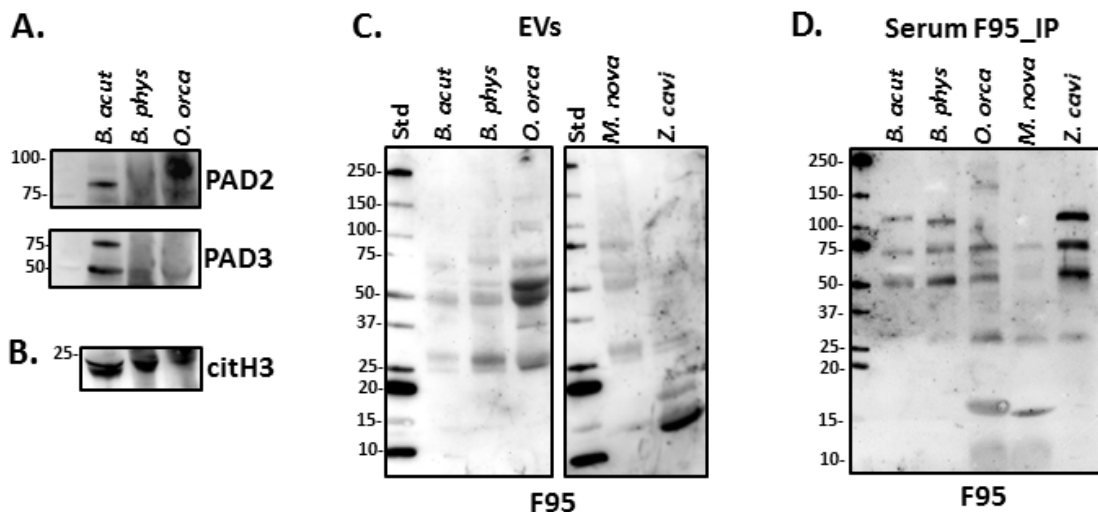
2660

**Fig. 2**



2661

**Fig. 3**



2662

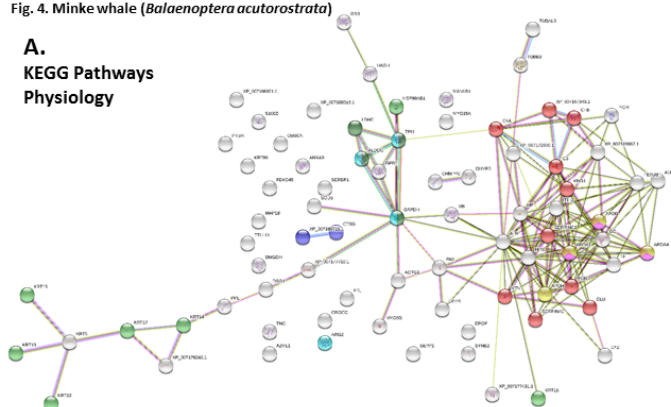
2663

2664

2665

Fig. 4. Minke whale (*Balaenoptera acutorostrata*)

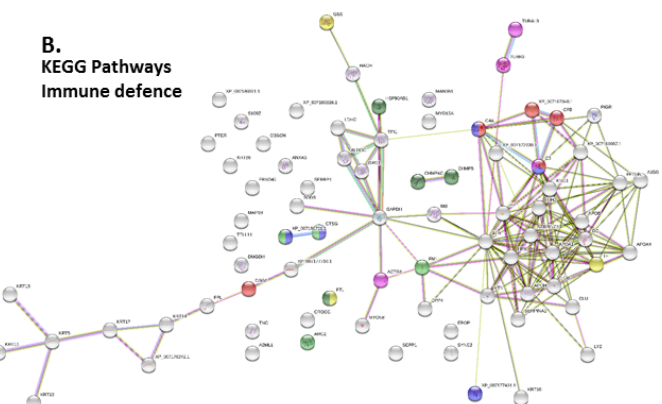
**A.**  
KEGG Pathways  
Physiology



**KEGG Pathways:**

- Complement and coagulation cascades
- Renin-angiotensin system
- Oestrogen signalling pathway
- Cholesterol metabolism
- Vitamin digestion and absorption
- Glycolysis/Gluconeogenesis
- Biosynthesis of amino acids
- Fat digestion and absorption

**B.**  
KEGG Pathways  
Immune defence



**KEGG Pathways:**

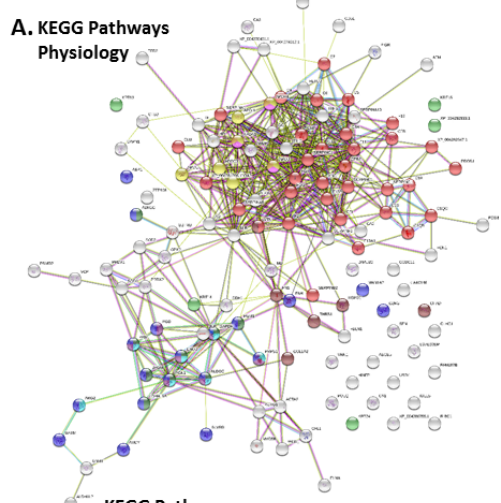
- *Staphylococcus aureus* infection
- Systemic lupus erythematosus
- Amoebiasis
- Ferroptosis
- Phagosome
- Necroptosis

2666

2667

Fig. 5. Fin whale (*Balaenoptera physalus*)

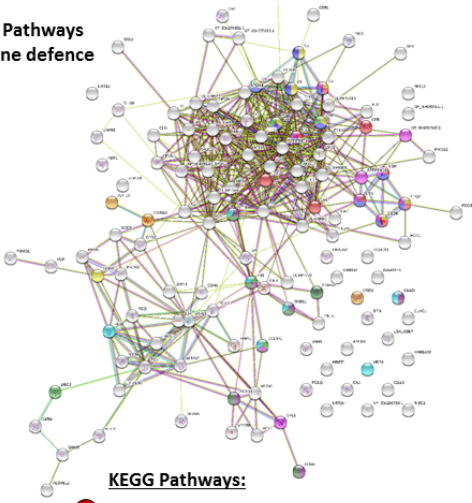
**A. KEGG Pathways**  
Physiology



**KEGG Pathways:**

- Complement and coagulation cascades
- Metabolic pathways
- Oestrogen signalling pathway
- Biosynthesis of amino acids
- Fat digestion and absorption
- Cholesterol metabolism
- Vitamin digestion and absorption
- Glycolysis/Gluconeogenesis
- Carbon metabolism
- ECM-receptor interaction

**B. KEGG Pathways**  
Immune defence



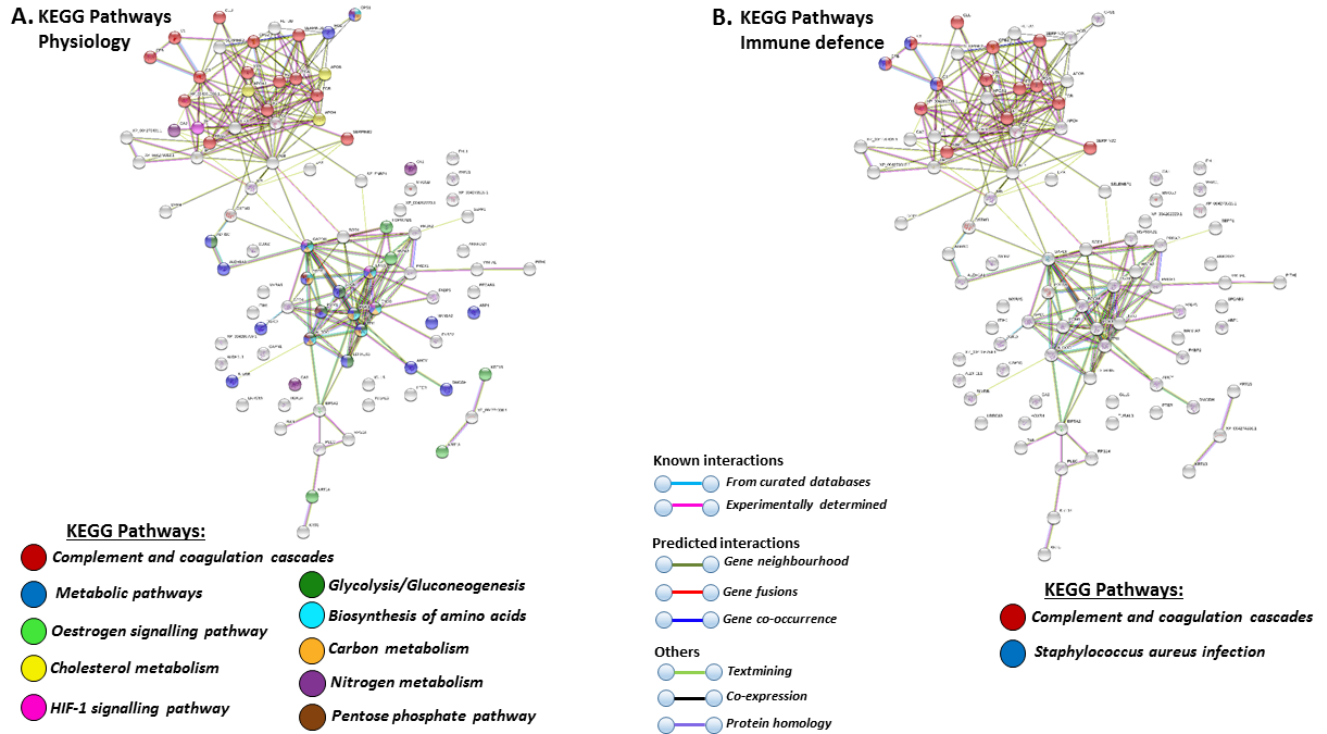
**KEGG Pathways:**

- *Staphylococcus aureus* infection
- Systemic lupus erythematosus
- Amoebiasis
- Prion diseases
- Human papillomavirus infection
- Pertussis
- Focal adhesion
- Proteoglycans in cancer
- Metabolism of xenobiotics by cytP450

2668

2669

Fig. 6. Humpback whale (*Megaptera novaeangliae*)

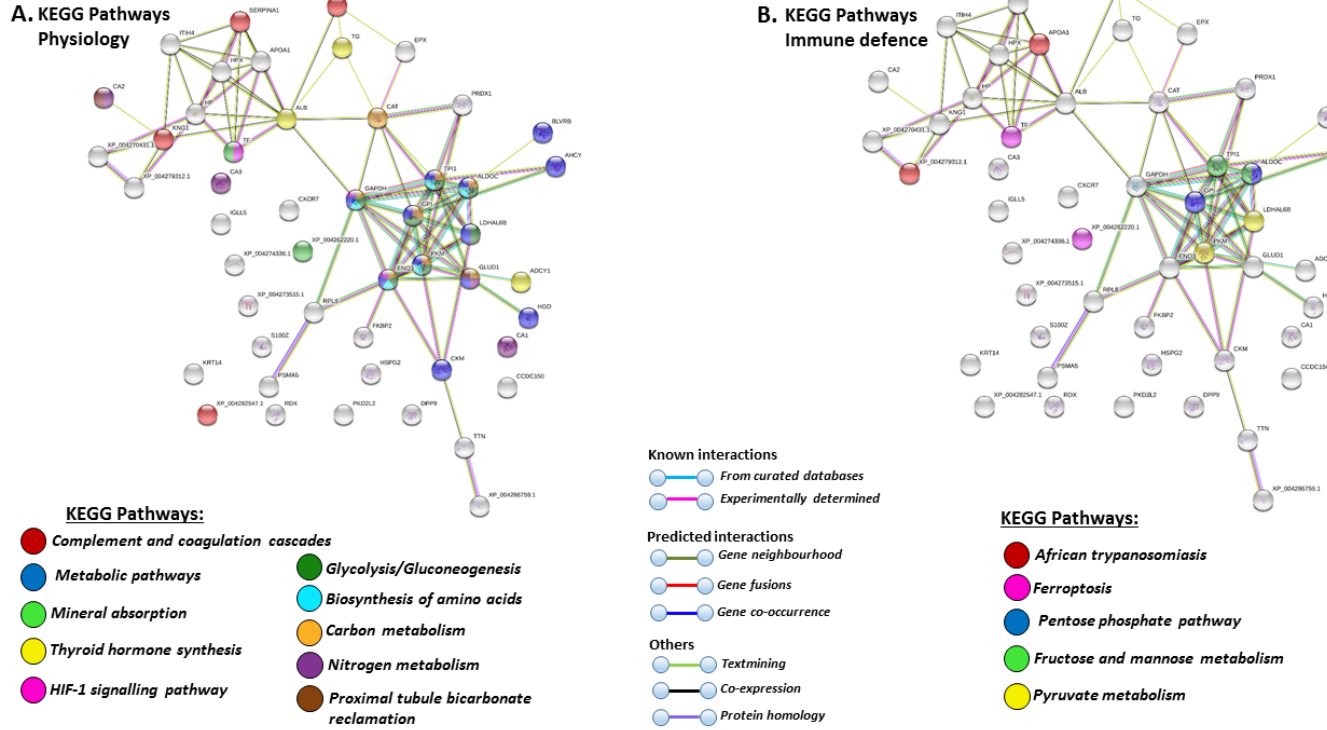


2670

2671

2672

Fig. 7. Cuvier's beaked whale (*Ziphis cavirostris*)

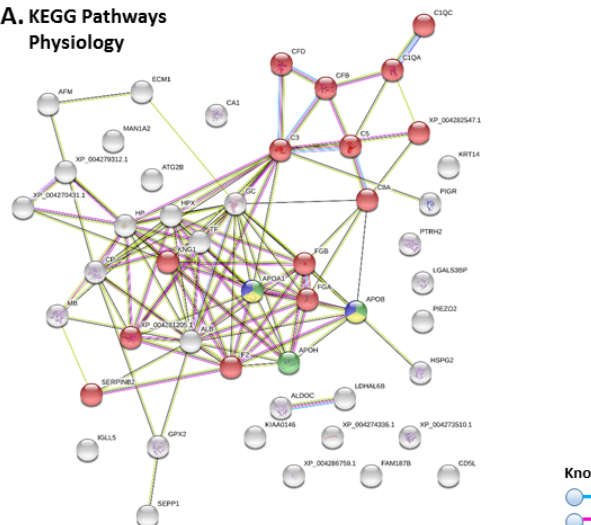


2673

2674

Fig. 8. Orca (*Orcinus orca*)

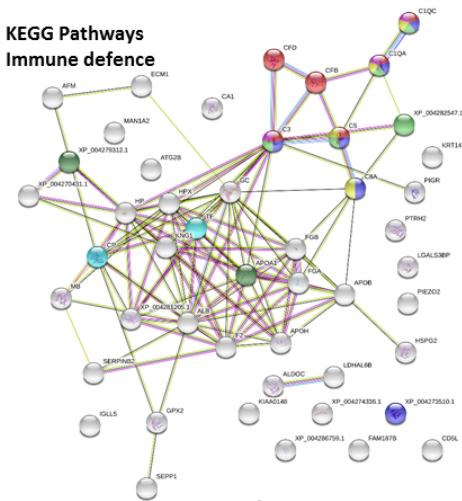
**A. KEGG Pathways Physiology**



**KEGG Pathways:**

- Complement and coagulation cascades
- Fat digestion and absorption
- Cholesterol metabolism
- Vitamin digestion and absorption

**B. KEGG Pathways Immune defence**



**Known interactions**

- From curated databases
- Experimentally determined

**Predicted interactions**

- Gene neighbourhood
- Gene fusions
- Gene co-occurrence
- Textmining
- Co-expression
- Protein homology

**Others**

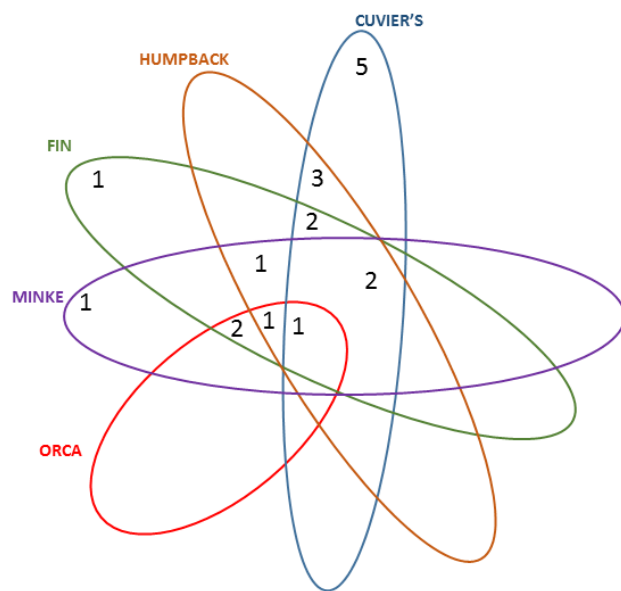
- KEGG Pathways:**
- *Staphylococcus aureus infection*
  - *Systemic lupus erythematosus*
  - *Pertussis*
  - *Prion diseases*
  - *Chagas disease (American trypanosomiasis)*
  - *African trypanosomiasis*
  - *Ferroptosis*

2675

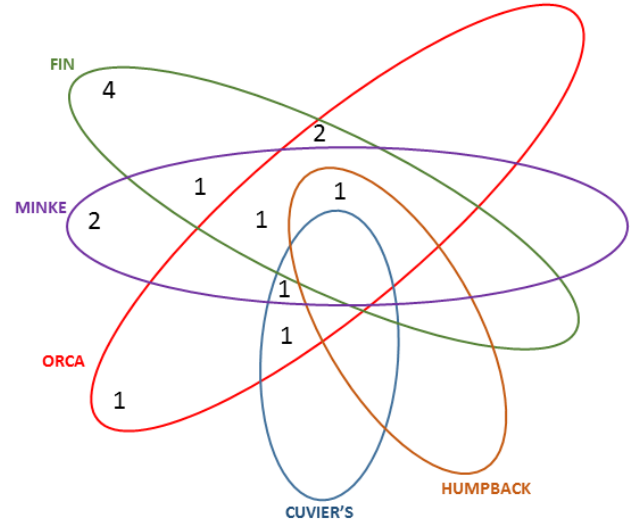
2676

Fig. 9.

**A. KEGG physiological pathways**



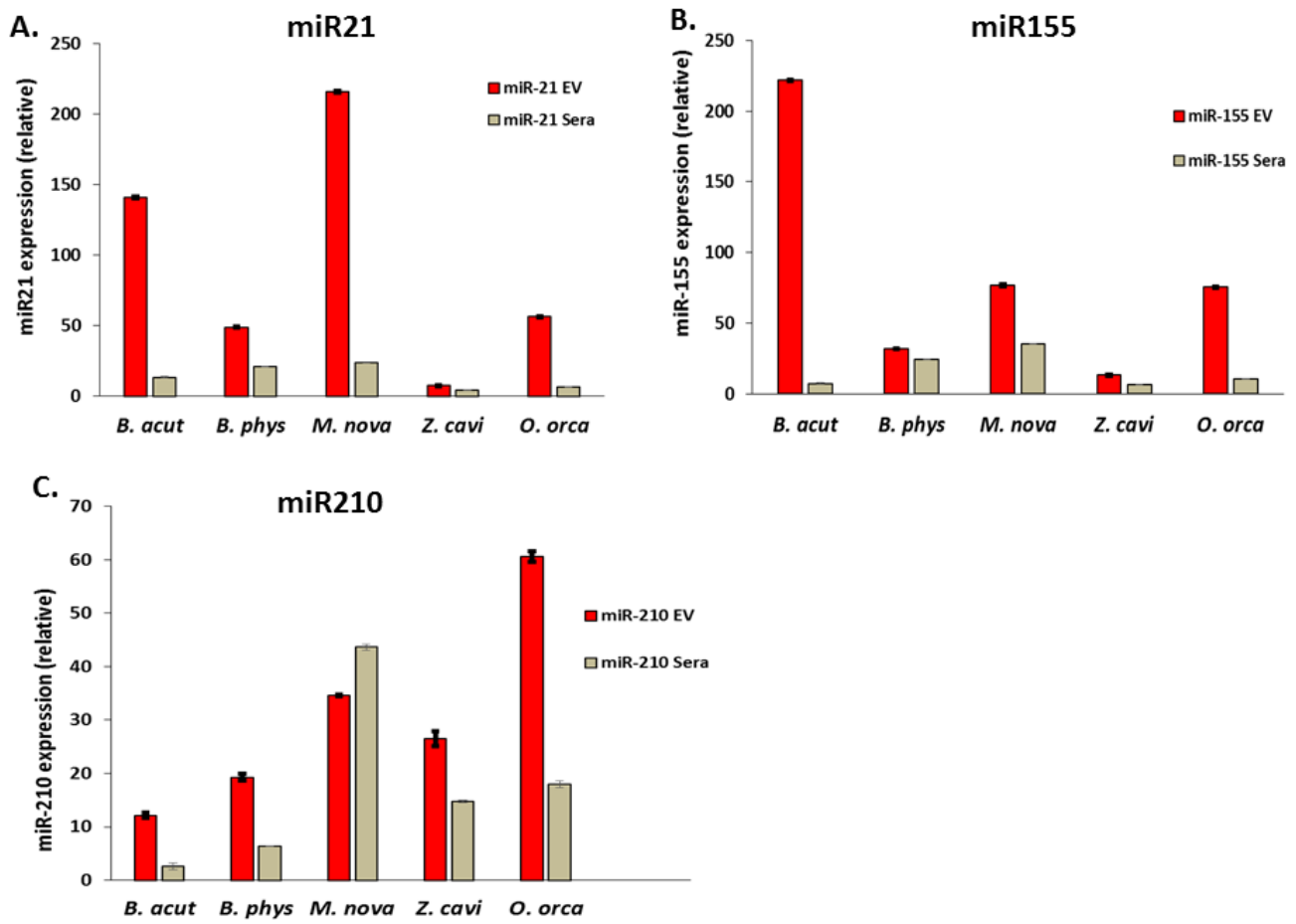
**B. KEGG immune pathways**



2677

2678

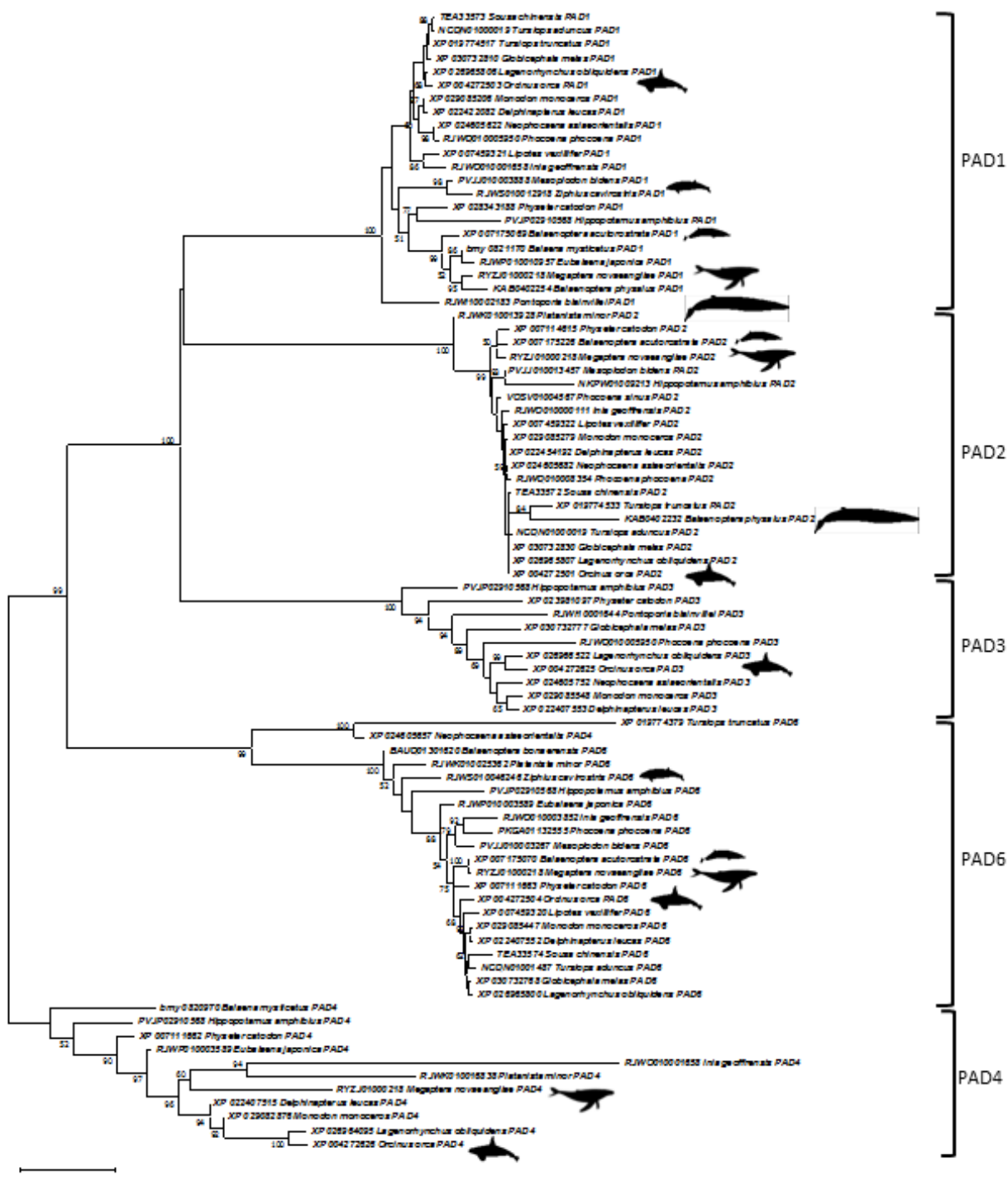
**Fig. 10**



2679

2680

2681



2683

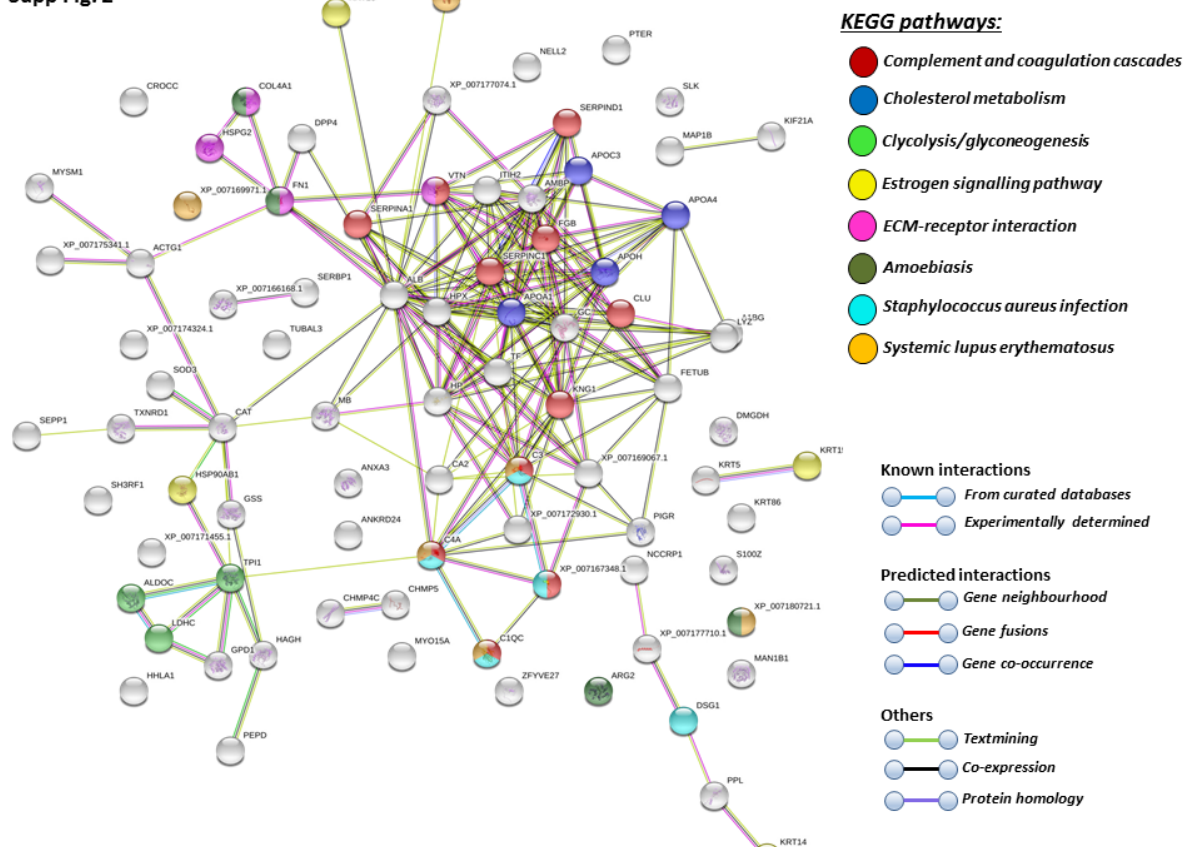
2684

2685

2686

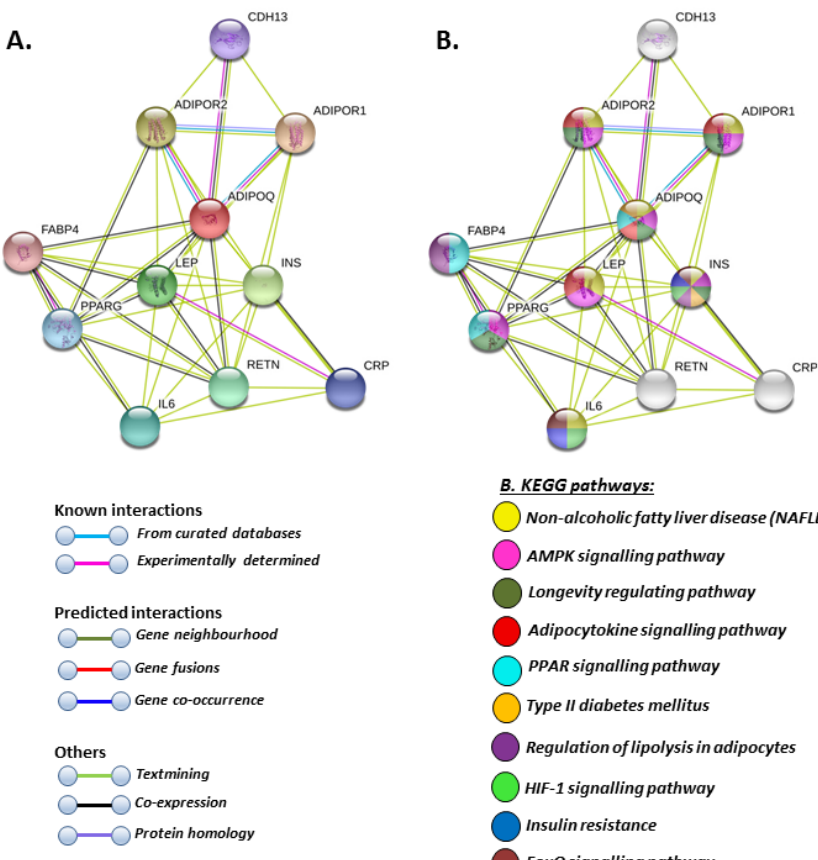
2687

Supp Fig. 2



2688

Supp. Fig. 3



2689

2690

2691

2692 **Supplementary Table 1.** Data summary for the individual cetaceans used in this study.

Common name	Species name	Sex	Maturity	Age (yrs)	Length /weight recorded	Location
Minke whale	<i>Balaenoptera acutorostrata</i>	male	mature	Not assessed	813 cm	South-Western Iceland (free ranging)
Fin whale	<i>Balaenoptera physalus</i>	female	anoestrous	33	2100 cm	South-Western Iceland (free ranging)
Humpback whale	<i>Megaptera novaeangliae</i>	female	immature	Not assessed	880 cm	South-Western Iceland (stranded)
Cuvier's beaked whale	<i>Ziphius cavirostris</i>	female	immature	Not assessed	605 cm	South-Eastern Iceland (stranded)
Orca	<i>Orcinus orca</i>	male	mature	22	5440 kg	South Iceland (captive)

2693

2694

2695   **Supplementary Table 2. Deiminated proteins identified by F95 enrichment in serum of Northern minke whale**  
 2696   **(*Balaenoptera acutorostrata*).** Deiminated proteins were isolated by immunoprecipitation using the pan-  
 2697   deimination F95 antibody. The F95 enriched eluate was analysed by LC-MS/MS and peak list files were submitted  
 2698   to mascot . Peptide hits scoring with the cetacean database (CCP\_Cetacea\_Cetacea\_20191213; 252,001  
 2699   sequences; 150,129,595 residues) are shown. Species hit names and total scores are shown.

Protein name	Species name	Common name	Total score ( <i>p</i> <0.05) <sup>t</sup>
AOA452CHV5_BALAS <b><i>apolipoprotein B-100</i></b>	<i>Balaenoptera acutorostrata scammoni</i>	Scammon's minke whale	3805
AOA384B912_BALAS <b><i>alpha-2-macroglobulin isoform X2</i></b>	<i>Balaenoptera acutorostrata scammoni</i>	Scammon's minke whale	3144
AOA2P4TBI3_BAMTH <b><i>apolipoprotein B-100</i></b>	<i>Lipotes vexillifer</i>	Baiji (white-finned dolphin)	2503
AOA383Z2B4_BALAS <b><i>complement C3</i></b>	<i>Balaenoptera acutorostrata scammoni</i>	Scammon's minke whale	2339
AOA383ZXRO_BALAS <b><i>serum albumin</i></b>	<i>Balaenoptera acutorostrata scammoni</i>	Scammon's minke whale	2314
AOA2Y9NK15_DELLE <b><i>alpha-2-macroglobulin isoform X3</i></b>	<i>Delphinapterus leucas</i>	Beluga whale	2152
AOA2U4AKU7_TURTR <b><i>alpha-2-macroglobulin-like</i></b>	<i>Tursiops truncatus</i>	Common bottlenose dolphin	2037
AOA4U1FPV0_MONMO <b><i>Uncharacterized protein</i></b>	<i>Monodon monoceros</i>	Narwhal	2033
AOA384ALG4_BALAS <b><i>ceruloplasmin isoform X2</i></b>	<i>Balaenoptera acutorostrata scammoni</i>	Scammon's minke whale	1968
AOA455BHA9_PHYMC <b><i>alpha-2-macroglobulin-like</i></b>	<i>Physeter macrocephalus</i>	Sperm whale	1848
AOA383Z5R5_BALAS <b><i>serotransferrin</i></b>	<i>Balaenoptera acutorostrata scammoni</i>	Scammon's minke whale	1707
AOA341C5T8_9CETA <b><i>serum albumin</i></b>	<i>Neophocaena asiaeorientalis asiaeorientalis</i>	Yangtze finless porpoise	1640
AOA2U3V5M2_TURTR <b><i>serum albumin isoform X1</i></b>	<i>Tursiops truncatus</i>	Common bottlenose dolphin	1610
AOA340XNP3_LIPVE <b><i>complement C3</i></b>	<i>Lipotes vexillifer</i>	Baiji (white-finned dolphin)	1548
AOA384B6G0_BALAS <b><i>kininogen-1</i></b>	<i>Balaenoptera acutorostrata scammoni</i>	Scammon's minke whale	1145
AOA383CJ5_BALAS <b><i>Hemopexin</i></b>	<i>Balaenoptera acutorostrata scammoni</i>	Scammon's minke whale	1094
AOA2F0B3C5_ESCRO <b><i>Keratin, type II cytoskeletal 5</i></b>	<i>Eschrichtius robustus</i>	Gray whale	1092
AOA2Y9MM41_DELLE <b><i>fibronectin isoform X6</i></b>	<i>Delphinapterus leucas</i>	Beluga whale	1047
AOA2Y9EED2_PHYMC <b><i>fibronectin isoform X5</i></b>	<i>Physeter macrocephalus</i>	Sperm whale	1045
AOA340XBS1_LIPVE <b><i>fibronectin</i></b>	<i>Lipotes vexillifer</i>	Baiji (white-finned dolphin)	1022
AOA384ALK4_BALAS <b><i>fibronectin</i></b>	<i>Balaenoptera acutorostrata scammoni</i>	Scammon's minke whale	1016
AOA2F0B042_ESCRO <b><i>Hemopexin</i></b>	<i>Eschrichtius robustus</i>	Gray whale	944
AOA383YWT8_BALAS	<i>Balaenoptera acutorostrata scammoni</i>	Scammon's minke whale	929

<b>complement factor H-like isoform X1</b>			
AOA383Z8T4_BALAS <b>C4b-binding protein alpha chain isoform X7</b>	<i>Balaenoptera acutorostrata scammoni</i>	Scammon's minke whale	864
APOA1_BALAS <b>Apolipoprotein A-I</b>	<i>Balaenoptera acutorostrata scammoni</i>	Scammon's minke whale	856
A0A384BF87_BALAS <b>Haptoglobin</b>	<i>Balaenoptera acutorostrata scammoni</i>	Scammon's minke whale	722
AOA2Y9N2V9_DELLE <b>kininogen-1 isoform X1</b>	<i>Delphinapterus leucas</i>	Beluga whale	707
A0A341CEB0_9CETA <b>Hemopexin</b>	<i>Neophocaena asiaeorientalis asiaeorientalis</i>	Yangtze finless porpoise	674
0A484GXQ7_SOUCHE <b>Hemopexin</b>	<i>Sousa chinensis</i>	Indo-Pacific humpbacked dolphin	625
AOA4U1EQC8_MONMO <b>apolipoprotein A-IV</b>	<i>Monodon monoceros</i>	Narwhal	623
AOA2Y9SJP9_PHYMC <b>keratin, type II cytoskeletal 6A</b>	<i>Physeter macrocephalus</i>	Sperm whale	586
AOA383ZI56_BALAS <b>inter-alpha-trypsin inhibitor heavy chain H4 isoform X2</b>	<i>Balaenoptera acutorostrata scammoni</i>	Scammon's minke whale	584
AOA140GN64_BALAC <b>Hemoglobin subunit beta</b>	<i>Balaenoptera acutorostrata</i>	Northern minke whale	583
AOA340Y1E6_LIPVE <b>keratin, type I cytoskeletal 14</b>	<i>Lipotes vexillifer</i>	Baiji (white-finned dolphin)	569
AV1_ESCRO <b>Keratin, type I cytoskeletal 14</b>	<i>Eschrichtius robustus</i>	Gray whale	517
AOA2Y9F6Z4_PHYMC <b>kininogen-1 isoform X1</b>	<i>Physeter macrocephalus</i>	Sperm whale	504
AOA383ZST7_BALAS <b>complement C5 isoform X1</b>	<i>Balaenoptera acutorostrata scammoni</i>	Scammon's minke whale	493
AOA384BAA9_BALAS <b>apolipoprotein A-IV</b>	<i>Balaenoptera acutorostrata scammoni</i>	Scammon's minke whale	491
AOA140GN67_MESDE <b>Hemoglobin subunit beta</b>	<i>Mesoplodon densirostris</i>	Blainville's beaked whale	466
AOA383Z9Z9_BALAS <b>Alpha-mannosidase</b>	<i>Balaenoptera acutorostrata scammoni</i>	Scammon's minke whale	456
AOA2FOBP97_ESCRO <b>Ig mu heavy chain disease protein</b>	<i>Eschrichtius robustus</i>	Gray whale	439
AOA4U1FIN2_MONMO <b>keratin, type I cytoskeletal 13</b>	<i>Monodon monoceros</i>	Narwhal	435
AOA383ZV20_BALAS <b>alpha-1-antitrypsin</b>	<i>Balaenoptera acutorostrata scammoni</i>	Scammon's minke whale	431
AOA340XV96_LIPVE <b>keratin, type I cytoskeletal 17</b>	<i>Lipotes vexillifer</i>	Baiji (white-finned dolphin)	409
AOA383ZW6_BALAS <b>keratin, type II cytoskeletal 6A-like isoform X2</b>	<i>Balaenoptera acutorostrata scammoni</i>	Scammon's minke whale	388
AOA2Y9P8E6_DELLE <b>desmoplakin isoform X1</b>	<i>Delphinapterus leucas</i>	Beluga whale	376
28_PONBL <b>Apolipoprotein B</b>	<i>Pontoporia blainvilliei</i>	La Plata dolphin	373
AOA140GN13_BALAC	<i>Balaenoptera acutorostrata</i>	Northern minke whale	365

<b>Hemoglobin subunit alpha</b>			
AOA384A3E4_BALAS <b>hemoglobin subunit alpha isoform X1</b>	<i>Balaenoptera acutorostrata scammoni</i>	Scammon's minke whale	346
AOA384AZC9_BALAS <b>Clusterin</b>	<i>Balaenoptera acutorostrata scammoni</i>	Scammon's minke whale	338
AOA384B1Q0_BALAS <b>vitamin D-binding protein</b>	<i>Balaenoptera acutorostrata scammoni</i>	Scammon's minke whale	328
AOA384A7N6_BALAS <b>dipeptidyl peptidase 4</b>	<i>Balaenoptera acutorostrata scammoni</i>	Scammon's minke whale	
AOA2Y9LVR1_DELLE <b>keratin, type I cytoskeletal 15</b>	<i>Delphinapterus leucas</i>	Beluga whale	299
AOA2F0B4J5_ESCRO <b>Hemoglobin subunit alpha</b>	<i>Eschrichtius robustus</i>	Gray whale	280
AOA383ZRY6_BALAS <b>junction plakoglobin</b>	<i>Balaenoptera acutorostrata scammoni</i>	Scammon's minke whale	275
AOA2Y9P876_DELLE <b>Tubulin beta chain</b>	<i>Delphinapterus leucas</i>	Beluga whale	272
AOA384AFQ0_BALAS <b>Plasminogen</b>	<i>Balaenoptera acutorostrata scammoni</i>	Scammon's minke whale	262
AOA140GN07_MESDE <b>Hemoglobin subunit alpha</b>	<i>Mesoplodon densirostris</i>	Blainville's beaked whale	257
AOA2U4AUY5_TURTR <b>dimethylglycine dehydrogenase, mitochondrial</b>	<i>Tursiops truncatus</i>	Common bottlenose dolphin	257
AOA140GN06_TURTR <b>Hemoglobin subunit alpha</b>	<i>Tursiops truncatus</i>	Common bottlenose dolphin	248
AOA340YDD2_LIPVE <b>xaa-Pro dipeptidase isoform X2</b>	<i>Lipotes vexillifer</i>	Baiji (white-finned dolphin)	240
AOA2U4AU60_TURTR <b>alpha-1B-glycoprotein</b>	<i>Tursiops truncatus</i>	Common bottlenose dolphin	216
AOA140GN09_KOGSI <b>Hemoglobin subunit alpha</b>	<i>Kogia sima</i>	Dwarf sperm whale	214
AOA2Y9S2C1_PHYMC <b>alpha-1B-glycoprotein</b>	<i>Physeter macrocephalus</i>	Sperm whale	203
AOA340WU44_LIPVE <b>immunoglobulin lambda-like polypeptide 5</b>	<i>Lipotes vexillifer</i>	Baiji (white-finned dolphin)	192
AOA2FOBAH8_ESCRO <b>Complement factor B</b>	<i>Eschrichtius robustus</i>	Gray whale	191
AOA2FOBNF0_ESCRO <b>Ig alpha-1 chain C region</b>	<i>Eschrichtius robustus</i>	Gray whale	186
AOA384B2W1_BALAS <b>complement C4</b>	<i>Balaenoptera acutorostrata scammoni</i>	Scammon's minke whale	181
AOA484GJZ6_SOUCHE <b>IF rod domain-containing protein</b>	<i>Sousa chinensis</i>	Indo-Pacific humpbacked dolphin	171
AOA384B7A3_BALAS <b>selenoprotein P</b>	<i>Balaenoptera acutorostrata scammoni</i>	Scammon's minke whale	160
AOA2F0BDQ6_ESCRO <b>Keratin, type I cytoskeletal 18</b>	<i>Eschrichtius robustus</i>	Gray whale	155
AOA452C4G6_BALAS <b>Lysozyme</b>	<i>Balaenoptera acutorostrata scammoni</i>	Scammon's minke whale	154

AOA2U4BA07_TURTR <i>Tubulin alpha chain</i>	<i>Tursiops truncatus</i>	Common bottlenose dolphin	153
AOA452C7H9_BALAS <i>Ferritin</i>	<i>Balaenoptera acutorostrata scammoni</i>	Scammon's minke whale	144
AOA340X0SO_LIPVE <i>desmoglein-1</i>	<i>Lipotes vexillifer</i>	Baiji (white-finned dolphin)	142
AOA340YAH5_LIPVE <i>Triosephosphate isomerase</i>	<i>Lipotes vexillifer</i>	Baiji (white-finned dolphin)	141
AOA2U4BSU8_TURTR <i>actin, cytoplasmic 2</i>	<i>Tursiops truncatus</i>	Common bottlenose dolphin	141
AOA2Y9F6J0_PHYMC <i>antithrombin-III</i>	<i>Physeter macrocephalus</i>	Sperm whale	136
AOA384AFN8_BALAS <i>Superoxide dismutase</i>	<i>Balaenoptera acutorostrata scammoni</i>	Scammon's minke whale	130
AOA452CDN2_BALAS <i>keratin, type I cytoskeletal 12</i>	<i>Balaenoptera acutorostrata scammoni</i>	Scammon's minke whale	120
AOA340XYI8_LIPVE <i>keratin, type I cytoskeletal 42-like</i>	<i>Lipotes vexillifer</i>	Baiji (white-finned dolphin)	120
AOA340WNM5_LIPVE <i>obscurin-like</i>	<i>Lipotes vexillifer</i>	Baiji (white-finned dolphin)	118
AOA384AEC5_BALAS <i>beta-2-glycoprotein 1</i>	<i>Balaenoptera acutorostrata scammoni</i>	Scammon's minke whale	111
AOA2U3V0A2_TURTR <i>Arginase</i>	<i>Tursiops truncatus</i>	Common bottlenose dolphin	109
AOA2F0B5A8_ESCRO <i>Fetuin-B</i>	<i>Eschrichtius robustus</i>	Gray whale	108
AOA4U1EJD5_MONMO <i>TAF domain-containing protein</i>	<i>Monodon monoceros</i>	Narwhal	108
AOA2U4CQQ1_TURTR <i>heat shock protein HSP 90-alpha</i>	<i>Tursiops truncatus</i>	Common bottlenose dolphin	108
AOA2F0B5X4_ESCRO <i>Heat shock protein HSP 90-beta</i>	<i>Eschrichtius robustus</i>	Gray whale	102
AOA2F0B035_ESCRO <i>Fructose-bisphosphate aldolase</i>	<i>Eschrichtius robustus</i>	Gray whale	101
AOA2U4B6K7_TURTR <i>inter-alpha-trypsin inhibitor heavy chain H2</i>	<i>Tursiops truncatus</i>	Common bottlenose dolphin	93
AOA384A960_BALAS <i>alpha-2-antiplasmin</i>	<i>Balaenoptera acutorostrata scammoni</i>	Scammon's minke whale	90
AOA383ZWG2_BALAS <i>keratin, type II cuticular Hb6</i>	<i>Balaenoptera acutorostrata scammoni</i>	Scammon's minke whale	82
AOA2U4BFU2_TURTR <i>unconventional myosin-Vb</i>	<i>Tursiops truncatus</i>	Common bottlenose dolphin	82
AOA2F0B3NO_ESCRO <i>Vitronectin</i>	<i>Eschrichtius robustus</i>	Gray whale	80
AOA2FOBB48_ESCRO <i>Phosphotriesterase-related protein</i>	<i>Eschrichtius robustus</i>	Gray whale	76
AOA452CPB6_BALAS <i>complement component C9</i>	<i>Balaenoptera acutorostrata scammoni</i>	Scammon's minke whale	76
AOA2Y9MHA0_DELLE	<i>Delphinapterus leucas</i>	Beluga whale	75

<b><i>unconventional myosin-XV</i></b>			
AOA2Y9PGE3_DELLE <b><i>protein dopey-1 isoform X4</i></b>	<i>Delphinapterus leucas</i>	Beluga whale	74
AOA2U4APV3_TURTR <b><i>L-lactate dehydrogenase</i></b>	<i>Tursiops truncatus</i>	Common bottlenose dolphin	74
AOA4U1EAQ3_MONMO <b><i>Ig-like domain-containing protein</i></b>	<i>Monodon monoceros</i>	Narwhal	73
AOA2U4ANF3_TURTR <b><i>14-3-3 protein epsilon</i></b>	<i>Tursiops truncatus</i>	Common bottlenose dolphin	68
AOA384A061_BALAS <b><i>cathepsin G-like</i></b>	<i>Balaenoptera acutorostrata scammoni</i>	Scammon's minke whale	66
AOA2F0BHJ5_ESCRO <b><i>Cathepsin G</i></b>	<i>Eschrichtius robustus</i>	Gray whale	66
AOA2U4BPE6_TURTR <b><i>nuclear mitotic apparatus protein 1 isoform X1</i></b>	<i>Tursiops truncatus</i>	Common bottlenose dolphin	65
AOA2U4BAA2_TURTR <b><i>protein kinase C-binding protein NELL2 isoform X3</i></b>	<i>Tursiops truncatus</i>	Common bottlenose dolphin	64
AOA340X2W3_LIPVE <b><i>C-type lectin domain family 4 member K</i></b>	<i>Lipotes vexillifer</i>	Baiji (white-finned dolphin)	63
AOA2FOBF69_ESCRO <b><i>Heparin cofactor 2</i></b>	<i>Eschrichtius robustus</i>	Gray whale	62
AOA2FOAY08_ESCRO <b><i>Glutathione synthetase</i></b>	<i>Eschrichtius robustus</i>	Gray whale	60
AOA2FOBHF1_ESCRO <b><i>Annexin</i></b>	<i>Eschrichtius robustus</i>	Gray whale	59
AOA341ACJ2_9CETA <b><i>charged multivesicular body protein 4c</i></b>	<i>Neophocaena asiaeorientalis asiaeorientalis</i>	Yangtze finless porpoise	58
AOA2U3V9U9_TURTR <b><i>charged multivesicular body protein 5</i></b>	<i>Tursiops truncatus</i>	Common bottlenose dolphin	57
AOA383Z9P7_BALAS <b><i>polymeric immunoglobulin receptor</i></b>	<i>Balaenoptera acutorostrata scammoni</i>	Scammon's minke whale	56
AOA484GZC1_SOUCHE <b><i>Ferritin</i></b>	<i>Sousa chinensis</i>	Indo-Pacific humpbacked dolphin	56
AOA2U3V9D2_TURTR <b><i>heterogeneous nuclear ribonucleoproteins A2/B1 isoform X4</i></b>	<i>Tursiops truncatus</i>	Common bottlenose dolphin	56
AOA340WWE6_LIPVE <b><i>periplakin</i></b>	<i>Lipotes vexillifer</i>	Baiji (white-finned dolphin)	56
AOA383ZLI1_BALAS <b><i>microtubule-associated protein 1B</i></b>	<i>Balaenoptera acutorostrata scammoni</i>	Scammon's minke whale	54
AOA2U4AKU6_TURTR <b><i>Glyceraldehyde-3-phosphate dehydrogenase</i></b>	<i>Tursiops truncatus</i>	Common bottlenose dolphin	54
AOA4U1ETF4_MONMO <b><i>Uncharacterized protein</i></b>	<i>Monodon monoceros</i>	Narwhal	54
AOA2FOAUI6_ESCRO <b><i>Ferritin</i></b>	<i>Eschrichtius robustus</i>	Gray whale	53

AOA2U4C9F5_TURTR <b><i>allergen Fel d 4-like</i></b>	<i>Tursiops truncatus</i>	Common bottlenose dolphin	52
AOA2U3V6F1_TURTR <b><i>tenascin isoform X2</i></b>	<i>Tursiops truncatus</i>	Common bottlenose dolphin	51
A2U4BRW1_TURTR <b><i>terminal uridylyltransferase 7 isoform X4</i></b>	<i>Tursiops truncatus</i>	Common bottlenose dolphin	51
AOA2U4AU11_TURTR <b><i>insulin-like growth factor 2 mRNA-binding protein 3</i></b>	<i>Tursiops truncatus</i>	Common bottlenose dolphin	48
AOA2U4B3V1_TURTR <b><i>E3 ubiquitin-protein ligase SH3RF1 isoform X2</i></b>	<i>Tursiops truncatus</i>	Common bottlenose dolphin	47
AOA2F0B098_ESCRO <b><i>Hydroxyacylglutathione hydrolase, mitochondrial</i></b>	<i>Eschrichtius robustus</i>	Gray whale	46
AOA2Y9P0R0_DELLE <b><i>F-box only protein</i></b>	<i>Delphinapterus leucas</i>	Beluga whale	46
AOA2F0AZL3_ESCRO <b><i>Histone H2B</i></b>	<i>Eschrichtius robustus</i>	Gray whale	45
AOA2U3V4Z9_TURTR <b><i>fibrinogen beta chain</i></b>	<i>Tursiops truncatus</i>	Common bottlenose dolphin	45
AOA340Y9E7_LIPVE <b><i>tubulin polyglutamylase TTLL11</i></b>	<i>Lipotes vexillifer</i>	Baiji (white-finned dolphin)	44
AOA2F0BHB3_ESCRO <b><i>Glycerol-3-phosphate dehydrogenase [NAD(+)]</i></b>	<i>Eschrichtius robustus</i>	Gray whale	44
AOA2Y9MUL0_DELLE <b><i>nesprin-2 isoform X1</i></b>	<i>Delphinapterus leucas</i>	Beluga whale	44
AOA2Y9LTS8_DELLE <b><i>complement C3-like isoform X1</i></b>	<i>Delphinapterus leucas</i>	Beluga whale	43
AOA2F0B9E6_ESCRO <b><i>Trypsin</i></b>	<i>Eschrichtius robustus</i>	Gray whale	43
<b><i>rootletin</i></b>	<i>Balaenoptera acutorostrata scammoni</i>	Scammon's minke whale	43
AOA2Y9FI42_PHYMC <b><i>coiled-coil domain-containing protein 190</i></b>	<i>Physeter macrocephalus</i>	Sperm whale	43
AOA341BVR7_9CETA <b><i>developmental pluripotency-associated protein 2-like</i></b>	<i>Neophocaena asiaeorientalis asiaeorientalis</i>	Yangtze finless porpoise	42
AOA2F0B364_ESCRO <b><i>Protein S100</i></b>	<i>Eschrichtius robustus</i>	Gray whale	42
AOA2Y9LCY9_DELLE <b><i>basement membrane-specific heparan sulfate proteoglycan core protein isoform X3</i></b>	<i>Delphinapterus leucas</i>	Beluga whale	42

2700      <sup>†</sup>Ions score is -10\*Log(P), where P is the probability that the observed match is a random event. Individual ions  
 2701      scores > 41 indicated identity or extensive homology ( $p < 0.05$ ). Protein scores were derived from ions scores as  
 2702      a non-probabilistic basis for ranking protein hits. Cut-off was set at Ions score 20.

2703  
2704

2705      **Supplementary Table 3. Deiminated proteins identified by F95 enrichment in serum of fin whale**  
 2706      (*Balaenoptera physalus*). Deiminated proteins were isolated by immunoprecipitation using the pan-deimination  
 2707      F95 antibody. The F95 enriched eluate was analysed by LC-MS/MS and peak list files were submitted to mascot.  
 2708      Peptide hits scoring with the cetacean database (CCP\_Cetacea\_Cetacea\_20191213; 252,001 sequences;  
 2709      150,129,595 residues) are shown. Species hit names and total scores are shown.

Protein name	Species name	Common name	Total score ( <i>p</i> <0.05) <sup>†</sup>
AOA384B912_BALAS <i>alpha-2-macroglobulin isoform X2</i>	<i>Balaenoptera acutorostrata scammoni</i>	Scammon's minke whale	3650
AOA383ZXRO_BALAS <i>serum albumin</i>	<i>Balaenoptera acutorostrata scammoni</i>	Scammon's minke whale	3062
AOA452CHV5_BALAS <i>apolipoprotein B-100</i>	<i>Balaenoptera acutorostrata scammoni</i>	Scammon's minke whale	2952
AOA383Z2B4_BALAS <i>complement C3</i>	<i>Balaenoptera acutorostrata scammoni</i>	Scammon's minke whale	2699
AOA341C5T8_9CETA <i>serum albumin</i>	<i>Neophocaena asiaeorientalis asiaeorientalis</i>	Yangtze finless porpoise	2447
AOA384ALG4_BALAS <i>ceruloplasmin isoform X2</i>	<i>Balaenoptera acutorostrata scammoni</i>	Scammon's minke whale	2325
AOA341AGH0_9CETA <i>alpha-2-macroglobulin-like isoform X2</i>	<i>Neophocaena asiaeorientalis asiaeorientalis</i>	Yangtze finless porpoise	2262
AOA4U1FPV0_MONMO <i>Uncharacterized protein</i>	<i>Monodon monoceros</i>	Narwhal	2249
AOA2U3V5M2_TURTR <i>serum albumin isoform X1</i>	<i>Tursiops truncatus</i>	Common bottlenose dolphin	2203
AOA340XUI9_LIPVE <i>apolipoprotein B-100</i>	<i>Lipotes vexillifer</i>	Baiji (white-finned dolphin)	2193
AOA2U4AKU7_TURTR <i>alpha-2-macroglobulin-like</i>	<i>Tursiops truncatus</i>	Common bottlenose dolphin	2181
AOA340Y7Z8_LIPVE <i>serum albumin</i>	<i>Lipotes vexillifer</i>	Baiji (white-finned dolphin)	2155
AOA383Z5R5_BALAS <i>serotransferrin</i>	<i>Balaenoptera acutorostrata scammoni</i>	Scammon's minke whale	2141
AOA340XNP3_LIPVE <i>complement C3</i>	<i>Lipotes vexillifer</i>	Baiji (white-finned dolphin)	2106
AOA384AFQ0_BALAS <i>Plasminogen</i>	<i>Balaenoptera acutorostrata scammoni</i>	Scammon's minke whale	2090
AOA340YAE1_LIPVE <i>alpha-2-macroglobulin-like</i>	<i>Lipotes vexillifer</i>	Baiji (white-finned dolphin)	2014
AOA2Y9TJG8_PHYMC <i>complement C3</i>	<i>Physeter macrocephalus</i>	Sperm whale	1908
AOA384ALK4_BALAS <i>fibronectin</i>	<i>Balaenoptera acutorostrata scammoni</i>	Scammon's minke whale	1871
AOA2U4BMT3_TURTR <i>fibronectin isoform X4</i>	<i>Tursiops truncatus</i>	Common bottlenose dolphin	1842
AOA2Y9EED2_PHYMC <i>fibronectin isoform X5</i>	<i>Physeter macrocephalus</i>	Sperm whale	1703
AOA383YWT8_BALAS <i>complement factor H-like isoform X1</i>	<i>Balaenoptera acutorostrata scammoni</i>	Scammon's minke whale	1662
AOA383Z1U4_BALAS <i>complement C3-like isoform X1</i>	<i>Balaenoptera acutorostrata scammoni</i>	Scammon's minke whale	1571

AOA384B2W1_BALAS <b><i>complement C4</i></b>	<i>Balaenoptera acutorostrata scammoni</i>	Scammon's minke whale	1479
AOA384B6G0_BALAS <b><i>kininogen-1</i></b>	<i>Balaenoptera acutorostrata scammoni</i>	Scammon's minke whale	1364
AOA383ZST7_BALAS <b><i>complement C5 isoform X1</i></b>	<i>Balaenoptera acutorostrata scammoni</i>	Scammon's minke whale	1362
AOA452C585_BALAS <b><i>pregnancy zone protein-like</i></b>	<i>Balaenoptera acutorostrata scammoni</i>	Scammon's minke whale	1272
PODMA6 APOA1_BALAS <b><i>Apolipoprotein A-I</i></b>	<i>Balaenoptera acutorostrata scammoni</i>	Scammon's minke whale	1269
AOA384BF87_BALAS <b><i>Haptoglobin</i></b>	<i>Balaenoptera acutorostrata scammoni</i>	Scammon's minke whale	1176
AOA340Y8V6_LIPVE <b><i>alpha-2-macroglobulin-like</i></b>	<i>Lipotes vexillifer</i>	Baiji (white-finned dolphin)	1169
AOA2U4CNJ2_TURTR <b><i>Plasminogen</i></b>	<i>Tursiops truncatus</i>	Common bottlenose dolphin	1127
AOA140GN64_BALAC <b><i>Hemoglobin subunit beta</i></b>	<i>Balaenoptera acutorostrata</i>	Northern minke whale	1078
AOA341CUQ2_9CETA <b><i>complement C5</i></b>	<i>Neophocaena asiaeorientalis asiaeorientalis</i>	Yangtze finless porpoise	1062
AOA340XE64_LIPVE <b><i>complement factor H-like</i></b>	<i>Lipotes vexillifer</i>	Baiji (white-finned dolphin)	1061
AOA2Y9FIB4_PHYMC <b><i>complement C5</i></b>	<i>Physeter macrocephalus</i>	Sperm whale	1045
AOA340XK77_LIPVE <b><i>complement C4-A</i></b>	<i>Lipotes vexillifer</i>	Baiji (white-finned dolphin)	1038
AOA4U1EQC8_MONMO <b><i>Uncharacterized protein</i></b>	<i>Monodon monoceros</i>	Narwhal	1012
AOA2F0B042_ESCRO <b><i>Hemopexin</i></b>	<i>Eschrichtius robustus</i>	Gray whale	966
AOA341ATW9_9CETA <b><i>complement factor H isoform X2</i></b>	<i>Neophocaena asiaeorientalis asiaeorientalis</i>	Yangtze finless porpoise	901
AOA384AY37_BALAS <b><i>complement component C6</i></b>	<i>Balaenoptera acutorostrata scammoni</i>	Scammon's minke whale	888
AOA2Y9N2V9_DELLE <b><i>kininogen-1 isoform X1</i></b>	<i>Delphinapterus leucas</i>	Beluga whale	869
AOA2F0BAH8_ESCRO <b><i>Complement factor B</i></b>	<i>Eschrichtius robustus</i>	Gray whale	832
AOA384B1Q0_BALAS <b><i>vitamin D-binding protein</i></b>	<i>Balaenoptera acutorostrata scammoni</i>	Scammon's minke whale	831
AOA383ZI56_BALAS <b><i>inter-alpha-trypsin inhibitor heavy chain H4 isoform X2</i></b>	<i>Balaenoptera acutorostrata scammoni</i>	Scammon's minke whale	824
AOA2Y9NIU7_DELLE <b><i>complement factor H isoform X1</i></b>	<i>Delphinapterus leucas</i>	Beluga whale	821
AOA2Y9FDR4_PHYMC <b><i>inter-alpha-trypsin inhibitor heavy chain H2</i></b>	<i>Physeter macrocephalus</i>	Sperm whale	812
AOA384B2P9_BALAS <b><i>complement factor B</i></b>	<i>Balaenoptera acutorostrata scammoni</i>	Scammon's minke whale	812
AOA384AGF6_BALAS <b><i>Fructose-bisphosphate aldolase</i></b>	<i>Balaenoptera acutorostrata scammoni</i>	Scammon's minke whale	804

AOA383YX88_BALAS <i>inter-alpha-trypsin inhibitor heavy chain H2</i>	<i>Balaenoptera acutorostrata scammoni</i>	Scammon's minke whale	801
AOA2F0B6R6_ESCRO <i>Apolipoprotein A-IV</i>	<i>Eschrichtius robustus</i>	Gray whale	782
AOA4U1EEK0_MONMO <i>complement factor B</i>	<i>Monodon monoceros</i>	Narwhal	764
AOA341C7J1_9CETA <i>vitamin D-binding protein</i>	<i>Neophocaena asiaeorientalis asiaeorientalis</i>	Yangtze finless porpoise	750
AOA384A1L0_BALAS <i>Prothrombin</i>	<i>Balaenoptera acutorostrata scammoni</i>	Scammon's minke whale	747
AOA383Z8T4_BALAS <i>C4b-binding protein alpha chain isoform X7</i>	<i>Balaenoptera acutorostrata scammoni</i>	Scammon's minke whale	740
AOA383ZI29_BALAS <i>inter-alpha-trypsin inhibitor heavy chain H1 isoform X1</i>	<i>Balaenoptera acutorostrata scammoni</i>	Scammon's minke whale	737
AOA383ZCJ5_BALAS <i>Hemopexin</i>	<i>Balaenoptera acutorostrata scammoni</i>	Scammon's minke whale	734
AOA341CEB0_9CETA <i>Hemopexin</i>	<i>Neophocaena asiaeorientalis asiaeorientalis</i>	Yangtze finless porpoise	728
AOA340YB71_LIPVE <i>complement component C6</i>	<i>Lipotes vexillifer</i>	Baiji (white-finned dolphin)	719
AOA384BAA9_BALAS <i>apolipoprotein A-IV</i>	<i>Balaenoptera acutorostrata scammoni</i>	Scammon's minke whale	713
AOA384AEC5_BALAS <i>beta-2-glycoprotein 1</i>	<i>Balaenoptera acutorostrata scammoni</i>	Scammon's minke whale	685
AOA383YNL2_BALAS <i>complement component C8 alpha chain</i>	<i>Balaenoptera acutorostrata scammoni</i>	Scammon's minke whale	662
AOA2Y9F6Z4_PHYMC <i>kininogen-1 isoform X1</i>	<i>Physeter macrocephalus</i>	Sperm whale	656
AOA383ZG27_BALAS <i>coagulation factor XI</i>	<i>Balaenoptera acutorostrata scammoni</i>	Scammon's minke whale	654
AOA140GN67_MESDE <i>Hemoglobin subunit beta</i>	<i>Mesoplodon densirostris</i>		653
AOA2Y9PXE8_DELLE <i>Prothrombin</i>	<i>Delphinapterus leucas</i>	Beluga whale	645
AOA4V5P7Z3_MONMO <i>inter-alpha-trypsin inhibitor heavy chain H3</i>	<i>Monodon monoceros</i>	Narwhal	638
AOA384AYR3_BALAS <i>complement component C7 isoform X2</i>	<i>Balaenoptera acutorostrata scammoni</i>	Scammon's minke whale	630
AOA340WSC2_LIPVE <i>keratin, type II cytoskeletal 5 isoform X1</i>	<i>Lipotes vexillifer</i>	Baiji (white-finned dolphin)	626
AOA2FOBBIO_ESCRO <i>Pregnancy zone protein</i>	<i>Eschrichtius robustus</i>	Gray whale	622
AOA484GV34_SOUCHE <i>Uncharacterized protein</i>	<i>Sousa chinensis</i>		604
AOA2U4AP99_TURTR <i>complement factor B</i>	<i>Tursiops truncatus</i>	Common bottlenose dolphin	572
AOA2U4B948_TURTR <i>serotransferrin</i>	<i>Tursiops truncatus</i>	Common bottlenose dolphin	568
AOA2Y9Q9H8_DELLE	<i>Delphinapterus leucas</i>	Beluga whale	559

<b>complement component C7</b>			
AOA383ZYJ4_BALAS <b>carbonic anhydrase 1</b>	<i>Balaenoptera acutorostrata scammoni</i>	Scammon's minke whale	553
AOA383ZJG1_BALAS <b>basement membrane-specific heparan sulfate proteoglycan core protein</b>	<i>Balaenoptera acutorostrata scammoni</i>	Scammon's minke whale	549
AOA383ZSR9_BALAS <b>gelsolin isoform X1</b>	<i>Balaenoptera acutorostrata scammoni</i>	Scammon's minke whale	542
AOA2FOAYW0_ESCRO <b>Ig lambda-6 chain C region</b>	<i>Eschrichtius robustus</i>	Gray whale	534
AOA452CPB6_BALAS <b>complement component C9</b>	<i>Balaenoptera acutorostrata scammoni</i>	Scammon's minke whale	533
AOA340YCM8_LIPVE <b>C4b-binding protein alpha chain-like</b>	<i>Lipotes vexillifer</i>	Baiji (white-finned dolphin)	523
AOA340XC23_LIPVE <b>serotransferrin</b>	<i>Lipotes vexillifer</i>	Baiji (white-finned dolphin)	522
AOA340Y1E6_LIPVE <b>keratin, type I cytoskeletal 14</b>	<i>Lipotes vexillifer</i>	Baiji (white-finned dolphin)	498
AOA2Y9FI53_PHYMC <b>gelsolin isoform X4</b>	<i>Physeter macrocephalus</i>	Sperm whale	497
AOA2Y9Q2M0_DELLE <b>betaine-homocysteine S-methyltransferase 1</b>	<i>Delphinapterus leucas</i>	Beluga whale	492
AOA140GN13_BALAC <b>Hemoglobin subunit alpha</b>	<i>Balaenoptera acutorostrata</i>	Northern minke whale	481
AOA2U4AKU6_TURTR <b>Glyceraldehyde-3-phosphate dehydrogenase</b>	<i>Tursiops truncatus</i>	Common bottlenose dolphin	465
AOA2FOBP97_ESCRO <b>Ig mu heavy chain disease protein</b>	<i>Eschrichtius robustus</i>	Gray whale	456
AOA344X2S6_GLOME <b>Hemoglobin subunit beta</b>	<i>Globicephala melas</i>		454
AOA383ZV20_BALAS <b>alpha-1-antitrypsin</b>	<i>Balaenoptera acutorostrata scammoni</i>	Scammon's minke whale	440
AOA383Z9Z9_BALAS <b>Alpha-mannosidase</b>	<i>Balaenoptera acutorostrata scammoni</i>	Scammon's minke whale	437
AOA384A3E4_BALAS <b>hemoglobin subunit alpha isoform X1</b>	<i>Balaenoptera acutorostrata scammoni</i>	Scammon's minke whale	436
AOA140GN07_MESDE <b>Hemoglobin subunit alpha</b>	<i>Mesoplodon densirostris</i>		421
AOA2FOB7Q7_ESCRO <b>Antithrombin-III</b>	<i>Eschrichtius robustus</i>	Gray whale	421
AOA140GN06_TURTR <b>Hemoglobin subunit alpha</b>	<i>Tursiops truncatus</i>	Common bottlenose dolphin	421
AOA2Y9T858_PHYMC <b>keratin, type I cytoskeletal 14 isoform X1</b>	<i>Physeter macrocephalus</i>	Sperm whale	420
AOA340XIR2_LIPVE <b>complement component C9</b>	<i>Lipotes vexillifer</i>	Baiji (white-finned dolphin)	415
AOA2FOB6I5_ESCRO <b>Alpha-1-antitrypsin</b>	<i>Eschrichtius robustus</i>	Gray whale	395

AOA383ZRG8_BALAS <i>keratin, type I cytoskeletal 15</i>	<i>Balaenoptera acutorostrata scammoni</i>	Scammon's minke whale	393
AOA2F0BAV1_ESCRO <i>Keratin, type I cytoskeletal 14</i>	<i>Eschrichtius robustus</i>		386
AOA384BCE5_BALAS <i>Fructose-bisphosphate aldolase</i>	<i>Balaenoptera acutorostrata scammoni</i>	Scammon's minke whale	378
AOA2U3V780_TURTR <i>carbonic anhydrase 2</i>	<i>Tursiops truncatus</i>	Common bottlenose dolphin	368
AOA383SX3_BALAS <i>protein AMBP</i>	<i>Balaenoptera acutorostrata scammoni</i>	Scammon's minke whale	368
AOA383ZA42_BALAS <i>CD5 antigen-like isoform X1</i>	<i>Balaenoptera acutorostrata scammoni</i>	Scammon's minke whale	364
AOA2F0B6G6_ESCRO <i>CD5 antigen-like</i>	<i>Eschrichtius robustus</i>	Gray whale	360
AOA2U4BSU8_TURTR <i>actin, cytoplasmic 2</i>	<i>Tursiops truncatus</i>	Common bottlenose dolphin	358
AOA383ZRJ1_BALAS <i>keratin, type I cytoskeletal 14</i>	<i>Balaenoptera acutorostrata scammoni</i>	Scammon's minke whale	355
AOA140GN14_PHYMC <i>Hemoglobin subunit alpha</i>	<i>Physeter macrocephalus</i>	Sperm whale	352
AOA340WLD3_LIPVE <i>fibrinogen beta chain isoform X2</i>	<i>Lipotes vexillifer</i>	Baiji (white-finned dolphin)	351
AOA2Y9SF59_PHYMC <i>L-lactate dehydrogenase</i>	<i>Physeter macrocephalus</i>	Sperm whale	350
AOA383ZYR5_BALAS <i>carbonic anhydrase 3</i>	<i>Balaenoptera acutorostrata scammoni</i>	Scammon's minke whale	349
AOA452C7C8_BALAS <i>complement component C8 beta chain</i>	<i>Balaenoptera acutorostrata scammoni</i>	Scammon's minke whale	345
AOA384AET4_BALAS <i>galectin-3-binding protein</i>	<i>Balaenoptera acutorostrata scammoni</i>	Scammon's minke whale	340
AOA383ZI45_BALAS <i>inter-alpha-trypsin inhibitor heavy chain H3 isoform X2</i>	<i>Balaenoptera acutorostrata scammoni</i>	Scammon's minke whale	338
AOA383ZNV5_BALAS <i>fibrinogen gamma chain isoform X1</i>	<i>Balaenoptera acutorostrata scammoni</i>	Scammon's minke whale	336
AOA383ZHT1_BALAS <i>apolipoprotein R-like</i>	<i>Balaenoptera acutorostrata scammoni</i>	Scammon's minke whale	335
AOA455B568_PHYMC <i>C4b-binding protein alpha chain</i>	<i>Physeter macrocephalus</i>	Sperm whale	324
AOA383ZW6_BALAS <i>keratin, type II cytoskeletal 6A-like isoform X2</i>	<i>Balaenoptera acutorostrata scammoni</i>	Scammon's minke whale	322
AOA384AUG3_BALAS <i>pantetheinase isoform X1</i>	<i>Balaenoptera acutorostrata scammoni</i>	Scammon's minke whale	315
AOA384A960_BALAS <i>alpha-2-antiplasmin</i>	<i>Balaenoptera acutorostrata scammoni</i>	Scammon's minke whale	311
AOA2F0AVP5_ESCRO <i>Apolipoprotein E</i>	<i>Eschrichtius robustus</i>	Gray whale	307
AOA2Y9ELN5_PHYMC <i>complement component C8 beta chain</i>	<i>Physeter macrocephalus</i>	Sperm whale	306

AOA2U4ANE4_TURTR <i>alpha-2-antiplasmin</i>	<i>Tursiops truncatus</i>	Common bottlenose dolphin	297
D3TTK4_DELDE <i>Hemoglobin beta5 chain</i>	<i>Delphinus delphis</i>		289
AOA2Y9MHB6_DELLE <i>filamin-A isoform X1</i>	<i>Delphinapterus leucas</i>	Beluga whale	287
APOE_BALAS <i>Apolipoprotein E</i>	<i>Balaenoptera acutorostrata scammoni</i>	Scammon's minke whale	286
AOA340WU44_LIPVE <i>immunoglobulin lambda-like polypeptide 5</i>	<i>Lipotes vexillifer</i>	Baiji (white-finned dolphin)	286
AOA2F0B376_ESCRO <i>Actin, aortic smooth muscle</i>	<i>Eschrichtius robustus</i>	Gray whale	281
AOA340XOE0_LIPVE <i>alpha-enolase isoform X1</i>	<i>Lipotes vexillifer</i>	Baiji (white-finned dolphin)	280
AOA2F0B4J5_ESCRO <i>Hemoglobin subunit alpha</i>	<i>Eschrichtius robustus</i>	Gray whale	276
AOA383Z577_BALAS <i>complement C1r subcomponent</i>	<i>Balaenoptera acutorostrata scammoni</i>	Scammon's minke whale	273
AOA2F0BHT3_ESCRO <i>Kininogen-2</i>	<i>Eschrichtius robustus</i>	Gray whale	270
AOA2U4A275_TURTR <i>selenium-binding protein 1 isoform X2</i>	<i>Tursiops truncatus</i>	Common bottlenose dolphin	269
AOA341CXM1_9CETA <i>heparin cofactor 2</i>	<i>Neophocaena asiaeorientalis asiaeorientalis</i>	Yangtze finless porpoise	269
AOA384A1C5_BALAS <i>inhibitor of carbonic anhydrase isoform X1</i>	<i>Balaenoptera acutorostrata scammoni</i>	Scammon's minke whale	269
AOA2Y9MKT1_DELLE <i>complement factor I</i>	<i>Delphinapterus leucas</i>	Beluga whale	264
AOA4U1FST8_MONMO <i>complement C1q subcomponent subunit C</i>	<i>Monodon monoceros</i>	Narwhal	258
AOA2Y9N8Q0_DELLE <i>keratin, type II cytoskeletal 6A-like</i>	<i>Delphinapterus leucas</i>	Beluga whale	257
AOA340XVX6_LIPVE <i>complement factor I</i>	<i>Lipotes vexillifer</i>	Baiji (white-finned dolphin)	253
AOA2F0B1I9_ESCRO <i>Beta-enolase</i>	<i>Eschrichtius robustus</i>	Gray whale	251
AOA2Y9FPJ2_PHYMC <i>Clusterin</i>	<i>Physeter macrocephalus</i>	Sperm whale	244
AOA383YVI2_BALAS <i>flavin reductase (NADPH)</i>	<i>Balaenoptera acutorostrata scammoni</i>	Scammon's minke whale	244
AOA2F0B3N0_ESCRO <i>Vitronectin</i>	<i>Eschrichtius robustus</i>	Gray whale	241
AOA2Y9NWCO_DELLE <i>complement component C8 gamma chain isoform X1</i>	<i>Delphinapterus leucas</i>	Beluga whale	230
AOA2Y9T005_PHYMC <i>complement C1q subcomponent subunit C</i>	<i>Physeter macrocephalus</i>	Sperm whale	225
AOA384B6M8_BALAS <i>fetuin-B</i>	<i>Balaenoptera acutorostrata scammoni</i>	Scammon's minke whale	224

AOA2Y9EH60_PHYMC <b>vitamin K-dependent protein S</b>	<i>Physeter macrocephalus</i>	Sperm whale	214
AOA2U3V7Z3_TURTR <b>peroxiredoxin-1</b>	<i>Tursiops truncatus</i>	Common bottlenose dolphin	211
Q9GL90_BALMY <b>Transferrin</b>	<i>Balaena mysticetus</i>		210
AOA383Z9P7_BALAS <b>polymeric immunoglobulin receptor</b>	<i>Balaenoptera acutorostrata scammoni</i>	Scammon's minke whale	208
AOA2F0AYU0_ESCRO <b>Ig lambda chain V-III region SH</b>	<i>Eschrichtius robustus</i>	Gray whale	208
AOA383ZRC7_BALAS <b>keratin, type I cytoskeletal 13</b>	<i>Balaenoptera acutorostrata scammoni</i>	Scammon's minke whale	208
AOA2F0B2V1_ESCRO <b>Glutathione peroxidase</b>	<i>Eschrichtius robustus</i>	Gray whale	202
AOA2Y9LPM6_DELLE <b>immunoglobulin lambda-1 light chain-like</b>	<i>Delphinapterus leucas</i>	Beluga whale	194
AOA2U4CLI2_TURTR <b>Adenosylhomocysteinase</b>	<i>Tursiops truncatus</i>	Common bottlenose dolphin	189
AOA2FOAXA3_ESCRO <b>Pyruvate kinase</b>	<i>Eschrichtius robustus</i>	Gray whale	188
AOA2Y9NH97_DELLE <b>L-lactate dehydrogenase</b>	<i>Delphinapterus leucas</i>	Beluga whale	187
AOA2Y9TCY0_PHYMC <b>keratin, type I cytoskeletal 42-like</b>	<i>Physeter macrocephalus</i>	Sperm whale	186
AOA2U4B8X2_TURTR <b>Amine oxidase</b>	<i>Tursiops truncatus</i>	Common bottlenose dolphin	179
AOA2Y9FE50_PHYMC <b>inhibitor of carbonic anhydrase isoform X2</b>	<i>Physeter macrocephalus</i>	Sperm whale	176
AOA383Z4U0_BALAS <b>complement C1s subcomponent isoform X2</b>	<i>Balaenoptera acutorostrata scammoni</i>	Scammon's minke whale	175
AOA383ZXQ7_BALAS <b>afamin</b>	<i>Balaenoptera acutorostrata scammoni</i>	Scammon's minke whale	173
AOAON9DSI7_BALOM <b>C1Q and collagen domain containing adiponectin</b>	<i>Balaenoptera omurai</i>	Omura's whale (dwarf fin whale)	170
AOA2F0BMU1_ESCRO <b>Fibrinogen alpha chain</b>	<i>Eschrichtius robustus</i>	Gray whale	169
AOA383ZJ84_BALAS <b>complement C1q subcomponent subunit B</b>	<i>Balaenoptera acutorostrata scammoni</i>	Scammon's minke whale	164
AOA452C5K2_BALAS <b>plasma protease C1 inhibitor</b>	<i>Balaenoptera acutorostrata scammoni</i>	Scammon's minke whale	156
AOA340XEE1_LIPVE <b>alpha-1B-glycoprotein-like</b>	<i>Lipotes vexillifer</i>	Baiji (white-finned dolphin)	155
AOA2U4BFU2_TURTR <b>unconventional myosin-Vb</b>	<i>Tursiops truncatus</i>	Common bottlenose dolphin	148
AOA340XVM8_LIPVE <b>keratin, type I cytoskeletal 15</b>	<i>Lipotes vexillifer</i>	Baiji (white-finned dolphin)	147

AOA340WNM5_LIPVE <i>obscurin-like</i>	<i>Lipotes vexillifer</i>	Baiji (white-finned dolphin)	144
AOA383YWX2_BALAS <i>coagulation factor XIII B chain</i>	<i>Balaenoptera acutorostrata scammoni</i>	Scammon's minke whale	144
AOA2Y9P2W5_DELLE <i>Glycine N-methyltransferase</i>	<i>Delphinapterus leucas</i>	Beluga whale	135
AOA2F0BNF0_ESCRO <i>Ig alpha-1 chain C region</i>	<i>Eschrichtius robustus</i>	Gray whale	129
AOA2FOB6Y0_ESCRO <i>Superoxide dismutase [Cu-Zn]</i>	<i>Eschrichtius robustus</i>	Gray whale	129
AOA2FOBBD2_ESCRO <i>Glutathione S-transferase</i>	<i>Eschrichtius robustus</i>	Gray whale	128
Q0KIY9 MYG_INDPC <i>Myoglobin</i>	<i>Indopacetus pacificus</i>	Tropical bottlenose whale	125
AOA2Y9MM08_DELLE <i>carbamoyl-phosphate synthase [ammonia], mitochondrial isoform X2</i>	<i>Delphinapterus leucas</i>	Beluga whale	125
AOA452C3Q2_BALAS <i>ficolin-1</i>	<i>Balaenoptera acutorostrata scammoni</i>	Scammon's minke whale	124
AOA2U3V999_TURTR <i>ribose-phosphate pyrophosphokinase 1</i>	<i>Tursiops truncatus</i>	Common bottlenose dolphin	122
AOA383ZZD6_BALAS <i>thrombospondin-1</i>	<i>Balaenoptera acutorostrata scammoni</i>	Scammon's minke whale	119
AOA2FOB025_ESCRO <i>Peroxiredoxin-2</i>	<i>Eschrichtius robustus</i>	Gray whale	118
AOA2Y9EQK7_PHYMC <i>transketolase isoform X1</i>	<i>Physeter macrocephalus</i>	Sperm whale	117
AOA2Y9LYW0_DELLE <i>apolipoprotein C-III</i>	<i>Delphinapterus leucas</i>	Beluga whale	115
AOA2Y9Q8L6_DELLE <i>selenoprotein P isoform X1</i>	<i>Delphinapterus leucas</i>	Beluga whale	114
AOA2Y9NVG6_DELLE <i>phosphoglucomutase-1 isoform X1</i>	<i>Delphinapterus leucas</i>	Beluga whale	112
AOA2Y9F8B3_PHYMC <i>fibrinogen alpha chain</i>	<i>Physeter macrocephalus</i>	Sperm whale	111
AOA2Y9FDN7_PHYMC <i>14-3-3 protein sigma</i>	<i>Physeter macrocephalus</i>	Sperm whale	109
AOA452CCB0_BALAS <i>immunoglobulin kappa light chain-like</i>	<i>Balaenoptera acutorostrata scammoni</i>	Scammon's minke whale	109
AOA384A668_BALAS <i>10-formyltetrahydrofolate dehydrogenase</i>	<i>Balaenoptera acutorostrata scammoni</i>	Scammon's minke whale	107
AOA2U3VAA7_TURTR <i>alcohol dehydrogenase E chain</i>	<i>Tursiops truncatus</i>	Common bottlenose dolphin	106
AOA2FOBNZ5_ESCRO <i>Fibrinogen gamma-B chain</i>	<i>Eschrichtius robustus</i>	Gray whale	106
AOA4U1ECF0_MONMO <i>Ig-like domain-containing protein</i>	<i>Monodon monoceros</i>	Narwhal	105

AOA383YWU0_BALAS <i>complement factor H isoform X1</i>	<i>Balaenoptera acutorostrata scammoni</i>	Scammon's minke whale	105
AOA341D7J4_9CETA <i>collagen alpha-2(I) chain</i>	<i>Neophocaena asiaeorientalis asiaeorientalis</i>	Yangtze finless porpoise	104
AOA2Y9NGE0_DELLE <i>ficolin-2-like isoform X2</i>	<i>Delphinapterus leucas</i>	Beluga whale	104
AOA2F0BEE8_ESCRO <i>Apolipoprotein A-II</i>	<i>Eschrichtius robustus</i>	Gray whale	103
AOA384BES7_BALAS <i>cadherin-1</i>	<i>Balaenoptera acutorostrata scammoni</i>	Scammon's minke whale	102
AOA2F0BQ50_ESCRO <i>Extracellular superoxide dismutase [Cu-Zn]</i>	<i>Eschrichtius robustus</i>	Gray whale	102
AOA383ZHH6_BALAS <i>keratin, type II microfibrillar-like</i>	<i>Balaenoptera acutorostrata scammoni</i>	Scammon's minke whale	98
AOA2U3V9F2_TURTR <i>Phosphoglycerate kinase</i>	<i>Tursiops truncatus</i>	Common bottlenose dolphin	91
AOA2Y9PJV8_DELLE <i>calpain-1 catalytic subunit</i>	<i>Delphinapterus leucas</i>	Beluga whale	84
AOA2U4BAA2_TURTR <i>protein kinase C-binding protein NELL2 isoform X3</i>	<i>Tursiops truncatus</i>	Common bottlenose dolphin	83
AOA2FOBAE6_ESCRO <i>Cofilin-1</i>	<i>Eschrichtius robustus</i>	Gray whale	83
AOA2FOB4Y4_ESCRO <i>Glycine amidinotransferase, mitochondrial</i>	<i>Eschrichtius robustus</i>	Gray whale	81
AOA2U3V6Z1_TURTR <i>complement C1q tumor necrosis factor-related protein 3 isoform X1</i>	<i>Tursiops truncatus</i>	Common bottlenose dolphin	80
AOA383Z8S9_BALAS <i>apolipoprotein R-like isoform X1</i>	<i>Balaenoptera acutorostrata scammoni</i>	Scammon's minke whale	76
AOA2FOBPF2_ESCRO <i>Angiotensinogen</i>	<i>Eschrichtius robustus</i>	Gray whale	74
AOA341B799_9CETA <i>WD repeat-containing protein 1</i>	<i>Neophocaena asiaeorientalis asiaeorientalis</i>	Yangtze finless porpoise	72
AOA2Y9FNF4_PHYMC <i>xaa-Pro dipeptidase isoform X3</i>	<i>Physeter macrocephalus</i>	Sperm whale	68
AOA2U4BCI8_TURTR <i>zinc finger protein 106 isoform X1</i>	<i>Tursiops truncatus</i>	Common bottlenose dolphin	64
AOA340XJB2_LIPVE <i>E3 ubiquitin-protein ligase UBR4</i>	<i>Lipotes vexillifer</i>	Baiji (white-finned dolphin)	62
AOA2U3V2I2_TURTR <i>Histone H4</i>	<i>Tursiops truncatus</i>	Common bottlenose dolphin	61
AOA2Y9FLP7_PHYMC <i>Fumarylacetoacetate</i>	<i>Physeter macrocephalus</i>	Sperm whale	61
AOA2Y9MHQ5_DELLE	<i>Delphinapterus leucas</i>	Beluga whale	61

<i>nuclear mitotic apparatus protein 1 isoform X2</i>			
AOA4U1EB65_MONMO <i>Ig-like domain-containing protein</i>	<i>Monodon monoceros</i>	Narwhal	60
AOA2F0BPQ3_ESCRO <i>Bisphosphoglycerate mutase</i>	<i>Eschrichtius robustus</i>	Gray whale	59
AOA2F0B2T1_ESCRO <i>Ig heavy chain V region 3-6</i>	<i>Eschrichtius robustus</i>	Gray whale	59
AOA2F0BQ37_ESCRO <i>Coagulation factor XIII A chain</i>	<i>Eschrichtius robustus</i>	Gray whale	58
AOA2U4AEQ4_TURTR <i>Alpha-1,4 glucan phosphorylase</i>	<i>Tursiops truncatus</i>	Common bottlenose dolphin	57
AOA2Y9LWI5_DELLE <i>junction plakoglobin</i>	<i>Delphinapterus leucas</i>	Beluga whale	56
AOA2Y9TGE0_PHYMC <i>ATP-binding cassette sub-family B member 5</i>	<i>Physeter macrocephalus</i>	Sperm whale	56
AOA452CFC8_BALAS <i>zinc finger protein 845-like</i>	<i>Balaenoptera acutorostrata scammoni</i>	Scammon's minke whale	56
AOA2U4AKS5_TURTR <i>complement C1s subcomponent</i>	<i>Tursiops truncatus</i>	Common bottlenose dolphin	55
AOA2F0B2N3_ESCRO <i>Cathepsin B</i>	<i>Eschrichtius robustus</i>	Gray whale	54
AOA2Y9LYJ2_DELLE <i>chondroadherin</i>	<i>Delphinapterus leucas</i>	Beluga whale	53
AOA2U4BYK3_TURTR <i>Clathrin heavy chain linker domain-containing protein 1</i>	<i>Tursiops truncatus</i>	Common bottlenose dolphin	52
AOA2U3V0A2_TURTR <i>Arginase</i>	<i>Tursiops truncatus</i>	Common bottlenose dolphin	52
AOA2FOBFV3_ESCRO <i>Protein Z-dependent protease inhibitor</i>	<i>Eschrichtius robustus</i>	Gray whale	51
AOA2U4C129_TURTR <i>RIB43A-like with coiled-coils protein 1</i>	<i>Tursiops truncatus</i>	Common bottlenose dolphin	51
AOA340XZH6_LIPVE <i>coiled-coil domain-containing protein 11</i>	<i>Lipotes vexillifer</i>	Baiji (white-finned dolphin)	51
AOA2F0B5J9_ESCRO <i>Transitional endoplasmic reticulum ATPase</i>	<i>Eschrichtius robustus</i>	Gray whale	51
AOA2F0B6H3_ESCRO <i>Coagulation factor X</i>	<i>Eschrichtius robustus</i>	Gray whale	50
AOA383ZRF2_BALAS <i>keratin, type I cytoskeletal 24</i>	<i>Balaenoptera acutorostrata scammoni</i>	Scammon's minke whale	49
AOA2Y9TDNO_PHYMC <i>IgGFc-binding protein</i>	<i>Physeter macrocephalus</i>	Sperm whale	49
AOA2F0B8P2_ESCRO <i>DnaJ subfamily B member 2</i>	<i>Eschrichtius robustus</i>	Gray whale	49
AOA384A3I0_BALAS <i>DNA polymerase theta</i>	<i>Balaenoptera acutorostrata scammoni</i>	Scammon's minke whale	

AOA2Y9MAX2_DELLE <i>stromelysin-1-like</i>	<i>Delphinapterus leucas</i>	Beluga whale	46
AOA2U4AZR9_TURTR <i>6-phosphogluconate dehydrogenase, decarboxylating</i>	<i>Tursiops truncatus</i>	Common bottlenose dolphin	46
AOA2U4ASA8_TURTR <i>NEDD4-binding protein 2 isoform X1</i>	<i>Tursiops truncatus</i>	Common bottlenose dolphin	45
AOA2F0B7K3_ESCRO <i>26S proteasome non-ATPase regulatory subunit 2</i>	<i>Eschrichtius robustus</i>	Gray whale	45
AOA2Y9Q0K2_DELLE <i>Fibulin-1</i>	<i>Delphinapterus leucas</i>	Beluga whale	44
AOA383ZV79_BALAS <i>plasma serine protease inhibitor</i>	<i>Balaenoptera acutorostrata scammoni</i>	Scammon's minke whale	44
AOA2U4B9G6_TURTR <i>U2 snRNP-associated SURP motif-containing protein isoform X2</i>	<i>Tursiops truncatus</i>	Common bottlenose dolphin	44
AOA384AEK3_BALAS <i>fas-binding factor 1 isoform X1</i>	<i>Balaenoptera acutorostrata scammoni</i>	Scammon's minke whale	44
AOA2F0B9R0_ESCRO <i>Carbonyl reductase [NADPH] 3</i>	<i>Eschrichtius robustus</i>	Gray whale	43
AOA341CAB3_9CETA <i>N-alpha-acetyltransferase 11-like isoform X2</i>	<i>Neophocaena asiaeorientalis asiaeorientalis</i>	Yangtze finless porpoise	41
AOA2U4BFX5_TURTR <i>carboxypeptidase B2</i>	<i>Tursiops truncatus</i>	Common bottlenose dolphin	41
AOA2F0B6A6_ESCRO <i>Dual serine/threonine and tyrosine protein kinase</i>	<i>Eschrichtius robustus</i>	Gray whale	40

2710       <sup>t</sup>Ions score is -10\*Log(P), where P is the probability that the observed match is a random event. Individual ions  
 2711       scores > 40 indicated identity or extensive homology ( $p < 0.05$ ). Protein scores were derived from ions scores as  
 2712       a non-probabilistic basis for ranking protein hits. Cut-off was set at Ions score 20.  
 2713  
 2714

2715      **Supplementary Table 4. Deiminated proteins identified by F95 enrichment in serum of humpback whale**  
 2716      (*Megaptera novaeangliae*). Deiminated proteins were isolated by immunoprecipitation using the pan-  
 2717      deimination F95 antibody. The F95 enriched eluate was analysed by LC-MS/MS and peak list files were submitted  
 2718      to mascot. Peptide hits scoring with the cetacean database (CCP\_Cetacea\_Cetacea\_20191213; 252,001  
 2719      sequences; 150,129,595 residues) are shown. Species hit names and total scores are shown.

Protein name	Species name	Common name	Total score ( <i>p</i> <0.05) <sup>t</sup>
AOA384B912_BALAS <i>alpha-2-macroglobulin isoform X2</i>	<i>Balaenoptera acutorostrata scammoni</i>	Scammon's minke whale	2926
AOA455BHA9_PHYMC <i>alpha-2-macroglobulin-like</i>	<i>Physeter macrocephalus</i>	Sperm whale	2174
AOA2Y9NK15_DELLE <i>alpha-2-macroglobulin isoform X3</i>	<i>Delphinapterus leucas</i>	Beluga whale	2132
AOA4U1FPV0_MONMO <i>Uncharacterized protein</i>	<i>Monodon monoceros</i>	Narwhal	2020
AOA2U4AKU7_TURTR <i>alpha-2-macroglobulin-like</i>	<i>Tursiops truncatus</i>	Common bottlenose dolphin	1993
AOA340YAE1_LIPVE <i>alpha-2-macroglobulin-like</i>	<i>Lipotes vexillifer</i>	Baiji (white-finned dolphin)	1907
AOA383Z2B4_BALAS <i>complement C3</i>	<i>Balaenoptera acutorostrata scammoni</i>	Scammon's minke whale	1900
AOA383ZXRO_BALAS <i>serum albumin</i>	<i>Balaenoptera acutorostrata scammoni</i>	Scammon's minke whale	1848
AOA340XNP3_LIPVE <i>complement C3</i>	<i>Lipotes vexillifer</i>	Baiji (white-finned dolphin)	1345
AOA2Y9TJG8_PHYMC <i>complement C3</i>	<i>Physeter macrocephalus</i>	Sperm whale	1286
AOA341C5T8_9CETA <i>serum albumin</i>	<i>Neophocaena asiaeorientalis asiaeorientalis</i>	Yangtze finless porpoise	1270
AOA452C585_BALAS <i>pregnancy zone protein-like</i>	<i>Balaenoptera acutorostrata scammoni</i>	Scammon's minke whale	1181
AOA384ALG4_BALAS <i>ceruloplasmin isoform X2</i>	<i>Balaenoptera acutorostrata scammoni</i>	Scammon's minke whale	1163
AOA2Y9M6G0_DELLE <i>complement C3 isoform X2</i>	<i>Delphinapterus leucas</i>	Beluga whale	1132
AOA140GN64_BALAC <i>Hemoglobin subunit beta</i>	<i>Balaenoptera acutorostrata</i>	Northern mine whale	1022
AOA383Z5R5_BALAS <i>serotransferrin</i>	<i>Balaenoptera acutorostrata scammoni</i>	Scammon's minke whale	978
AOA340Y8V6_LIPVE <i>alpha-2-macroglobulin-like</i>	<i>Lipotes vexillifer</i>	Baiji (white-finned dolphin)	960
PODMA6 APOA1_BALAS <i>Apolipoprotein A-I</i>	<i>Balaenoptera acutorostrata scammoni</i>	Scammon's minke whale	663
AOA2Y9PL94_DELLE <i>Fructose-bisphosphate aldolase</i>	<i>Delphinapterus leucas</i>	Beluga whale	646
AOA384BF87_BALAS <i>Haptoglobin</i>	<i>Balaenoptera acutorostrata scammoni</i>	Scammon's minke whale	556
AOA140GN67_MESDE <i>Hemoglobin subunit beta</i>	<i>Mesoplodon densirostris</i>	Blainville's beaked whale	549
AOA384B6G0_BALAS <i>kininogen-1</i>	<i>Balaenoptera acutorostrata scammoni</i>	Scammon's minke whale	518
AOA2FOB042_ESCRO	<i>Eschrichtius robustus</i>	Gray whale	480

<b>Hemopexin</b>			
AOA140GN13_BALAC <b>Hemoglobin subunit alpha</b>	<i>Balaenoptera acutorostrata</i>	Northern minke whale	439
AOA2Y9F931_PHYMC <b>carbonic anhydrase 2 isoform X1</b>	<i>Physeter macrocephalus</i>	Sperm whale	423
AOA384A3E4_BALAS <b>hemoglobin subunit alpha isoform X1</b>	<i>Balaenoptera acutorostrata scammoni</i>	Scammon's minke whale	412
AOA2F0B3C5_ESCRO <b>Keratin, type II cytoskeletal 5</b>	<i>Eschrichtius robustus</i>	Gray whale	387
AOA383ZLC8_BALAS <b>betaine-homocysteine S-methyltransferase 1</b>	<i>Balaenoptera acutorostrata scammoni</i>	Scammon's minke whale	387
AOA384B1Q0_BALAS <b>vitamin D-binding protein</b>	<i>Balaenoptera acutorostrata scammoni</i>	Scammon's minke whale	356
AOA4U1FNC5_MONMO <b>Hemoglobin subunit alpha</b>	<i>Monodon monoceros</i>	Narwhal	351
AOA2Y9SJP9_PHYMC <b>keratin, type II cytoskeletal 6A</b>	<i>Physeter macrocephalus</i>	Sperm whale	341
AOA140GN07_MESDE <b>Hemoglobin subunit alpha</b>	<i>Mesoplodon densirostris</i>	Blainville's beaked whale	338
AOA340XC23_LIPVE <b>serotransferrin</b>	<i>Lipotes vexillifer</i>	Baiji (white-finned dolphin)	333
AOA2FOBK75_ESCRO <b>Glyceraldehyde-3-phosphate dehydrogenase</b>	<i>Eschrichtius robustus</i>	Gray whale	330
AOA2U4AKU6_TURTR <b>Glyceraldehyde-3-phosphate dehydrogenase</b>	<i>Tursiops truncatus</i>	Common bottlenose dolphin	328
AOA383ZID2_BALAS <b>L-lactate dehydrogenase</b>	<i>Balaenoptera acutorostrata scammoni</i>	Scammon's minke whale	322
Q06YY0_STECO <b>Beta-actin</b>	<i>Stenella coeruleoalba</i>	Striped dolphin	312
AOA383Z8T4_BALAS <b>C4b-binding protein alpha chain isoform X7</b>	<i>Balaenoptera acutorostrata scammoni</i>	Scammon's minke whale	307
AOA4U1FI99_MONMO <b>IF rod domain-containing protein</b>	<i>Monodon monoceros</i>	Narwhal	293
AOA4U1FIN2_MONMO <b>Keratin, type I cytoskeletal</b>	<i>Monodon monoceros</i>	Narwhal	291
AOA2U3V5B8_TURTR <b>antithrombin-III isoform X2</b>	<i>Tursiops truncatus</i>	Common bottlenose dolphin	275
AOA2Y9SF59_PHYMC <b>L-lactate dehydrogenase</b>	<i>Physeter macrocephalus</i>	Sperm whale	274
AOA383ZYJ4_BALAS <b>carbonic anhydrase 1</b>	<i>Balaenoptera acutorostrata scammoni</i>	Scammon's minke whale	271
AOA140GN68_KOGSI <b>Hemoglobin subunit beta</b>	<i>Kogia sima</i>	Dwarf sperm whale	271
AOA384B2W1_BALAS <b>complement C4</b>	<i>Balaenoptera acutorostrata scammoni</i>	Scammon's minke whale	268
AOA383YRF9_BALAS <b>Amine oxidase</b>	<i>Balaenoptera acutorostrata scammoni</i>	Scammon's minke whale	260

AOA2U3V7Z3_TURTR <i>peroxiredoxin-1</i>	<i>Tursiops truncatus</i>	Common bottlenose dolphin	260
AOA384A7N6_BALAS <i>dipeptidyl peptidase 4</i>	<i>Balaenoptera acutorostrata scammoni</i>	Scammon's minke whale	259
AOA2FOAYW0_ESCRO <i>Ig lambda-6 chain C region</i>	<i>Eschrichtius robustus</i>	Gray whale	258
AOA2Y9PHY7_DELLE <i>Amine oxidase</i>	<i>Delphinapterus leucas</i>	Beluga whale	249
AOA384AFQ0_BALAS <i>Plasminogen</i>	<i>Balaenoptera acutorostrata scammoni</i>	Scammon's minke whale	244
AOA2F0BP97_ESCRO <i>Ig mu heavy chain disease protein</i>	<i>Eschrichtius robustus</i>	Gray whale	243
AOA2F0BAV1_ESCRO <i>Keratin, type I cytoskeletal 14</i>	<i>Eschrichtius robustus</i>	Gray whale	238
AOA2U3VAA7_TURTR <i>alcohol dehydrogenase E chain</i>	<i>Tursiops truncatus</i>	Common bottlenose dolphin	235
AOA2U4CBA9_TURTR <i>keratin, type II cytoskeletal 6A-like</i>	<i>Tursiops truncatus</i>	Common bottlenose dolphin	234
AOA383ZW6_BALAS <i>keratin, type II cytoskeletal 6A-like isoform X2</i>	<i>Balaenoptera acutorostrata scammoni</i>	Scammon's minke whale	226
AOA2F0B434_ESCRO <i>Cytosolic 10-formyltetrahydrofolate dehydrogenase</i>	<i>Eschrichtius robustus</i>	Gray whale	223
AOA2F0B4J5_ESCRO <i>Hemoglobin subunit alpha</i>	<i>Eschrichtius robustus</i>	Gray whale	219
AOA2U4B5X8_TURTR <i>flavin reductase (NADPH)</i>	<i>Tursiops truncatus</i>	Common bottlenose dolphin	215
AOA1KOFUJ2_TURTR <i>Globin B1</i>	<i>Tursiops truncatus</i>	Common bottlenose dolphin	214
AOA384B6I8_BALAS <i>L-lactate dehydrogenase</i>	<i>Balaenoptera acutorostrata scammoni</i>	Scammon's minke whale	205
AOA383ZYR5_BALAS <i>carbonic anhydrase 3</i>	<i>Balaenoptera acutorostrata scammoni</i>	Scammon's minke whale	190
AOA384AL46_BALAS <i>carbamoyl-phosphate synthase [ammonia], mitochondrial</i>	<i>Balaenoptera acutorostrata scammoni</i>	Scammon's minke whale	186
AOA340WU44_LIPVE <i>immunoglobulin lambda-like polypeptide 5</i>	<i>Lipotes vexillifer</i>	Baiji (white-finned dolphin)	180
AOA384BCE5_BALAS <i>Fructose-bisphosphate aldolase</i>	<i>Balaenoptera acutorostrata scammoni</i>	Scammon's minke whale	173
AOA4U1ECY9_MONMO <i>Uncharacterized protein</i>	<i>Monodon monoceros</i>	Narwhal	169
AOA2U4A337_TURTR <i>selenium-binding protein 1 isoform X1</i>	<i>Tursiops truncatus</i>	Common bottlenose dolphin	166
AOA484GJZ6_SOUCHE <i>IF rod domain-containing protein</i>	<i>Sousa chinensis</i>	Indo-Pacific humpbacked dolphin	165

AOA2F0BAH8_ESCRO <b>Complement factor B</b>	<i>Eschrichtius robustus</i>	Gray whale	163
AOA383ZNS6_BALAS <b>fibrinogen beta chain</b>	<i>Balaenoptera acutorostrata scammoni</i>	Scammon's minke whale	161
AOA384AFN8_BALAS <b>Superoxide dismutase</b>	<i>Balaenoptera acutorostrata scammoni</i>	Scammon's minke whale	156
AOA2U4AUY5_TURTR <b>dimethylglycine dehydrogenase, mitochondrial</b>	<i>Tursiops truncatus</i>	Common bottlenose dolphin	156
AOA2F0B025_ESCRO <b>Peroxiredoxin-2</b>	<i>Eschrichtius robustus</i>	Gray whale	155
AOA340YDD2_LIPVE <b>xaa-Pro dipeptidase isoform X2</b>	<i>Lipotes vexillifer</i>	Baiji (white-finned dolphin)	150
AOA2FOBB82_ESCRO <b>Glycerol-3-phosphate dehydrogenase [NAD(+)]</b>	<i>Eschrichtius robustus</i>	Gray whale	146
AOA383ZRC7_BALAS <b>keratin, type I cytoskeletal 13</b>	<i>Balaenoptera acutorostrata scammoni</i>	Scammon's minke whale	146
AOA2F0B5C3_ESCRO <b>Factor XIIa inhibitor (Fragment)</b>	<i>Eschrichtius robustus</i>	Gray whale	145
AOA383ZPB5_BALAS <b>fibrinogen alpha chain</b>	<i>Balaenoptera acutorostrata scammoni</i>	Scammon's minke whale	136
AOA2Y9FBW7_PHYMC <b>selenoprotein P</b>	<i>Physeter macrocephalus</i>	Sperm whale	134
AOA384A1C5_BALAS <b>inhibitor of carbonic anhydrase isoform X1</b>	<i>Balaenoptera acutorostrata scammoni</i>	Scammon's minke whale	131
AOA452C7H9_BALAS <b>Ferritin</b>	<i>Balaenoptera acutorostrata scammoni</i>	Scammon's minke whale	123
AOA340YEK8_LIPVE <b>keratin 16</b>	<i>Lipotes vexillifer</i>	Baiji (white-finned dolphin)	121
AOA383ZI56_BALAS <b>inter-alpha-trypsin inhibitor heavy chain H4 isoform X2</b>	<i>Balaenoptera acutorostrata scammoni</i>	Scammon's minke whale	121
AOA341BL15_9CETA <b>apolipoprotein B-100</b>	<i>Neophocaena asiaeorientalis asiaeorientalis</i>	Yangtze finless porpoise	118
AOA2Y9FIB4_PHYMC <b>complement C5</b>	<i>Physeter macrocephalus</i>	Sperm whale	111
AOAON9DSI7_BALOM <b>C1Q and collagen domain containing adiponectin</b>	<i>Balaenoptera omurai</i>	Omura's whale (dwarf fin whale)	111
AOA383ZHI2_BALAS <b>four and a half LIM domains protein 1 isoform X1</b>	<i>Balaenoptera acutorostrata scammoni</i>	Scammon's minke whale	111
AOA2Y9Q8L6_DELLE <b>selenoprotein P isoform X1</b>	<i>Delphinapterus leucas</i>	Beluga whale	109
AOA2Y9NVG6_DELLE <b>phosphoglucomutase-1 isoform X1</b>	<i>Delphinapterus leucas</i>	Beluga whale	109
AOA2F0BG39_ESCRO <b>Eosinophil peroxidase</b>	<i>Eschrichtius robustus</i>	Gray whale	107
AOA2F0B5X4_ESCRO	<i>Eschrichtius robustus</i>	Gray whale	102

<b>Heat shock protein HSP 90-beta</b>			
AOA2Y9M0C5_DELLE <b><i>nesprin-1 isoform X9</i></b>	<i>Delphinapterus leucas</i>	Beluga whale	99
AOA2F0BF69_ESCRO <b><i>Heparin cofactor 2</i></b>	<i>Eschrichtius robustus</i>	Gray whale	99
AOA2F0B1I9_ESCRO <b><i>Beta-enolase</i></b>	<i>Eschrichtius robustus</i>	Gray whale	98
AOA2Y9S2C1_PHYMC <b><i>alpha-1B-glycoprotein</i></b>	<i>Physeter macrocephalus</i>	Sperm whale	97
AOA383YWT8_BALAS <b><i>complement factor H-like isoform X1</i></b>	<i>Balaenoptera acutorostrata scammoni</i>	Scammon's minke whale	96
AOA2F0B6Y0_ESCRO <b><i>Superoxide dismutase [Cu-Zn]</i></b>	<i>Eschrichtius robustus</i>	Gray whale	96
AOA383Z9Z9_BALAS <b><i>Alpha-mannosidase</i></b>	<i>Balaenoptera acutorostrata scammoni</i>	Scammon's minke whale	93
AOA2U3ZZ88_TURTR <b><i>alpha-1-antitrypsin-like</i></b>	<i>Tursiops truncatus</i>	Common bottlenose dolphin	93
AOA2U3V1L4_TURTR <b><i>alpha-enolase</i></b>	<i>Tursiops truncatus</i>	Common bottlenose dolphin	90
AOA2FOAUI6_ESCRO <b><i>Ferritin</i></b>	<i>Eschrichtius robustus</i>	Gray whale	87
AOA2Y9F7I5_PHYMC <b><i>fetuin-B isoform X1</i></b>	<i>Physeter macrocephalus</i>	Sperm whale	85
AOA2F0BB0D2_ESCRO <b><i>Glutathione S-transferase</i></b>	<i>Eschrichtius robustus</i>	Gray whale	85
AOA384AAI3_BALAS <b><i>heat shock-related 70 kDa protein 2</i></b>	<i>Balaenoptera acutorostrata scammoni</i>	Scammon's minke whale	84
AOA4V5P683_MONMO <b><i>Histone H2B</i></b>	<i>Monodon monoceros</i>	Narwhal	84
AOA2F0B3E9_ESCRO <b><i>Superoxide dismutase</i></b>	<i>Eschrichtius robustus</i>	Gray whale	81
AOA2F0AVC4_ESCRO <b><i>Fatty acid-binding protein, epidermal</i></b>	<i>Eschrichtius robustus</i>	Gray whale	80
AOA2Y9MBI0_DELLE <b><i>keratin, type II cytoskeletal 8-like</i></b>	<i>Delphinapterus leucas</i>	Beluga whale	77
AOA340WNM5_LIPVE <b><i>obscurin-like</i></b>	<i>Lipotes vexillifer</i>	Baiji (white-finned dolphin)	75
AOA340XVM8_LIPVE <b><i>keratin, type I cytoskeletal 15</i></b>	<i>Lipotes vexillifer</i>	Baiji (white-finned dolphin)	75
AOA2U4BYT9_TURTR <b><i>GTP-binding nuclear protein Ran</i></b>	<i>Tursiops truncatus</i>	Common bottlenose dolphin	73
AOA2F0B364_ESCRO <b><i>Protein S100</i></b>	<i>Eschrichtius robustus</i>	Gray whale	70
AOA2Y9PGE3_DELLE <b><i>protein dopey-1 isoform X4</i></b>	<i>Delphinapterus leucas</i>	Beluga whale	70
AOA2U3V4G0_TURTR <b><i>PITH domain-containing protein 1</i></b>	<i>Tursiops truncatus</i>	Common bottlenose dolphin	69
AOA2U4CEL7_TURTR <b><i>importin-7 isoform X1</i></b>	<i>Tursiops truncatus</i>	Common bottlenose dolphin	69

AOA384AEC5_BALAS <b><i>beta-2-glycoprotein 1</i></b>	<i>Balaenoptera acutorostrata scammoni</i>	Scammon's minke whale	68
AOA2U3V8D9_TURTR <b><i>Peptidyl-prolyl cis-trans isomerase</i></b>	<i>Tursiops truncatus</i>	Common bottlenose dolphin	68
AOA2F0BDE3_ESCRO <b><i>Carboxypeptidase B2</i></b>	<i>Eschrichtius robustus</i>	Gray whale	68
AOA2U4ANF3_TURTR <b><i>14-3-3 protein epsilon</i></b>	<i>Tursiops truncatus</i>	Common bottlenose dolphin	67
AOA2U3V999_TURTR <b><i>ribose-phosphate pyrophosphokinase 1</i></b>	<i>Tursiops truncatus</i>	Common bottlenose dolphin	67
AOA340XWI8_LIPVE <b><i>Adenosylhomocysteinase</i></b>	<i>Lipotes vexillifer</i>	Baiji (white-finned dolphin)	67
AOA2FOB177_ESCRO <b><i>Clusterin</i></b>	<i>Eschrichtius robustus</i>	Gray whale	67
Q0KIY1 MYG_BALBO <b><i>Myoglobin</i></b>	<i>Balaenoptera borealis</i>	Sei whale	64
AOA2Y9EU52_PHYMC <b><i>Triosephosphate isomerase</i></b>	<i>Physeter macrocephalus</i>	Sperm whale	63
AOA341BER1_9CETA <b><i>homeobox protein Hox-B4</i></b>	<i>Neophocaena asiaeorientalis asiaeorientalis</i>	Yangtze finless porpoise	63
AOA2FOBB48_ESCRO <b><i>Phosphotriesterase-related protein</i></b>	<i>Eschrichtius robustus</i>	Gray whale	62
AOA383ZHH6_BALAS <b><i>keratin, type II microfibrillar-like</i></b>	<i>Balaenoptera acutorostrata scammoni</i>	Scammon's minke whale	62
AOA340XTH9_LIPVE <b><i>plectin</i></b>	<i>Lipotes vexillifer</i>	Baiji (white-finned dolphin)	61
AOA2FOBAJ8_ESCRO <b><i>Eukaryotic translation initiation factor 5A</i></b>	<i>Eschrichtius robustus</i>	Gray whale	60
AOA2FOB748_ESCRO <b><i>Homogentisate 1,2-dioxygenase</i></b>	<i>Eschrichtius robustus</i>	Gray whale	57
AOA384A960_BALAS <b><i>alpha-2-antiplasmin</i></b>	<i>Balaenoptera acutorostrata scammoni</i>	Scammon's minke whale	57
AOA341AVJ1_9CETA <b><i>EF-hand calcium-binding domain-containing protein 6</i></b>	<i>Neophocaena asiaeorientalis asiaeorientalis</i>	Yangtze finless porpoise	56
AOA2FOBHS2_ESCRO <b><i>Inter-alpha-trypsin inhibitor heavy chain H1</i></b>	<i>Eschrichtius robustus</i>	Gray whale	56
AOA2Y9MWF5_DELLE <b><i>protocadherin Fat 1 isoform X1</i></b>	<i>Delphinapterus leucas</i>	Beluga whale	54
AOA2U4BA07_TURTR <b><i>Tubulin alpha chain</i></b>	<i>Tursiops truncatus</i>	Common bottlenose dolphin	53
AOA2U4BFU2_TURTR <b><i>unconventional myosin-Vb</i></b>	<i>Tursiops truncatus</i>	Common bottlenose dolphin	53
AOA2FOBDR3_ESCRO <b><i>Calpain-1 catalytic subunit</i></b>	<i>Eschrichtius robustus</i>	Gray whale	52
AOA2U4BFQ3_TURTR <b><i>Diacylglycerol kinase</i></b>	<i>Tursiops truncatus</i>	Common bottlenose dolphin	52

AOA452C841_BALAS <i>ankyrin repeat domain-containing protein 24</i>	<i>Balaenoptera acutorostrata scammoni</i>	Scammon's minke whale	49
AOA2U4C9K2_TURTR <i>unconventional myosin-Va isoform X2</i>	<i>Tursiops truncatus</i>	Common bottlenose dolphin	49
AOA2U4AHH7_TURTR <i>40S ribosomal protein S14</i>	<i>Tursiops truncatus</i>	Common bottlenose dolphin	49
AOA2F0BPQ3_ESCRO <i>Bisphosphoglycerate mutase</i>	<i>Eschrichtius robustus</i>	Gray whale	48
AOA2F0B3N0_ESCRO <i>Vitronectin</i>	<i>Eschrichtius robustus</i>	Gray whale	48
AOA455BTV8_PHYMC <i>echinoderm microtubule-associated protein-like 1 isoform X2</i>	<i>Physeter macrocephalus</i>	Sperm whale	47
AOA2FOAVI7_ESCRO <i>EF-hand domain-containing protein</i>	<i>Eschrichtius robustus</i>	Gray whale	47
AOA4U1F4C5_MONMO <i>SAC domain-containing protein</i>	<i>Monodon monoceros</i>	Narwhal	47
AOA2F0BJB3_ESCRO <i>Prothrombin</i>	<i>Eschrichtius robustus</i>	Gray whale	47
AOA2U4C8L6_TURTR <i>protein KIBRA</i>	<i>Tursiops truncatus</i>	Common bottlenose dolphin	46
AOA2Y9MWH7_DELLE <i>pericentriolar material 1 protein isoform X5</i>	<i>Delphinapterus leucas</i>	Beluga whale	46
AOA2Y9PYI9_DELLE <i>fer-1-like protein 4</i>	<i>Delphinapterus leucas</i>	Beluga whale	46
AOA455AIA8_PHYMC <i>eIF-2-alpha kinase activator GCN1 isoform X2</i>	<i>Physeter macrocephalus</i>	Sperm whale	46
AOA2U4C9F5_TURTR <i>allergen Fel d 4-like</i>	<i>Tursiops truncatus</i>	Common bottlenose dolphin	45
AOA340X7R4_LIPVE <i>leucine-rich repeat-containing protein 69</i>	<i>Lipotes vexillifer</i>	Baiji (white-finned dolphin)	44
AOA384B088_BALAS <i>uncharacterized protein C3orf20 homolog</i>	<i>Balaenoptera acutorostrata scammoni</i>	Scammon's minke whale	43
AOA340XGD2_LIPVE <i>matrix-remodeling-associated protein 5</i>	<i>Lipotes vexillifer</i>	Baiji (white-finned dolphin)	42
AOA2FOBBC1_ESCRO <i>Retinal dehydrogenase 1</i>	<i>Eschrichtius robustus</i>	Gray whale	42
AOA2F0BPS3_ESCRO <i>Phosphoglycerate kinase</i>	<i>Eschrichtius robustus</i>	Gray whale	41

2720      <sup>t</sup>Ions score is -10\*Log(P), where P is the probability that the observed match is a random event. Individual ions  
 2721      scores > 41 indicated identity or extensive homology ( $p < 0.05$ ). Protein scores were derived from ions scores as  
 2722      a non-probabilistic basis for ranking protein hits. Cut-off was set at Ions score 20.

2723  
2724

2725 **Supplementary Table 5. Deiminated proteins identified by F95 enrichment in serum of Cuvier's beaked whale**  
 2726 (*Ziphius cavirostris*). Deiminated proteins were isolated by immunoprecipitation using the pan-deimination F95  
 2727 antibody. The F95 enriched eluate was analysed by LC-MS/MS and peak list files were submitted to mascot.  
 2728 Peptide hits scoring with the cetacean database (CCP\_Cetacea\_Cetacea\_20191213; 252,001 sequences;  
 2729 150,129,595 residues) are shown. Species hit names and total scores are shown.

Protein name	Species name	Common name	Total score ( <i>p</i> <0.05) <sup>‡</sup>
AOA383ZXRO_BALAS <i>serum albumin</i>	<i>Balaenoptera acutorostrata scammoni</i>	Scammon's minke whale	1159
AOA341C5T8_9CETA <i>serum albumin</i>	<i>Neophocaena asiaeorientalis asiaeorientalis</i>	Yangtze finless porpoise	1156
AOA2U3V5M2_TURTR <i>serum albumin</i>	<i>Tursiops truncatus</i>	Common bottlenose dolphin	1088
AOA140GN64_BALAC <i>Hemoglobin subunit beta</i>	<i>Balaenoptera acutorostrata</i>	Northern minke whale	1003
AOA384AGF6_BALAS <i>Fructose-bisphosphate aldolase</i>	<i>Balaenoptera acutorostrata scammoni</i>	Scammon's minke whale	970
AOA384B912_BALAS <i>alpha-2-macroglobulin isoform X2</i>	<i>Balaenoptera acutorostrata scammoni</i>	Scammon's minke whale	932
AOA140GN67_MESDE <i>Hemoglobin subunit beta</i>	<i>Mesoplodon densirostris</i>	Blainville's beaked whale	847
AOA2Y9NE67_DELLE <i>alpha-2-macroglobulin isoform X2</i>	<i>Delphinapterus leucas</i>	Beluga whale	736
AOA344X2S6_GLOME <i>Hemoglobin subunit beta</i>	<i>Globicephala melas</i>	Long-finned pilot whale	714
P02182 MYG_ZIPCA <i>Myoglobin</i>	<i>Ziphius cavirostris</i>	Cuvier's beaked whale	696
AOA140GN07_MESDE <i>Hemoglobin subunit alpha</i>	<i>Mesoplodon densirostris</i>	Blainville's beaked whale	637
AOA2Y9NWW8_DELLE <i>L-lactate dehydrogenase</i>	<i>Delphinapterus leucas</i>	Beluga whale	559
AOA2Y9EHS1_PHYMC <i>hemoglobin subunit beta-1/2 isoform X2</i>	<i>Physeter macrocephalus</i>	Sperm whale	520
AOA140GN06_TURTR <i>Hemoglobin subunit alpha</i>	<i>Tursiops truncatus</i>	Common bottlenose dolphin	447
AOA140GN13_BALAC <i>Hemoglobin subunit alpha</i>	<i>Balaenoptera acutorostrata</i>		445
AOA140GN14_PHYMC <i>Hemoglobin subunit alpha</i>	<i>Physeter macrocephalus</i>	Sperm whale	403
AOA340WLD3_LIPVE <i>fibrinogen beta chain isoform X2</i>	<i>Lipotes vexillifer</i>	Baiji (white-finned dolphin)	390
AOA140GN09_KOGSI <i>Hemoglobin subunit alpha</i>	<i>Kogia sima</i>	Dwarf sperm whale	364
AOA140GN68_KOGSI <i>Hemoglobin subunit beta</i>	<i>Kogia sima</i>	Dwarf sperm whale	348
AOA4U1FNC5_MONMO <i>Uncharacterized protein</i>	<i>Monodon monoceros</i>	Narwhal	346
AOA2U4AKU6_TURTR <i>glycine amidinotransferase, mitochondrial isoform X1</i>	<i>Tursiops truncatus</i>	Common bottlenose dolphin	269
AOA2Y9EYT5_PHYMC <i>Catalase</i>	<i>Physeter macrocephalus</i>	Sperm whale	269

AOA340WJU5_LIPVE <b><i>alpha-1-antitrypsin isoform X2</i></b>	<i>Lipotes vexillifer</i>	Baiji (white-finned dolphin)	269
AOA2U4AKU6_TURTR <b><i>Glyceraldehyde-3-phosphate dehydrogenase</i></b>	<i>Tursiops truncatus</i>	Common bottlenose dolphin	260
AOA383ZV20_BALAS <b><i>alpha-1-antitrypsin</i></b>	<i>Balaenoptera acutorostrata scammoni</i>	Scammon's minke whale	246
AOA341AN91_9CETA <b><i>Haptoglobin</i></b>	<i>Neophocaena asiaeorientalis asiaeorientalis</i>	Yangtze finless porpoise	244
AOA4U1EJD5_MONMO <b><i>TAF domain-containing protein</i></b>	<i>Monodon monoceros</i>	Narwhal	243
AOA2FOAZL3_ESCRO <b><i>Histone H2B</i></b>	<i>Eschrichtius robustus</i>	Gray whale	238
AOA2FOAXA3_ESCRO <b><i>Pyruvate kinase</i></b>	<i>Eschrichtius robustus</i>	Gray whale	237
AOA2F0B4J5_ESCRO <b><i>Hemoglobin subunit alpha</i></b>	<i>Eschrichtius robustus</i>	Gray whale	235
AOA2F0BMF7_ESCRO <b><i>Histone H2B</i></b>	<i>Eschrichtius robustus</i>	Gray whale	231
AOA340Y1E6_LIPVE <b><i>keratin, type I cytoskeletal 14</i></b>	<i>Lipotes vexillifer</i>	Baiji (white-finned dolphin)	226
AOA2Y9FPM0_PHYMC <b><i>phosphoglucomutase-1 isoform X2</i></b>	<i>Physeter macrocephalus</i>	Sperm whale	220
AOA2FOBAV1_ESCRO <b><i>Keratin, type I cytoskeletal 14</i></b>	<i>Eschrichtius robustus</i>	Gray whale	206
AOA2U4AC17_TURTR <b><i>homogentisate 1,2-dioxygenase</i></b>	<i>Tursiops truncatus</i>	Common bottlenose dolphin	198
AOA2U4AM45_TURTR <b><i>carbonic anhydrase 3</i></b>	<i>Tursiops truncatus</i>	Common bottlenose dolphin	186
AOA2FOB1I9_ESCRO <b><i>Beta-enolase</i></b>	<i>Eschrichtius robustus</i>	Gray whale	184
AOA2U4CBF1_TURTR <b><i>keratin, type II cytoskeletal 5</i></b>	<i>Tursiops truncatus</i>	Common bottlenose dolphin	168
AOA383ZJG1_BALAS <b><i>basement membrane-specific heparan sulfate proteoglycan core protein</i></b>	<i>Balaenoptera acutorostrata scammoni</i>	Scammon's minke whale	164
AOA2Y9EU52_PHYMC <b><i>Triosephosphate isomerase</i></b>	<i>Physeter macrocephalus</i>	Sperm whale	163
AOA2Y9MCX1_DELLE <b><i>Hemopexin</i></b>	<i>Delphinapterus leucas</i>	Beluga whale	163
AOA383Z5R5_BALAS <b><i>serotransferrin</i></b>	<i>Balaenoptera acutorostrata scammoni</i>	Scammon's minke whale	163
AOA2U3V7Z3_TURTR <b><i>peroxiredoxin-1</i></b>	<i>Tursiops truncatus</i>	Common bottlenose dolphin	159
AOA340XVL6_LIPVE <b><i>Ferritin</i></b>	<i>Lipotes vexillifer</i>	Baiji (white-finned dolphin)	158
AOA2U3V0H1_TURTR <b><i>betaine-homocysteine S-methyltransferase 1</i></b>	<i>Tursiops truncatus</i>	Common bottlenose dolphin	157
AOA384BCE5_BALAS <b><i>Fructose-bisphosphate aldolase</i></b>	<i>Balaenoptera acutorostrata scammoni</i>	Scammon's minke whale	156
AOA2F0B042_ESCRO <b><i>Hemopexin</i></b>	<i>Eschrichtius robustus</i>	Gray whale	150

AOA341AG71_9CETA <i>titin</i>	<i>Neophocaena asiaeorientalis asiaeorientalis</i>	Yangtze finless porpoise	148
AOA2Y9N3W5_DELLE <i>keratin, type II cytoskeletal 5-like</i>	<i>Delphinapterus leucas</i>	Beluga whale	143
AOA2U4BKU4_TURTR <i>protein 4.1 isoform X5</i>	<i>Tursiops truncatus</i>	Common bottlenose dolphin	136
AOA2U4B9J5_TURTR <i>ceruloplasmin isoform X2</i>	<i>Tursiops truncatus</i>	Common bottlenose dolphin	135
AOA2Y9M110_DELLE <i>complement C3 isoform X1</i>	<i>Delphinapterus leucas</i>	Beluga whale	134
AOA2FOAYW0_ESCRO <i>Ig lambda-6 chain C region</i>	<i>Eschrichtius robustus</i>	Gray whale	127
AOA2U3V5S9_TURTR <i>kininogen-1 isoform X1</i>	<i>Tursiops truncatus</i>	Common bottlenose dolphin	122
AOA2Y9F6G6_PHYMC <i>fibrinogen gamma chain isoform X2</i>	<i>Physeter macrocephalus</i>	Sperm whale	115
AOA384ANK3_BALAS <i>thyroglobulin</i>	<i>Balaenoptera acutorostrata scammoni</i>	Scammon's minke whale	112
AOA2FOAYR9_ESCRO <i>Glucose-6-phosphate isomerase</i>	<i>Eschrichtius robustus</i>	Gray whale	96
AOA383YWT8_BALAS <i>complement factor H-like isoform X1</i>	<i>Balaenoptera acutorostrata scammoni</i>	Scammon's minke whale	89
AOA2U3VA32_TURTR <i>Protein S100</i>	<i>Tursiops truncatus</i>	Common bottlenose dolphin	87
AOA2U3V321_TURTR <i>four and a half LIM domains protein 1 isoform X2</i>	<i>Tursiops truncatus</i>	Common bottlenose dolphin	86
AOA2U4B948_TURTR <i>serotransferrin</i>	<i>Tursiops truncatus</i>	Common bottlenose dolphin	76
AOA340WU44_LIPVE <i>immunoglobulin lambda-like polypeptide 5</i>	<i>Lipotes vexillifer</i>	Baiji (white-finned dolphin)	75
AOA2Y9M0C5_DELLE <i>nesprin-1 isoform X9</i>	<i>Delphinapterus leucas</i>	Beluga whale	73
AOA2Y9F931_PHYMC <i>carbonic anhydrase 2 isoform X1</i>	<i>Physeter macrocephalus</i>	Sperm whale	73
AOA2F0BGI8_ESCRO <i>Prelamin-A/C</i>	<i>Eschrichtius robustus</i>	Gray whale	70
AOA2U4CLI2_TURTR <i>Adenosylhomocysteinase</i>	<i>Tursiops truncatus</i>	Common bottlenose dolphin	70
AOA2FOBP97_ESCRO <i>Ig mu heavy chain disease protein</i>	<i>Eschrichtius robustus</i>	Gray whale	69
AOA2U3VA11_TURTR <i>carbonic anhydrase 1</i>	<i>Tursiops truncatus</i>	Common bottlenose dolphin	64
AOA2U4AJY5_TURTR <i>glutamate dehydrogenase 1, mitochondrial</i>	<i>Tursiops truncatus</i>	Common bottlenose dolphin	64
AOA2FOBN89_ESCRO <i>Inter-alpha-trypsin inhibitor heavy chain H4</i>	<i>Eschrichtius robustus</i>	Gray whale	63

AOA2U3V937_TURTR <b><i>Proteasome subunit alpha type</i></b>	<i>Tursiops truncatus</i>	Common bottlenose dolphin	62
APOA1_BALAS <b><i>Apolipoprotein A-I</i></b>	<i>Balaenoptera acutorostrata scammoni</i>	Scammon's minke whale	61
AOA2FOBG39_ESCRO <b><i>Eosinophil peroxidase</i></b>	<i>Eschrichtius robustus</i>	Gray whale	60
AOAON7EHN7_DELCA <b><i>C1Q and collagen domain containing adiponectin</i></b>	<i>Delphinus capensis</i>	Long-beaked common dolphin	60
AOA340WNM5_LIPVE <b><i>obscurin-like</i></b>	<i>Lipotes vexillifer</i>	Baiji (white-finned dolphin)	57
AOA384AT03_BALAS <b><i>coiled-coil domain-containing protein 150</i></b>	<i>Balaenoptera acutorostrata scammoni</i>	Scammon's minke whale	57
AOA2Y9EWF4_PHYMC <b><i>Alpha-1,4 glucan phosphorylase</i></b>	<i>Physeter macrocephalus</i>	Sperm whale	55
AOA2U4BQ96_TURTR <b><i>adenylate cyclase type 1</i></b>	<i>Tursiops truncatus</i>	Common bottlenose dolphin	55
AOA2FOBCJ0_ESCRO <b><i>Complement C4-B</i></b>	<i>Eschrichtius robustus</i>	Gray whale	54
AOA383ZUH3_BALAS <b><i>DNA excision repair protein ERCC-6 isoform X2</i></b>	<i>Balaenoptera acutorostrata scammoni</i>	Scammon's minke whale	53
AOA2FOBKF1_ESCRO <b><i>60S ribosomal protein L8</i></b>	<i>Eschrichtius robustus</i>	Gray whale	52
AOA340YCM8_LIPVE <b><i>C4b-binding protein alpha chain-like</i></b>	<i>Lipotes vexillifer</i>	Baiji (white-finned dolphin)	48
AOA2Y9P779_DELLE <b><i>creatine kinase M-type</i></b>	<i>Delphinapterus leucas</i>	Beluga whale	45
AOA2U4BWA9_TURTR <b><i>radixin isoform X1</i></b>	<i>Tursiops truncatus</i>	Common bottlenose dolphin	45
AOA2U4B5X8_TURTR <b><i>flavin reductase (NADPH)</i></b>	<i>Tursiops truncatus</i>	Common bottlenose dolphin	44
AOA2U4B008_TURTR <b><i>cilia- and flagella-associated protein 45 isoform X1</i></b>	<i>Tursiops truncatus</i>	Common bottlenose dolphin	43
AOA340X7S9_LIPVE <b><i>Plasminogen</i></b>	<i>Lipotes vexillifer</i>	Baiji (white-finned dolphin)	42
AOA2FOAV78_ESCRO <b><i>Dipeptidyl peptidase 9</i></b>	<i>Eschrichtius robustus</i>	Gray whale	42
AOA2Y9FG23_PHYMC <b><i>Peptidyl-prolyl cis-trans isomerase</i></b>	<i>Physeter macrocephalus</i>	Sperm whale	42
AOA2U3V024_TURTR <b><i>C-C motif chemokine 17</i></b>	<i>Tursiops truncatus</i>	Common bottlenose dolphin	41

2730      \*Ions score is -10\*Log(P), where P is the probability that the observed match is a random event. Individual ions  
 2731      scores > 41 indicated identity or extensive homology ( $p < 0.05$ ). Protein scores were derived from ions scores as  
 2732      a non-probabilistic basis for ranking protein hits. Cut-off was set at Ions score 20.  
 2733  
 2734

2735 **Supplementary Table 6. Deiminated proteins identified by F95 enrichment in serum of orca (*Orcinus orca*).**  
 2736 Deiminated proteins were isolated by immunoprecipitation using the pan-deimination F95 antibody. The F95  
 2737 enriched eluate was analysed by LC-MS/MS and peak list files were submitted to mascot . Peptide hits scoring  
 2738 with the cetacean database (CCP\_Cetacea\_Cetacea\_20191213; 252,001 sequences; 150,129,595 residues) are  
 2739 shown. Species hit names and total scores are shown.

Protein name	Species name	Common name	Total score ( <i>p</i> <0.05) <sup>‡</sup>
AOA341C5T8_9CETA <i>serum albumin</i>	<i>Neophocaena asiaeorientalis asiaeorientalis</i>	Yangtze finless porpoise	2358
AOA2U3V5M2_TURTR <i>serum albumin isoform X1</i>	<i>Tursiops truncatus</i>	Common bottlenose dolphin	2336
AOA2U4B948_TURTR <i>serotransferrin</i>	<i>Tursiops truncatus</i>	Common bottlenose dolphin	2322
AOA2Y9QJ69_DELLE <i>serum albumin</i>	<i>Delphinapterus leucas</i>	Beluga whale	2149
AOA383ZXRO_BALAS <i>serum albumin</i>	<i>Balaenoptera acutorostrata scammoni</i>	Scammon's minke whale	2086
AOA2Y9NK15_DELLE <i>alpha-2-macroglobulin isoform X3</i>	<i>Delphinapterus leucas</i>	Beluga whale	1928
AOA4U1FPV0_MONMO <i>Uncharacterized protein</i>	<i>Monodon monoceros</i>	Narwhal	1883
AOA2U3V5S9_TURTR <i>kininogen-1 isoform X1</i>	<i>Tursiops truncatus</i>	Common bottlenose dolphin	1880
AOA384B912_BALAS <i>alpha-2-macroglobulin isoform X2</i>	<i>Balaenoptera acutorostrata scammoni</i>	Scammon's minke whale	1800
AOA2U4AKU7_TURTR <i>alpha-2-macroglobulin-like</i>	<i>Tursiops truncatus</i>	Common bottlenose dolphin	1763
AOA340Y7Z8_LIPVE <i>serum albumin</i>	<i>Lipotes vexillifer</i>	Baiji (white-finned dolphin)	1762
AOA2Y9P4F8_DELLE <i>serotransferrin-like</i>	<i>Delphinapterus leucas</i>	Beluga whale	1703
AOA2Y9N2V9_DELLE <i>kininogen-1 isoform X1</i>	<i>Delphinapterus leucas</i>	Beluga whale	1590
AOA2U4CD99_TURTR <i>fibronectin isoform X4</i>	<i>Tursiops truncatus</i>	Common bottlenose dolphin	1374
AOA455BHA9_PHYMC <i>alpha-2-macroglobulin-like</i>	<i>Physeter macrocephalus</i>	Sperm whale	1290
AOA341DCM8_9CETA <i>kininogen-1 isoform X2</i>	<i>Neophocaena asiaeorientalis asiaeorientalis</i>	Yangtze finless porpoise	1173
AOA2U4CD99_TURTR <i>hemopexin</i>	<i>Tursiops truncatus</i>	Common bottlenose dolphin	1046
AOA484GXQ7_SOUCHE <i>Hemopexin</i>	<i>Sousa chinensis</i>	Indo-Pacific humpbacked dolphin	1039
AOA340WVC6_LIPVE <i>kininogen-1 isoform X1</i>	<i>Lipotes vexillifer</i>	Baiji (white-finned dolphin)	867
AOA341CEB0_9CETA <i>Hemopexin</i>	<i>Neophocaena asiaeorientalis asiaeorientalis</i>	Yangtze finless porpoise	801
AOA387L946_PSECS <i>Complement component 4A</i>	<i>Pseudorca crassidens</i>	False killer whale	750
AOA140GN64_BALAC <i>Hemoglobin subunit beta</i>	<i>Balaenoptera acutorostrata</i>	Northern minke whale	748
AOA2Y9MCX1_DELLE <i>Hemopexin</i>	<i>Delphinapterus leucas</i>	Beluga whale	741

AOA2Y9MIR4_DELLE <b>complement C4-like isoform X1</b>	<i>Delphinapterus leucas</i>	Beluga whale	712
AOA340XNP3_LIPVE <b>complement C3</b>	<i>Lipotes vexillifer</i>	Baiji (white-finned dolphin)	707
AOA2F0B042_ESCRO <b>Hemopexin</b>	<i>Eschrichtius robustus</i>	Gray whale	694
AOA2Y9M110_DELLE <b>complement C3 isoform X1</b>	<i>Delphinapterus leucas</i>	Beluga whale	670
AOA341BIQ3_9CETA <b>complement C3</b>	<i>Neophocaena asiaeorientalis asiaeorientalis</i>	Yangtze finless porpoise	612
AOA2U3V5U9_TURTR <b>complement factor H isoform X1</b>	<i>Tursiops truncatus</i>	Common bottlenose dolphin	565
AOA140GN67_MESDE <b>Hemoglobin subunit beta</b>	<i>Mesoplodon densirostris</i>	Blainville's beaked whale	546
AOA383Z5R5_BALAS <b>serotransferrin</b>	<i>Balaenoptera acutorostrata scammoni</i>	Scammon's minke whale	534
AOA2U4CNJ3_TURTR <b>Plasminogen</b>	<i>Tursiops truncatus</i>	Common bottlenose dolphin	531
AOA2U4CQ05_TURTR <b>C4b-binding protein alpha chain</b>	<i>Tursiops truncatus</i>	Common bottlenose dolphin	472
AOA455BL00_PHYMC <b>ceruloplasmin</b>	<i>Physeter macrocephalus</i>	Sperm whale	445
AOA383Z9Z9_BALAS <b>Alpha-mannosidase</b>	<i>Balaenoptera acutorostrata scammoni</i>	Scammon's minke whale	437
AOA4U1ETI6_MONMO <b>Alpha-mannosidase</b>	<i>Monodon monoceros</i>	Narwhal	435
AOA2Y9N1N7_DELLE <b>inter-alpha-trypsin inhibitor heavy chain H4 isoform X4</b>	<i>Delphinapterus leucas</i>	Beluga whale	434
AOA484GU10_SOUCHE <b>Uncharacterized protein</b>	<i>Sousa chinensis</i>	Indo-Pacific humpbacked dolphin	428
AOA2U4B9J5_TURTR <b>ceruloplasmin isoform X2</b>	<i>Tursiops truncatus</i>	Common bottlenose dolphin	401
AOA340XE64_LIPVE <b>complement factor H-like</b>	<i>Lipotes vexillifer</i>	Baiji (white-finned dolphin)	397
AOA2Y9MD96_DELLE <b>CD5 antigen-like</b>	<i>Delphinapterus leucas</i>	Beluga whale	393
AOA344X2S6_GLOME <b>Hemoglobin subunit beta</b>	<i>Globicephala melas</i>	Long-finned pilot whale	389
AOA2Y9TJG8_PHYMC <b>complement C3</b>	<i>Physeter macrocephalus</i>	Sperm whale	382
AOA484GS12_SOUCHE <b>Haptoglobin</b>	<i>Sousa chinensis</i>	Indo-Pacific humpbacked dolphin	357
AOA140GN13_BALAC <b>Hemoglobin subunit alpha</b>	<i>Balaenoptera acutorostrata</i>	Northern minke whale	309
AOA341BX82_9CETA <b>C4b-binding protein alpha chain isoform X2</b>	<i>Neophocaena asiaeorientalis asiaeorientalis</i>	Yangtze finless porpoise	302
AOA384ALG4_BALAS <b>ceruloplasmin isoform X2</b>	<i>Balaenoptera acutorostrata scammoni</i>	Scammon's minke whale	299
AOA2U4COC1_TURTR <b>apolipoprotein B-100</b>	<i>Tursiops truncatus</i>	Common bottlenose dolphin	287

AOA2U4AL13_TURTR <i>pregnancy zone protein-like</i>	<i>Tursiops truncatus</i>	Common bottlenose dolphin	272
AOA14GN07_MESDE <i>Hemoglobin subunit alpha</i>	<i>Mesoplodon densirostris</i>	Blainville's beaked whale	270
AOA2FOAYW0_ESCRO <i>Ig lambda-6 chain C region</i>	<i>Eschrichtius robustus</i>	Gray whale	265
AOA4U1FNC5_MONMO <i>Uncharacterized protein</i>	<i>Monodon monoceros</i>	Narwhal	264
AOA340WU44_LIPVE <i>immunoglobulin lambda-like polypeptide 5</i>	<i>Lipotes vexillifer</i>	Baiji (white-finned dolphin)	261
AOA2U4B4R7_TURTR <i>vitamin D-binding protein</i>	<i>Tursiops truncatus</i>	Common bottlenose dolphin	251
AOA14GN68_KOGSI <i>Hemoglobin subunit beta</i>	<i>Kogia sima</i>	Dwarf sperm whale	251
AOA2Y9LCY9_DELLE <i>basement membrane-specific heparan sulfate proteoglycan core protein isoform X3</i>	<i>Delphinapterus leucas</i>	Beluga whale	244
AOA2F0B4J5_ESCRO <i>Hemoglobin subunit alpha</i>	<i>Eschrichtius robustus</i>	Gray whale	243
AOA341CUQ2_9CETA <i>complement C5</i>	<i>Neophocaena asiaeorientalis asiaeorientalis</i>	Yangtze finless porpoise	235
AOA2Y9NPG1_DELLE <i>pregnancy zone protein-like</i>	<i>Delphinapterus leucas</i>	Beluga whale	235
AOA2U4BJL8_TURTR <i>basement membrane-specific heparan sulfate proteoglycan core protein</i>	<i>Tursiops truncatus</i>	Common bottlenose dolphin	228
AOA2U3V9T1_TURTR <i>fibrinogen alpha chain</i>	<i>Tursiops truncatus</i>	Common bottlenose dolphin	218
AOA2Y9LZH5_DELLE <i>apolipoprotein A-I</i>	<i>Delphinapterus leucas</i>	Beluga whale	213
AOA383Z8T4_BALAS <i>C4b-binding protein alpha chain isoform X7</i>	<i>Balaenoptera acutorostrata scammoni</i>	Scammon's minke whale	212
AOA2U4CBF1_TURTR <i>keratin, type II cytoskeletal 5</i>	<i>Tursiops truncatus</i>	Common bottlenose dolphin	206
AOA383ZRJ1_BALAS <i>keratin, type I cytoskeletal 14</i>	<i>Balaenoptera acutorostrata scammoni</i>	Scammon's minke whale	201
AOA14GN09_KOGSI <i>Hemoglobin subunit alpha</i>	<i>Kogia sima</i>	Dwarf sperm whale	188
AOA340WSC2_LIPVE <i>keratin, type II cytoskeletal 5 isoform X1</i>	<i>Lipotes vexillifer</i>	Baiji (white-finned dolphin)	186
AOA2U4AXD6_TURTR <i>selenoprotein P</i>	<i>Tursiops truncatus</i>	Common bottlenose dolphin	164
AOA2FOBAV1_ESCRO <i>Keratin, type I cytoskeletal 14</i>	<i>Eschrichtius robustus</i>	Gray whale	162
AOA2Y9F6G6_PHYMC <i>fibrinogen gamma chain isoform X2</i>	<i>Physeter macrocephalus</i>	Sperm whale	156
PODMA6 APOA1_BALAS <i>Apolipoprotein A-I</i>	<i>Balaenoptera acutorostrata scammoni</i>	Scammon's minke whale	152
AOA2U3V4Z9_TURTR <i>fibrinogen beta chain</i>	<i>Tursiops truncatus</i>	Common bottlenose dolphin	151

AOA2Y9F6G0_PHYMC <i>fibrinogen beta chain isoform X1</i>	<i>Physeter macrocephalus</i>	Sperm whale	150
AOA484H0L9_SOUCHE <i>Uncharacterized protein</i>	<i>Sousa chinensis</i>	Indo-Pacific humpbacked dolphin	136
AOA340WCV4_LIPVE <i>alpha-1-antitrypsin isoform X1</i>	<i>Lipotes vexillifer</i>	Baiji (white-finned dolphin)	125
AOA340WNM5_LIPVE <i>obscurin-like</i>	<i>Lipotes vexillifer</i>	Baiji (white-finned dolphin)	118
AOA340WNM5_LIPVE <i>Fructose-bisphosphate aldolase</i>	<i>Lipotes vexillifer</i>	Baiji (white-finned dolphin)	114
AOA4U1EB65_MONMO <i>Ig-like domain-containing protein</i>	<i>Monodon monoceros</i>	Narwhal	109
AOA484H0M4_SOUCHE <i>IGv domain-containing protein</i>	<i>Sousa chinensis</i>	Indo-Pacific humpbacked dolphin	109
AOA2Y9PG29_DELLE <i>Glutathione peroxidase</i>	<i>Delphinapterus leucas</i>	Beluga whale	100
AOA2FOBP97_ESCRO <i>Ig mu heavy chain disease protein</i>	<i>Eschrichtius robustus</i>	Gray whale	98
AOA2U3V1T4_TURTR <i>complement C1q subcomponent subunit A</i>	<i>Tursiops truncatus</i>	Common bottlenose dolphin	98
AOA2U4BME2_TURTR <i>galectin-3-binding protein</i>	<i>Tursiops truncatus</i>	Common bottlenose dolphin	91
AOA4U1ECF0_MONMO <i>Ig-like domain-containing protein</i>	<i>Monodon monoceros</i>	Narwhal	85
AOA2U4APV3_TURTR <i>L-lactate dehydrogenase</i>	<i>Tursiops truncatus</i>	Common bottlenose dolphin	82
AOA2U3V4E2_TURTR <i>beta-2-glycoprotein 1 isoform X1</i>	<i>Tursiops truncatus</i>	Common bottlenose dolphin	81
AOA2FOAY95_ESCRO <i>Complement C1q subcomponent subunit C</i>	<i>Eschrichtius robustus</i>	Gray whale	76
AOA2FOBAH8_ESCRO <i>Complement factor B</i>	<i>Eschrichtius robustus</i>	Gray whale	69
AOA2U3V982_TURTR <i>immunoglobulin J chain isoform X2</i>	<i>Tursiops truncatus</i>	Common bottlenose dolphin	65
AOA2U4AGU1_TURTR <i>RNA-binding protein 27 isoform X1</i>	<i>Tursiops truncatus</i>	Common bottlenose dolphin	56
QOKIY9 MYG_INDPC <i>Myoglobin</i>	<i>Indopacetus pacificus</i>	Tropical bottlenose whale	52
AOA2Y9NX77_DELLE <i>Piezo-type mechanosensitive ion channel component</i>	<i>Delphinapterus leucas</i>	Beluga whale	51
AOA2U4BAA2_TURTR <i>protein kinase C-binding protein NELL2 isoform X3</i>	<i>Tursiops truncatus</i>	Common bottlenose dolphin	51

AOA2U3VA11_TURTR <b><i>carbonic anhydrase 1</i></b>	<i>Tursiops truncatus</i>	Common bottlenose dolphin	49
AOA2F0AZJ9_ESCRO <b><i>Histone H2A</i></b>	<i>Eschrichtius robustus</i>	Gray whale	49
AOA2Y9SDE6_PHYMC <b><i>SEC14-like protein 3</i></b>	<i>Physeter macrocephalus</i>	Sperm whale	49
AOA4U1EBP7_MONMO <b><i>IGv domain-containing protein</i></b>	<i>Monodon monoceros</i>	Narwhal	48
AOA2F0B5R5_ESCRO <b><i>Complement component C8 alpha chain</i></b>	<i>Eschrichtius robustus</i>	Gray whale	48
AOA340WK61_LIPVE <b><i>autophagy-related protein 2 homolog B</i></b>	<i>Lipotes vexillifer</i>	Baiji (white-finned dolphin)	47
AOA2U3V609_TURTR <b><i>afamin</i></b>	<i>Tursiops truncatus</i>	Common bottlenose dolphin	47
AOA2Y9MDP5_DELLE <b><i>extracellular matrix protein 1 isoform X1</i></b>	<i>Delphinapterus leucas</i>	Beluga whale	45
AOA2Y9FWE7_PHYMC <b><i>complement factor D</i></b>	<i>Physeter macrocephalus</i>	Sperm whale	43
AOA2Y9QED7_DELLE <b><i>huntingtin-interacting protein 1-related protein isoform X2</i></b>	<i>Delphinapterus leucas</i>	Beluga whale	43
AOA2Y9Q1L2_DELLE <b><i>polymeric immunoglobulin receptor</i></b>	<i>Delphinapterus leucas</i>	Beluga whale	42
AOAON7EHN7_DELCA <b><i>C1Q and collagen domain containing adiponectin</i></b>	<i>Delphinus capensis</i>	Long-beaked common dolphin	42
AOA383ZKS2_BALAS <b><i>DENN domain-containing protein 5B isoform X2</i></b>	<i>Balaenoptera acutorostrata scammoni</i>	Scammon's minke whale	41
AOA2F0BJB3_ESCRO <b><i>Prothrombin</i></b>	<i>Eschrichtius robustus</i>	Gray whale	41
AOA2F0BL32_ESCRO <b><i>Peptidyl-tRNA hydrolase 2, mitochondrial</i></b>	<i>Eschrichtius robustus</i>	Gray whale	41

2740      <sup>a</sup>Ions score is -10\*Log(P), where P is the probability that the observed match is a random event. Individual ions  
 2741      scores > 41 indicated identity or extensive homology ( $p < 0.05$ ). Protein scores were derived from ions scores as  
 2742      a non-probabilistic basis for ranking protein hits. Cut-off was set at Ions score 20.  
 2743  
 2744